Protein Factors Involved in the Biogenesis of the Mitochondrial Ribosome

Aaron Raynold D'Souza

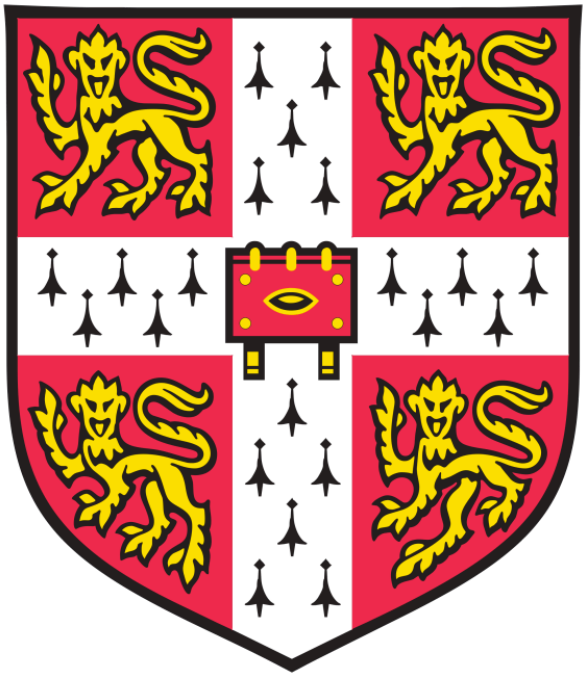

Dissertation submitted to the Board of Graduate Studies in partial fulfilment of the requirements for the degree of Doctor of Philosophy

MRC Mitochondrial Biology Unit
University of Cambridge, UK

Homerton College
September 2017

Declaration

I hereby declare that except where specific reference is made to the work of others, the contents of this dissertation are original and have not been submitted in whole or in part for consideration for any other degree or qualification in this, or any other University. This dissertation is the result of my own work and includes nothing which is the outcome of work done in collaboration, except where specifically indicated in the text. This dissertation contains fewer than 60,000 words excluding appendices, bibliography, footnotes and tables.

Aaron Raynold D'Souza

September 30th 2017

Acknowledgements

First and foremost, I would like to thank my SUPERvisor, Dr Michal Minczuk for giving me the opportunity to do this PhD support, for his mentorship, encouragement, friendship and patience, without which I would not be the scientist I am today. Thank you for giving me the independence to pursue my curiosity and for your belief in me.

I would also like to thank my colleagues through the years with whom I was able to discuss my work and work through my problems, who taught me the basics and tricks of the trade. You were a pleasure to collaborate with. I am especially gratefully for the wonderful members of the Minczuk lab, past and present, who would take time away from their work to help me work through my issues when things were inevitably not going according the plan. Thank you for your friendship and for the inappropriate humour I don't think I can find anywhere else.

I would like to thank my friends in the Homerton MCR, Homerton College Charter Choir and the Imperial College Chamber Choir. You helped me escape the stresses of my PhD and kept me from going insane.

Finally, I would like to thank my parents and my brother for their constant and unfailing love, support and encouragement.

This work is yours as much as it is mine. This work is dedicated to you.

Abstract

The mammalian mitochondria contain their own genome that encodes thirteen polypeptide components of the oxidative phosphorylation (OxPhos) system, and the mitochondrial (mt-) rRNAs and tRNAs required for their translation. The maturation of the mitochondrial ribosome requires both mt-rRNAs to undergo post-transcriptional chemical modifications, folding of the rRNA and assembly of the protein components assisted by numerous biogenesis factors. The post-transcriptional modifications of the mt-rRNAs include base methylations, 2'-O-ribose methylations and pseudouridylation. However, the exact function of these modifications is unknown. Many mitoribosome biogenesis factors still remain to be identified and characterised. This work aims to broaden our understanding of two proteins involved in mitoribosome biogenesis through the study of the function of an rRNA methyltransferase and a novel biogenesis factor.

Firstly, we characterised MRM1 (mitochondrial rRNA methyltransferase 1), a highly conserved 2'-*O*-ribose methyltransferase. We confirmed that MRM1 modifies a guanine in the peptidyl (P) transferase region of the 16S mt-rRNA that specifically interacts with the 3' end of the tRNA at the ribosomal P-site. In bacteria, the modification is dispensable for ribosomal biogenesis and cell viability under standard conditions. However, in yeast mitochondria, Mrm1p is vital for ribosomal assembly and function. We generated knockout cells lines using programmable nuclease technology, and characterised the possible effects of MRM1 depletion on mitochondrial translation and mitoribosome biogenesis. We demonstrated that neither the enzyme nor the modification is required for human mitoribosomal assembly and translation in our experimental setup.

Secondly, we identified a novel mitochondrially-targeted putative RNA endonuclease, YbeY. Using YbeY knockout cell lines, we showed that depletion of YbeY leads to loss of cell viability and OxPhos function as a consequence of a severe decrease in mitochondrial translation. Northern blotting and transcriptomic analysis using next generation RNA-Seq revealed transcript-specific changes to steady state levels. This analysis identified mt-tRNA^{Ser} as a potential target of YbeY. We investigated the effect of YbeY deficiency on mitoribosomal assembly by quantitative sucrose gradient fractionation and mass spectrometry. This analysis showed that the mt-SSU is

depleted in YbeY knockout cells. Further, immunoaffinity purification identified MRPS11 as a key interactor of YbeY. We propose that YbeY is a multifunctional protein that performs endonucleolytic functions in the mitochondria and also acts as a mitochondrial ribosome biogenesis factor, assisting small subunit assembly through its interaction with MRPS11.

Contents

Abbreviations

Amino acid abbreviations, standard units and abbreviations are as decribed in the 'Instructions to Authors' of the Biochemical Journal (Biochem J. (1998) 329, 1-16) unless stated here.

Acetyl-coA	Acetyl coenzyme A
cRT-PCR	Circularisation reverse transcription polymerase chain reaction
CO	Cytochrome c oxidase
CSB	Conserved sequence blocks
DDM	n-Dodecyl-b-D-maltopyranoside
DMEM	Dulbecco's modified eagle medium
DTT	1,4-dithiothreitol
$FADH_2$	Flavin adenine dinucleotide
GTB	Glycerol tolerant buffer
H-Strand	mtDNA heavy strand
HDR	Homology directed recombination
HEK	Human embryonic kidney
HEPES	2-[4-(2-hydroxyethyl)piperazin-1-yl]ethanesulfonic acid
HSP	Heavy strand promoter
IMM	Inner mitochondrial membrane
L-strand	mtDNA light strand
LSP	Light strand promoter
LSU	Large ribosomal subunit
Mt-	Mitochondrial
MOMP	Mitochondrial outer membrane permeabilisation
MOPS	3-(N-morpholino)propanesulfonic acid
MPAT	Mitochondrial poly(A) tail assay
MRGs	Mitochondrial RNA granules
MRM1	Mitochondrial RNA methyltransferase I
MRM1 (-/-)	MRM1 knockout cell line
MRPL	Mitochondrial ribosomal protein of the large subunit
MRPS	Mitochondrial ribosomal protein of the small subunit
MRPP	Mitochondrial RNase P protein

MSH	Mannitol-sucrose-HEPES
mtRPF	Mitochondrial ribosome profiling footprint
MTS	Mitochondrial targeting sequence
NADH	Nicotinamide adenine dinucleotide
NCR	Non-coding region
ND	NADH dehydrogenase
NHEJ	Non-homologous end joining
OCR	Oxygen consumption rate
OLB	Oligonucleotide labeling buffer
OMM	Outer mitochondrial membrane
OXPHOS	Oxidative phosphorylation
PBS-T	Phosphate buffered saline-Triton X-100
PDE12	Phosphodiesterase 12
PNK	Polynucleotide kinase
PNPase	Polynucleotide phosphorylase
PPR	Pentatricopeptide repeat containing
PVDF	Polyvinylidene fluoride
RPMI	Roswell Park Memorial Institute
SOC	Super optimal broth with catabolite repression
SSC	Saline-sodium citrate
SSU	Small ribosomal subunit
TBE	Tris-borate-EDTA
TCA	Tricarboxylic acid
TEMED	N,N,N ',N '-tetramethylethylenediamine
TOM	Translocase of the outer membrane
TRIS	Tris(hydroxymethyl)aminomethane
YbeY (-/-)	YbeY knockout cell line
YbeY (+/-)	YbeY heterozygous cell line
YbeY (-/m)	YbeY Hemizygous cell line
ZFN	Zinc finger nucleases

1 Introduction

1.1 – The mitochondrion – evolution and structure

The turning point in driving the success of the eukaryotic domain of life was the evolution of compartmentalisation in eukaryotic cells. This allowed the development of specialised compartments within the cell that could perform more complex functions and, therefore, could be more tightly regulated. These compartments, called organelles, allowed the development of more specialised cells that could evolve to adapt to changing demands put on the cell and eventually evolve into multicellular organisms (Lane and Martin, 2010). One of these organelles is the mitochondrion. Mitochondria are double membrane-bound sub-compartments of the cells that that emerged during an endosymbiotic merger between an anaerobic archaebacterium and a protobacterium similar to the α-proteobacteria of the order, Rickettsiales (Williams et al, 2007; Anderson et al., 1981; Andersson et al., 1998; Sagan, 1967; Martin & Müller, 1998).

In mammalian cells, these organelles have changed substantially since their protobacterial origins approximately 1.5 billion years ago. Over time, the mitochondrion has specialised through a drastic reduction of the genome, now encoding less than 1% of the proteins found in the mitochondria. About 99% of the proteins (~1500) are now encoded in the nucleus, synthesised in the cytosol and imported into mitochondria (Lopez et al, 2000; Calvo et al, 2016).

The structure and function of mitochondria are closely linked. Even though mitochondria are normally depicted as small rod-like structures, they are a continually changing between dynamic network of reticula or a fragmented state, constantly dividing and fusing with other mitochondria, interacting with other organelles like the endoplasmic reticulum, and communicating with the cell. Mitochondria are a double membrane-bound structure, where the outer mitochondrial membrane (OMM) is partially permeable to small molecules (<5kDa) from the cytosol, and the inner mitochondrial membrane (IMM), enclosing the mitochondrial matrix, is extremely impermeable. The inner membrane is further specialised in that it is highly invaginated into structures called cristae, consisting of large complexes of the respiratory chain. This means that, to shuttle proteins synthesised in the cytosol, through the outer mitochondrial membrane, most nuclear encoded proteins carry a

N-terminal amphipathic helix mitochondrial targeting signal (MTS), and both membranes have evolved to contain multicomponent translocation machineries to recognise and import these proteins (Dudek et al., 2013). Furthermore, the inner mitochondrial membrane, being impervious to passive diffusion, contains a large variety of mitochondrial carriers to import substrates for the mitochondrial enzymes.

1.2 – Functions of the mitochondria

1.2.1 Powerhouse of the cell

The mitochondria are often described as the 'powerhouse of the cell'. However, this is an inadequate description of the function of the mitochondrion because it is not only responsible for the generation of a majority of the ATP required to drive the endergonic functions of the cell, but it is also the house for various other important cellular processes (figure 1.1). At least part of the biosynthetic pathways of iron-sulphur clusters, haem and pyrimidines happen in the mitochondria (Pearce et al., 2017).

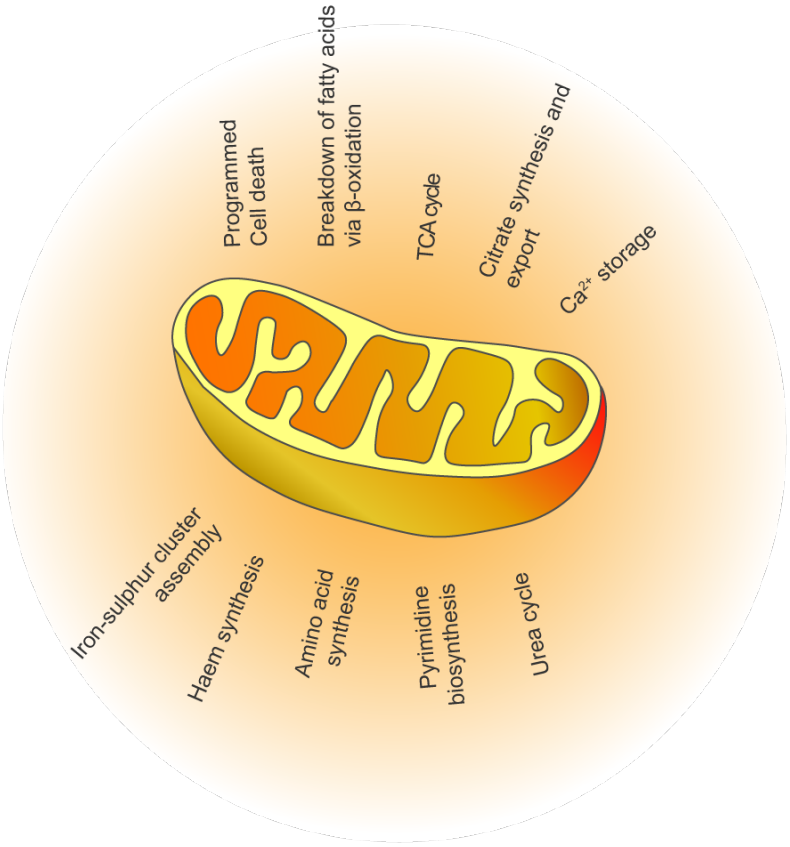

Figure 1.1 Summary of mammalian mitochondrial functions

A major function of the mitochondria is the production of ATP. A small proportion of ATP is derived through glycolysis. The pathway that generates ATP begins in the cytosol with the oxidation of glucose into pyruvate, producing 2 molecules of ATP per glucose molecule. However, a majority of ATP is derived from oxidative phosphorylation. This process begins with the import of into the mitochondrial matrix that is used by the pyruvate dehydrogenase complex to produce acetyl-CoA pyruvate (Bricker et al., 2012; Herzig et al., 2012). Mitochondria are also produce acetyl-CoA through β-oxidation of fatty acids. The acetyl-CoA is fed into the TCA cycle which through a series of sequential reactions leads to the reduction of NAD^+ and FAD cofactors to NADH and $FADH_2$, which are used in the electron transport chain. The electrons from these reduced cofactors are then consumed in the respiratory chain at NADH dehydrogenase (Complex I) and succinate dehydrogenase (Complex II). In the electron transport chain, the electrons are first passed onto ubiquinone. The lipid soluble ubiquinol product of ubiquinone reduction carries the electrons to cytochrome c (by Complex III), which itself passes the electrons to Complex IV (cytochrome c oxidase). Finally, the electrons are used to reduce molecular oxygen to produce water. The series of redox reactions and transfer of these electrons is tightly coupled to the transport of protons out of the mitochondrial matrix establishing an electrochemical gradient (proton motive force) across the IMM. This proton motive force created by the gradient of charge and proton concentration is used by the mitochondria to transport proteins into the mitochondria and drives the rotations of the central domain of the ATP synthase (Complex V). This rotary catalysis mechanism facilitates the generation of ATP from ADP and inorganic phosphate (P_i) (Walker, 2013). The ATP is then exported out of the matrix by adenine nucleotide translocators to be used in endergonic cellular processes. Mitochondria produce oxaloacetate for aspartate and asparagine synthesis, and 2-oxogluterate for glutamate, glutamine, arginine and proline synthesis. The mitochondria are also involved in the early and final steps of heme synthesis, and a part of pyrimidine biosynthesis and the urea cycle.

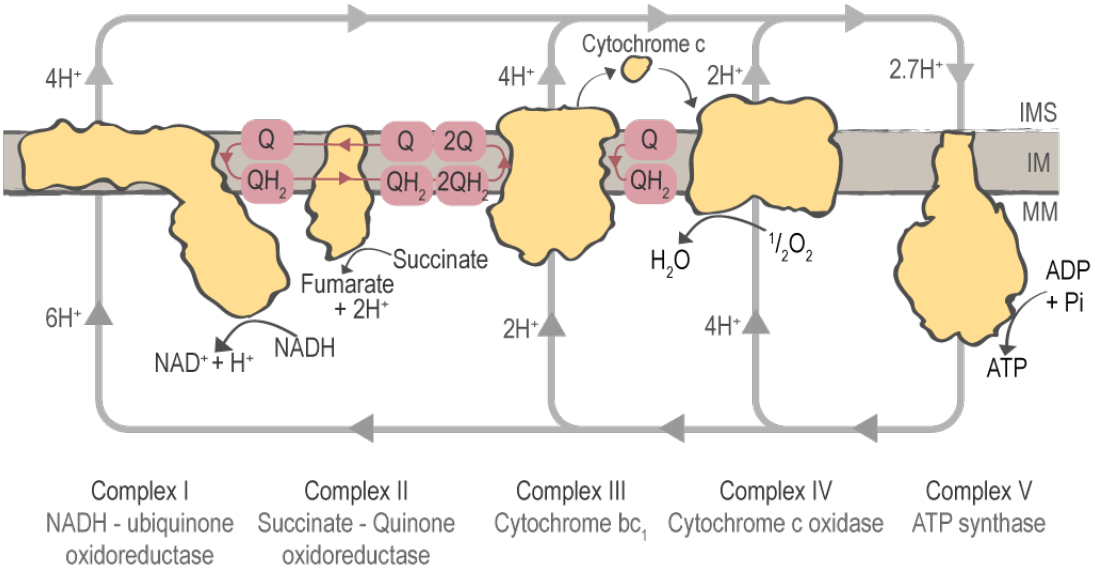

Figure 1.2 Schematic of the electron transport chain. Complex I and II reduce obiquinone to ubiquinol. Complex III oxidises ubiquinol and oxidises cytochrome c. Finally, the electrons are passed from cytochrome c on to molecular oxygen by complex IV producing H_2O. The movement of electrons is used to catalyse the translocation of protons across the inner membrane which generates a proton gradient that is used to fuel ATP synthase activity. IMS, intermembrane space, IM, inner membrane; MM, mitochondrial matrix; Q, ubiquinone; QH_2

The respiratory complexes can also associate with each other to form 'supercomplexes' such as the supercomplexes containing complex I+III, I+III+IV, and III+IV. Complex II does not seem to associate with any other complex and complex V dimerises with itself. Overall, these complicated superstructures facilitate efficient transport of electrons between them (Chaban et al., 2014).

1.2.2 Mitochondria and programmed cell death

Mitochondria also play a key role in programmed cell death. This is led by mitochondrial outer membrane permeabilization and cristae remodelling which cause the release of apoptotic factors such as cytochrome c, Diablo/SMAC and apoptosis initiating factor (Uren et al., 2005). Moreover, the mitochondria also maintain cellular calcium homeostasis by acting as a Ca^{2+} store and coordinating intracellular calcium signalling. Dysregulation of calcium homeostasis is associated with the formation of the permeability transition pore in the outer membrane, which releases the pro-apoptotic factors that stimulate caspase-mediated apoptosis.

1.3 Mitochondrial DNA

1.3.1 Organisation and Structure

The mitochondria derive its genome from its protobacterial ancestor. Mammalian mitochondrion contains ~1000 copies of the mitochondrial genome, each ~16 kb in length. Mitochondrial DNA is tightly packed into nucleoprotein complexes called nucleoids, that are commonly associated with the inner membrane (Albring et al., 1977, Brown et al., 2011). These mitochondrial nucleoids are focal points for mtDNA maintenance, replication and transcription, consisting of proteins such as Mitochondrial Transcription Factor A (TFAM), mitochondrial single-stranded DNA-binding protein (mtSSB), DNA Polymerase γ and mtRNA polymerase (Garrido et al., 2003, Bogenhagen et al., 2008). TFAM is a highly abundant mobility group box protein that facilitates the compact nature of the mtDNA. This core transcription factor causes the genome to undergo negative supercoiling causing the mtDNA to become severely compacted (Ngo et al., 2011; Rubio-Cosials et al., 2011). A recent study showed that nucleoids predominantly consist of a single mtDNA molecule compacted into the nucleoidal structure through the action of TFAM (Kukat et al., 2015). In the absence of TFAM, the mtDNA becomes unstable and mitochondrial transcription is impaired (Larsson et al., 1998; Matsushima et al., 2003).

The double stranded mitochondria DNA (mtDNA) is divided into the heavy strand (H-strand) and light strand (L-strand). The heavy strand is rich in guanine nucleotides, and this difference in composition results in different bouyancies in caesium chloride gradients, as one is heavier than the other. The circular genome encodes 13 polypeptide components of the respiratory complexes (I, III, IV and V), and functional RNAs, 22 tRNAs and 2 rRNAs of the translation machinery that are required to synthesise these proteins (figure 1.2). Unlike the nuclear genome, no introns are found in the mitochondrial genome.

An important region of the genome is a ~1.1 kb major non-coding region (NCR) containing the H- strand (HSP) and L- strand (LSP) promoters of transcription and the H-strand origin of replication (O_H). On the other strand, the L-strand origin of replication (O_L) lies two-thirds along the circular genome in a cluster of five tRNAs. A large portion of the NCR is a three-stranded region called the D-loop containing a third 7S DNA strand necessary for mtDNA replication (figure 1.3).

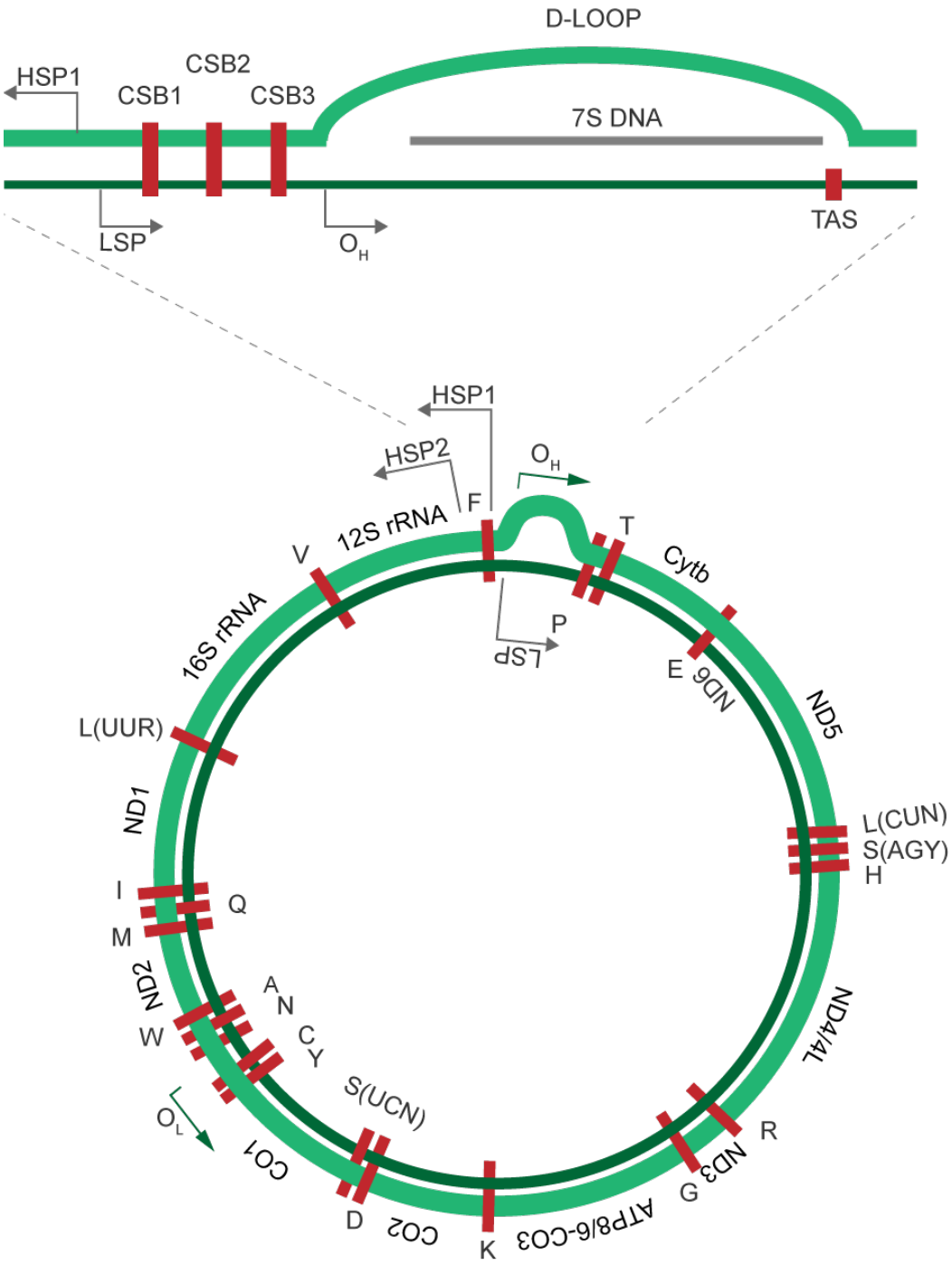

Figure 1.3 Schematic representation of the mammalian mitochondrial genome. The DNA can be divided into a heavy strand (light green) and light strand (dark green). Protein coding regions are generally punctuated by tRNAs (Dark red bars in circular genome). The major non-coding region (above) of the genome contains the D-loop where replication of the H-strand begins showing the 7S DNA, supposed heavy strand promoters (HSP1, HSP2, LSP), three conserved sequence boxes (CSB1-3), Heavy strand origin or replication (OH) and termination associated sequence (TAS). The light strand origin of replication (OL) is also indicated two-thirds along the genome in a non-coding region in a cluster of 5 mt-tRNAs (W, A, N, C, Y).

1.3.2 Mitochondrial replication

1.3.2.1 The mitochondrial replisome

In vitro experiments showed that the mtDNA replisome can be fundamentally separated into to three main components, Polγ, Twinkle and mtSSB (Korhonen et al., 2004). Polγ is a heterotrimeric complex consisting of a catalytic subunit (PolγA) consisting of the 5'-3' DNA polymerase and 3'-5' proofreading exonuclease, and a homodimer (PolγB) that ensures high binding affinity. The Twinkle helicase is responsible for the mtDNA duplex denaturation stimulated by single-strand binding protein, mtSSB (Spelbrink et al., 2001; Melenkovic et al., 2013, Tiranti et al., 1993). The tetrameric mtSSB binds to single stranded DNA stabilising the replication fork (Korhonen et al., 2003; Korhonen et al., 2004).

However, other factors have also been shown to be involved in replication in living cells. The mitochondrial RNA polymerase POLRMT (Fusté et al., 2010), RNaseH1 (Cerritelli et al., 2003), DNA ligase III (Gao et al. , 2011; Simsek et al. , 2011) and MGME1 (Szczesny et al., 2013; Kornblum et al. 2013, Nicholls et al., 2014). Recently, a DNA polymerase-primase called PrimPol was also identified that facilitates the progression of the mtDNA replication fork at lesions, replication blocks or DNA damaged sites and may be responsible for mtDNA repair (Garcia-Gomez et al., 2013; Matinez-Jimenez et al., 2015).

1.3.2.2 Models of mtDNA replication

There are three competing models of mtDNA replication − the strand displacement model (SDM), ribonucleotide incorporation throughout the lagging strand (RITOLS) and strand-coupled replication.

In the strand displacement model, replication begins at O_H in the NCR primed by 7S DNA. The 7S DNA is produced when transcription initiated from the LSP transitions to DNA synthesis. There are three conserved sequence blocks (CSB) within this region that facilitates the switch from RNA synthesis to DNA synthesis (figure 1.2) (Chang and Clayton, 1985). CSB2, in particular, produces G-quadruplexes, which terminate transcription of the 7S RNA, allowing synthesis of 7S DNA (Wanrooij et al., 2010; Wanrooij et al, 2012). The termination of 7S DNA is associated with the termination-associated sequence (TAS) in the D-loop. However, the mechanism for the synthesis of the 7S DNA is still being elucidated (figure 1.2).

During H-strand synthesis, extension of 7S DNA proceeds unidirectionally producing the H-strand until it passes the O_L, two-thirds along the circular DNA (Clayton, 1982). Concurrently, mtSSB binds to the displaced ssDNA strand, preventing the recruitment of POLRMT and the initiation of L-strand synthesis at a wrong site. The formation of a stem loop structure at the O_L hinders mtSSB binding, stimulating POLRMT to produce an RNA primer for the initiation of L-strand replication by Polγ. The replication of both strands then progresses until they terminate at their site of origin (Fuste et al., 2010; Wanrooij et al., 2012).

The RITOLS model of mtDNA replication progresses very similarly to the SDM model. However, it does not require mtSSB to bind to the displaced strand during H-strand synthesis. Instead, RNA intermediates produced during transcription bind to the ssDNA stabilising it, until the RNA is displaced or degraded during lagging strand DNA synthesis (Yasukawa et al., 2006; Reyes et al., 2013). Unlike asynchronous replication at the O_H and O_L proposed by SDM and RITOLS, the strand coupled replication suggests a bidirectional replication bubble initiating in a 5000 bp 'Ori-z' zone spanning MT-CYB, mt-ND6 and mt-ND5 (Holt et al., 2000, Bowmaker et al.,2003; Reyes et al., 2005).

Before the completion of H-strand synthesis, the 7S RNA is degraded by RNaseH1, and the 7S DNA upstream of the O_H is removed by MGME1 (Cerritelli et al, 2003; Holmes et al., 2015; Kornblum et al., 2013; Nicholls et al., 2014; Uhler and Falkenberg, 2015). Finally, mtDNA replication is terminated when the 5' and 3' ends are ligated together by DNA ligase III (Lakshmipathy et al., 1999; Puebla-Osorio et al., 2006).

1.4 Mitochondrial transcription

The transcription of the mitochondrial genome produces polycistronic RNA molecules which encode 22 tRNAs, 13 polypeptides of the oxidative phosphorylation system and 2 rRNAs. Eight of these tRNAs and the ND6 gene are produced from the light strand template transcribed under a single light strand promoter (LSP) (Montoya et al 1982; Montoya et al 1983).

1.4.1 Initiation and termination

Transcription of the mitochondrial genome is led by separate promoters for the light and the heavy strand. The LSP contains the initiation site for 7S RNA production and also the promoter which initiates transcription along the light strand. The transcription of the H-strand is said to be under the control of two promoter sites, HSP1 and HSP2, located in the non-coding region (Figure 1.3) (Montoya et al, 1982; Montoya et al, 1983, Chang and Clayton, 1984). In the classical model, transcription initiating at HSP1, 19 bp upstream of tRNA-Phe produces tRNA-Phe, tRNA-Val and the two rRNAs (12S and 16S), terminating at the tRNA-Leu(UUR) gene. On the other hand, transcription initiating at HSP2, begins just upstream of the 12S mt-rRNA gene and does not terminate at the tRNA-Leu(UUR) site, instead producing a transcript spanning the entire genome, encoding two rRNAs, 12 mRNAs and 14 tRNAs. This transcript terminates at an A/T-rich region of the NCR named D-TERM (Camasamudram et al, 2003). However, this two-promoter model of transcription of the H-strand and termination at tRNA-Leu(UUR) is not supported by more recent *in* vivo (Terzioglu et al., 2013) and *in vitro* results (Litonin et al, 2010).

1.4.2 Transcription machinery

Transcription in the mitochondria is driven by POLRMT, a DNA-dependent RNA polymerase homologous to RNA polymerases in T3 and T7 bacteriophages (Tiranti et al., 1997). The C-terminal domain contains the functionally important, highly conserved, catalytic domain. In yeast, POLRMT contains a unique N-terminal sequence that is dispensable for transcription initiation but is important for mtDNA replication (Wang and Shadel, 1999). This has not been demonstrated in mammals. The mechanism by which the N-terminus contributes to POLRMT function is unclear. In bacteriophages, the N-terminal domain is responsible for recognition and binding to the promoter region. However, in mitochondria, POLRMT uses

additional factors to perform this function (Ringel et al., 2011). In yeast, an additional N-terminal extension is present, which is responsible for interacting with other proteins required for intron splicing (Rodeheffer et al., 2001). However, due to the compact nature of the mammalian mitochondrial genome, there are no introns to be spliced. Yet, a similar N-terminal extension is observed in POLRMT. This extension contains two penticopeptide repeat (PPR) domains that may function to provide site-specific RNA interactions. However, the function of these PPR domains remains to be elucidated (Ringel et al., 2011).

As mentioned earlier, POLRMT works in concert with a collection of proteins to control mitochondrial transcription. Activation and initiation of mitochondrial transcription requires the association of POLRMT with mitochondrial transcription factors B2 (TFB2M) and TFAM (Shi et al., 2012). Produced through a gene duplication event, TFB1M and TFB2M are both homologous to a bacterial SSU rRNA methyltransferase (Cotney and Shadel., 2006). Both these proteins retain their methyltransferase activity. However, it has been shown that the primary function of TFB1M is the dimethylation of mtSSU rRNA (see Section 3.1.1), and the primary function of TFB2M is to induce promoter melting required for initiation of transcription (Falkenberg et al., 2002; McCulloch et al., 2002; Seidel-Rogol et al., 2003). Transcription begins with the binding of TFAM to the DNA causing bending and melting. Then, a POLRMT+TFB2M complex is recruited to the initiation site with TFAM acting to stabilize the DNA-protein complex for initiation of transcription (Posse and Gustafsson, 2017; Ramachandran et al., 2017).

TFAM, in addition of being a mitochondrial transcriptional activator, has non-specific DNA binding capabilities that allows it to function as a DNA packaging protein in the nucleoid (Fisher and Clayton, 1985; Parisi and Clayton, 1991). TFAM has been shown to interact with TFB1M and TFB2M (Dairaghi et al., 1995; McCulloch and Shadel, 2003). It has also been suggested that phosphorylation, acetylation and targeted degradation of TFAM by the Lon protease may lead to dynamic regulation of TFAM-mediated transcription (Lu et al., 2012; Matsushima et al., 2010; Bestwick and Shadel., 2013). *In vitro* reconstitution of mitochondrial transcription shows that TFAM concentrations can determine promoter-specific transcription. TFAM can activate transition from HSP1 and LSP. However, high concentration of TFAM can suppress transcription from the supposed HSP2 site (Lodiero et al., 2012; Zollo et al,

2012). And since H-strand replication is tightly linked to transcription from the LSP promoter, it could be envisaged that TFAM levels could be linked to replication.

Elongation of transcripts in mitochondria is coordinated by mitochondrial transcription elongation factor, TEFM. Transcription from the LSP is often prematurely terminated at the conserved sequence block 2 in the major non-coding region. Though this process is required to prime replication of the mtDNA, this is inhibitory to the progression of transcription (Tan et al., 2016). This protein interacts with POLRMT with its conserved C-terminal domain, without interacting with initiation factors TFB2M and TFAM. Moreover, reduction in TEFM causes a depletion of promoter-distal elongation products (Minczuk et al., 2011). TEFM allows POLRMT to pass this region and allows the transcription of the L-strand primary transcript (Posse et al., 2015). TEFM has been shown to facilitate communication between transcription and replication *in vitro* (Agaronyan et al., 2015). However, this has not been demonstrated *in vivo*.

MTERF1 (mitochondrial transcription termination factor 1) is the protein responsible for termination of transcription. It was initially suggested that MTERF1 binds to the HSP1 promoter site and the site of termination in tRNA-Leu(UUR), thereby facilitating termination of transcription by base flipping and DNA unwinding, and the recycling of the transcription machinery back to the promoter site. (Martin et al., 2005, Yakubovskaya et al., 2010; Jimenez-Menendez et al., 2010). This model was put forward to explain the 50-fold abundance of the rRNAs in the mitochondrial relative to other mitochondrial RNAs (Martin et al., 2005). However, studies in MTERF knockout mice do not show differences in the supposed rRNA products of HSP1 transcription (Terzioglu et al., 2013). This suggests that the high abundance of rRNA is a consequence of their higher stability and half-life rather than due to additional transcription from an alternative promoter. Recent evidence states that MTERF instead plays a role in preventing the progression of the replication fork into the rRNA sequence while it is being transcribed, and prevents the transcription of the anti-sense sequence of the rRNAs (Hyvarinen et al., 2010; Terzioglu et al., 2013; Shi et al., 2016).

Additional factors that have been implicated in transcription regulation include a mt-LSU component, MRPL12, which interacts with POLRMT and activates transcription *in vitro* (Surovtseva et al., 2011; Wang et al., 2007). A depletion of MRPL12 leads to a depletion in POLRMT (Nouws et al., 2016). This suggests a

possible communication between the translation apparatus and transcription machinery.

1.5 Maturation of transcription products

1.5.1 Cleavage of the primary transcript

The mitochondrial genome is transcribed as long polycistronic molecules. The genes coding for mRNA and rRNA are punctuated by tRNA-coding regions. Removal of the tRNA from these molecules generates RNA products for translation and assembly into the ribosome (Anderson et al., 1981; Ojala et al., 1981). This model that defines the processing of this primary transcript is called the 'tRNA Punctuation Model'.

A majority of tRNA excision and mt-RNA processing is performed by RNase P and RNase Z (ELAC2). In eight out of thirteen polypeptides encoded in the mitochondrial genome, the mRNA sequences immediately precede tRNA-coding sequences (Ojala et al., 1981). The RNase P enzyme is responsible for the 5'-end maturation of tRNA precursors and is vital for the endonucleolytic activity required for the release of different RNA species from the primary transcript. Unlike previously characterised RNAse P enzymes in the cytoplasm or bacteria, the mitochondrial version contains no RNA component. RNase P is a heterotrimer composed of three entirely proteinaceous subunits (mitochondrial RNase P proteins 1, 2, and 3 (MRPP1-3)) that independently have separate functions but moonlight as components of the heterotrimeric RNase P complex (Holzmann et al., 2008).

MRPP1 (TMRT10C or RG9MTD1) is the mammalian homologue of yeast tRNA m^1G9-methylase Trm10, which in RNase P, is responsible for tRNA binding. MRPP2 (17β-hydroxysteroid dehydrogenase type 10 (HSD10) or SDR5C1) is a 2-methyl 3-hydrobutyryl-coA-dehydrogenase (MHBD) involved in isoleucine metabolism. Together, MRPP1 and MRPP2 also form a heterodimer that methylates adenines or guanines in position 9 of mt-tRNAs. This modification is vital for mt-tRNA folding and is independent of the mtRNA processing activity. Patients with a recessive mutation in MRPP1 that lacks precursor processing, show a retention of methyltransferase activity suggesting that endonucleolytic activity is independent of the methyltranferase activity of the protein (Metodiev et al., 2016).

The catalytic domain of RNase P lies in the third MRPP3 subunit. It interacts with MRPP1 and MRPP2 in a salt-labile manner, and without this interaction, the

catalytic site of MRPP3 cannot present a correct conformation (Holzmann et al., 2008, Rossmanith and Karwan, 1998). The C-terminal of MRPP3 contains two pentatricopeptide repeats (PPR) motifs which assist in RNA binding, and a metalloprotease domain containing a Mg^{2+} ion required for the hydrolysis of the RNA phosphodiester bond.

Together, the three components of RNase P recognise and cleave the nascent precursor transcript at the 5' end of tRNA (Holzmann et al., 2008; Rossmanith & Holzmann, 2009). Knockdown of the different protein components of RNase P causes an accumulation of precursor molecules (Holzmann et al., 2008). MRPP1 knockdown reduces steady state levels of mature tRNAs which has a detrimental effect on translation. Knockdown of MRPP1 or MRPP3 leads to a reduction in mature mRNAs, bicistronic mRNAs and rRNAs. However, knockdown of MRPP1 or MRPP3 affects the precursor levels to different extents, suggesting different level of contribution of the components to tRNA processing. Moreover, overexpression of these proteins does not have any effect on steady state levels of these RNAs indicating that their concentration is not the rate-limiting step in catalysis (Lopez Sanchez et al., 2011).

The release of tRNAs from the primary transcript also required the action of RNaseZ at the 3' end of the tRNA sequence. ELAC2 is an endonuclease which exhibits RNase Z activity on both nuclear and mitochondrial pre-tRNAs *in vitro* (Rossmanith, 2011). Consequently, depletion of ELAC2 causes the accumulation of tRNA precursors. However, mt-mRNA and mt-rRNA levels, and translation are not significantly affected (Brzezniak et al 2011; Sanchez et al 2011). In patients with missense mutations in ELAC2, increased levels of RNA processing precursors are observed, which leads to translational dysfunction and respiratory defect (Haack et al., 2013). Interestingly, RNase Z endonuclease activity is dependent on RNase P activity. ELAC2 only cleaves 5'-processed mt-tRNA cleavage products of RNase P suggesting a hierarchical processing of RNA (Brzezniak et al., 2011; Rackam et al., 2016).
Other factors have also been identified in the precursor RNA processing, namely G-rich sequence factor 1 (GRSF1) and penticopeptide repeat-containing proteins, PTCD1 and PTCD2. GRSF1 is an RNA-binding protein that binds to L-strand transcripts at consensus sequences in ND6 mRNA and the non-coding regions near ND5 and Cytb. The protein is strongly linked with early stage processing of the RNA

precursor as it is shown to interact with RNase P in RNA granules (see section 1.8) and knockdown of GRSF1 leads to an accumulation of RNA precursors produced by the inactivity of RNase P (Jourdain et al., 2013). Depletion of GRSF1 leads to instability of mt-RNA, decreased expression of mitochondrially-encoded polypeptides, impaired ribosomal assembly and mitochondrial dysfunction (Antonicka et al., 2013; Jourdain et al., 2013).

Both PTCD1 and PTCD2 are PPR-containing proteins that confers the ability to bind RNA (Small and Peeters, 2000). PTCD1 has been shown to interact with ELAC2. A deficiency in PTCD1 accompanies a dysregulation of 3' tRNA processing, especially mt-tRNA-Leu(UUR) and mt-tRNA-Leu(CUN). Therefore, it is possible that PTCD1 also plays a role in sequence-specific tRNA metabolism (Lopez Sanchez et al., 2011; Rackham et al., 2009). PTCD2, on the other hand, has been implicated in the processing of the non-canonical cleavage site between ND5 and CytB (Figure 4.5), as the junction does not contain a mt-tRNA. A depletion of PTCD2 in mouse models causes an accumulation of the precursor and a reduction in the activity of complex III (ubiquinol-cytochrome c reductase), where CytB is the catalytic core (Xu et al., 2008)

1.5.2 Exceptions to the tRNA punctuation model

Out of approximately forty-three cleavage events observed in the mitochondrial polycistronic transcript, there are various elements that do not follow this 'tRNA punctuation model'. These include the overlapping reading frames of ND4/4L, and ATP8/6, and other bicistronic transcripts like ATP8/6-CO3 that are not separated by tRNAs. The 5' end of CO1 and CytB, and the 3' end of ND6 show cleavage sites that do not depend on the presence of tRNAs (Temperley et al., 2010). The 3' end of ND6 shows multiple ends and is found approximately 500 nt (nucleotides) downstream of the translation termination codon (Slomovic et al., 2005).

The accuracy of cleavage at the junction between genes is variable. The 5' ends of ATP8/6-CO3, ND1 and CO1 have been observed with 1-3 nt long untranslated regions (UTR). CO1, ND6 and ND5 have 3' UTR that code for genes in the antisense strand. The 3' end of 12S rRNA has been seen with minor truncations and with the addition of 3-4 nt. A majority of 16S rRNA molecules seem to show additional residues at the 3' end, whether it be oligoadenylation, or nucleotides from

the 5' end of the downstream tRNA-Leu(UUR) gene (Temperley et al., 2010, Pearce et al., 2017).

There are no common sequence motifs within CO1, CO3 and CytB that signal a common mechanism of cleavage, suggesting that the different sites might have different nucleases acting on them. It has been suggested that ELAC2 and RNase P might contribute to processing of these sites. However, knockdown of the proteins and analysis using northern blotting shows no effect on the levels of the non-conventional cleavage sites (Brzezniak et al., 2011). On the other hand, knockdown and qPCR shows that RNase P is required for 5' end endonucleolytic activity on CO1 mRNA, which, if true, might be due directed by tRNA-like secondary structures present at the 5' end (Sanchez et al., 2011).

FASTKD2 has been implicated as one of the enzyme involved in non-canonical cleavage. A depletion of the protein leads to the accumulation of various precursors with the non-canonical cleavage sites (Antonicka and Shoubridge, 2015). Knockout of FASTKD2 leads to an accumulation of misprocessed precursors of 16S rRNA and ND6 mRNA. CLIP-based analysis of the RNA targets of FASTKD2 identify both 16S rRNA and ND6 as its targets (Popow et al., 2015). As described earlier, PTCD2 has been implicated in the processing of the ND5-CytB precursor. However, the mechanism of cleavage of the precursor transcripts of FASTKD2 and PTCD2 needs to be investigated further.

1.5.3 Post-cleavage maturation of RNA

1.5.3.1 Polyadenylation

After being released from the primary transcript, the mitochondrial mRNAs, except for ND6, undergo 3' polyadenylation (Slomovic et al., 2005). Compared to nuclearly-encoded transcripts which have poly(A) tails ranging between 150-200 nucleotides, mt-mRNAs have a significantly shorter poly(A) tail at roughly 45-55 nucleotides (Ojala et al., 1981; Proudfoot, 2011). In mammals, mitochondrial rRNAs contains little to no adenylation at the 3' ends, while in *Drosophila melanogaster*, ND6 and both rRNAs are polyadenylated (Stewart et al., 2009; Bratic et al, 2011).

Poladenylation in mitochondria is catalysed by a homodimeric polyadenylic acid RNA polymerase (mtPAP) (Tomecki et al., 2004; Bai et al., 2011; Lapkouski and Hallberg., 2015). The function of polyadenylation in RNA stability in mitochondria is unclear. They might serve to complete stop codons because seven of thirteen mt-mRNAs have lost their 3' stop codon and require 3' adenylation to complete the open reading frame.

In various other systems, polyadenylation of RNA is used to control stability of the molecule. In bacteria and plant mitochondria, the poly(A) tail decreases stability of the transcript (Schuster and Stern, 2009). However, whether the presence of a poly(A) tail has any effect on mammalian mitochondrial RNA stability is unclear. Knockdown of mtPAP causes a mRNA-specific effect on steady state levels, causing an increase in complex I mRNAs, ND1 and ND2, a decrease in complex IV transcripts and no difference in the steady state levels of the other transcripts (Tomecki et al., 2004; Nagaike et al., 2005). Defective mtPAP in patient cells also showed differential sequence-specific changes to RNA steady state levels (Wilson et al., 2014). However, in all the cells studied, a short oligoadenyl tail was still observed in the absence of mtPAP (Slomovic et al., 2005).

A knockout of mtPAP in *D. melanogaster* causes a complete loss of all poly(A) tails except 12S rRNA, suggesting the presence of an alternative 12S-specific oligoadenylase. In these deadenylated mRNAs, the lack of poly(A) tails made the molecules susceptible to 3' end degradation. Moreover, no overall change in steady state level of processed transcripts was observed, regardless of whether the 3' stop codon was encoded or not (Bratic et al., 2016). This suggests that polyadenylation in

mitochondria is not a determinant of steady state level but may protect the 3' terminus of the sequence from being exonucleolytically degraded.

The polyadenylation status of some RNAs in the mitochondria is controlled by PDE12. PDE12 is a mitochondrially-targeted member of the exonuclease/ endonuclease/ phosphate family (Poulson et al., 2011; Rorbach et al.,2011). *In vitro* assays show 3'-5' poly(A)-specific (and to a lesser extend poly(U)) exonuclease activity (Rorbach et al., 2011). As such, overexpression of PDE12 *in vivo* leads to 3' deadenylation of poly(A) tails. Similar to experiments in which mtPAP was depleted, mRNAs for ND1 and ND2 showed increase in steady state levels while steady state levels of complex IV increased. This suggested that polyadenylation has different effects on the steady state levels of different mRNAs. Knockout of PDE12 from human cells does not have any significant effect on the mt-mRNA poly(A) lengths or its stability. However, PDE12 was shown to be required for the maturation of the 3' end of 16S mt-rRNA and certain mt- tRNAs by the removal of spurious 3' adenylation. Depletion of PDE12 caused a strong mitochondrial dysfunction as a result of impaired protein synthesis. However, this translation defect was not caused by misassembled ribosomes. On the contrary, spurious oligoadenylation at the 3' end of 16S rRNA did not affect its assembly into the ribosome. Instead, translation was impaired by the ribosomal stalling caused by dysfunctional polyadenylated tRNAs. Therefore, it can be concluded that PDE12 is required in the mitochondria to counteract excessive mistargeted adenylation (Pearce et al, 2017)

A translational defect was also observed in cells where exogenous expression of deadenylases were used to remove poly(A) tails (Wydro et al., 2010). However, deadenylation caused as a by-product of ablation of LRPPRC (see section 1.6.1), does not affect levels of translation (Ruzzenente et al., 2012). Therefore, it can be concluded that the translational defect is not directly caused by lack of a poly(A) tail, but due to the lack of a stop codon. The function of a long poly(A) tail still remains to be elucidated.

Polyadenylation also seems to be associated with RNA processing. Patient cell lines with a μΔ9205 deletion which removes the termination codon from the bicistron encoding ATP6, does not show any effect on the processing of the junction between ATP8/6 and CO3, or the stability of processed CO3 mRNA. However, it does produce a truncated mRNA caused by excessive exoribonuclease activity, and leads to the decreased stability of the processed ATP8/6 molecule. Unlike mRNA from

control cell lines, which show a poly-A tail of about 45-56 nt, the patient cell line showed three discrete populations of mRNA with normal poly-A tails (A45-56), shorter poly-A tails (A26-37) and severely truncated 3' termini (A[-1]-11) (Temperley et al., 2003). This suggests that polyadenylation and 3' end of the transcript are linked and processing and polyadenylation may happen concurrently in RNA granules (see section 1.8).

1.5.4 Mitochondrial tRNA Maturation

The 22 mitochondrial tRNAs produced from the action of RNase P and ELAC2 undergo a series of extensive maturation steps comprising of chemical modifications, polymerase activity and processing. Major chemical modifications that have been identified in tRNAs include methylation, pseudouridylation, taurine modification, formylation, isopentenyl modification and methylthio modification. The modifications have a structural role in making additions to the sequence which are not coded in the genome and stabilisation of the tRNA structure, and a functional role in expanding anticodon-codon recognition, and ensuring efficiency and accuracy of this recognition. Many of the enzymes involved in these modifications have been identified. However, many are yet to be discovered.

The encoded tRNA sequence is not always complete and requires additional polymerase activity to produce a functional unit. Mitochondrial tRNAs do not encode a 3' CCA sequence which is required for aminoacylation by aminoacyl-tRNA synthetases. In humans, this CCA is post-transcriptionally added on by tRNA-nucleotidyltransferase 1 (TRNT1), which specifically selects CTP and ATP for polymerisation without the need for a template sequence, terminating polymerisation immediately after CCA addition (Nagaike et al., 2001). Similarly, unlike bacteria, yeast and mammalian mitochondrial tRNA-His does not encode a 5' guanine which is required for the recognition and activity of its cognate aminoacyl-tRNA synthetase. This is performed by a 3'-5' polymerase activity (Nakamura et al., 2013; Powell et al., unpublished data).

The tRNA exists as a cloverleaf structure with four distinct base-paired stems - the acceptor stem, T-stem, anticodon stem and the D-stem, with three non-base paired loops. The L-shaped tertiary structure of tRNAs is formed by the interactions of the distal loops. This structure positions the acceptor stem perpendicular to the anticodon stem. There are two exceptions to the common tRNA structure in the mitochondria.

Mitochondrial tRNA-Ser(UCN) contains a longer acceptor arm, a reduced D-loop and a reduced linker region between the acceptor and D-stems. However, alternative interactions allow the tRNA to still maintain the required conformation (Watanabe et al., 1994). Similarly, mitochondrial tRNA-Ser(AGY) is highly shortened, completely lacking the D-arm. However, a more flexible core allows the molecule to mould to the correct structural dimensions (Frazer-Abel and Hagerman, 2008). The strong conservation of the tRNA conformation illustrates its importance in its function. The high efficiency of translation is enabled by the chemical modifications that stabilise this conformation (Perret et al., 1990; Harrington et al., 1993, Helm et al., 1998; Helm et al., 1999). These modifications work collaboratively to fine-tune the structure and functional fidelity of the individual tRNAs (Motorin and Helm, 2010). Hence, deficiencies are not necessarily observed on removal of a modification and may require combinatorial deficiencies of multiple chemical modifiers and additional translational inhibitors before a deficit in translation is observed (Alexandrov et al., 2006; D'Silva et al., 2011; Okamoto et al., 2014).

Methylation and pseudouridylation are the two main ways of influencing structural conformation. Methylation of tRNA is used to block hydrogen bonding and to prevent the formation of helices. This is seen in TRMT1 which dimethylates G26 and inhibits base pairing with cytosine, and the methylation of A9 by the MRPP1/MRPP2 (TRMT10C/HSD17B10) subcomplex (two components of the RNase P complex (see section 1.4.1)), which inhibits base pairing with U64 in the T-stem (Voigts-Hoffmann et al., 2007; Vilardo et al., 2012). TRMT61B is responsible for the m^1A58 modification of multiple mt-tRNAs, and TRMT5 methylates G37 in mt-tRNAs (Chujo and Suzuki, 2012; Powell et al., 2015). In bacteria and yeast, m^1G37 prevents frameshift-based errors at the ribosome (Urbonavicius et al., 2001). However, the function of these modification in mitochondria is still unknown (Brule et al, 2004; Chujo and Suzuki, 2012).

Instead of disrupting hydrogen bonds, modifications can also be made to encourage hydrogen bonding, as seen in the isomerisation of uracil to pseudouridine. This presents an extra hydrogen bond donor on the Watson-Crick base pairing edge of the nucleotide. This stronger bond is used by the tRNA to strengthen and stabilize the structure (Davis, 1995; Newby and Greenbaum, 2002). PUS1 is a well characterised pseudouridine synthetase, which in mitochondria modifies U27 and U28 on tRNAs and various other non-coding RNAs (Patton et al., 2005, Zhao et al., 2004). Loss of

PUS1 leads to defect in mitochondrial translation, and in patients leads to symptoms associated with mitochondrial dysfunction, such as lactic acidosis, myopathy and sideroblastic anemia (Patton et al., 2005; Zeharia et al., 2005; Fernandez-Vizarra et al., 2007). Recently, a RNA-granule localising (See section 1.8) pseudouridine synthetase, RPUSD4, was identified, that pseudouridylates 16S mt-rRNA at position 1397, which is suggested to be required for the stability of 16S rRNA and the assembly of the mt-LSU (Antonicka et al., 2017; Zaganelli et al., 2017). CLIP-based analysis identified that RPUSD4, in addition to 16S rRNA, also interacts with tRNA-Phe and tRNA-Met. However, knockdown of RPUSD4 only caused a reduction of ψ39 on tRNA-Phe but no change in pseudouridylation of tRNA-Met. Overall, a loss of RPUSD4 led to a defect in ribosomal biogenesis and therefore, mitochondrial translation (Zaganelli et al., 2017).

During translation, tRNAs communicate the information from the triplet codon on the mRNA to the peptidyl transferase centre. This requires the tRNA to correctly recognise the mRNA codon and provide the appropriate amino acid. However, there is a high degree of degeneracy of the genetic code in mitochondria. That is, many codons can code for the same amino acid. The tRNA compensates for this by chemically modifying the third position of the cognate anticodon (position 34). The post-transcriptional modification of this 'wobble' base encourages non-conventional base pairing and diversifies the possible scenarios in which the tRNA can be used. Moreover, conversely, the unmodified uracil is also naturally 'wobbly' and so, modification of the base can restrict its codon recognition.

For example, in tRNAs for Leu(UUR), Trp, Lys, Gln and Glu, the encoded uridine at position 34 is modified to 5-tauromethyluridine (Suzuki and Suzuki, 2014). This is performed by GTP binding protein 3 (GTPBP3) and mitochondrial tRNA optimisation 1 (MTO1) (Villarroya et al., 2008; Li et al., 2002). Of these five modified uridines, tRNAs for Lys, Gln and Glu undergo further thiolation to 5-taurinomethyl-2-thiouridine by TRMU (MTU1). Patients and animal models lacking these modifications and their modifying enzymes have been shown to present deficiencies in the respiratory chain (Suzuki et al., 2002; Ghezzi et al., 2012; Gaignard et al., 2013; Kopajtich et al., 2014; Becker et al., 2014). Deletion of the yeast homologs of TRMT1, GTPBP3 or MTO1 in yeast do not cause respiratory deficiencies if knocked out on their own. However, a combinatorial double or triple knockout of the three

genes leads to complete loss of tRNAs and mitochondrial protein synthesis (Wang et al., 2010).

Similarly, the cytosine found at the wobble position of mt-tRNA^{Met} is formylated. This is because, in mitochondria, the codons encoding methionine are expanded to also include AUA, alongside AUG (Fernley and Walker, 1987). The modification that allows this expansion of recognised codons is a two-step process, which includes the methylation of the position by NSUN3 and further oxidation to a formyl group by ABH1 (Haag et al., 2016; Nakano et al., 2016; Van Haute et al., 2016; Van Haute et al., 2017)

The other nucleotides surrounding the anticodon triplet are also modified. Position 37 is found downstream of the anticodon triplet, namely position 36, which base pairs with the first position of the codon triplet on the mRNA. TRIT1 (tRNA isopentenyltransferase 1) catalyses the formation of isopentenyladenosine and, in some cases, this can be further methylthiolated by CDK5RAP1 (Cyclin-dependant kinase 5 regulatory subunit associated protein 1) (Yarham et al., 2014; Reiter et al. 2012; Wei et al., 2015). This is particularly important in cases where position 1 of the codon triplet is a uridine. This modification stabilises the weak A-U base pairing between the codon and the anticodon, increasing accuracy and fidelity (Lamichhane et al., 2013).

1.6 Mitochondrial RNA turnover

1.6.1 Regulation of mitochondrial RNA stability

The steady state levels of transcripts in the mitochondria are maintained by two RNA-binding proteins, LRPPRC and SLIRP. LRPPRC (Leucine-rich penticopeptide rich domain containing protein), is a highly abundant protein that localises to the mitochondria (Sterky et al., 2010). Loss of LRPPRC leads to a loss of steady state levels of mt-mRNAs, but not mt-rRNAs and mt-tRNAs. This is accompanied by a defect in translation and consequently, a loss of assembled respiratory complexes (Gohil et al., 2010; Sasarman et al., 2010a; Sondheimer et al., 2010; Ruzzenente et al., 2012; Mourier et al., 2014). A LRPPRC knockout mouse model exhibits a loss of stability of all H-strand-derived transcripts, loss of long poly(A) tails and a severe translational defect (Ruzzenente et al., 2012).

Similarly, SLIRP (Stem-loop interacting RNA binding protein) is an RNA-binding protein that, when knocked down, leads to a destabilisation of mRNA transcripts in

cells, which causes disassembly of the OXPHOS subunits and OXPHOS deficiency (Baughman et al., 2009). However, this is not observed in a knockout mouse model (Lagouge et al., 2015). In the mitochondria, LRPPRC forms a complex with SLIRP which controls the stability of mRNAs, independent of the transcriptional and translational apparatuses (Sasarman et al., 2010b; Ruzzenente et al., 2012; Harmel et al., 2013). Moreover, the steady state levels of both proteins are linked to the steady state levels of the other. Knockdown of one of the protein leads to destabilisation of the other (Chujo et al., 2012; Ruzzenente et al., 2012). It has been suggested that the LRPPRC/SLIRP complex associates with the mRNAs, especially, translationally-inactive transcripts, suppressing degradation by the PNPase/SUV3 degradosome (Chujo et al., 2012; Ruzzenente et al., 2012; Lagouge et al., 2015)). Moreover, this binding activity prevents secondary structures from forming, thus making the 3' ends available for polyadenylation by mtPAP. As such, a decrease in polyadenylated mRNAs is observed in cells where LRPPRC and to a small extent when SLIRP are reduced. Conversely, an increase in the levels of the complex, *in vitro*, leads to an increase in polyadenylated mt-mRNAs (Chujo et al., 2012; Wilson et al., 2014).

Recently, FASTKD3 was also implicated in RNA stability. Loss of FASTKD3 leads to an increase in stability of mRNAs for ND2, ND3, CYTB, COX2, and ATP8/6 without affecting steady state levels of unprocessed precursors. In addition, it has also been shown to be necessary for the translation of complex IV subunit CO1 through regulation of translation. Unlike other members of the FASTK family, FASTKD3 does not co-localise in the RNA granule (see section 1.8), suggesting that its role is not at the level of the nascent transcript (Boehm et al., 2016).

1.6.2 Mitochondrial RNA degradation

In yeast mitochondria, RNA degradation is mediated by an RNA degradosome consisting of helicase SUV3 and RNase Dss1. This degradasome is required for the removal of introns and misprocessed RNA (Dziembowski et al., 2003; Malecki et al., 2007). In these degradosomes, SUV3 unwinds the RNA secondary structure in an ATP-dependent manner, making ssRNA available for Dss1 3'-5' ssRNA exoribonuclease activity. In humans, the homolog of Dss1 has not been identified. However, the human homolog of helicase SUV3 (hSUV3) has been localised to the mitochondrial matrix (Michal et al., 2002). Knockout of SUV3 in *Drosophila melanogaster* leads to an increase in abundance of mt-mRNA, while rRNAs are not

affected and tRNA levels are reduced. This suggests that the degradosome may not be responsible for rRNA turnover. Moreover, an accumulation of tRNA precursors suggests that SUV3 helicase activity may have a role to play in the punctuation model (Clemente et al., 2015).

The RNase component of the mitochondrial degradosome has been assigned to PNPase. PNPase is a mitochondrially-targeted enzyme that contains both 3'-5' exonuclease activity and 5'-3' polymerase activity (Piwowarski et al., 2003). PNPase has been localised to the mitochondrial matrix (Borowski et al., 2013). However, its function in the mitochondria is constantly under debate. Some have shown that PNPase is vital for mRNA and precursor stability and control of polyadeylation, while others have observed no effect of PNPase depletion (Nagaike et al, 2005; Slomovic and Schuster, 2008; Wang et al., 2010). However, *in vitro* assays show PNPase heterodimerising with matrix SUV3 helicase to form a mitochondrial ssRNA degradation complex (Wang et al., 2014). *In vivo* assays localise PNPase to the mitochondrial matrix in RNA granules (see section 1.8) forming a degradosome with hSUV3 (Borowski et al., 2012). Both the components of the degradosome have also been shown to be vital for the removal of 3' UTR of ND6, reinforcing the idea of a collaborative role in RNA turnover (Jourdain et al., 2015).

PNPase was also localised to the intermembrane space suggesting a role for PNPase in this region. PNPase has been implicated in transporting cytoplasmic RNA across the inner membrane, however, evidence for the presence of cytoplasmic RNA in the matrix is inconclusive and contradictory (Wang et al., 2010; Matilainen et al., 2017; Sato et al., 2017). The RNA import function of PNPase suggests that PNPase import RNA component of RNase P and the 5S rRNA into the mitochondria. However, both these RNA components have been shown to be obsolete in the mitochondria. The RNase P in the mitochondria is completely composed of a homotrimeric protein complex which functions without the need of an RNA component (Holtzmann et al., 2008), and the 5S rRNA in the mt-LSU has been replaced by tRNA-Val or tRNA-Phe (Amunts et al., 2015; Greber et al., 2015; Rorbach et al., 2016).

It has been suggested that polyadenylation of transcripts in the mitochondria are linked to their stability. The PNPase/hSUV3 complex has been shown to directly interact with mtPAP and thus, indirectly control levels of polyadenylation (Wang et al., 2014). Consequently, a depletion in PNPase has been shown to lead to a lengthening of poly(A) tails, though the strength of this effect differs between different

publications (Nagaike et al., 2005; Slomovic and Schuster, 2008). Furthermore, a depletion in hSUV3 leads to an extension of poly(A) tails (Szczesny et al., 2010). It is not clear whether an increase in polyadenylation causes an increase in stability, or whether an increase in stability of the transcripts allows for more opportunities for polyadenylation. Knockdown of mtPAP results in an increase in stability of mt-mRNAs for ND1, ND2, ND3 and ND4/4L, and a decrease in stability of CO3 and ATP8/6, even though a reduction in polyadenylation is observed (Piechota et al., 2006). This suggests that the effect of polyadenylation on stability is transcript-specific. This differential polyadenylation-dependent pattern of stability is observed in various studies where mtPAP was depleted (Piechota et al., 2006; Nagaike et al., 2005; Nagao et al., 2009; Crosby et al., 2010; Bratic et al., 2016) and where mitochondrially-targeted deadenylases (PARN and PDE12) were overexpressed in cell lines (Wydro et al., 2010; Rorbach et al., 2011).

The mitochondrial degradosome is incapable of degrading short RNA molecules. Therefore, REXO2, a mitochondrially-targeted exoribonuclease has been attributed the function of completing RNA degradation (Bruni et al., 2013). *In vitro*, REXO2 is able to perform 3'-5' degradation of ssRNA and DNA fragments (Nguyen et al., 2000). Interestingly, a reduction of REXO2 causes a deficiency in mt-DNA replication, transcription and translation, suggesting that it plays a more fundamental role in nucleic acid metabolism in the mitochondria (Bruni et al., 2013).

In addition to the degradosome and REXO2, LACTB2 has been identified as a mitochondrially-localised ssRNA endonuclease, homologous to ELAC2 (Levy et al., 2016). Knockdown of the protein causes an accumulation in mt-RNAs, as identified via qPCR, and a general mitochondrial dysfunction (Levy et al., 2016). However, its RNA targets and its function within the mitochondria are still to be elucidated.

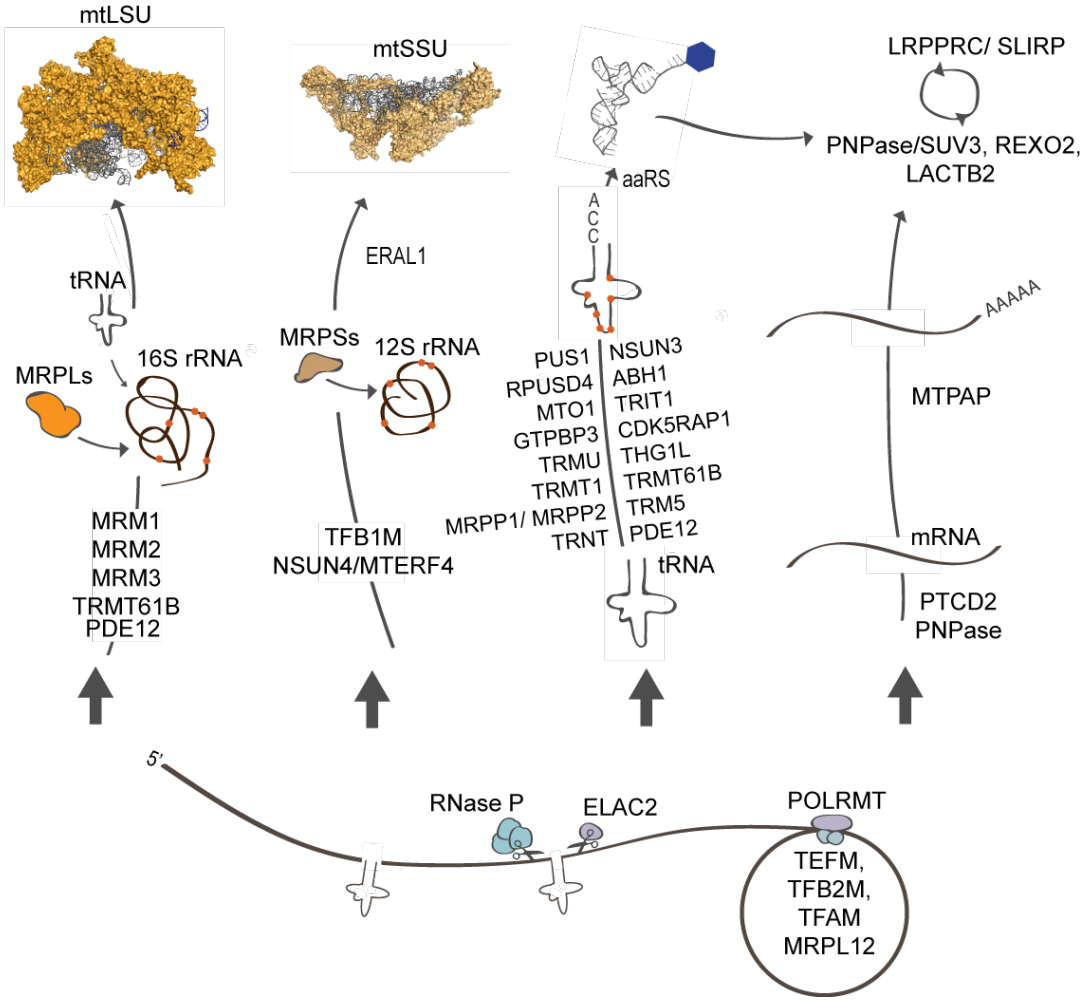

Figure 1.4 Summary of major steps and players in RNA processing and maturation in the mitochondria. The mtDNA is transcribed from the LSP and HSP promoters. The polycistronic transcript is mostly processed through the excision of punctuating tRNA sequences. Other mRNAs are also released through non-canonical cleavage and processing. The mt-LSU and mt-SSU rRNAs are chemically modified by various methyl transferases and pseudouridylases during folding and assembly of mitoribosomal protein components, coordinated by various trans-acting assembly factors. The tRNAs are processed through 5' and 3' polymerase activity and chemical modification before being aminoacylated by aminoacyl-tRNA synthetases (aaRS). The mRNAs undergo polyadenylation and deadenylation. The stability of mt-RNAs are controlled by various factors including RNA-stabilising complexes, degradosome, endonucleases and exonucleases.

1.7 Mitochondrial translation

Mitochondrial translation requires a large plethora of nuclearly-encoded factors including initiation, elongation and termination factors.

In eubacteria, translation is initiated through the action of three initiation factors – IF1, IF2 and IF3. Of these, IF1 and IF2 are present in all domains of life and commonly referred to as 'universal translation initiation factors' (Choi et al., 1998, Lee et al., 1999). However, in the mammalian mitochondria, IF1 is absent. Translation is initiated through the action of IF2 and IF3. A 37-amino acid insertion into IF2 compensates for the loss of IF1 (Figure 1.5). A bacterial strain lacking IF1 and IF2 can be complemented with mitochondrial IF2, and if the 37 aa insert is lost, requires IF1 to be present (Gaur et al., 2008).

Prokaryotic translation elongation is mediated through three factors that are all found in mammalian mitochondria – mt-EFTu, mt-EFTs and mt-EFG (Hammarsund et al., 2001; Ling et al., 1997). In addition to these, in mitochondria, two homologs of mt-EFG (1 and 2) exist. However, mt-EFG2 may be dispensable as depletion, in yeast, does not lead to a translation defect. It may be responsible for ribosome recycling (Tsuboi et al., 2009).

Termination of translation in bacteria is under the control of four factors, release factors RF1, RF2, RF3 and ribosome recycling factor (RRF) (Bertram et al., 2001). RF1 and RF2 catalyse stop codon-specific hydrolysis of peptidyl tRNA, while RF3 acts to stimulate these release factors and their release from the ribosome. In the mitochondria, three termination factors have been identified, namely mtRF1, mtRF1a and mtRRF (Nozaki et al., 2008; Soleimanpour-Lichaei et al., 2007; Zhang et al., 1998; Rorbach et al., 2008). Analogous to bacterial RF1, mtRF1 terminates translation at the UAA and UAG stop codon (Soleimanpour-Lichaei et al., 2007).

Transcript-specific regulation of translation has also been observed. In yeast, these translational activation factors have been observed for all the eight mitochondrially-encoded genes. These are generally membrane-associated and facilitate the co-translational insertion of the proteins (Towpik, 2005; Chacinska and Boguta, 2000; Zeng et al., 2007). Mdm38 controls the synthesis of CO1 and CytB by binding to Mba1 (see section 1.7.1.5). A loss of Mba1 and Mrm38 (paralog of human protein, Letm1) in yeast cells causes a loss of biogenesis of cytochrome reductase and cytochrome oxidase, independent of a defect in membrane association. This suggests

the synthesis of the mitochondrially-encoded polypeptides can be regulated in an mRNA-specific manner (Bauerschmitt et al., 2010).

The difference between yeast and mammalian transcripts is that yeast mRNAs contain 5' UTRs to which the translational activators can bind. In mammalian mitochondrial, this is absent and therefore, any activator would have to modulate translation in a different way. As such, various factors have been identified that can regulate the synthesis of complex IV subunit CO1. CCDC44 (TACO1) was identified as a regulator of mitochondrially-encoded CO1, as depletion of the protein led to a loss of CO1 translation and complex IV deficiency, despite no changes to levels of CO1 mRNA (Weraarpachai et al., 2009). Similarly, depletion of components of the mitochondrial translation regulation assembly intermediate of cytochrome c oxidase (MITRAC), C12orf62 and MITRAC12, leads to a reduction of CO1 synthesis, possibly through an associated loss in the assembly of the complex (Szklarczyk et al., 2012; Weraarpachai et al., 2012).

Due to the lack of a 5' UTR or cap that would allow the ribosome to identify the mRNA, the mitoribosome must have evolved mechanisms for recognition of these transcripts. Recent cryo-EM structures have identified the recruitment of an RNA-binding PPR protein, mS39 at the entrance to the mRNA entry site (figure 1.8) (Amunts et al., 2015; Greber et al., 2015). Initiation begins with the association of the mRNA with the free mt-SSU. This is mediated by mt-IF3 which inhibits the premature association of the mt-LSU and facilitates the positioning of the AUG start codon at the peptidyl site (Bhargava and Spremulli; 2005; Liao and Spremulli; 1989; Haque et al., 2008). This initiation complex also requires the entry of fMet-tRNA-Met which is facilitated by mtIF2 in a GTP-dependant manner. The interaction between mtIF2 and fMet-tRNA-Met is strengthened by the association with mt-mRNA. The formation of a stable complex leads to the assembly of the monosome (Liao and Spremulli, 1990; Ma and Spremulli, 1996). Similar to their bacterial equivalents, dissociation of the initiation factors is accompanied by the hydrolysis of GTP (figure 1.5). In the case of ND4/ND4L and ATP8/6 mRNAs, the open reading frames of both genes are overlapping. The mechanism by which the ribosome identifies and begins translation of the second ORF is unclear.

Mitochondrial translational elongation is very similar to elongation in prokaryotic systems. This begins with the mtEFTu which forms a complex with GTP and amino-acyl tRNA. After a proofreading step, mtEFTu carries the tRNA to the acceptor (A)

site where it binds to the mRNA through codon-anticodon interactions on the mt-SSU. This stimulates the hydrolysis of GTP which releases the elongation factor and moves the tRNA into the peptidyl (P) site. This catalyses peptide bond formation. mtEFTu is recycled through the action of nucleotide exchange proteins that replace the GDP for a GTP. Then, mtEFG1 (bound to GTP) moves the tRNAs in the A and P site to the P and exit (E) sites respectively. This also causes the mRNA to move along by one codon, making the next codon available for recognition (figure 1.5). In the mitoribosome, the E site is not well defined, as many of the residues involved with interactions between the bacterial ribosome and the tRNA in the E-site, have been lost in the mitochondria (Sharma et al., 2003; Mears et al., 2002; Mears et al., 2006). Cryo-EM studies of the ribosome have identified the presence of an altered binding pocket which may serve an alternative E-site (Amunts et al., 2-15; Greber et al., 2015). Termination of translation is triggered by the presence of a stop codon in the A site. This causes the hydrolysis of the bond between the tRNA and the nascent polypeptide, allowing it to be released. In the case of mRNAs for CO1 and ND6, the sequence ends with AGA and AGG, instead of the conventional UAA and UAG stop codons. However, this issue can be resolved by a -1 frameshift which brings a UAG stop codon into frame possibly caused by the action of the mt-LSU component ICT1 (Temperley et al., 2010a, Temperley et al., 2010b). Recent data suggests that ICT1 behaves like a release factor as it is capable of hydrolysing peptidyl-tRNA on stalled ribosomes (Feaga et al., 2016). However, contradictory data suggests ICT1 may not be directly involved in termination of translation of these transcripts (Chrzanowska-Lightowlers and Lightowlers, 2015). Finally, the release factors, mtRF1, mtRRF and mtEFG2 catalyse the release of the mRNA and the deacetylated tRNA, and the dissociation of the ribosome, making the translation apparatus available for reuse. The hydrolysis of GTP then catalyses dissociation of the release factors (Bhargava et al., 2004).

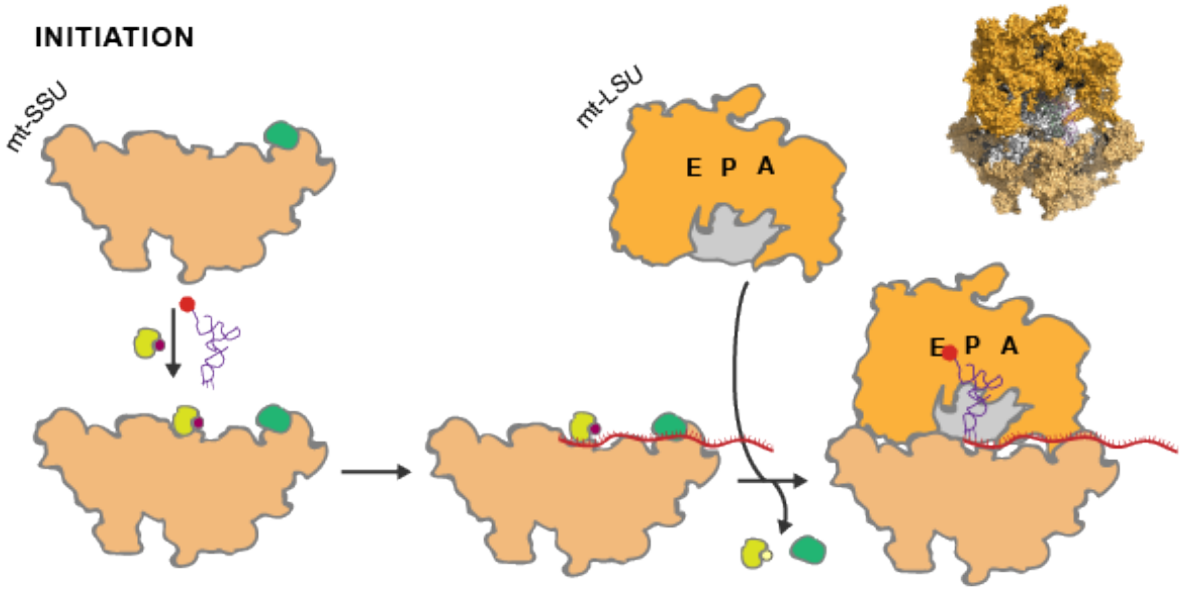
INITIATION
mt-SSU
mt-LSU
E P A
E P A

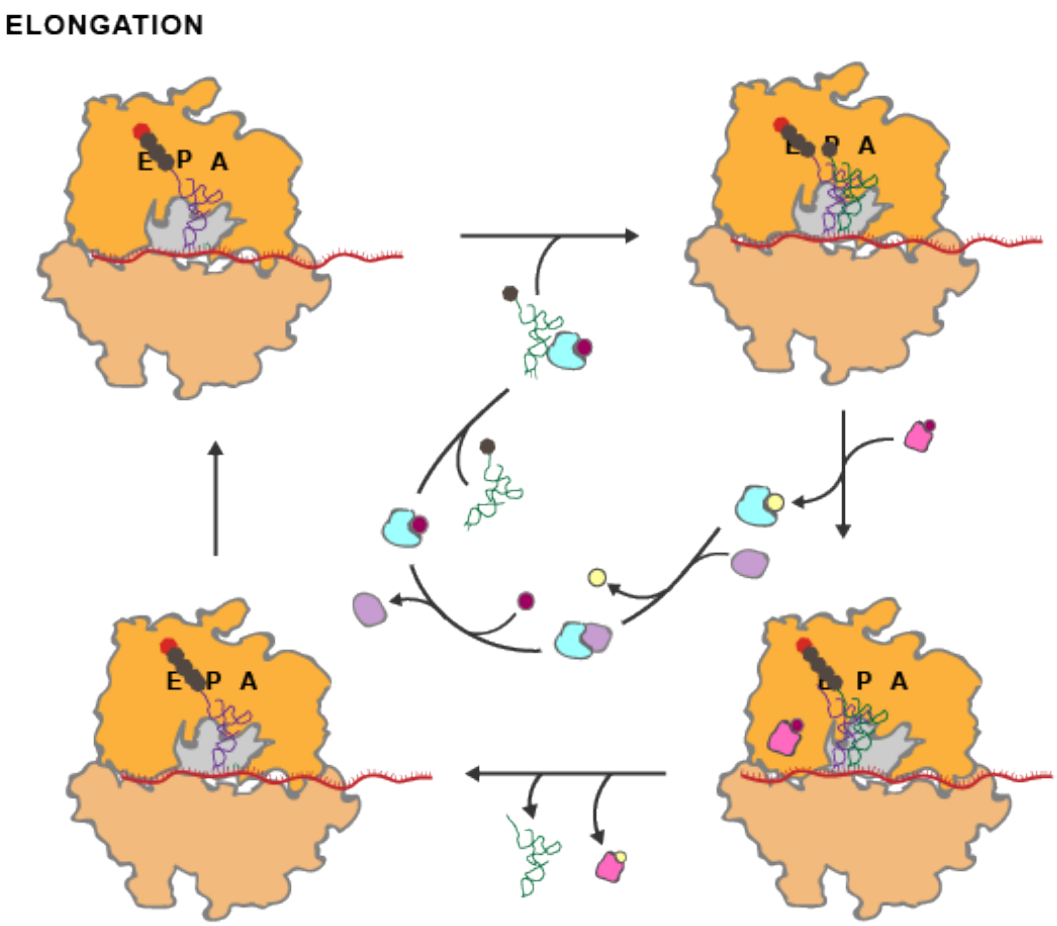
ELONGATION
E P A
E P A
E P A
E P A

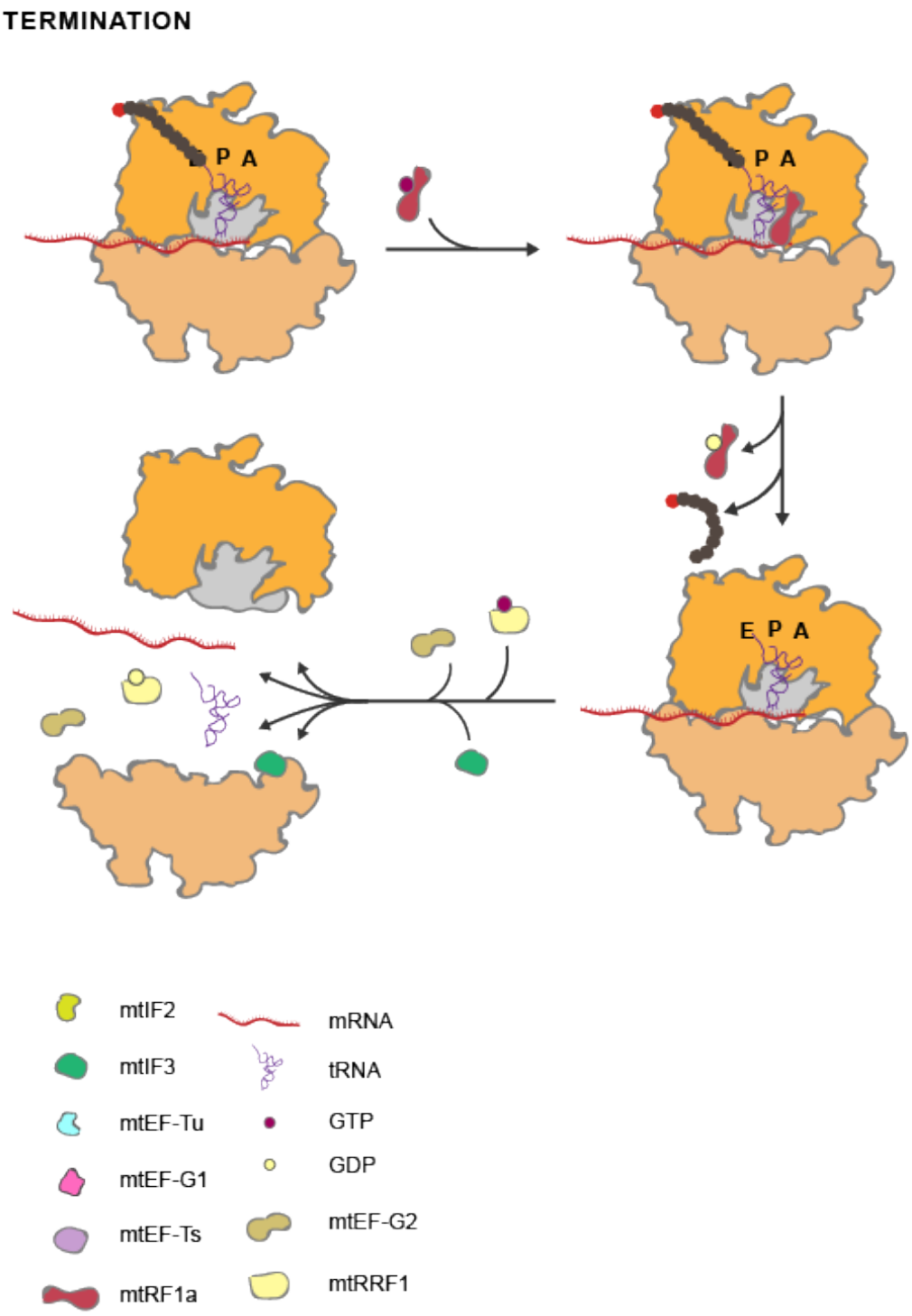

Figure 1.5 Schematic diagram of mitochondrial protein synthesis consisting of three phases of initiation, elongation and termination. The key indicates the identity of the factors and RNAs involved. Hydrolysis of GTP is indicated by a change of colour from purple to yellow. GTPases are shown attached to GTP. The formylmethionine amino acid starting the polypeptide chain is shown in red. The large subunit is shown in orange and the small subunit is shown in light orange. The structure of the mammalian mitoribosome is shown for reference at the top right (PDB: 5AJ4)

1.8 Mitochondrial ribosome

The mammalian mitoribosome is a large ribonucleoprotein complex required for translation of the 13 polypeptides encoded in the mitochondrial genome. It consists of a large 39S (mt-LSU) and a small 28S (mt-SSU) subunit. The large subunit, the site of the peptidyl transferase activity, is a ribonucleoprotein complex containing a catalytic 16S RNA component, encased in approximately 50 protein components and an additional tRNA component. The small subunit, the site of mRNA binding and decoding, contains a smaller 12S catalytic RNA component encapsulated by 30 protein components.

1.8.1 Specialisation of the mitochondrial ribosome

1.8.1.1 Architecture of the mitochondrial ribosome

Despite evolving from a eubacterial ancestor, the mammalian mitoribosome is unique in structure and composition from its bacterial, yeast mitochondrial and cytoplasmic equivalents. This is seen in the mammalian mitoribosomes' substantially lower sedimentation coefficient. While the bacterial, yeast mitochondrial and cytoplasmic ribosomes sediment with a coefficient of 70S, 74S and 80S respectively, the mammalian mitoribosome sediments at a coefficient of 55S (figure 1.6). The yeast mitoribosome contains a larger 37S mt-SSU with a 15S rRNA component and 38 mitochondrial ribosomal proteins (MRPs), and a larger 54S mt-LSU consisting of a 21S rRNA and 46 MRPs (Smits et al., 2007; Herrmann et al., 2012). In yeast, 12 SSU MRPs (MRPSs) and 16 LSU MRPs (MRPLs) are specific to the mitoribosome and not homologous to bacterial ribosomal proteins (Smits et al., 2007; Amunts et al., 2014). Similarly, the mammalian mitoribosome has substantially smaller rRNA components, and 14 MRPSs and 22 MRPLs that do not have homologs in bacteria. These proteins are generally found attached at the periphery of the complex while the core of the complex is highly conserved (figure 1.7) (Sharma et al., 2003; Greber et al., 2014; Brown et al., 2014; Greber et al., 2014; Kaushal et al., 2014).

Figure 1.6 Overview of the protein and RNA composition of the ribosomes in bacteria, the eukaryotic cytosol, human mitochondria and yeast mitochondria. Pink, LSU rRNA; blue, SSU rRNA; maroon, LSU; green, SSU. The number of protein components of the SSUs and LSUs is indicated in the circles. Data was acquired from Greber and Ban (2016).

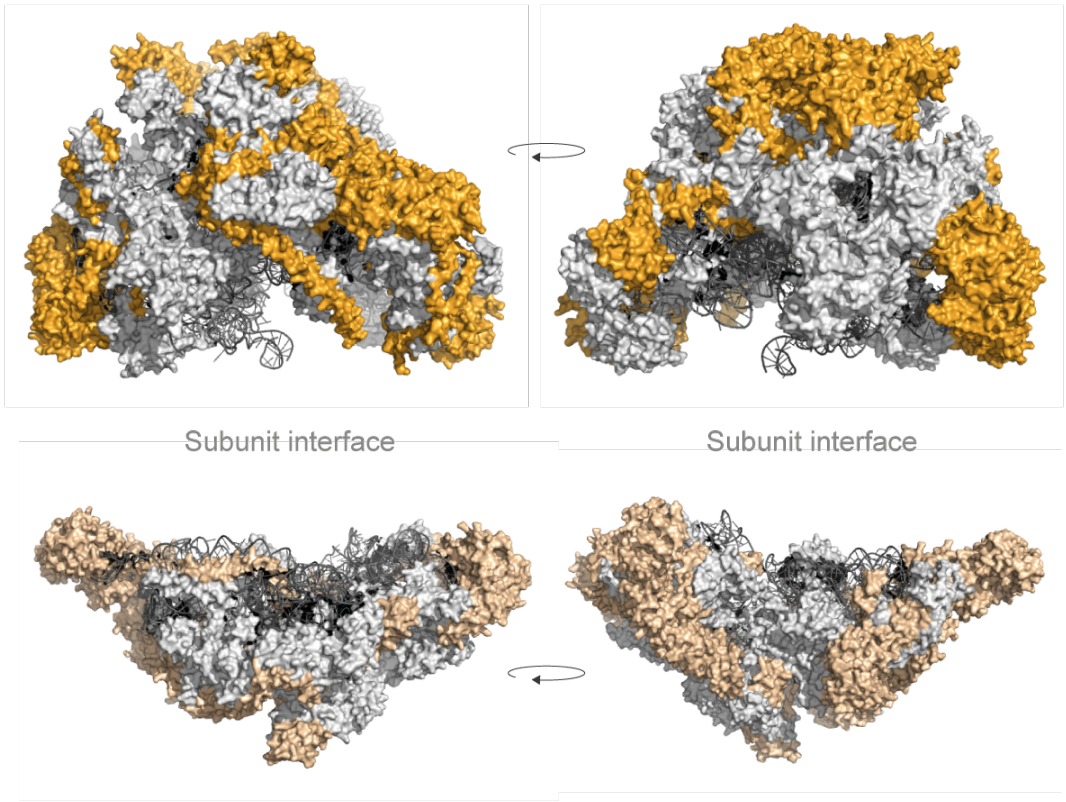

Figure 1.7 Mammalian mitochondria-specific components. Protein components of the LSU (above, orange) and the SSU (below, wheat) that do not have bacterial homologs have been coloured (PDB: 5AJ4)

1.8.1.2 Replacement of rRNA domains in the mitoribosome with protein components

This diminution of the mitoribosome is a consequence of the reductive evolution of the mitochondrial genome. In particular, this is seen in the halving of the core RNA component of the mitoribosome. To compensate for this, the mitoribosome has undergone extensive remodelling. New protein subunits and protein-mediated interactions have been recruited to replace the lost functional domains. For example, the bacterial ribosome contains various zinc-binding proteins that coordinate a zinc ion to stabilize the quaternary interactions and architecture of the complex, such as bS18. In the mitoribosome, the abundance of these motifs is increased. Mitochondria-specific MRPs such as MRPS18b (bS18m), MRPL10 (uL10m), MRPS6 (bS6m), MRPS16 (bS16m) and MRPS25 (mS25) all contain zinc-binding residues that coordinate three zinc ions between them (Greber and Ban, 2016). Moreover, various RNA-RNA bridges have also been substituted with RNA-protein or protein-protein interactions. For example, in bacteria, the uL24 subunit interacts with domain I of

23S rRNA. However, this lost domain in the mitoribosome is replaced by the protein-protein interactions between the mL45 and uL29m subunits (Sharma et al., 2003; Amunts et al., 2014).

1.8.1.3 A structural tRNA in the mammalian mitochondrial ribosome

In all three domains of life, the mt-LSU contains a second smaller 5S rRNA component in the central protuberance (Magalhaes et al., 1998; Smirnov et al., 2011). This 5S rRNA acts as a scaffold connecting the large subunit to the small subunit and the tRNAs in the intersubunit space (Yusupov et al., 2001). However, recently, cryo-EM structures of the human and porcine mitoribosome identified that, in mammals, this moiety has been replaced (Amunts et al., 2015; Greber et al., 2015). In the absence of an RNA import mechanism, the mitoribosome has incorporated a tRNA in its place. Interestingly, further studies identified this component to be either tRNA-Val or tRNA-Phe depending on the species or context. It was shown that the incorporated tRNA is a tRNA-Val in human and rat tissues, and tRNA-Phe in porcine and bovine tissues. Moreover, when the steady state levels of tRNA-Val are reduced in human tissues, the mitoribosomes incorporate tRNA-Phe in its place to produce functional ribosomes (Rorbach et al., 2016). These tRNAs are encoded proximal to the rRNAs in the genome and transcribed concurrently with the rRNAs. This allows for a stoichiometric expression of the tRNAs and the rRNAs, and co-transcriptional maturation and assembly into the mitoribosome.

The mitoribosome has also evolved synchronously with the mt-tRNAs. In the mitochondria, the D and T-stems of the mt-tRNAs show a high level of variability. To accommodate this, the mitochondria has lost the ribosomal structures that interact with these regions on the tRNAs. For example, the A-site finger (consisting of uL25m and rRNA helix H38), and uL5m and the H48 helix in the P-site are absent. Therefore, the mitoribosome has evolved a P-site finger structure protruding from the central protruberance connecting the A and P site tRNAs and compensating for the absence of the A-site finger. The tRNAs in the P site bind more strongly with the P-site finger via their T-loop, than in the bacterial P-site. Conversely, the mitoribosome has retained regions that bind to conserved sections of the tRNAs. This includes regions involved in the interactions with the 3' CCA, the anticodon loop, the mRNA decoding region and the peptidyl transferase centre (Greber et al., 2014; Greber et al., 2015; Amunts et al., 2015).

The mitoribosome has also recruited a GTPase, MRPS29 (mS29) in the mt-SSU that sits in the interface between the two subunits. Here, the protein may use its GTPase activity to facilitate intersubunit bridge formation (Suzuki et al., 2001). However, this has not been proven experimentally.

1.8.1.4 Adaptation in the mRNA channel in the mitoribosome

Mitochondrial transcripts also differ from their bacterial and cytoplasmic counterparts by not having a 5' UTR with a Shine-Dalgarno sequence or a 5' cap. In the cases where there are overlapping genes, the second protein could be considered to have a long untranslated region. These motifs help the ribosome identify the start codon for translation. However, in the mitoribosome, the ORF can begin directly at the 5' end. This means that the start codon needs to be identified by the mt-SSU or other initiation factors (Herrmann et al., 2013). To facilitate the entry of the mRNA into the ribosome, the site of entry of the mRNA has been remodelled (figure 1.8). Bacterial ribosomal component uS4 and an mRNA helicase domain of uS3 have been lost (Amunts et al., 2015). Instead, mitochondrial uS5m has an extension which forms a 'latch' across the mRNA channel and PPR-domain containing MRP, mS39 is positioned close to this entry site (Amunts et al., 2015; Greber et al., 2015). Whether the RNA-binding properties of the PPR domain is recruited for mRNA threading is yet to be elucidated. However, depletion of mS39 leads to a defect in translation (Davies et al., 2009).

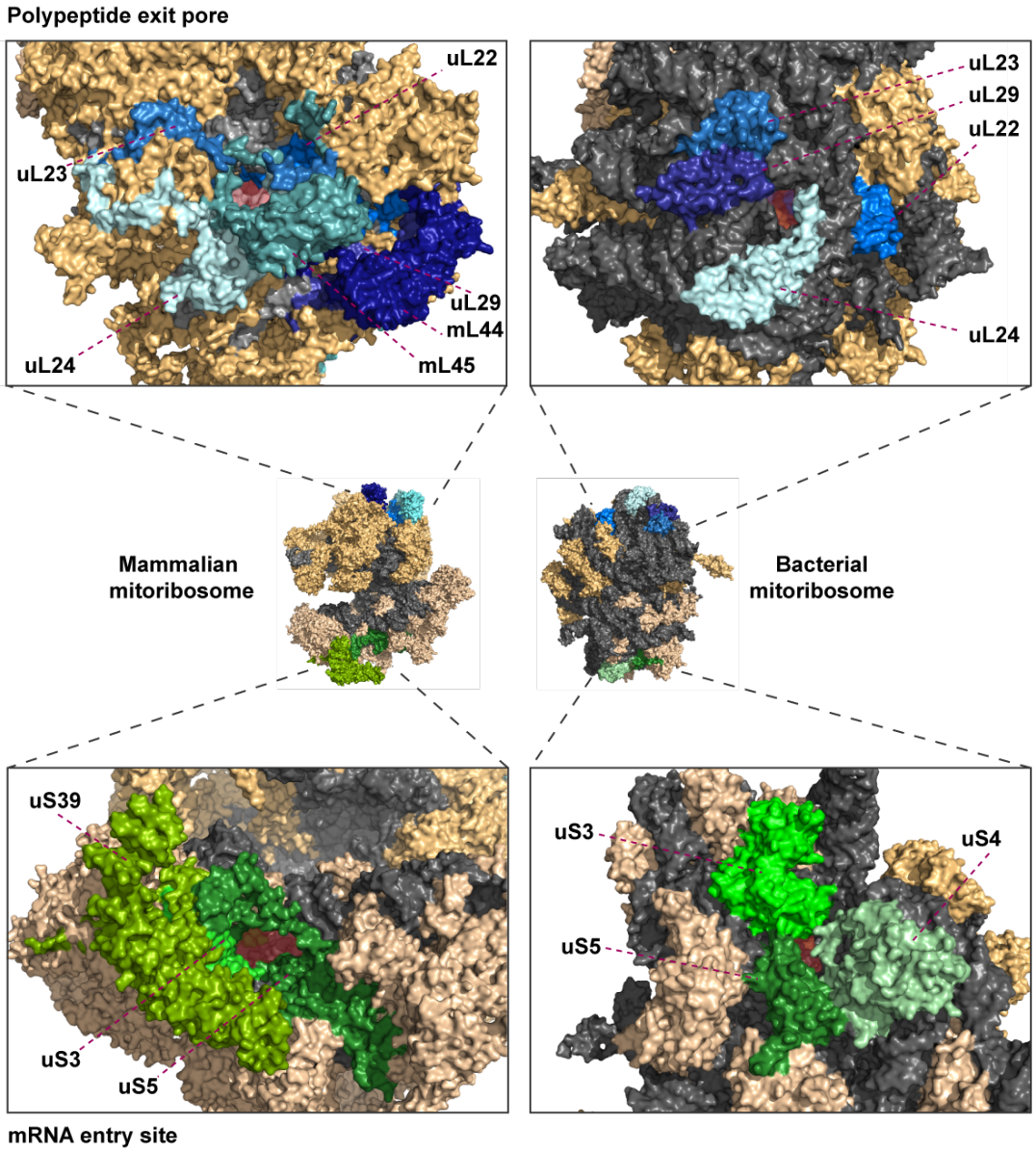

Figure 1.8 Changes to the polypeptide exit pore and mRNA entry site. (Above) Ribosomal proteins surrounding the polypeptide exit site are shown in shades of blue. Two additional components have been recruited in the mitoribosome including mL45 which assists in ribosome-membrane association (figure 1.9). (Below) Ribosomal proteins surrounding the mRNA entry site have been coloured in shades of green. No mitochondria-specific proteins have been recruited at the site. However, substantial changes have occurred in the orientation and the size of the proteins surrounding the mRNA entry site (Bacterial ribosome, PDB: 4V4Q; Mammalian mitoribosome, PDB: 3J9M).

1.8.1.5 Adaptations in the exit tunnel in the mitoribosome

Unlike other ribosomes, the mammalian mitoribosome specifically caters to the production of the 13 polypeptides encoded in the mammalian mitochondrial genome. All these proteins are highly hydrophobic and form components of the membrane-spanning respiratory complexes. Since the biochemical properties of all the polypeptides are similarly hydrophobic, the exit tunnel of the mitoribosome is lined with hydrophobic residues (especially from MRPL22(uL22m)) to regulate the efficiency of exit of the newly synthesized polypeptide from the mitoribosome (Brown et al., 2014).

Moreover, the mitoribosome assists with co-translational assembly of the proteins by associating with the membrane and feeding the newly synthesised polypeptides into the inner membrane (Liu et al., 2000; Ott et al., 2006; Pfeffer et al., 2015). Biochemical studies have shown that a significant proportion of the mitochondrial ribosome is found associated to the inner membrane via electrostatic interactions between the membrane, membrane-bound proteins and MRPs (Liu and Spremulli, 2000). One of the proteins identified that perform this function is OXA1L which controls the insertion of proteins into the inner membrane (Hennon et al., 2015). The c-terminus of mitochondrial OXA1L binds to MRPL13 (uL13m), MRPL20 (bL20m), MRPL28 (uL28m), MRPL48 (mL48), MRPL49 (mL49) and MRPL51 (mL51) (Haque et al., 2010). However, these MRPs are not located near the polypeptide exit site. In addition, similar to OXA1L, LetM1 was also identified as a protein that interacts with the mitoribosome (via MRPL36 (bL36m)) and has yeast homologs that facilitate mitoribosome-inner membrane anchoring (Piao et al., 2009).

Compared to the bacterial ribosome, in yeast mitoribosomes, the newly synthesised polypeptides take a new path to the exit site. This new exit site is surrounded by bacterial bL33, and mitochondria-specific MRPs, MRPL44 (mL44) and MRPL50 (mL50). These two MRPs form a protuberance that extends out towards the inner membrane and may facilitate interactions with the membrane (Greber et al., 2014; Brown et al., 2014). Cryo-EM tomography showed that, in yeast, the Mba1 protein spatially orientates the translation machinery to the inner membrane with the insertion machinery (Pfeffer et al., 2015). In the mammalian mitoribosome, a homolog of Mba1, MRPL45 (mL45) binds to the ribosome at the exit tunnel and has been proposed to perform the same function as Mba1 (figure 1.9) (Greber et al., 2014).

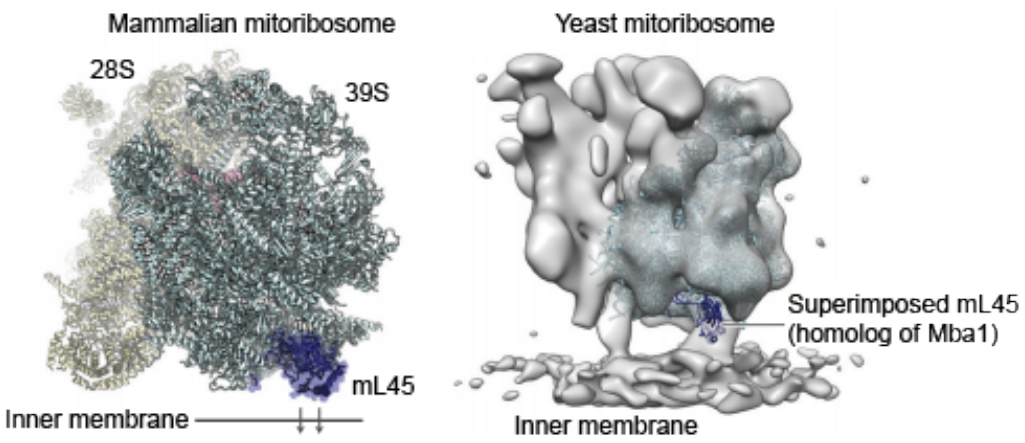

Figure 1.9. Hypothetical membrane association of the mt-LSU via mL45 (yeast homolog of Mba1). (Left) MRPL45 (Dark blue) is located adjacent to the polypeptide exit tunnel in the mammalian mitoribosome. Cyan, mitoribosome; yellow, small subunit; dark blue, MRPL45. (Right) MRPL45 superimposed onto Mba1, yeast homolog of MRPL45 which mediates interaction with the inner membrane. Cyan, large subunit; yellow, small subunit. Cryo-EM tomographic reconstruction (grey surface) of the yeast mitoribosome (EMD identification number 2826). Cyan, yeast mt-LSU structure; PDB: 3J6B; Figure adapted from Greber and Ban (2016)

1.8.2 Ribosomal biogenesis in bacteria

Assembly of the bacterial ribosome has been well characterised. Since the mitoribosome is derived from a common eubacterial ancestor, the steps in the biogenesis of the bacterial ribosome may inform the biogenesis of the mitoribosome.

The *E. coli* ribosomal RNAs are transcribed on one polycistronic transcript. They are released by the action of five nucleases. From this primary transcript, RNase III produces a 16S rRNA precursor (17S rRNA), 23S rRNA precursor and a 5S rRNA precursor (9S rRNA) (Dunn and Studier, 1973; Nikolaev et al., 1973; Ginsburg and Steitz, 1975). The 17S rRNA is further matured by RNase E and RNase G (Li et al., 1999a). The maturation of the 5' and 3' end of the 16S is finally completed through the removal of transcribed spacer regions by endoribonuclease YbeY (Davies et al., 2010). Similarly, YbeY also facilitates the 5' end maturation of the 23S (Davies et al., 2010). RNase T, then performs the final maturation of 23S rRNA (Li et al., 1999b). RNase T and RNase E, along with YbeY complete the maturation of the 5S rRNA (Figure 1.10) (Misra and Apirion, 1978).

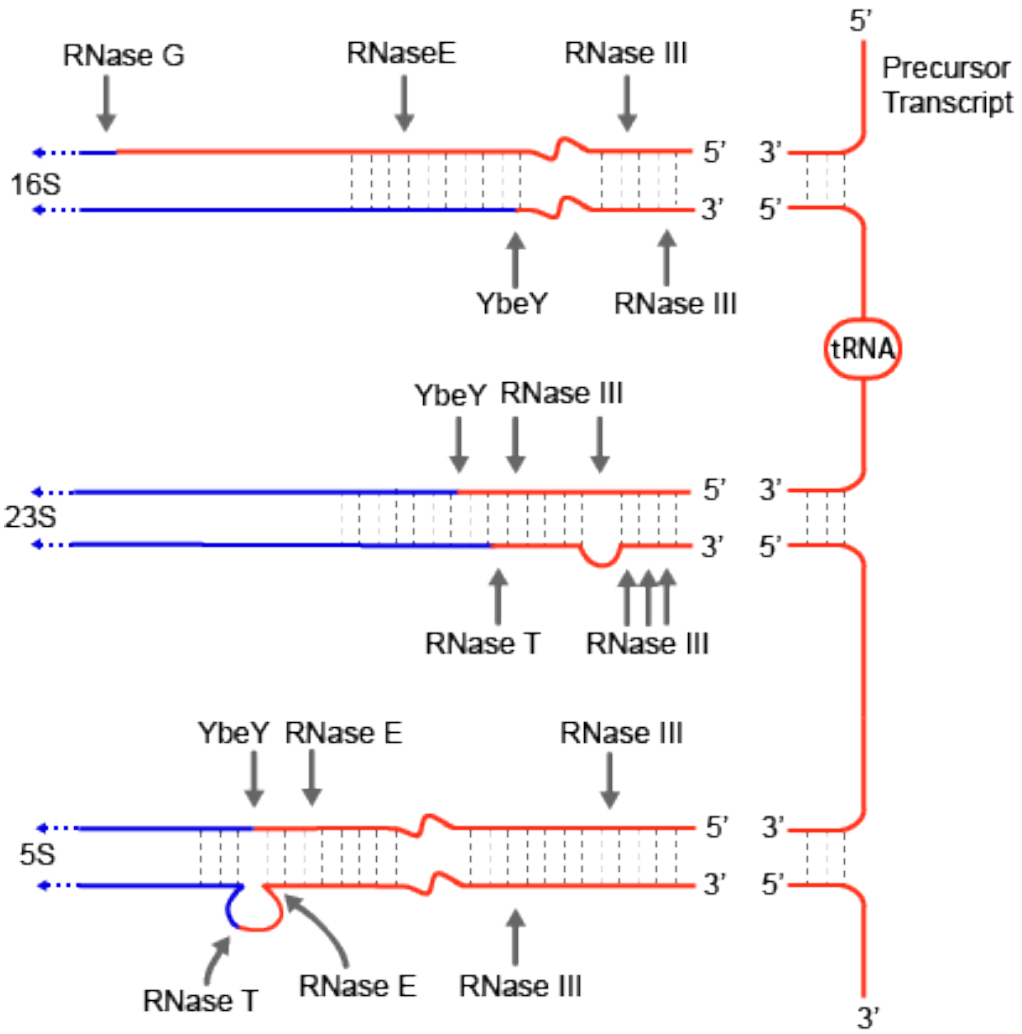

Figure 1.10 Maturation of precursor bacterial rRNA showing nuclease endonuclease activity of RNase G, RNase E, RNase III, YbeY and RNase T. Blue lines indicate the rRNA regions. Red lines indicate non-ribosomal RNA sequences in the precursor. Adapted from Shajani et al. (2011)

Following this, the 16S rRNA undergoes 11 chemical modifications including one pseudouridylation and 10 methylations, and the 23S rRNA undergoes 25 chemical modifications (1 unknown, 14 methylations, 9 pseudouridylations and 1 methylated pseudouridylation) (Kaczanowska and Ryden-Aulin, 2007; Chow et al., 2007; Decatur and Fournier, 2002). Interestingly, the modified 16S rRNA can be assembled *in vitro* to produce a catalytically active ribosome. But, this is not the case for modified 23S rRNA (Krzyzosiak et al., 1987; Green and Noller, 1999)

Numerous *in vitro* assembly experiments with individually purified proteins (Mizushima and Nomura, 1970; Held et al., 1973), recombinant ribosomal proteins (Culver and Noller, 1999; Culver and Noller, 2000) and in vitro transcribed 16S

rRNA (Krzyzosiak et al., 1987) identified that the assembly of the bacterial ribosome happens in a hierarchical and parallel manner. The 30S small subunit (with 16S rRNA) can be divided into three domains, namely the 5' body, the central platform region and the 3' head. First, primary proteins (uS4, uS7, uS8, uS15, uS17, bS20) bind the 16S rRNA, which drives conformational changes on the RNA. This causes more secondary and then, tertiary components to assemble onto the ribosome (Traub et al., 1968; Held et al., 1973; Sieber et al., 1978; Stern et al., 1989). The bS16 and bS18 were shown to be required for assembly but not function (Held and Nomura, 1975). However, further studies identified that ribosome assembly can occur through multiple different parallel pathways leading to a heterogenous population of assembly intermediates (Adilakshmi et al., 2008; Talkington et al., 2005; Mulder et al., 2010; Bubunenko et al., 2006; Sykes et al., 2010). This is confirmed by the observation that the assembly of a primary 23S component uS15 can be circumvented by alternate assembly pathways, suggesting that there may not be one definitive assembly pathway (Bubunenko et al., 2006).

Different components of the bacterial ribosome are dispensable for assembly. This includes uL9, uL15, bL21, uL24, bL27, uL29, uL30, bL34, uS9, and uS17. However, it is suggested that they are necessary for accurate and efficient translation (Shoji et al., 2011). Furthermore, *in vivo* SILAC labelling, sucrose gradient fractionation and mass spectrometric analysis, and aptamer-based RNA-tagging and affinity purification, have been used to identify assembly intermediates and their composition (Li et al., 2013; Sashital et al., 2014; Gupta and Culver, 2014). These methods have also identified that bacterial SSU assembly occur through various different pathways that happen concurrently in the cell.

The 50S large subunit was also reconstituted *in vitro* under non-physiological conditions. This identified three intermediates - 33S (23S rRNA + 22 proteins), 41-43S (induced by change in temperature and ionic conditions) and 48S (+11 proteins). The conversion from one intermediate stage to another relied on the addition of certain specific ribosomal proteins, changes to temperature and ionic conditions. For example, the maturation of the 33S to the 41-43S intermediate require the addition of uL4, uL13, bL20, uL22, uL24 and 23S rRNA (Spillman et al., 1977).

Earlier *in vivo* analysis of ribosomal intermediates identified 32S (23S rRNA + 16 proteins), 43S (+8 proteins) and immature 50S (+6 proteins) intermediates. Analysis of the assembly pathways of the LSU showed that functionally important domains like

the tRNA-binding sites remain immature until the final stages of assembly. This is probably to prevent the ribosome from beginning protein synthesis with an immature ribosome. More recent investigations identified two 45S intermediates that differ only in their interaction with 5S rRNA. The final maturation step of these 45S intermediates is the assembly of the central protuberance (Li et al., 2013; Jomaa et al., 2014).

1.8.3 Mitoribosomal biogenesis in yeast

In *S. cerevisiae*, the mitochondrial genome encodes 8 polypeptides, 7 of which are components of the respiratory complex, and one is a component of the mtSSU (Var1). The genome is transcribed as polycistronic molecules from 11 promoters, containing intronic regions. Very little is known about the stages of and factors involved in the biogenesis of the yeast mitoribosome. All the precursors contain 5' and 3' extension which require further processing. This is carried out by RNase P (encoded by RPMI) and tRNase Z (encoded by TRZ1) activity (Morales et al, 1992; Chen et al., 1988). The mt-LSU 21S rRNA precursor contains a 1.2 kb intronic region and a 3' extension that requires SUV3 to be processed (Stepien et al., 1995). The mt-SSU 15.5S rRNA precursor also contains a 5' extension and a tRNA-Trp. However, the mechanism of processing of this precursor is still unclear (Osinga et al., 1981). The assembly of the large subunit (54S) occurs at the inner membrane. Here, a pre-54S intermediate is proteolytically matured by YtA10/Yta12 with the final incorporation of MRPL32 (bL32m) (Nolden et al., 2005; Kaur and Stuart, 2011).

1.8.4 Mitoribosomal biogenesis in mammals

The assembly pathway of the mammalian mitoribosome is still mostly unknown. The maturation of the rRNA involves ten conserved chemical modifications of the rRNA. The mt-SSU is methylated at positions 429, 839, 841, 936 and 937. The mt-LSU is methylated at positions 947, 1145, 1369 and 1370, and pseudouridylated at position 1397. The enzymes involved in introducing these modifications and the function of these modifications are further elaborated in section 3.1.1.

The assembly of the RNA and proteins components of the mitoribosome into a functional ribosome involves a combination of spontaneous interactions and folding, and the assistance of additional ribosome assembly factors. These include GTPases and ATP-dependent RNA helicases which force the conformation of the assembling

ribonucleoparticle in a specific direction. Four GTPases have been identified as factors that associate with the mitoribosome during biogenesis. These include mitochondrial GTPBP7, MTG2/ObgH1 and C4ORF14, which are found in yeast and humans, and mitochondria-specific ERAL1.

1.8.4.1 GTPases

MTG1 (or GTPBP7) is a conserved protein related to bacterial RbgA. In bacteria, RbgA assists in the assembly and maturation of the large subunit. It associates with the immature LSU, connecting the helix 38 and the central protuberance, and only dissociates after it hydrolyses GTP, after the assembly of a 50S LSU. Depletion of RbgA causes an accumulation of an immature 50S assembly intermediate and leads to the inhibition of cell growth (Matsuo et al, 2006; Achila et al., 2012; Matsuo et al., 2007; Uicker et al, 2006). In yeast, loss of mtg1 leads to a reduction in mt-LSU 21S rRNA levels and severe translation defect (Kotani et al., 2013). This phenotype can be partially rescued with human MTG1, suggesting a conservation of function. In humans, the equivalent of helix 38 is not present and therefore, the mechanism of MTG1 action is not clear (Barrientos et al., 2003).

MTG2/ ObgH1 (or GTPBP5) is related to bacterial ObgE. In *E. coli*, ObgE binds to both the SSU and the LSU. Lack of ObgE causes an impairment of 70S ribosome assembly, leading to the accumulation of free subunits and the accumulation of immature 50S assembly intermediates (Sato et al., 2005). Sucrose gradient sedimentation of Mtg2 in yeast showed that it interacts with the mt-LSU and can be used to alleviate the symptoms of mrm2 depletion. This suggest that, in yeast, mtg2 may perform its role ahead of mrm2 modification. Since, both these proteins are conserved in the mammalian mitoribosome, it is possible that their role and order of activity in the maturation of the mitoribosome may be conserved. Both MTG1 and MTG2/ObgH1 are found associated with the mt-LSU at the inner membrane, and require their GTPase activity to facilitate this interaction, suggesting a membrane-associated maturation of the mt-LSU. However, a knockdown of MTG2/ObgH1 did not lead to a defect in mt-LSU assembly (Kotani et al., 2013). Therefore, the exact role of these factors in mitoribosomal biogenesis remains unclear.

C4ORF14 (MTG3 or NOA1) is a member of the YqeH protein family. In bacteria, YqeH binds to the SSU, depending on the GTP:GDP ratio, and facilitates the assembly of the small subunit, and thus the 70S ribosome (Anand et al., 2010). It does

this by controlling the maturation of the 15S rRNA. Depletion of Mtg3 also leads to the accumulation of misprocessed 15S precursors in yeast mitochondria (Paul et al., 2012). Sucrose gradient sedimentation analysis showed that in humans, C4ORF14 binds to the small subunit (Al-Furoukh et al., 2013). However, knockdown of human C4ORF14 leads to misassembly of the mt-LSU and a translational defect (He et al., 2012; Kolanczyk et al., 2011). Furthermore, overexpression of the GTPase leads to increased oxidative phosphorylation and ATP production in a GTP-dependent manner (Heidler et al., 2011). Similar to other GTPase involved in mitoribosomal biogenesis, the hydrolysis of GTP is required for its dissociation from the mt-SSU. Moreover, it is found associated with the mitochondrial nucleoid, suggesting the mt-SSU assembly may occur at this site (He et al., 2012).

ERAL1 is a mitochondrial GTPase with RNA-binding properties. It is a homolog of Era in *E. coli*, which binds to a 3' stem-loop structure (helix 45) of the 16S SSU rRNA and is required for ribosomal assembly (Sharma et al., 2005). In bacteria, this highly conserved 3' helix binds to the Shine-Dalgarno sequence. In humans, the anti-Shine Dalgarno sequence and helix is lost. Instead, ERAL1 binds to a different 33-nucleotide 3' terminal stem-loop of the mt-SSU 12S rRNA. This region contains the two adenine residues dimethylated by TFB1M. Furthermore, these modifications may be necessary for ERAL1 binding and SSU maturation, as knockout of TFB1M leads to a similar phenotype as ERAL1 depletion (Uchiumi et al., 2010). Patients with defective ERAL1 show compromised 28S SSU assembly and lower steady state levels of 12S rRNA, leading to a translation defect (Dennerlein et al., 2010; Chatzipyrou et al., 2017).

Investigation of protein interactors of ERAL1 identified mitoribosomal proteins, transcription factor A, TFAM, which is required for nucleoid formation, and mitochondrial ribosome recycling factor, mtRRF (Dennerlein et al., 2010; Uchiumi et al., 2010). Moreover, the removal of ERAL1 and the subsequent targeted degradation of ERAL1 is required for the control of 28S SSU assembly. In the absence of this degradation pathway, ERAL1 is accumulated and strongly associates with the assembling subunit preventing maturation (Szczepanowska et al., 2016).

1.8.4.2 RNA helicases involved in mitoribosome biogenesis

RNA helicases bind and unwind RNA and ribonucleoprotein complexes using NTP hydrolysis. They contain a helicase core domain that binds RNA and external domains that confer specificity. A common group of ribosomal RNA helicases fall in the DEAD box family of helicases, recognised by a common Asp-Glu-Ala-Asp motif. The helicase core in these proteins contains two domains connected by a linker. When these two domains come together, they form a cleft which hold the RNA and ATP at either end. Helicase activity is linked to ATP hydrolysis. In many cases, substrate specificity may be specified by additional co-factors that bind to the helicase (Linder et al., 2011; Cordin et al., 2006; Fairman-Wiliams et al., 2010; Young et al., 2013).

Members of the DExD/H-box ATP-dependent RNA helicase family participate in a large number of RNA metabolism pathways. In *E. coli*, four out of the five identified DExD/H-ATPases play a role in ribosome biogenesis, RNA degradation or translation (Kaberdin et al., 2013). The RhlE helicase activity is required at early stages of ribosome assembly to direct rRNA folding (Nierhaus, 1991). After this, SrmB leads the maturation of the 23S intermediate to the 32S intermediate of 50S LSU maturation. Then, the DeaD/CsdA helicases direct the late stage assembly stage. Loss of DeaD/CsdA and SrmB leads to an accumulation of a 40S assembly intermediates and reduction in ribosome biogenesis (Peil et al., 2008; Charallais et al., 2003). DbpA is another DEAD box ATP-dependent helicase that is specifically activated by interaction with helix 92 of the 23S SSU rRNA. Knockout of the protein does not affect ribosome biogenesis. However, an accumulation of 45S assembly intermediates, lacking key proteins near the peptidyl transferase centre, can be induced through the expression of a dominant negative mutant (Fuller-Pace et al., 1993; Diges et al., 2001; Sharpe Elles et al., 2009).

Mitoribosome assembly has recruited a different set of helicases to control biogenesis. In yeast mitochondria, helicase Mrh4 was identified as essential for mt-LSU biogenesis. In the presence of a catalytically inactive Mrh4, mt-LSU is halted, causing an accumulation of a pre-54S particle lacking MRPs, MRPL9(bL9m), MRPL16(uL16m), MRPL33(bL33m), similar to the *dbpa* dominant mutant in *E. coli*. Sucrose gradient experiments show that Mrh4 co-sediments with the pre-54S particle. This assembly intermediate contains a fully matured 21S rRNA, suggesting that Mrh4 activity occurs later in the assembly pathway. This is further corroborated by the interaction of Mrh4 with 21S mt-LSU rRNA, subassemblies of the mitoribosome and

the fully-assembled ribosome (De Silva et al., 2013). Interestingly, the MTG1 and MTG2 GTPases also co-sediment with the pre-54S particle (De Silva et al., 2013). This indicated that they may function earlier in the assembly of the mt-LSU. In mammals, Mrh4 is closely related to helicase DDX28, an RNA-sensitive ATPase, which dually localises to the mitochondria and the nucleolus (Valgardsdottir et al., 2001; Valgardsdottir et al., 2003). Similar to Mrh4, DDX28 interacts with 16S mt-LSU rRNA and the mt-LSU. Knockdown of the protein leads to a decrease in steady state level of 16S rRNA and mt-LSU MRPs, mtLSU assembly and consequently, protein synthesis. However, loss of DDX28 does not have any effects on mRNA stability and 16S rRNA processing or modification. This suggests that DDX28 functions at an earlier stage of mt-LSU assembly, but after 16S processing (Tu and Barrientos, 2015)

DHX30 was recently identified as another mtLSU assembly factor. Knockdown of the protein leads to an absence of assembled ribosomes, which results in a severe inhibition of protein synthesis. It was shown to interact with mt-LSU, mt-SSU and monosome, suggesting that it plays a role in all stages of assembly. Intriguingly, DDX38 and DHX30 are both found in RNA granules (see section 1.9). This suggests that they act on the nascent transcript and have an early influence on mitoribosome biogenesis (Antonicka and Shoubridge, 2015).

1.8.4.3 Additional factors in mitoribosomal biogenesis

MTERF3 (MTERFD1) and MTERF4 are members of a family of mitochondrial transcription termination factors that have been implicated in mitoribosomal biogenesis. A depletion of MTERF3 not only causes an activation repression of mitochondrial transcription, but also leads to instability of the mt-LSU (Wrendenberg et al., 2013). MTERF4, on the other hand, functions in combination with a methyltransferase, NSUN4 (Camara et al., 2011). NSUN4 can modify the 12S rRNA independent of MTERF4 interactions. However, it requires MTERF4 to facilitate monosome formation (Spahr et al., 2102; Metodiev et al., 2014).

Recently, NGRN, a highly conserved protein with a Pfam domain was localised to the mitochondria. The protein was shown to bind to 16S mt-LSU rRNA and its precursor but not 12S mt-SSU rRNA. In addition, depletion of the protein leads to a reduction of MRPs and a deficiency in translation. This suggests that NGRN may play a role in the early stages of mitoribosome biogenesis. Analysis of the interactome of NGRN

identified WBSCR16, FASTKD2 (see below) and pseudouridine synthases, RPUSD3, RPUSD4 (see section 3.1.1) and TRUB2, which were required for 16S rRNA stability and mitochondrial translation (Arroyo et al., 2016).

MALSU1 (or C7orf30) is another mitoribosome biogenesis factor that specifically associates with the large subunit through uL14 (Rorbach et al., 2012, Fung et al., 2013, Wanschers et al., 2012). Sucrose gradient analysis identified that MALSU interacts with the free 39S subunit and not with the assembled ribosome. Furthermore, depletion of MALSU inhibits assembly of the mt-LSU which leads to a translation phenotype and respiratory incompetence (Rorbach et al., 2012; Wanschers et al., 2012). As a member of the DUF143 family of nucleotidyltransferases, MALSU1, similar to other members of the family, may facilitate the interaction of various subunits of larger complexes. As such, in the mitoribosome, MALSU1 may inhibit assembly of the immature assembly intermediate into a monosome until it is properly matured (Rorbach et al., 2012). Recently, a cryo-EM structural analysis of the human mitoribosomal large subunit identified two assembly factors L0R8F8 and mt-ACP which associate with MALSU forming a 65 Å module in the subunit interphase and possibly preventing the premature subunit from forming a monosome. L0R8F8 is a eukaryote-specific protein that is synthesized from an alternate open reading frame in a bicistronic transcript that encodes a outer mitochondrial membrane transmembrane protein, MID51. Mt-ACP a protein that acts as a scaffold in fatty-acid synthesis. However, in mt-LSU biogenesis, they together interact with MALSU sterically blocking association of the mitoribosomal subunits (Brown et al., 2017).

FASTKD2 is a mitochondrially-targeted RNA-binding protein. iCLIP analysis of RNA targets of the protein identified the 16S mt-LSU rRNA and NADH dehydrogenase (Complex I) subunit 6 (ND6) mRNA. Depletion of the protein led to the accumulation of precursors of these transcripts. In addition, loss of the protein leads to instability of the mt-LSU and the monosome, and a respiratory defect (Antonicka and Shoubridge, 2015; Popow et al., 2015). However, the mechanism of action of the protein is still unknown. Another member of the FATK family, FASTKD3, has been recently shown to selectively regulate CO1 translation without affecting CO1 mRNA stead state levels. However, unlike other members of the FASTK family like FASTKD2, it does not co-localise the mitochondrial RNA granules. (Boehm et al., 2016).

MPV17L2 is an integral inner membrane protein that co-sediments with mt-LSU and the monosome. Knockdown of the protein leads to a decrease in mt-LSU and mt-SSU stability, and a translation defect. In these cells, the mt-SSU is unable to associate with the mt-LSU, suggesting a role of the protein in monosome formation (Dalla Rosa et al., 2014). The mechanism of this function still remains to be elucidated. Similar to C4orf14, MPV17L2 is associated with the mitochondrial nucleoid, suggesting that 28S mt-SSU assembly may happen at the nucleoid (He et al., 2012; Dalla Rosa et al., 2014)

GRSF1 is an integral component of mitochondrial RNA granules (Section 1.9). In the RNA granule, it interacts with the mt-SSU, as identified by sucrose gradient fractionation (Tu and Barrientos, 2015). A depletion of GRSF1 leads to reduced mt-SSU biogenesis and a translation defect (Antonicka et al., 2013; Jourdain et al., 2013). Its presence in the RNA granules suggests that it acts on the newly transcribed 12S rRNA at an early stage of mitoribosome biogenesis.

Assembly factors	12S rRNA	mt-SSU	16S rRNA	mt-LSU	Monosome	References
ERAL1		✓				Uchiumi et al. (2010), Dennerlein et al. (2010)
C4ORF14		✓				Al-Furoukh et al. (2013)
GRSF1		✓				Tu and Barrientos (2015)
NGRN			✓			Arroyo et al. (2016)
FASTKD2			✓			Popow et al. (2015)
DDX28			✓	✓		Tu and Barrientos (2015)
MALSU				✓		Rorbach et al. (2012), Fung et al. (2013)
L0R8F8 – mt-ACP				✓		Brown et al. (2017)
MTG1				✓		Kotani et al. (2013)
MTG2				✓		Kotani et al. (2013)
MPV17L2				✓	✓	Dalla Rosa et al. (2014)
DHX30		✓		✓	✓	Antonicka and Shoubridge (2015)

Table 1.1 Summary of co-sedimentation experiments, showing the ribosomal subassemblies that the assembly factors have been shown to interact with. It must be noted that absence of a tick only indicates insufficient evidence and not absence of interaction. In addition, some proteins have been located in MRGs (GRSF1, DHX30, DDX28) and nucleoids (MPV17L2, C4ORF14), indirectly suggesting that they may be involved at early stages of assembly. However, this information has not been included in the table.

1.9 Mitochondrial RNA granules

Several recent studies have identified the colocalization of proteins involved in gene expression in distinct foci called mitochondrial RNA granules (MRGs). These subcompartments bring together RNA processing enzymes onto nascent transcripts to allow only fully mature RNA molecules to be released for use by the translation apparatus. As seen in the ribonucleoparticles in stress granules and processing bodies in the cytosol (Anderson and Kedersha, 2009; Jourdain et al., 2016), this spatial,

temporal and functional delineation of RNA maturation is hypothesised to allows for more efficient and accurate gene expression.

By studying the co-localisation of 5'-bromouridine-incorporated nascent transcripts and RNA-processing proteins, it was shown that MRGs are found near but distinct from nucleoids (Jourdain et al, 2013; Antonicka et al., 2013). Proteins in these granules include GRSF1 (Jourdain et al, 2013; Antonicka et al., 2013), RNase P subunits (Jourdain et al., 2013), mtPAP (Wilson et al., 2014), nucleotide modifying enzymes (MRM2, MRM3 (Lee et al., 2013), TFB1M, PUS1 (Antonicka et al.,2015)), and TRMT10C (MRPP1) (Vilardo et al., 2012).Of these, GRSF1 (RBP G-rich sequence factor 1) was shown to be an essential component of the MRGs, as loss of GRSF1 leads to aberrant processing of mt-RNAs and translation defects (Jourdain et al, 2013). Recently, a systematic analysis of the MRG proteome has identified more factors involved in mt-RNA metabolism, including Fas-activated serine/threonine kinase (FASTK) proteins, FASTK and FASTK5 (Antonicka et al., 2015; Jourdain et al., 2015) which have been implicated in non-canonical processing of the primary transcript (Antonicka and Shoubridge, 2015).

Moreover, MRGs are also considered as centres for mitoribosomal biogenesis as they contain such assembly factors as MTERF3/MTERFD1, ERAL1, DDX28, FASTK-family proteins (Antonicka and Shoubridge, 2015; Tu and Barrientos, 2015) and mt-rRNA and mitoribosomal proteins (Hu et al., 2012; Bogenhagen et al., 2008). This suggests that the MRGs facilitate co-transcriptional assembly of the ribosome (Bogenhagen et al., 2014; Rackham et al., 2016).

Similarly, D-foci are said to contain the mitochondrial degradosome components, PNPase and SUV3 (Jourdain et al., 2015; Borowski et al., 2012; Minczuk et al., 2002; Piwowarski et al., 2003; Szczesny et al., 2010). The D-foci are found in close proximity to MRGs and is involved in co-transcriptional degradation of non-functional antisense RNAs and misprocessed RNAs, RNA maturation which requires 3' end exonuclease activity like ND6, and RNA turnover (Jourdain et al., 2013).

1.10 Aim

Of the numerous chemical modifications present in the cytoplasmic and bacterial ribosomal RNAs, only a few are conserved in the mammalian mitochondria. This work aims to identify the function of one such modification at G1145 on the 16S rRNA of the large subunit through identification of interactors of the responsible methyltransferase, MRM1 using immunoaffinity purification, the generation of knockout cell lines, the analysis of changes to the mitoribosomes composition and function using proteomic approaches upon loss of MRM1, and any consequential effects on mitochondrial function upon loss of MRM1.

This work also aimed to characterise a homolog of bacterial endonuclease, YbeY that is predicted to localise in the mitochondria. This involved the confirmation of location of YbeY to the mitochondria and analysis of the role of the endonuclease in the processing of the non-canonical cleavage site between the mRNAs encoding ATP8/6 and CO3. Analysis of the YbeY-deficient cells showed a severe defect in mitochondrial function, particularly in mitochondrial translation. Therefore, this work aimed to elucidate the role of YbeY in mitochondrial translation through the analysis of mitochondrial RNA metabolism via northern blotting and RNA-Seq, the identification of protein interactors of YbeY using immunoaffinity purification, and the role YbeY plays in mitoribosome biogenesis using proteomic approaches.

2 Material and methods

2.1.1 Chemicals and reagents

1 kb plus DNA Ladder, Hygromycin, Lipofectamine 2000, Lipofectamine RNAiMax, Cyquant NF cell proliferation assay kit, NativePAGE reagents, NuPAGE MOPS SDS running buffers, NuPAGE LDS sample buffer, random hexamers, SimplyBlue Safe Stain, SYBR Safe, TaqMan gene expression master mix and UltraPure agarose were purchased from Invitrogen.

5' Terminator exonuclease and 5' RNA polyphosphatase were purchased from Epicentre.

[^{32}P]-labelled a-UTP, α-dCTP and γ-ATP were purchased from Hartmann Analytic.

[^{35}S]-labelled methionine was purchased from Perkin Elmer.

Acrylamide/Bis solution (19:1) , DC assay kit and Precision Plus Protein Kaleidoscope prestained protein standard were purchased from Bio-Rad.

Alpha Select Silver Efficiency Competent Cells was purchased from Bioline Reagents.

All restriction enzymes, Klenow polymerase, T4 DNA Ligase, T4 Polynucleotide Kinase and T4 RNA Ligase were purchased from New England Biolabs.

Amaxa Nucleofector Kit V was purchased from Lonza.

Ammonium persulphate, β-mercaptoethanol, CompoZr zinc finger nucleases, DDM, DNA oligonucleotides, doxycycline, emetine dihydrochloride, FCCP, glucose, galactose, L-glutamine, mannitol, MMS, oligomycin, phenol, PMSF, rotenone, TEMED, Trizma base, hexadimethrine bromide and uridine were purchased from Sigma-Aldrich.

Ampicillin sodium salt and DTT were purchased from Melford Laboratories.

Benzonase Nuclease and Immobilon-P PVDF membrane were purchased from Merck Millipore.

Blasticidin and Zeocin were purchased from Invivogen.

Bromophenol blue, disodium phosphate, DMSO, EDTA, ethidium bromide, formaldehyde, glycerol, glycine, HEPES, hydrochloric acid, isopropanol, magnesium chloride, methanol, orthophosphoric acid, potassium chloride, sodium chloride, sucrose, mMessage mMachine T7 transcription kit and Triton-X100 were purchased from Fisher Scientific.

BSA, sodium hydroxide and urea were purchased from VWR International.

DMEM (Dulbecco's Modiefied Eagle's Medium) variants, Iscove's Modified Dulbecco's Medium (IMDM), RPMI (Roswell Park Memorial Institute) medium, Glutamax, Opti-MEM, D-PBS (phosphate buffered saline), Penicillin-Streptomycin (10,000 U/ml), sodium pyruvate and trypsin-EDTA (0.25%) were purchased from Gibco.

DNeasy Blood and Tissue kits, miRNeasy RNA isolation kits, Omniscript reverse transcription kits, QIAquick Gel Extraction kits, QIAquick PCR Purification kits, QIAprep Miniprep kits and QIAzol were purchased from QIAGEN.

dNTPs, ECL, ECL prime, Hybond N+ nylon membrane and storage phosphor screens were purchased from GE Healthcare.

Gel Loading Buffer II, Glycoblue Coprecipitant, nuclease-free water, RNaseZap, T7 Maxiscript In Vitro Transcription Kit, TRIzol and TRIzol LS were purchased from Ambion.

Hap1 control and knockout cells (Product ID: HZGHC002765c022) were purchased from Horizon Discovery.

High Sensitivity D1000 Screentape was purchased from Agilent Technologies.

Hybond-N+ membrane was purchased from Amersham.

Low-melt agarose was purchased from Biogene.

Milk Powder was purchased from Marvel.

Proteinase Inhibitor tablets were purchased from Roche.

Tetracycline-free fetal bovine serum (FBS) was purchased from Biochrom AG.

TruSeq Stranded Total RNA LT Kit and MiSeq reagent kits were purchased from Illumina.

X-Ray film was purchased from Fujifilm.

2.1.2 Solutions

ACA BUFFER: 1.5M aminocaproic acid, Bis-Tris (pH 7)

BUFFER A: 2M HEPES pH 6.6

BUFFER B: 1.25 M Tris-HCl pH 8, 125 mM MgCl2, 1.8% 2-mercaptoethanol, 0.5 mM dATP, 0.5 mM GTP, 0.5 mMTTP

FREEZING MEDIUM: 20 % v/v DMSO, 80 % FBS

GRADIENT BUFFER: 50 mM Tris–HCl (pH 7.2), 20 mM Mg(OAc)2, 80 mM NH4Cl, 0.1 M KCl, 1 mM PMSF

GTB BUFFER (20x): 1.78 M tris base, 0.57 M taurine, 10 mM EDTA.

HYBRIDISATION BUFFER: 7 % SDS, 0.25 M Sodium Phosphate (pH 7.6)

LYSIS BUFFER 1: 50 mM TRIS HCl, 150 mM NaCl, 1 mM EDTA, 1% Triton, 1 x Roche Protease Inhibitor Tablet

MITOBUFFER: 0.6 M mannitol, 10 mM Tris HCl pH 7.4, 1 mM EDTA

MOPS BUFFER (10 X): 200 mM MOPS, 10 mM EDTA, 50 mM Sodium Acetate (pH 7.0).

MOPS RUNNING BUFFER: 5 ml of 10 x MOPS, 5 mL of 37 % formaldehyde (0.3 M fc), 10 µg/mL EtBr, and 220 mL of water

PIC: 1 x PBS, 1 x tablet of Roche protease inhibitor/ 50 ml

PBSS: 5% FBS v/v, 95% PBS

PBS-T (1x): 1x PBS, 0.1 % (v/v) Triton X-100

SILAC MEDIUM: 10% dialysed FBS (20% for YbeY (-/-) cells), 200 mg/L proline, 0.398 mM arginine, 0.798 mM lysine (Light-R_0K_0, Heavy-$R_{10}K_8$)

SOC MEDIUM: 0.5 % (w/v) yeast extract, 2 % (w/v) tryptone, 10 mM NaCl, 2.5 mM KCl, 10 mM MgCl2, 20 mM MgSO4, 20 mM glucose

SONICATION BUFFER: 20 MM Tris HCl PH 7.5, 200 mM NaCl, 10% ethylene glycol, 1 x Roche Protease inhibitor tablet/ 50 ml

SSC (20 X): 3 M NaCl, 0.3 M sodium citrate (pH 7.0).

WASH BUFFER: 50 mM HEPES pH 8.0, 150mM NaCl, 0.05% DDM, 2 mM DTT, 2 mM EDTA, 1 Roche protease inhibitor tablet/50 ml

2.2 Basic techniques

2.2.1 Cloning

A plasmid containing the open reading frame of YbeY was purchased as an IMAGE cDNA clone (IRAUp969G02109D; GeneScript Item number: SC1010) from Source Bioscience, and then cloned into pcDNA5/FRT/TO constructs.

Primers:

YBEY + FLAG	
Overhang+BamH1+FP	CTTTCTTGGATCCAATGAGTTTGGTGATTAGAAATCTGCAGCG
Overhang+Not1+Flag+RP	CTCTCCGCGGCCGCCTACTTATCGTCGTCATCCTTGTAATCGCTCCCTCCGAAGAGGCC
YBEY (FLAG + STREP)	
Overhang + Age1 + RP	CTCTCCACCGGTGCTCCCTCCGAAGAGGC
YBEY (R59A catalytic mutant)	
RP for site directed mutagenesis	GCACATCGGTTGGGACATTTCTATCCGCGTAGATTCTATTAATGTGC
FP for site-directed mutagenesis	GCACATTAATAGAATCTACGCGGATAGAAATGTCCCAACCGATGTGC
YBEY (H117A mutant)	
RP for site directed mutagenesis	CCTGACTGTGACGGCCACCGCAGGACTCTGTCACTTGCTGGGATTCACA
FP for site-directed mutagenesis	TGTGAATCCCAGCAAGTGACAGAGTCCTGCGGTGGCCGTCACAGTCAGG

DNA concentrations were determined using a Nanodrop 1000 Spectrophotometer.
MRM1 cloned into pcDNA5/FRT/TO was kindly gifted by Dr Joanna Rorbach.
pBMN plasmid was kindly gifted by Luther Davis.

2.2.2 Sanger sequencing

PCR products or plasmid sequencing was performed by Source Bioscience sequencing service. 96-well plates of bacterial colonies were sequenced by GENEWIZ sequencing service.

2.2.3 TBE-agarose gel electrophoresis

PCR products of restriction enzyme digestion products (with 1 x SYBR Safe DNA statin) were resolved on a 1% agarose gel prepared in 1 x TBE buffer. The gel was run at 95V for 40 minutes. Bands were visualised using UV light and bands were cut

out (if necessary) using scalpels. DNA was extracted from the gels using QIAquick gel extraction kit, according to manufacturer's instructions.

2.2.4 Restriction digestion

Restriction digests of PCR products and plasmids were performed using manufacturer's (New England Biolabs) instructions. 1 x NEBuffer (1.1, 2.1 or 3.1) was added to 1 μg of plasmid or the PCR mix with 10 units of the restriction endonuclease. The reaction was incubated at 37° for 1 hour.

2.2.5 DNA ligation

PCR-generated, restriction endonuclease-cleaved PCR products were mixed with the restriction endonuclease-cleaved vector at a molar ratio of 1:3. This was added to a 20 μl reaction mix containing 1 x T4 DNA ligase and 400 units of T4 DNA ligase. The ligation mix was incubated at 16 °C overnight. This vector was then transformed into chemically competent bacteria for expansion.

2.2.6 Transformation of chemically competent *E. coli*

DNA was added to 50 μl of α-select chemically competent *E. coli* cells (defrosted on ice), and incubated on ice for 10 minutes. Cells were then heated to 42°C for 45 seconds and chilled in ice for 2 minutes. 500 ml of *SOC MEDIUM* was added to the cells. The mixture was incubated in a shaking incubator at 37°C for 1 hour. The mixture was centrifuged at 2000g for 3 minutes. 250 μl of medium was removed. The cells were resuspended in the rest of the medium and spread onto pre-warmed LB agar plates containing either 50 mg/ml ampicillin or 50 mg/ml kanamycin, depending on selection requirements. The plates were incubated at 37°C overnight.

2.2.7 Western blotting

A confluent 9 cm dish of HEK293 or Hap1 cells was washed with PBS and pelleted at 1200 rpm for 3 minutes. The cells (or isolated mitochondria) were resuspended in 100 μl of *LYSIS BUFFER 1* and kept on ice for 15 minutes. Then, the lysed cells were centrifuged at 8000 rpm for 5 minutes. The supernatant was transferred to a new tube. Protein concentration was determined using the BCA kit according to manufacturer's instructions.

25 µg of cell lysate were boiled at 95°C for 5 minutes with 33.3% NuPAGE LDS 4 x sample buffer containing 200 mM DTT. The boiled solution was loaded onto 4-12% Bis-Tris NuPAGE polyacrylamide gels and run at 200 V for 30 minutes. The proteins were transferred onto nitrocellulose membranes with the Bio-Rad Trans-Blot SD Semi-Dry Transfer Cell at 1 mA/cm2 for 90 minutes, or the iBlot 2 Dry Blotting System using protocol 'P0'. Gels were then stained using SimplyBlue Safestain to confirm equal loading. The nitrocellulose membrane was blocked using 5% non-fat milk in *PBS-T* at room temperature on rollers. The blocking solution was removed and replaced with the primary antibody solution (diluted in *PBS-T*). The membrane was incubated with the antibodies overnight on rollers at 4°C. The membrane was washed 3 times for 10 minutes on rollers with *PBS-T* and incubated with secondary antibody diluted in *PBS-T*. The membrane was washed again, three times, as before. Finally, the membrane was developed using ECL and exposed to X-ray film in a dark room.

The antibodies used are detailed in table 2.1.

Primary antibodies

Epitope	Source	Species	Dilution
TOM22	Abcam ab10436	Mouse	1:2000
GAPDH	Abcam ab10436	Mouse	1:2000
YbeY	Atlas HPA018162	Rabbit	1:500
Histone H4	Abcam ab10158	Rabbit	1:1000
MRM1	Atlas HPA021598	Rabbit	1:1000
Flag	Sigma F3165	Mouse	1:1000
MRPL12	Proteintech 14795-1-AP	Rabbit	1:2000
MRPL3	Atlas HP043665	Rabbit	1:2000
MRPS18b	Proteintech 16139-1-AP	Rabbit	1:2000
MRPS17	Proteintech 18881-1-AP	Rabbit	1:2000
β-actin	Sigma A2228	Mouse	1:50,000
NDUFS1	Abcam ab169540	Rabbit	1:2500
OXPHOS cocktail	Abcam ab110411	Mouse	1:1000

Secondary antibodies

Epitope	Source	Dilution
Goat anti-rabbit IgG HRP	Promega W4011	1:1000
Goat anti-mouse IgG HRP	Promega W4021	1:2000

Table 2.1 Antibodies for western blotting

2.2.8 Mitochondrial isolation using Dounce homogeniser (and cell fractionation)

This method was used predominantly for cell fractionation to identify protein localisation. Text in bold indicate fractions that need to be kept aside for western blot analysis. All steps of the mitochondrial isolation were carried out at 4 °C. 15 plates of confluent 15 cm dishes of HEK293 cells were harvested and washed with 1 x PBS. The cell pellet was resuspended in 15 ml of *MITOBUFFER* containing 0.1% BSA (100 µl was kept aside for total fraction). 2 ml of this suspension was put in a Dounce homogeniser and homogenised with 15 strokes with a tight pestle. This homogenised solution was transferred to a new 2 ml tube. This was repeated with all the remaining resuspended cells. The tubes were centrifuged at 400g for 10 minutes. The supernatant was kept aside. The pellet from each tube was resuspended in 2ml of *MITOBUFFER* containing 0.1% BSA. The homogenisation and centrifugation steps were repeated. The supernatant was put into new 1.5 ml tubes (100 µl was kept aside as debris fraction). All the supernatant kept aside was centrifuged at 400g for 5 minutes. The supernatant from these centrifuged tubes was transferred to a new tube and centrifuged at 11,000g for 10 minutes. The supernatant was removed (100 µl was kept aside as the cytoplasmic fraction). The pellet was resuspended in 1 ml of *MITOBUFFER*. 50U/ml of Benzonase was added to this and incubated for 15 minutes. The suspension was centrifuged at 11,000g for 10 minutes. The mitochondrial pellet can be lysed in the same manner as cell lysis (section 2.2.7).

For cell fractionation, the mitochondrial pellet was resuspended in 120 µl of *MITOBUFFER*. This was divided into 3 aliquots. The first aliquot was used as the mitochondrial fraction. The second aliquot was incubated with 4 µg/mg of Proteinase K and incubated for 30 minutes. This was the Proteinase K fraction. The third

aliquot was incubated with Proteinase K as described, and 0.2 µl of Triton X. This was the proteinase K and Triton-X fraction. The three fractions were centrifuged at 11,000g for 5 minutes. The pellet was resuspended in *WASH BUFFER* containing 1 µM PMSF. The pellets and the fractions collected were then lysed and analysed by western blotting (section 2.2.7).

2.2.9 Mitochondrial isolation using Balch homogeniser

A minimum of 10 x 15 cm confluent dishes of HEK293 or Hap1 cells were harvested and washed with cold 1 x PBS. All further steps were performed at 4 °C. The Balch homogeniser was kept on ice. 2 ml of *HYPOTONIC BUFFER* was introduced into the assembled homogeniser containing the ball bearing (10 µm clearance for Hap1 cells and 12 µm clearance for HEK293 cells). The cells were resuspended in 3 ml of *HYPOTONIC BUFFER* per gram of cells and incubated for 10 minutes. The cells were passed through the homogeniser chamber between two syringes repeatedly (3 passes for HEK293 cells/ 7 passes for Hap1 cells). The homogenised cells were put in a new 50 ml falcon and neutralised with 2.5 x *MSH* buffer (0.68 ml/ml of cells). The final homogenised cell suspension was diluted in up to 50 ml of 1 x *MSH* buffer. This was centrifuged at 1000 g for 10 minutes. The pellet was discarded. The supernatant was again centrifuged at 1000 g for 10 minutes. The pellet was discarded and the supernatant was transferred to a new tube and centrifuged at 8500 rpm for 10 minutes. Again, the supernatant was transferred to a new tube and centrifuged at 8500 rpm for 10 minutes. The pellets from the 8500 rpm spins were pooled and resuspended in 1 ml of 1 x *MSH*. 50U/ml of Benzonase was added to this and incubated for 15 minutes. The suspension was centrifuged at 8500 rpm for 10 minutes.

The pellet was reusupended in 1 x MSH. This was loaded onto a 1.5 M – 1 M – 0.5 M step sucrose gradient (prepared in 10 mM HEPES pH 7.8 containing 5 mM EDTA) (tube number: 344060). The tube was centrifuged at 26,000 rpm for 60 minutes in a SW40Ti rotor. The mitochondria formed a pellet in the interface between the 1 M and 1.5 M solutions. The pellet was extracted and diluted in 4 volumes of 1 x MSH and centrifuged at 8,000 rpm for 10 minutes at 4 °C. The pellet was the isolated mitochondria. This can be lysed for immunoaffinity purification or western blot analysis, in the same manner as cell lysis.

2.2.10 Polymerase Chain Reaction (PCR)

All PCR reactions were performed using Novagen KOD Hot Start DNA polymerase as per manufacturer's instructions. PCR was performed for 35 cycles, using a Tm of 58-65 °C depending on the primers.

2.3 Cell Culture

2.3.1 Maintenance of cell lines

All cell lines were maintained at 5% CO_2 and 37°C in humidified incubators. The HEK and HeLa cells were cultured in Dulbecco's Modified Eagle Medium (DMEM), containing 4.5 g/L glucose, 110 mg/L sodium pyruvate, supplemented with 10 % (v/v) foetal bovine serum (FBS), 100 U/ml penicillin and 100 µg/ml streptomycin. Hap1 cells were cultured in Iscove's Modified Dulbecco's Medium (IMDM) containing 4.5 g/L glucose, 110 mg/L sodium pyruvate, supplemented with 10 % foetal bovine serum (v/v) (FBS), 100 U/ml penicillin and 100 µg/ml streptomycin. In the case of the YbeY knockout Hap1 cells, 20% of foetal bovine serum was used.

Flp-In T-Rex HEK293 cells were gown supplemented DMEM containing 15 µg/ml blasticidin and 100 µg/ml Zeocin (*BZ MEDIUM)*. After transfection, 15 µg/ml blasticidin and 50 µg/ml hygromycin were used instead (*HB MEDIUM*).

2.3.2 Freezing and thawing cell lines

A confluent 9 cm dish was trysinised, neutralised with medium (DMEM or IMDM, depending on the cell type), centrifuged at 1200 rpm for 3 minutes, washed with phosphate buffer saline (PBS) and re-centrifuged. The pellet was resuspended in 1ml of FBS and transferred into a cryovial. 1 ml of *FREEZING MEDIUM* was added to the cryovial. The solutions were mixed by inversion. The cryovials were transferred to a Mr Frosty isopropanol container at -80°C. The vials could be transferred to liquid nitrogen tanks after 24 hours.

For thawing cells, cells were quickly defrosted in a 37°C water bath. The contents of the cryovial were transferred to 10 ml of non-selective supplemented medium, mixed by inversion and centrifuged at 1200 rpm for 3 minutes. The supernatant was aspirated. The cells were resuspended in 1 ml of supplemented DMEM and plated in a 9 cm dishes with 10 ml of supplemented medium.

2.3.3 Lipofectamine 2000 transfection

2 µg of DNA was incubated in 100 µl of optimem for 5 minutes, while 3 µl of Lipofectamine 2000 was also incubated in 100 µl of optimum for 5 minutes at room temperature. They were mixed and incubated at room temperature for 10 minutes. Then, they were added to the cells in supplemented DMEM and mixed by swirling.

2.3.4 Transient DNA transfection for immunofluorescence imaging

HeLa or HEK cells were plated on coverslips in a well of a 6 well tissue culture plate until 80% confluency for 24 hours. 2 µg of pcDNA5 vector containing the relevant gene were transfected into the cells using lipofectamine 2000. 24 hours later, the cells were prepared for immunocytochemistry.

2.3.5 Immunocytochemistry

All the steps were performed at room temperature.

The cells were grown on coverslips in a well of a 6-well plate. After 24 hours of transfection, the cells were washed with PBS. The PBS was aspirated and the cells were incubated in 4 % formaldehyde in 1x PBS for 15 minutes. The formaldehyde was removed and the cells were washed with PBS. 0.1 % Triton-X in PBS (PBS-T) was added for 5 minutes to permeabilise the cells. Cells were incubated for 1 hour in *PBSS* buffer and then primary antibodies (diluted in *PBSS*) were applied for 1.5 hours. The cells were washed in PBSS for 5 minutes on a rocker, three times and secondary antibodies (diluted in PBSS) were added for one hour. Following this incubation, cells were washed two times in *PBSS* and one time in PBS (5 minute washes), and mounted in Vectashield mounting medium. The cells were then visualised by fluorescence microscopy. Immunofluorescence images were captured using a Zeiss LSM 510 META confocal microscope.

Primary antibodies

Epitope	Source	Dilution
Flag	Sigma F3165	1:200
Tom20	Santa Cruz sc-11415	1:500

Secondary antibodies

Epitope	Source	Dilution
Alexa Fluor 488-conjugated goat anti-mouse	Molecular Probes A1101	1:1000
Alexa Fluor 594-conjugated goat anti-rabbit	Molecular Probes A11037	1:1000

Table 2.2 Antibodies for immunocytochemistry

2.3.6 Stable DNA transfection of Flp-In 293 T-Rex cell lines

Prior to transfection, parental Flp-In 293 T-REx HEK (HEK293) cells were grown to 50% confluency in a well of a 6 well tissue culture plate in *BZ MEDIUM*. Just before transfection, the medium was changed to supplement non-selective DMEM. 0.2 µg pcDNA5/FRT/TO construct and 1.8 µg pOG44 vector were stably transfected into cells using Lipofectamine 2000. After 24 hours, media was replaced with non-selective media. After another 24 hours, cells were plated in selective *HB MEDIUM* in a 9 cm dish. The medium was replaced every three days until colonies were formed. Clones were isolated and grown in new 9 cm dishes. The selected clones were induced with 100 ng/ml doxycycline for 24 hours and harvested for screening by western blotting using antibodies against epitope tags (flag) or against endogenous proteins.

2.3.7 Lentiviral infection (Complementation of YbeY (-/-) Hap1 cells)

Phoenix-AMPHO cells were plated at 20 % confluency in 2 x 10 cm dishes in supplemented Roswell Park Memorial Institute (RPMI) medium (with 10% (v/v) FBS, 100 U/ml penicillin and 100 µg/ml streptomycin, 4.5 g/L glucose, 2 mM L-glutamine). After 24 hours, the medium was changed to supplemented RPMI medium (without penicillin and streptomycin). The Phoenix cells were transfected with 140 µg of pBMN plasmid containing the wildtype YbeY or catalytic mutant YbeY) using Lipofectamine 2000. To do this, 50 µl of Lipofectamine 2000 was incubated in 3 ml of Optimem for 5 minutes. Simultaneously, 140 µg of the pBMN vector (in 14 µl nuclease free water) was incubated in 1.5 ml of Optimem for 5 minutes. After 5 minutes, 1.5 of the lipofectamine-containing Optimem was added to each of the 1.5 ml of plasmid-containing Optimem. This was incubated at room temperature for 20 minutes. 3 ml of the Optimem containing the lipofectamine-DNA complexes were added to the Phoenix cells and incubated for 24 hours in a 32 °C incubator. After 24 hours, the medium was replaced with warmed supplemented IMDM medium.

Meanwhile, YbeY (-/-) knockout cells were cultured to 50 % confluency in a 10 cm dish. After 24 hours, 15 µl of 1000 x polybrene (5mg/ml hexadimethrine bromide in 1x PBS) was added to 3 ml of IMDM medium in two tubes. 12 ml of medium from the Phoenix cell plates was transferred into the tubes through a 0.45 µm Millex syringe filter and mixed by inversion. This was applied to the YbeY (-/-) cells and incubated in a 37 °C incubator. After 24 hours, the medium was changed to supplemented IMDM medium (containing 200 µg/ml hygromycin selection) and allowed to recover for 1 week in a 37 °C incubator.

2.3.8 siRNA transfection

In a well of a 6 well plate, 250 µl of optimum was mixed with 2 µl of Lipofectamine RNAiMAX. To this, 2.5 µl of 20 mM siRNA was added. This was incubated for 5 minutes at room temperature. Meanwhile, 50,000 cells were pelleted. Then, the cells were resuspended in 1.5 ml of medium and added to the well. This was mixed by swirling and incubated for 72 hours. The siRNA could be repeated again after this period for further depletion of the protein, before cells were harvested for analysis.

siRNA	Product code
siRNA 1	HSS147611
siRNA 2	HSS147612
siRNA 3	HSS182431

2.3.9 Growth rate measurement using Incucyte

A confluent 9 cm dish of cells was trypsinised for 3 minutes at 37°C and the trypsin was neutralised using medium. The cells were centrifuged at 1200 rpm for 3 minutes and the pellet was resuspended in 4 ml of medium. For HEK293 cells, glucose-free DMEM medium was used. For Hap1 cells, supplemented IMDM was used.

For HEK293 cells, 2 ml of pre-warmed glucose-free medium was plated in wells of a 6 well plate. Glucose or galactose was added to these cells to a final concentration of 4.5 g/L and 0.9 g/L respectively. For IMDM, 2 ml of pre-warmed, supplemented IMDM (20 % (v/v) FBS) was put in each well.

10,000 cells were counted using the Countess automated cell counter and added to each well. The plates were placed in the Incucyte High Definition Imaging Mode.

Growth rate was measured as a function of changing cell confluency at 4 hour intervals.

2.3.10 Measurement of cellular oxygen consumption

24 hours prior to the beginning the assay, 200 µl of calibrant solution was put in each well of the bottom plate of a 96 well sensor cartridge and incubated in a 37 °C non-CO_2 incubator.

For HEK293 cells, the XF 96-well cell culture microplates (Seahorse Bioscience) were coated with poly-L-lysine (20 minutes of 20 µl of 0.1 mg/ml poly-L-lysine in PBS for 20 minutes followed by a PBS wash and air drying for 2 hours). Cells were counted using the Countess automated cell counter and 15,000 cells were plated per well 24 hours prior to beginning the assay.

For Hap1 cells, the cells were plated at 40,000 cells per well 4 hours before beginning the assay. Both cell types were incubated at 37 °C in 5% CO_2 incubators.

One hour before the assay, the growth medium was removed, washed with 200 µl *SEAHORSE ASSAY MEDIUM* and 175 µl of the *SEAHORSE ASSAY MEDIUM* was added to each well and incubated for 1 hour in a 37 °C non-CO_2 incubator. Analysis of oxygen consumption was measured using a XF96 Extracellular Flux analyser (Seahorse Bioscience). The wells were sequentially injected with 2 µM oligomycin (ATP synthase inhibitor), 0.2 µM Bam15 (uncoupler) and 1 µM Antimycin and Rotenone (Complex III and I inhibitors respectively). Oxygen consumption was measured every 5 minutes before and after injection.

To quantify cell density per cell, for HEK293 cells, the Cyquant NF cell proliferation assay kit as per manufacturer's instructions. For Hap1 cells, 20 µl of *LYSIS BUFFER 1* was added to each well and incubated at 37 °C for 30 minutes. 10 µl of this solution was used for Pierce BCA assay. Quantification of cell density was used to normalise the oxygen consumption rate.

2.3.11 Generation of HEK293 knockouts using zinc-finger nucleases

2.3.11.1 Transfection and single cell cloning

Transient transfection of the two ZFNs were performed into Flp-In T-Rex 293 HEK cells by nucleofection. The cells were harvested by trypsinisation and 1,000,000 cells

were counted using the Countess automated cell counter. These cells were pelleted by centrifugation at 200 g for 10 minutes. The cell pellets were resuspended in 100 µl of Nucleofector solution. 2.5 µg of each ZFN was added to the cell suspension. This was transferred to a nucleofection cuvette and into an Amaxa Nucleofector. Program A-23 was run. The cell suspension was immediately transferred to a 9 cm dish containing supplemented DMEM and incubated in a 37 °C 5% CO_2 incubator.

After 72 hours, the cells were trypsinised and counted in a Countess automated cell counter. 8 x 96 well plated were plated at a cell density of 1 cell per 5 wells. This ensured that colonies produced would be derived from a single colony. These plates were incubated again for about 2 weeks until colonies were visible. These colonies were then plated into 24 well plates until confluent. These were allowed to expand to >80% confluency. Then, these were split into three 24 well plates, one for freezing, one for gDNA extraction and one for protein extraction. Then, these plates were allowed to grow. One plate was frozen by resuspending the cells in each well in 400 µl of FBS containing 10% DMSO. Plates were sealed and placed on dry ice for 5 minutes and then transferred to -80 °C for long term storage.

2.3.11.2 Screening using western blotting and sequencing

For western blotting, cells were resuspended in 100 µl of *LYSIS BUFFER 2* per well and incubated on ice for 15 minutes. 7 µl was used from each well was used for western blotting (section 2.2.7).

For sequencing, 50 µl of Lysis for Blood (Sigma) reagent was added to each well and plate was heated at 75 °C for 15 minutes. 450 µl of water was added to each well. 4 µl from each well was used for PCR (section 2.2.10). Primers are detailed in table 2.3. The PCR products were sent for sequencing using the forward primer as the sequencing primer. The sequences for each clone were manually assessed for a lack of consensus in the sequence trace at and beyond the ZFN target site.

If western blotting and sequencing identified possible candidates for knockout, the PCR products were cloned into pCR4 vectors using the Zero Blunt TOPO PCR Cloning Kit and sequenced using the M13 forward sequencing primer.

Name	Sequence
YbeY forward	AAAGTGATCTGATTGCGCGT
YbeY reverse	CTGGGAAGATGGGCTAGACA
MRM1 forward	CTGGAGCTTCTGTTTGGCAT
MRM1 reverse	TGACCTTATCCACTCCGAGG

Table 2.3 Primers used to screen for successful knockouts

2.4 RNA-related assays

2.4.1 RNA extraction

Total cell RNA from a confluent well of a 6 well plate at 80% confluency was extracted using 500 µl Ambion TRIzol Reagent using the manufacturer's instructions.

2.4.2 Terminator assay

For phosphatase treatment, 10 µg of RNA was treated with RNA 5' polyphosphatase (Epicentre) according to manufacturer's instructions. The Terminator exonuclease (epicentre) was a 5'-phosphate dependant exonuclease. 5 µg of Total HEK293 cell RNA or 10 µl of the polyphosphatase reaction was used in a 20 µl reaction as per manufacturer's instructions. The RNA was resolved on a low resolution polyacrylamide gel and analysed by northern blotting (section 2.4.8).

2.4.3 End labelling

50 pmol of DNA oligonucleotide substrate was 5' end labelled in a 20 µl reaction using T4 polynulceotide kinase and 2 µl of [γ^{32}P]-ATP (111 TBq/mmol) using the manufacturer's instructions.

2.4.4 Primer extension

2.4.4.1 *In vitro* transcription for negative control for primer extension

PCR products were generated with 5' T7 promoter and *in vitro* transcribed using the mMessage mMachine T7 transcription kit (Thermo Fisher Scientific) as per manufacturer's instructions (mRNA synthesis, DNase treatment, RNA purification with phenol chloroform extraction). Primers detailed in table 2.4.

Name	Sequence
Negative control PCR forward primer	CCAGTGAAATTGACCTGCCC
Negative control PCR reverse primer	TGTCCTTTCGTACAGGGAGG
Primer extension Primer 1	TGGGTTCTGCTCCGAGGTCGC
Primer extension Primer 2	GTTGGGTTCTGCTCCGAGGTC

Table 2.4 Primers used for the construction of the negative control and as primers for reverse transcription

2.4.4.2 Hybridisation and reverse transcription

In this procedure, reverse transcription is limited by the omission of a specific dNTP which is required for extension after the modification. This causes all the primers extended after the modification to be completely stalled. This required the primer to be designed such that the specific dNTP is not required before the modification.

For primer extension, DNA oligonucleotides, which bind upstream to the site of the modification being investigated, are used as primers for reverse transcriptase. These oligonucleotides are 5' end labelled as described in section 2.4.3. Extension is paused at the site of modification and stalled when a specific dNTP requirement is not met.

25 nmoles of labelled oligonucleotide was added to total 1 µl of RNA in a 10 µl reaction containing 10 mM Tris-HCl (pH 8.0) and 1 mM EDTA. The sample was heated to 80 °C for 2 minutes and the temperature was slowly lowered at the rate of 0.02 °C/s to 45 °C where it was held for 1 minutes, followed by a 0.02 °C/s decrease to 4 °C.

This was mixed with a 10 µl reverse transcription mix (1 x RT buffer, 40 nM dNTP of each of the three dNTPs required for primer extension, 0.5 µl RNasin inhibitor, 1 µl Omniscript Reverse Transcriptase, 4.5 µl nuclease free water) and incubated at 37 °C for 1 hour. After this incubation step, 4 µl of Gel loading buffer II was added and the DNA was resolved on a 10 % high-resolution polyacrylamide gel as per section 2.4.5. Gels were dried at 80 °C overnight and scanned using a Typhoon 9410 scanner. Bands were quantified using Image J. The ratio of the pausing at the modification to the stalled primer extension is used to quantify the level of modification of RNA.

2.4.5 High-resolution polyacrylamide gel electrophoresis

21 g (7.3M) Urea was dissolved in a 50 ml solution containing 1 x *GTB BUFFER*, 25% v/v of 40% 19:1 Acrylamide:Bis stock solution. Polymerisation was activated using 400 µl of 10 % APS and 20 µl TEMED, mixed and immediately injected into a Sequi-Gel GT tank. This was left to polymerise for 45 minutes and gel was warmed by pre-running it for 2 hours at 50 W in 1 x *GTB BUFFER*. After the temperature of the gel reached 50 °C. 12 µl of the sample was run in well at 50 W for approximately between 1 – 2 hours depending on the size of the product length being analysed.

The gel was them transferred onto a sheet of Whatman 3 MM blotting paper and dried using a Bio-Rad Model 583 gel dryer at 80 °C overnight. The dried gel was then removed, wrapped in cling film, exposed to a storage phosphor screen and scanned using a Typhoon 9410 scanner. Bands were quantified using Image J.

2.4.6 Riboprobe generation

Templates were generated using PCR (primers detailed in table 2.5) from HeLa total cell DNA (section 2.2.10) with a T7 promoter introduced at the 5' terminus of the reverse primer. 100 ng of the PCR product was then transcribed using the MaxiScript T7 transcription kit (1 x transcription buffer, 500 µM ATP, 500 µM GTP, 500 µM CTP, 30 units of T7 polymerase) as per the manufacturer's instructions using [α^{32}P]-UTP (2.5 µl) instead of the UTP provided in the kit.

For 5S rRNA loading control for northern blots, a DNA oligo was radiolabelled and used as a probe. The oligos were end-labelled using T4 polynucleotide kinase and [γ^{32}P]-ATP (section 2.4.3).

One these were prepared, they were added to 10 ml of *HYBRIDISATION BUFFER* in the hybridisation tube containing the membrane.

Transcript		Sequence
ND3	Forward	ATAAACTTCGCCTTAATTTTAATAATC
	Reverse	TAATACGACTCACTATAGGGATTCGGTTCAGTCT AATCCTTTTTGTAG
ND6	Forward	GGGGTTTTCTTCTAAGCCTTC
	Reverse	TAATACGACTCACTATAGGGCCCCCGAGCAATCT CAATTAC

CO3	Forward	CCTGAGAACCAAAATGAACG
	Reverse	TAATACGACTCACTATAGGGGCCAGGGCTATTGG TTGAATG

Table 2.5 Primers for the constructions of PCR templates for ssRNA probe generation

2.4.7 DNA probe generation

BUFFER A and *BUFFER B* were mixed ('OLB') in a ratio of 5:2. 50 ng of the PCR product (primers detailed in table 2.6) were denatured at 95 °C for 5 minutes in a 20 µl solution and immediately placed on ice for 2 minutes. The labelling reaction was setup containing 10 µl OLB, 2 µg of BSA, 5U Klenow polymerase and 3 µg of Invitrogen Random Hexamers. The denatured DNA was mixed with the labelling reaction and 3 µl of [α^{32}P]-dCTP was added. The reaction was incubated at 37 °C for 1 hour. The labelled probe was denatured at 95 °C for 5 minutes and immediately placed on ice for 2 minutes before being added to the hybridisation tube.

Transcript		Sequence
12S	Forward	CACTGAAAATGTTTAGACGGG
	Reverse	GGCTCCTCTAGAGGGATATG
16S	Forward	TAGATATAGTACCGCAAGGG
	Reverse	GACTTGTTGGTTGATTGTAG
ND1	Forward	AACCTCAACCTAGGCCTCC
	Reverse	AATGCTAGGGTGAGTGGTAGG
ND2	Forward	TCCCAGAGGTTACCCAAG
	Reverse	GAGTAGTGTGATTGAGGTGGAG
ND4/4L	Forward	ACTACCACTGACATGACTTTCC
	Reverse	GGAGTCATAAGTGGAGTCCG
ND5	Forward	GTAGCATTGTTCGTTACATGG
	Reverse	ACTGCTGCGAACAGAGTG
CO1	Forward	CTTATTCGAGCCGAGCTG
	Reverse	GGTATAGAATGGGGTCTCCTC
CO2	Forward	GCGCAAGTAGGTCTACAAGACGC

	Reverse	GCATGAAACTGTGGTTTGCTCC
ATP8/6	Forward	CCCATACTCCTTACACTATTCC
	Reverse	GTTAGCGGTTAGGCGTAC
CytB	Forward	CTACCTTCACGCCAATGG
	Reverse	TTTGTTAGGGACGGATCG

Table 2.6 Primers for the constructions of PCR templates for dsDNA probe generation

2.4.8 Northern blotting

2.4.8.1 Low-resolution polyacrylamide gel electrophoresis

A 50 ml gel containing 1.2 % UltraPure agarose, 1 x MOPS BUFFER and 1.11% formaldehyde was cast in a Bio-Rad Mini-Sub cell GT set. The gel was run in 250 ml of MOPS RUNNING BUFFER. The RNA sample containing 50% Gel Loading Buffer II was heated for 10 minutes at 55 °C, cooled on ice for 2 minutes and then loaded onto the gel. The gel was run at 80 V for 2 hours and 20 minutes, at 4 °C. The gels were semi-dry blotted onto moistened positively-charged nylon membrane (Hybond – N+) with 3 x 3 mm Whatmann paper. 3 to 5 cm of absorbent paper was placed on top of this followed by an additional 1 kg of weight. Gels were left to blot overnight. Then, the RNA was cross-linked to the membrane by exposing it to 120 mJ/cm^2 of 254 nm UV light.

2.4.8.2 Hybridisation and washes

For hybridisation, the membrane was placed in a hybridisation tube and washed with 20 ml of *HYBRIDISATION BUFFER* for 90 minutes at 65 °C in a hybridisation oven. The buffer was then replaced with 10 ml of *HYBRIDISATION BUFFER*. The riboprobe or DNA probe was added to the buffer and allowed to hybridise overnight at 65 °C.

The following day, the probe was removed and the membrane was washed 5 times for 20 minutes with 1 x *SSC* buffer. The membrane was then removed and wrapped in cling film and exposed to a storage phosphor screen and scanned using a Typhoon 9410 scanner. Bands were quantified using Image J.

2.4.9 Circularisation reverse transcription PCR

5 μg of total RNA was circularised using T4 RNA ligase (1 x T4 RNA ligase reaction buffer, 10 units of T4 RNA ligase, 1 mM ATP, 2 units Turbo DNase, 40 units RNasin) at 37 °C for 1 hour. This was diluted to 100 μl in nuclease free water and subjected to phenol:chloroform (1:1) extraction. For this, 100 μl of phenol:chloroform was added and the mixture was vigorously vortexed for 20 seconds. The mixture was centrifuged at 16,300 g for 30 seconds at room temperature. 100 μl of the aqueous phase was removed and the DNA was precipitated at -80 °C for 1 hour in 1/10th volume of 3 M NaOAc at pH 5.2,3 volumes of 100 % ethanol and 1 μl of Glycoblue coprecipitant.

The circularised RNA was pelleted by centrifugation at 20,000 g for 30 minutes at 4 °C. The pellet was resuspended in 20 μl nuclease free water. 5 μl of this solution was used (in a 20 μl reaction) for reverse transcription across the circularised junction using the Ominiscript reverse trascriptase kit as per the manufacturer's instructions. 5 μl of this reaction was used for PCR to amplify the reverse transcribed junction sequence using Omniscript reverse transcriptase as per manufacturer's instrcucitons. The PCR product was then resolved on a 1% agarose gel (section 2.2.3). Concatenation of tRNAs can lead to incrementally larger products. Hence, gel extraction of the PCR product at the predicted product size was required. The DNA was extracted from the gel slice using the QIAquick Gel Extractionkit and then cloned into a Zero Blunt TOPO PCR cloning kit according to their respective manufacturers' instructions. The insert was then sequenced using the M13 forward sequencing primer.

Primers are given in table 2.7. Note that the reverse primer was used for the reverse transcription and the PCR.

Transcript		Sequence
12S	Forward	AAACTTAAGGGTCGAAGGTG
	Reverse	GGTTAATCACTGCTGTTTCC
16S	Forward	GCAGCCGCTATTAAAGGTTC
	Reverse	GCGGTACTATATCTATTGCGC
Ile	Forward	TAATAGGAGCTTAAACCCCC
	Reverse	CTCTATCAAAGTAACTC
Gln	Forward	ATTCTCAGGGATGGGTTCGA
	Reverse	CCAAAATTCTCCGTGCCACC

Leu(UUR)	Forward	CAGTCAGAGGTTCAATTCC
	Reverse	GTTTTATGCGATTACCGGGC
Ser(AGY)	Forward	CCCATGTCTAACAACATGGC
	Reverse	GGCATGAGTTAGCAGTTCTTG

Table 2.7 Primers used for reverse transcription and PCR across the junction caused by circularisation of RNA

2.4.10 RNA-seq

2.4.10.1 Library preparation

RNA was extracted (section 2.4.1) from isolated mitochondria (section 2.2.9). 1 μg was used to prepare a RNA-seq library using the Illumina TruSeq Stranded Total RNA LT Kit A as per the manufacturer's instructions. Ribosomal RNA was depleted using RiboZero Gold kit treatment. The library was quantified using the Agilent TapeStation and the High Sensitivity D1000 Screentape with a v2 MiSeq Reagent kit. The library was sequenced on the MiSeq Illumnia sequencer using a paired-end 500 cycle run (2 x 250 cycles).

2.4.10.2 Bioinformatic analysis

Adapter sequences from the generated FASTQ file were trimmed using *Tim_Galore!*. The reads were then filtered to remove any sequences that were below 20 nt in length. The remaining reads were mapped to the revised Cambridge reference sequence for mtDNA using *TopHat* (Trapnell et al., 2009). 12S and 16S rRNA reads were then removed by the *Samtools* filter (Li et al., 2009). Then, *Bedtools* was used to generate strand-specific coverage files for each sample (Quinlan and Hall, 2010). *Rsubread* was used to produce count tables for the sense and antisense mitochondrially-encoded transcripts to determine steady state levels for each of the transcripts (Liao et al., 2013). *DESeq2* was then used to analyse differential gene expression statistically (Love et al., 2014).

Reads per kilobase of transcript per million mapped reads = 10^9C/N*L, where,

C = Number of reads mapped to a gene, N = Total mapped reads in an experiment and L= mt-mRNA length in base pairs

2.5 Analysis of mitoribosomes

2.5.1 Sucrose gradient fractionation

2 ml of 10-30% linear sucrose gradients in 1 x *GRADIENT BUFFER* were prepared in 11 x 35 mm thin wall polypropylene ultracentrifuge tubes using Biocomp Gradient station. 750 µg of cell lysate or mitochondrial lysate was loaded onto the top of the tube. The tube was centrifuged for 2 hours and 15 minutes at 100,000 g at 4 °C (39,000 rpm, Beckman Coulter TLS-55 rotor). 100 µl fractions were taken from the top of the gradient. 7 µl from each fraction were used for Western blotting (section 2.2.7).

2.5.2 Quantitative- gradient fractionation – mass spectrometry (qGFMS)

For qGFMS, 6 x 15 cm dishes of Hap1 control and YbeY (-/-) Hap1 cells were grown in heavy *SILAC MEDIUM* and 6 of both were grown in light *SILAC MEDIUM*. The 4 different conditions (heavy control, heavy knockout, light control, light knockout) were harvested and pelleted by centrifugation at 1200 rpm for 3 minutes, washed with 1 x PBS and re-pelleted. The cells were resuspended in 20 ml of 1 x PBS and quantified using the Pierce BCA protein assay kit as per manufacturer's instructions. The induced heavy cells were mixed with light uninduced cells in equal concentrations. Similarly, uninduced heavy and induced light cells were mixed in equal concentration. 50 µg of the heavy cells was kept aside. The cells were pelleted and mitochondria were isolated using the Balch homogeniser (section 2.2.9). The mitochondria were lysed with 100 µl of *LYSIS BUFFER 1* and incubated on ice for 15 minutes. This was centrifuged at 8000 rpm for 5 minutes at 4 °C. 750 µg of lysate was run on a 10-30% sucrose gradient as described in section 2.5.1. The fractions were run 4 mm into 4-12% Bis-Tris polyacrylamide gel (section 2.2.7). The gel was stained for 1 hour in SimplyBlue Safestain and destained for 1 hour (20% methanol, 10% acetic acid). The stained 4 mm region was cut and the slice was analysed by mass spectrometry as described in section 2.5.3.4.

2.5.3 Complexomic profiling

2.5.3.1 Mitochondrial fractionation

Cells of control and induced/ knockout cells were harvested and mitochondria were isolated using the Balch homogeniser (section 2.2.9). For SILAC-complexomic profiling, the different cell lines were grown in heavy or light *SILAC MEDIUM* for 7 doublings and mixed in equal proportion as quantified using the Pierce BCA protein assay kit as per manufacturer's instructions. The pellet was resuspended in 2.5 ml of *SONICATION BUFFER* and sonicated at amplitude 25% for 10 second bursts with 50 second processing time until 100 J had been transferred into the sample, using a Q-700 sonicator using a 1/8" microtip. The samples were centrifuged at 40,000 rpm using a MLA80 rotor for 30 minutes at 4 °C. The supernatant was stored on ice and is the soluble fraction. The soluble fraction and the pellet resuspended in 5 ml of *ACA BUFFER* were centrifuged at 40,000 rpm for 30 minutes. The pellet was then resuspended in 15 µl of *ACA BUFFER* and homogenised using a 100 µl Dounce homogeniser. This formed the membrane fraction. The soluble fraction was concentrated further to a volume of 250 ml with a 3 kDA MWCO Sartorius Vivaspin 2 centrifugal filter at 7,000 g at 4 °C.

2.5.3.2 Blue native PAGE

9 µg of soluble protein was made up to 10 µl *ACA BUFFER*. 25 µg of membrane protein was made up to 10 µl with *ACA BUFFER* and 0.45% DDM. This was incubated for 20 minutes on ice. Both the soluble and membrane fraction solutions were centrifuged for 30 minutes at 14,000 rpm at 4 °C. After this, the supernatant fraction and solubilised membrane fractions were transferred to new tubes and 0.1125% Coomassie G250 was added to the membrane fraction. 10 µl of BN NativePage 4X sample buffer was added to both samples. The sample was run in duplicates in 3-12% Bis-Tris NativePAGE gels, in duplicate, for western blotting and complexomic profiling. The inner chamber of the gel tank was filled with 1 x NativePAGE running buffer with 1 x cathode buffer. The outer chamber was filled with 1 x NativePAGE running buffer. This gel was then run for 1 hour at 80 V. After one hour, the inner chamber buffer was replaced with 1 x NativePAGE running buffer with 0.1 x NativePAGE cathode buffer additive. The gel was run at 200 V until

the front of the gel has started to leave the bottom of the gel. For western blotting, the gel was briefly washed with methanol before transferring using the wet transfer onto methanol-activated polyvinylidene fluoride (PVDF) membrane in a Mini Trans-Blot electrophoresis transfer cell at a constant current of 300 mA for 60 minutes. For complexomic profiling, the gel was destained using destain (20% methanol, 10% acetic acid) for 1-2 hours. Each lane was then cut into 64 x 1 mm slices using a razor blade and transferred to 1.5 ml tubes (previously washed with 50% methanol and dried).

2.5.3.3 In-gel tryptic digestion

Each slice was washed with 100 µl HPLC water for 30 minutes and then washed again with 20 mM Tris-HCl (pH 8) for 60 minutes. The liquid was removed and the slice was incubated in 100 µl of 20mM Tris-HCl (pH 8) and 50% acetonitrile (ACN) for 1 hour at RT. The solution was removed and 20 µl 100 % ACN and incubated for 15 minutes. The liquid was then removed and the gel was dessicated in a Thermo Savant SpeedVac at 37 °C. The gel was then resuspended in 12.5ng/ml trypsin containing 20 mM Tris HCl (pH 8), 5 mM CaCl2 and incubated at 37 °C overnight. The digested peptides were incubated with 15 µl of 60% ACN, 4% formic acid solution. The liquid from this reaction was centrifuged for 15 minutes. The liquid was then dessicated in a Speedvac (37 °C for 15 minutes). The residual pellet was resuspended in 14 µl of 2% ACN and 0.1% formic acid.

2.5.3.4 Mass spectrometry and analysis

The peptides were analysed with LC-MS/MS on a Thermo Scientific Orbitrap LTQ XL spectrometer with a nanospray inlet interface coupled with a Proxeon EasynLC nano chromatography. For accurate mass measurements, the internal 'lock mass' standard of 445.120m/z was used.

For each lane, all samples were run starting with the highest molecular weight slice and, to ensure that chromatographic conditions were maintained throughout the batch, each sample was analysed with no intervening washes.

To identify peptides, resulting data files were processed using Proteome Discoverer software (Thermo). Resulting spectra from the RAWfile were submitted to the in-house Mascot server and peptides were assigned using the Uniprot *Homo sapiens*

protein database, specifying parameters for use of trypsin digest, allowing for the possibility of one uncleaved lysine or arginine residue per peptide, allowing for peptides to carry a deviation of 10 ppm around calculated peptide values to allow matches with experimentally observed values, and fragment size was set at 0.5 Da. Following quantification of each identified peptide using Protein Discoverer, a multi-consensus report was generated, allowing the relative quantification of proteins to be obtained from the relative quantification of peptides. For this, the mean value for the three highest intensity peptides for each protein was taken and this was used as a representative value for that protein. This was performed for each gel slice and a profile for each protein for each lane can be determined.

2.5.3.5 Analysis of SILAC samples

Generally, SILAC (stable isotope labelling of amino acids in cell culture) was performed in duplicates with reciprocal labelling. Comparing protein ratios can then be compared from both experiments on a scatter plot. Proteins that behave differently in both experiments can be discarded.

Proteins were identified using the ANDROMEDA algorithm of the MAXQUANT software package by comparing the proteins to the human UniProt database. The peptide information from both dataset pairs were combined and filtered using the PERSEUS software, removing proteins only identified by site, that matched a decoy database of random peptides deliberately introduced to identify noise, and those peptides identified as contaminants. Then, proteins identified by one peptides and those proteins that were identified by two or fewer peptides were removed. The reciprocal of the protein orientation was calculated for the reverse labelling orientation. Ratios for both samples and a base two logarithm were calculated. The processed data was plotted on a X-Y scatter plot using Prism 7. Preliminary assessment of heavy label incorporation was performed by manually processing the peptide information of the heavy-only lanes by MAXQUANT.

2.6 qPCR to measure mtDNA copy number

The DNA was extracted from Hap1 cells using DNeasy Blood and Tissue kit as per manufacturer's instructions. Mitochondrial DNA copy number was quantified by measuring two mitochondrial amplicons relative to a nuclear control gene, B2M, using the $2^{-\Delta\Delta CT}$ method. The average of the two amplicons was used as the mtDNA

copy number. 10 ng of gDNA was used as a template and all samples were amplified in quadruplicates in 25 µl reactions. The TaqMan gene expression master mix was used with 900 mM forward primer and 250 nM probe. The reaction was performed as per the manufacturer's instructions. Sequence of the primers and probes are detailed in table 2.8.

Primer/ Probe		Sequence
B2M	Forward	TGCTGTCTCCATGTTTGATGTATCT
	Reverse	TCTCTGCTCCCCACCTCTAAGT
	Probe	Fam-TTGCTCCACAGGTAGCTCTAGGAGG-Tamra
mt3211	Forward	CACCCAAGAACAGGGTTTGT
mt3298	Reverse	TGGCCATGGGTATGTTGTTAA
mt3242	Probe	Fam-TTACCGGGCTCTGCCATC T-Tamra
mt9827	Forward	CGT CATTATTGGCTCAAC
mt9974	Reverse	GATGGAGACATACAGAAATAG
mt9852	Probe	Fam-ACTATCTGCTTCATCCGCCACTAA-Tamra

Table 2.8 DNA oligonucleotide and probe sequences used for qPCR

2.7 [^{35}S]-L-methionine labelling of mitochondrially-translated proteins

Al incubation steps were performed at 37 °C and 5% CO_2. HEK293 or Hap1 cells were grown in 6 well corning dishes to up to 80% confluency. Initially, the cells were washed twice with methionine and cysteine-free medium and incubated with this medium for 5 minutes. After 5 minutes, this was replaced with DMEM supplemented with 2 mM Glutamax, 110 mg/L sodium pyruvate, 96 mg/ml cysteine and 5% dialysed FBS and incubated for 20 minutes. Then, 100 µg of cytoplasmic translation inhibitor, emetine was added and the cells were incubated for 30 minutes at 37 °C. 166.6 mCi/ml [^{35}S]-L-methionine was added to each well and incubated for 30 minutes (this incubation time was increase for time course assays). The cells were harvested and centrifuged at 5000 rpm for 3 minutes. The pellet was washed with 1 x PBS and centrifuged again.

The pellet was resuspended in 20 µl of *PIC* buffer. 0.1 % DDM and 50 U Benzonase was added and incubate on ice for 20 minutes. 1% SDS was added and vortexed vigorously. This was left on ice for 30 minutes. The protein was then quantified using

the BioRAD DC assay kit as per manufacturer's instructions. 30 μg of protein was made up to 15 μl loading volume with water, containing 1 x NuPAGE LDS Sample buffer. This was incubated at room temperature for 20 minutes. This was loaded onto a 10-20% Tris-glycine gradient SDS polyacrylamide gel and run at 85V for 3 hours or until the gel front has reached the bottom of the gel. The gel was briefly washed with water and stained with SimplyBlue Safestain for 1 hour. The gel was then destained with coomassie destain/fixer (20% methanol, 7% acetic acid, 3% glycerol) for 1 hour and dried using a Bio-Rad Model 583 gel dryer at 80 °C for 1 hour. The gel was exposed to a storage phosphor screen and scanned using a Typhoon 9410 scanner

Modifications to this protocol:
For added chloramphenicol treatment, cells were incubated for 22 hours with 40 mg/ml chloramphenicol, prior to the assay.

2.8 Immunoaffinity purification (with and without SILAC)
12 x 15 cm dishes of HEK293 cells containing the doxycycline-inducible flag/strep2-tagged gene were grown in heavy and light *SILAC* MEDIUM each. After 7 doublings, 6 plates of the heavy and 6 plates of the light-labelled cells were induced with 100 ng/ml for 24 hours. The 4 different conditions (heavy induced, heavy uninduced, light induced, light uninduced) were harvested and pelleted by centrifugation at 1200 rpm for 3 minutes, washed with 1 x PBS and re-pelleted. The cells were resuspended in 20 ml of 1 x PBS and quantified using the Pierce BCA protein assay kit as per manufacturer's instructions. The induced heavy cells were mixed with light uninduced cells in equal concentrations. Similarly, uninduced heavy and induced light cells were mixed in equal concentration. 50 μg of the heavy cells was kept aside. The cells were pelleted and mitochondria were isolated using the Balch homogeniser (section 2.2.9). The mitochondrial were lysed with 500 μl of *LYSIS BUFFER 1* and incubated on ice for 15 minutes. The solutions were centrifuged at 8000 rpm for 5 minutes. Anti-flag antibody coated beads were washed according to the Sigma-Aldrich FLAG immunoprecipitation kit manufacturer's instructions. The supernatant was then incubated on the beads for 3 hours on a roller at 4 °C. The proteins were eluted as per the manufacturer's instructions. All the protein and 25 μg of the heavy cell protein

was run on a 4-12% Bis-tris polyacrylamide gel as described in section 2.2.7. The gel was stained for 1 hour with SimplyBlue Safestain and destain for 1 hour (20% methanol, 10% acetic acid). All the lanes were cut into 10 equal slices. For the immunoaffinity purified proteins-containing lanes, all the 10 slices were submitted, while only three slices were sent for the heavy-only lanes. These gel slices were analysed as described in section 2.5.3.3 and 2.5.3.5. If proteins were not SILAC-labelled, proteins were analysed according to section 2.5.3.3 and 2.5.3.4.

3 MRM1 – A strongly conserved large ribosomal RNA-modifying enzyme

3.1 MRM1 – A methyltransferase that modifies 16S rRNA of the mitochondrial large subunit

3.1.1 Mitoribosomal epitranscriptome

The ribosome consists of protein components encapsulating a catalytic RNA core. This ribosomal RNA (rRNA) core undergoes various post-transcriptional chemical modifications. The rRNA of bacterial and eukaryotic cytoplasmic ribosomes contain over 30 and 200 chemical post-transcriptional modifications, respectively, including base methylation, 2'-*O*-ribose methylation and pseudouridylation. However, of these, only a few modifications are conserved in mitochondrial ribosomes.

In yeast, the mitoribosome is composed of a 37S small subunit with a 15S rRNA component, and a 54S large subunit with a 21S rRNA component. The 15S rRNA contains one known modification, a pseudouridylation of which the enzyme and the exact site of modification still need to be identified. The 21S mt-LSU RNA contains one pseudouridylation at position 2819 and two 2'-*O*-ribose methylations at G2270 and U2791 in the peptidyl transferase centre of the ribosome (Klootwijk et al., 1975; Sirum-Connolly et al, 1995).

The mammalian mitochondrial ribosome consists of a 28S small subunit with a 12S rRNA and a 39S large subunit with a 16S rRNA. Both rRNAs have five conserved modified nucleotides each. The small subunit undergoes methylations at U429, C839, C841, A936 and A937 (human numbering) (Figure 3.1.1). The large 16S rRNA contains three 2'-*O*-ribose methylations at G1145, U1369 and U1370, a pseudouridylation of U1397 and the base methylation of A947 (Figure 3.1.2). The exact function of the modifications is unknown, but it is suggested that they may be required for RNA recognition during translation, to induce and maintain correct RNA secondary structure or to facilitate inter-ribosome subunit association (Decatur and Fournier, 2002; Sirum-Connolly et al., 1995; Rorbach & Minczuk, 2012).

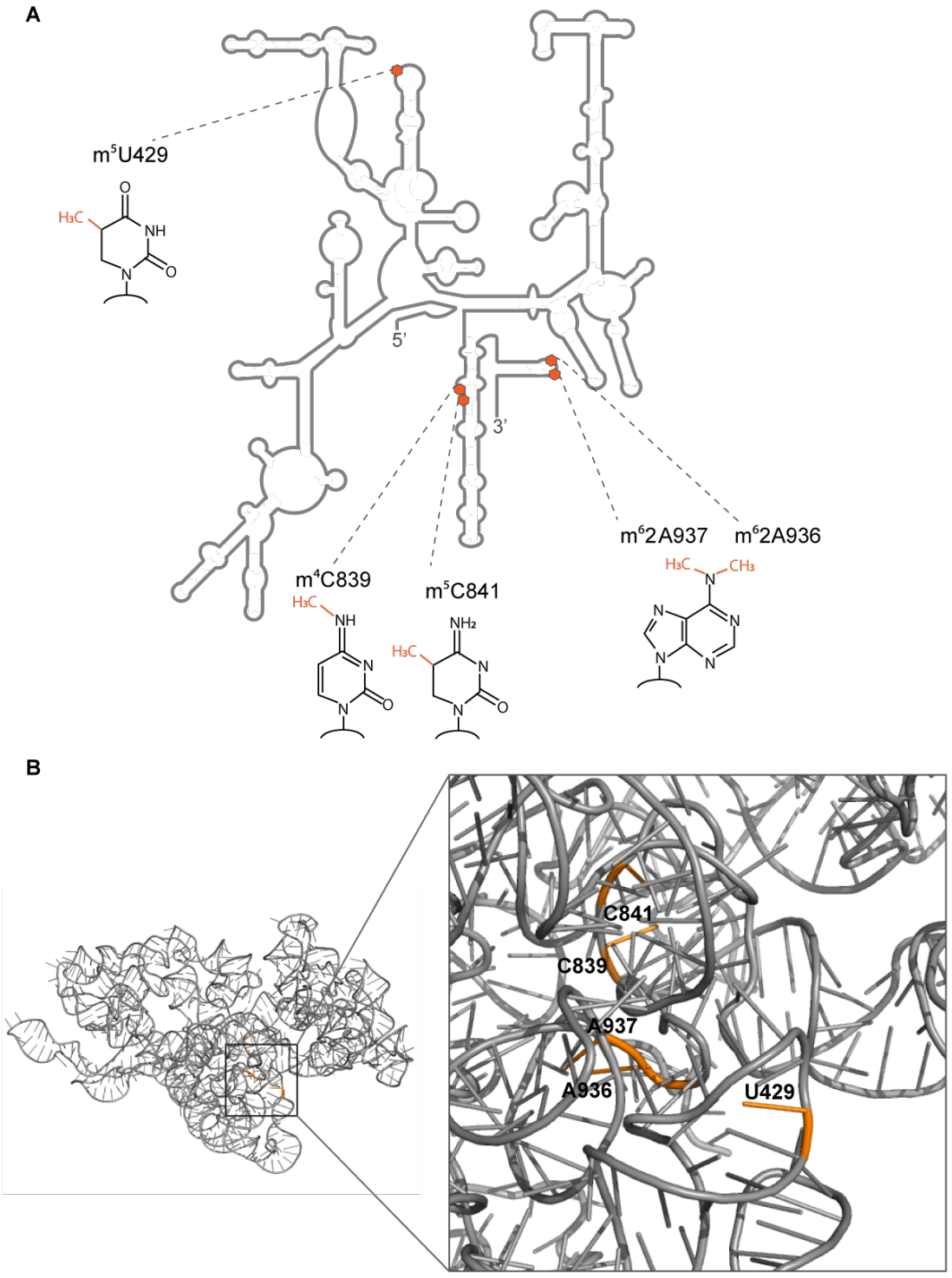

Figure 3.1.1 Chemical modifications of the 12S mt-SSU rRNA. (A) Schematic representation of the secondary structure of the mammalian 12S rRNA and the positions of the chemical modifications on it. (B) The tertiary structure of the 12S rRNA (facing the rRNA from the subunit interface) showing the close proximity of the modified residues to each other and to the subunit interphase where the recognition of the mRNA occurs. (PDB: 5AJ4)

The modifications on the mt-SSU rRNA occur at the site of mRNA recognition near the subunit interphase (Figure 3.1.1). The best characterized mt-SSU rRNA modifying enzyme is a dimethyladenosine transferase, TFB1M, which performs a highly conserved dimethylation at adenines residues, A936 and A937 (based on human numbering) on the 12S rRNA mammalian mitochondrial rRNA (Seidel-Rodol *et al.*,2003). In bacteria (positions A1518 and A1519 modified by KsgA) and yeast cytoplasm (positions A1779 and A1770 modified by Dim1p), loss of the equivalent modifications from the rRNA does not cause a significant decrease in mt-SSU biogenesis (LaFontaine et al., 1998; Xu et al., 2008). The modification is not present in yeast mitochondrial rRNA. However, in mammalian mitochondria, knockout of TFB1M causes a reduction in 12S rRNA steady state levels, mtSSU assembly and mitochondrial translation. A loss of TFB1M is embryonic lethal in mice. However, a conditional knockout of TFB1M leads to impaired mt-SSU biogenesis and translational defects (Metodiev *et al.*, 2009).

Another modifier of 12S rRNA is NSUN4, which methylates C841 in (human numbering). In bacteria, the NSUN4 homolog, YebU methylates at equivalent position 1407 of the SSU rRNA. It performs this function only after the rRNA has been assembled into the SSU. Loss of the protein leads to a growth phenotype and a loss of cell viability (Andersen and Douthwaite, 2006). Similar to TFB1M, loss of mammalian mitochondrial NSUN4 leads to embryonic lethality and a conditional knockout in mice leads to a severe translational defect (Metodiev *et al.*, 2014). Unlike homologous methyltransferases in bacteria, NSUN4 does not have a RNA binding domain. Hence, NSUN4 forms a complex with a RNA-binding protein MTERF4, and together, the complex assists in mt-LSU assembly. Moreover, this function in mt-LSU biogenesis is independent of the NSUN4 ability to catalyse the methylation of C841 (Camara *et al.,* 2011; Metodiev et al., 2014; Spahr et al., 2012). Knockout of NSUN4 does not affect the modification of A936 and A937 by TFB1M suggesting that the two modifications happen independent of each other (Metodiev et al., 2014). The mammalian mt-SSU rRNA has two further modifications of which the responsible methyltransferases have yet to be identified (m^5U429 and m^4C839) (Rorbach and Minczuk, 2012).

The catalysis of peptide bond formation in the ribosome occurs in the large subunit, namely at the peptidyl transferase centre. This region is divided into the A-site which

binds the aminoacyl tRNA and the P-site which binds the peptidyl-tRNA, and the rRNA domains that binds to the tRNAs in these sites are called the A-loop and P-loop respectively. Chemical modification of the rRNA conserved in the mitoribosome are concentrated on the A-loop and P-loop.

The A-loop is modified at positions U1369 and G1370 (human numbering) which directly interacts with the aminoacyl-tRNA (Greber et al., 2015, Rorbach et al., 2014). In *E.* coli, RrmJ methylates U2552 (equivalent to human mitochondrial U1369 and yeast mitochondrial U2791). This modification occurs at later stages of ribosomal assembly (Caldas et al., 2000a; Caldas et al., 2000b). Absence of RrmJ causes a loss of programmed frameshifting, decreased translation and consequently, a growth defect (Caldas et al., 2000a). In yeast mitochondria, the equivalent methylation is performed by Mrm2p. Mrm2p associates with the assembled mt-LSU, suggesting that, similar to bacterial RrmJ, it is also involved with late stage maturation of the LSU. Additionally, a loss of Mrm2p in yeast leads to a thermosensitive growth defect (Pintard et al., 2002). In the mammalian mitoribosome, MRM2, an ortholog of bacterial RrmJ and yeast Mrm2p, methylates U1369 on the A-loop. Sucrose gradient fractionation of mammalian mitochondria shows that MRM2 co-migrates with the mt-LSU and the fully associated ribosome. Moreover, depletion of MRM2 causes a loss of stability of the mt-LSU and leads to a translational defect and respiratory deficiencies (Rorbach et al., 2014).

On the other hand, the G1370 modification is not conserved in bacteria or yeast mitochondria. In the mammalian mitoribosome, this residue in the 16S mt-rRNA, also found on the A-loop, is methylated by MRM3. Sucrose gradient fractionation and western blot analysis shows that MRM3 associates with the mt-LSU, but, unlike MRM2, it does not associate with the assembled ribosome. A loss of MRM3 and/or Gm1370 leads to instability of the mt-LSU and a defect in translation. Notably, the G1370 modification is reduced if the G1369 modification is not present. This suggests a hierarchical pathway of modifications that control mitoribosome biogenesis (Lee et al., 2013; Rorbach et al., 2014). However, not all modifications are hierarchical. As described earlier, the TFB1M modifications of the 12S rRNA are not dependent on NSUN4 modifications (Metodiev et al., 2014).

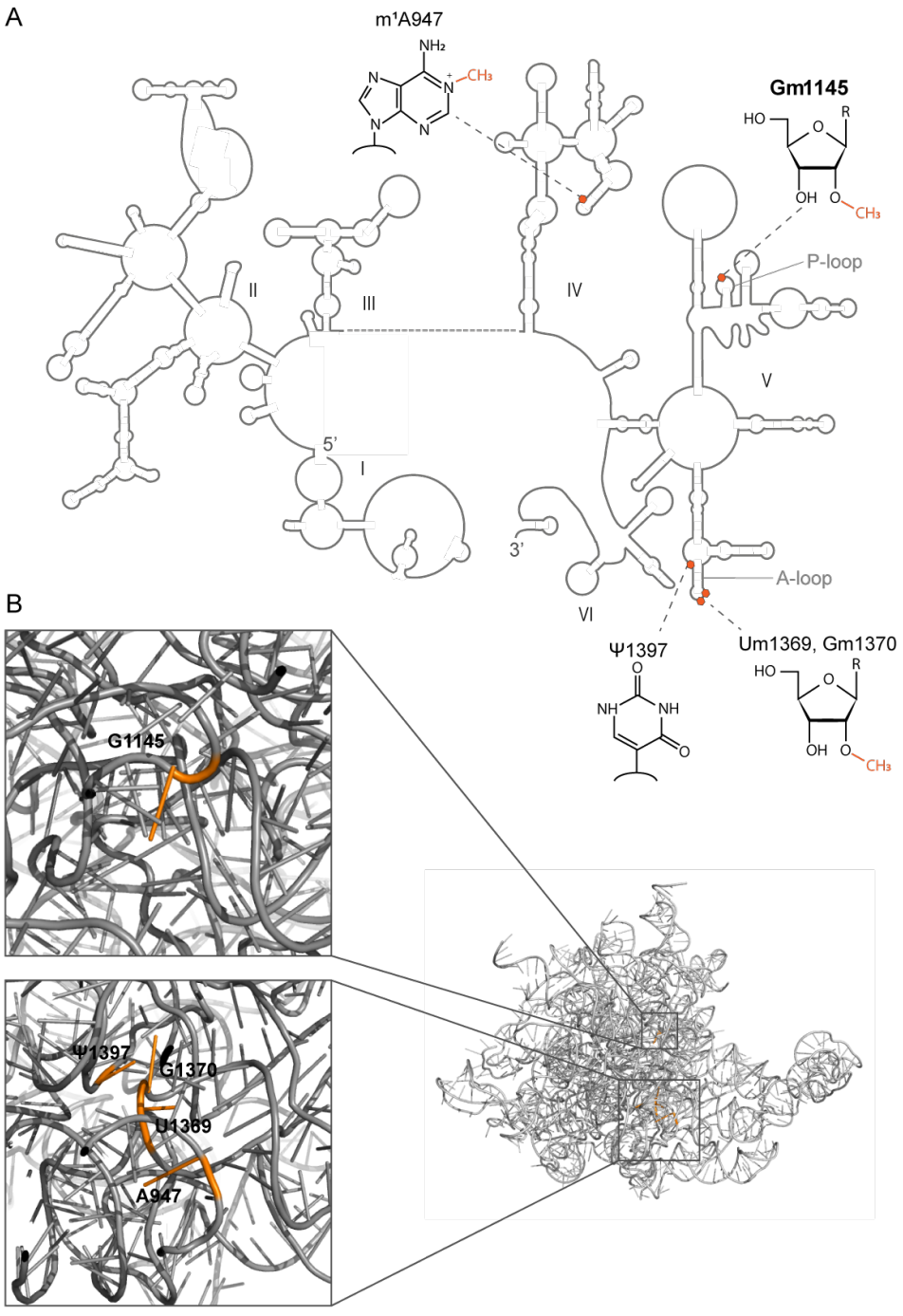

Figure 3.1.2 Chemical modifications of the 16S mt-SSU rRNA. (A) Schematic representation of the secondary structure of the 16S rRNA and the positions of the chemical modifications on it. The catalytically important P-loop in the peptidyl (P) site and the A-loop in the aminoacyl (A) site have been indicated. These loops are important in the recognition and binding to their respective tRNAs. (B) The tertiary structure of the 16S rRNA (facing the rRNA from the subunit interface) showing the close proximity of the modified residues to each other and to the subunit interface where the recognition of the mRNA occurs. It shows that even though A947 is not close to the A-loop in the secondary structure, it is brought close to the A-site after RNA folding. (PDB: 5AJ4)

Recently, analysis of the difference between RNA sequences and the DNA template sequence identified TRMT61B, a tRNA-modifying enzyme, as the enzyme responsible for the formation of m^1A947 in the mt-LSU rRNA. In bacteria, mutation of this position causes a deficiency in translation (Bar-Yaacov *et al.*, 2016). Analysis of the conservation of this modification through evolution suggests that it is not a universal modification. In about 10% of mammalian species, mitoribosomes and cytoplasmic ribosomes do not carry this modification and this nucleotide is replaced by a uridine. In bacteria, this position is replaced by an unmodified guanine. The adoption of a tRNA-modifying enzyme to control modification, instead of an encoded adenine or guanine at this site, suggests an additional level of control on the biogenesis of the ribosome. (Bar-Yaacov et al., 2016; Bohnsack and Sloan, 2017). However, the fact that this modification evaded detection until only recently suggests that there might be more rRNA modifications and modifying enzymes yet to be discovered.

Mammalian 16S rRNA also has a pseudouridine conversion at position 1397. Recently, a potential candidate responsible for this modification was identified as pseudouridine synthase, RPUSD4 (Antonicka et al., 2017; Zaganelli et al., 2017). This enzyme was shown to bind to 16S rRNA, $tRNA^{Met}$ and $tRNA^{Phe}$, and knockdown of the protein in human cells led to a reduction in the steady state levels of 16S rRNA and a defect in mt-LSU assembly, resulting in a loss of mitochondrial translation (Arroyo et al., 2016; Antonicka et al., 2017; Zaganelli et al., 2017). However, the corresponding modification in yeast is dispensable (Ansmant *et al.*, 2000).

3.1.2 MRM1 and the 16S rRNA modification Gm1145

The P-loop of the 16S rRNA is an important part of mitoribosomal the peptidyl transferase centre, as it plays a role in the peptidyl-tRNA binding in the P-site. In human mitochondria, the P-loop undergoes a 2'-*O*-ribose methylation at G1145 (Baer & Dubin, 1981). In *E. coli*, the equivalent site on the LSU rRNA, G2251, is modified by the methyltransferase RlmB. Knockout of RlmB in *E. coli* showed no effect on ribosome assembly and function (Lovgren & Wikstrom, 2001). However, ablation of the homologous mitochondrial protein Mrm1p (Pet56p) in yeast causes a loss of the Mrp7p protein component of the mitochondrial ribosomal LSU (homologous to human mitochondrial L27 and *E.coli* 27 ribosomal protein) (Sirum-Connolly & Mason., 1993; Sirum-Connolly et al., 1995).

In mammalian mitochondria, this highly conserved modification is introduced by MRM1. Human MRM1 is a member of the SpoU superfamily. It is highly conserved except in certain fungal and metazoan clades (Figure 3.1.3). Like other 2'-*O*-methyltransferases in this family, MRM1 contains a S-adenosyl-L-methionine (AdoMet)-binding motif and the SpoU-type guanosine 2'-*O*-methyltransferase domain. However, the importance of this methylation to cell viability and translation varies between organisms (Rorbach *et al.*, 2014).

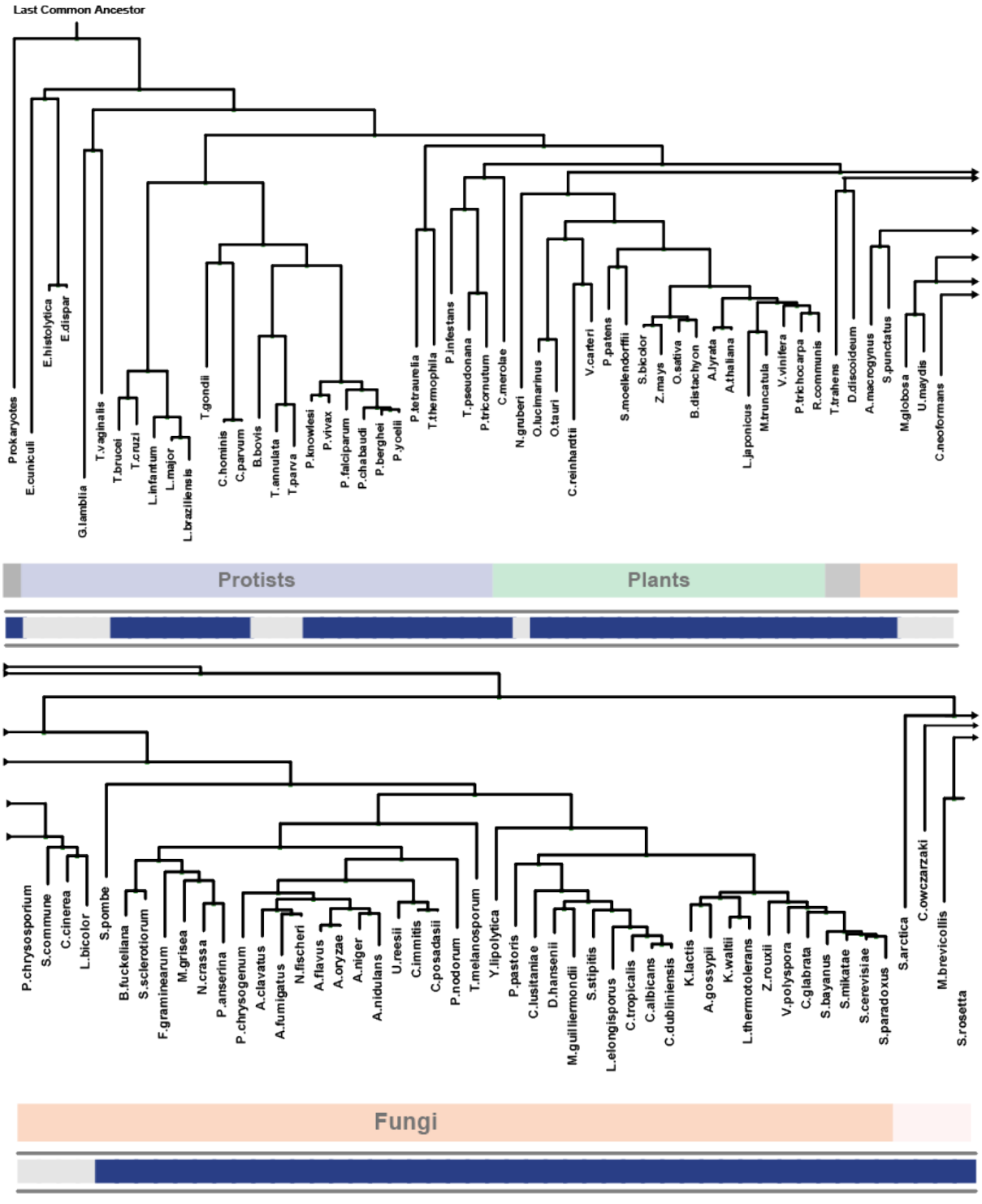

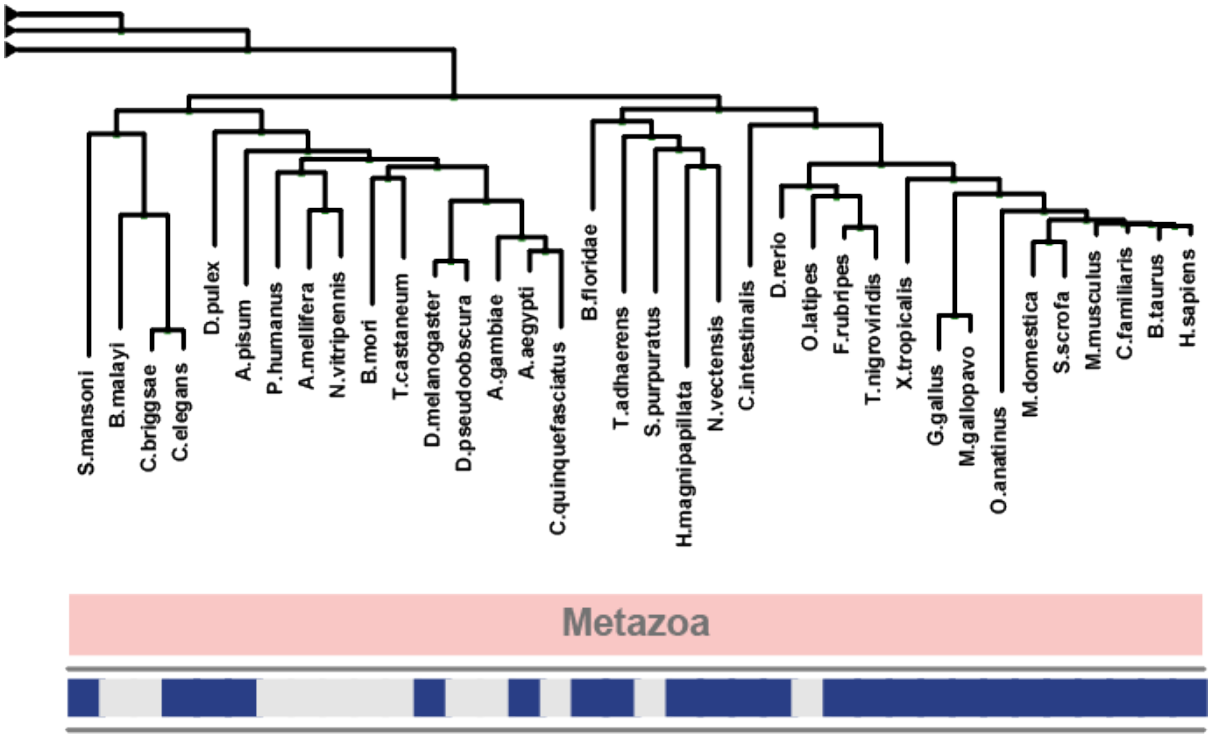

Figure 3.1.3 Conservation and phylogeny of MRM1. Evolutionary conservation of MRM1 was calculated using CLIME portal online web service (gene-clime.org). The bottom bar indicates the presence of the protein in the species indicated above on the evolutionary tree. Grey indicates absence of the protein while blue indicates presence of the protein. The length of the branches in the phylogenetic tree indicate divergence of the protein since a common ancestor.

Mitochondrial localisation of MRM1 was shown by immunofluorescence. A strong co-localisation signal between transiently expressed MRM1 with mitochondria was observed. In addition, subcellular fractionation of HeLa cells in combination with western blotting confirmed that MRM1 is localised in the mitochondrial matrix (Rorbach *et al.*, 2014).

Recently, work using an alternative DNAzyme strategy showed that that MRM1 is required for the ribose methylation of G1145. This method relies on the ability of 2'-*O*-ribose methylated RNA to resist site-specific cleavage by DNAzymes. This experiment showed that upon siRNA knockdown of MRM1, the sensitivity of the 16S rRNA to DNAzyme-cleavage at the G1145 site increases (Lee and Bogenhagen, 2014).

The function of MRM1 and the G1145 modification is still unclear. In the bacterial ribosome, G2252 and G2251 (equivalent to human mitochondrial G1146 and the MRM1 target G1145) in the P-loop form Watson-Crick base pairs with the C74 and

C75 positions at the 3' end of tRNAs (Jenni & Ban, 2003). Analysis of the porcine mitoribosomal cryo-EM structure shows that this interaction is retained in mammals (Greber *et al.*, 2015). The modification of G2251 may influence base pairing with the two tRNA cytidines, therefore ensuring efficient peptidyl transferase activity. G2251 interacts with U2585 on domain V. Upon tRNA entry into the P-site, a local conformational change occurs. This disrupts the interaction between G2251 and U2585 and mediating progression of peptidyl-transferase activity (Green et al., 1997).

2'-O-ribose methylations also serve various other roles depending on the context. It is a highly prevalent modification, found in tRNAs, rRNAs, mRNAs and miRNAs in all three domains of life. It provides stability to RNA in conditions of extreme temperature and pH by reducing the availability of the oxygen at the 2' site and preventing nucleophilic attack and cleavage of the phosphodiester bond (Motorin and Helm, 2010). Methylation has also been implicated in regulation of gene expression, resistance to aminoglycoside antibiotics in bacteria, as markers of innate immunity, and as regulators of translation of viral mRNAs (Marchand *et al.* 2016).

In many previous studies, knockout cell lines and mouse models were used to demonstrate the function of specific modifications within the larger context of mitochondrial translation and ribosomal biogenesis. Therefore, to identify the role of MRM1 and the Gm1145 modification in the human mitochondrial ribosome, we generated MRM1 knockout cell lines to characterise mitochondrial function in the absence of MRM1 and to elucidate the purpose of the MRM1 modification within the mitochondrial translation apparatus.

3.2 Results – Identification of the function of MRM1 through the generation and characterisation of MRM1 overexpression and knockout cells

3.2.1 Identification of MRM1 interactors using immunoaffinity purification

Firstly, to deduce the function of MRM1 in the mitochondria, doxycycline-inducible MRM1 overexpressing cell lines were generated by transfecting HEK293T cell lines with pcDNA5 vector containing the cDNA for MRM1 with a flag tag and selecting for successful integration using hygromycin selection. Doxycycline induced expression was tested in several clones by Dr Joanna Rorbach (data not shown). Flag epitope immunoaffinity purification of overexpressed MRM1 was used to identify interactors of MRM1 in the mt-LSU. Mitochondria were isolated from 100 ng/ml doxycycline-

induced cells expressing flag/strep2-tagged MRM1. Mitochondrial lysate was incubated with flag immunoaffinity beads and eluted using flag peptide. Preliminary immunopurification identified various non-mitoribosomal associated protein interactors (HSP70, HSPD1, H2A, H2B, H4A, H2A, NDK), mt-LSU components (MRPL19, MRPL28, MRP49, MRPL41), mt-SSU components (MRPS30, MRPS18b, MRPS23, MRPS10, MEPS14, MRPS6, MRPS33), other RNA-binding proteins (LRPPRC, DHX30, PTCD3 and GRSF1) and a nucleotide diphosphate kinase (NME4) (Figure 3.2.1). However, immunoaffinity purification of MRM1 was repeated with SILAC labelling of cells to quantify the strength of interaction with MRM1 (Figure 3.2.2 A, B). Furthermore, Benzonase treatment was also applied to remove possible indirect interactions that may be caused via the MRM1's interaction with RNA (Figure 3.2.3 A, B). This pulldown experiment did not identify mitoribosomal components but mitoribosome biogenesis factor ERAL1 was one of the proteins that were purified.

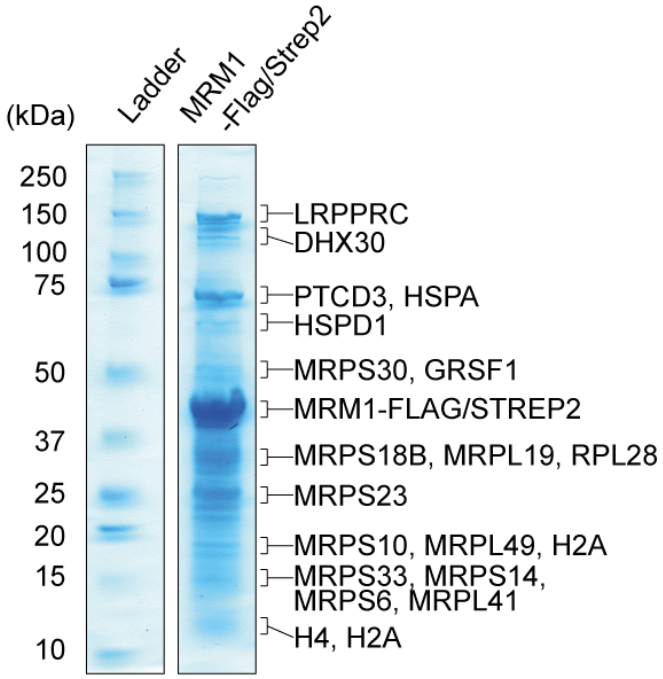

Figure 3.2.1 Immunoaffinity purification of MRM1. Overexpression of MRM1-Flag/Strep2 was induced using 100 ng/ml doxycycline in a HEK293T Flp-In cell line. After 24 hours, the cells were harvested, mitochondria were isolated and the mitochondrial lysate was incubated with beads attached to antibodies against the flag epitope. The beads were washed and the bound proteins were eluted using flag peptide. 30 μg of the eluted protein was resolved on a 4-12% Bis-Tris SDS PAGE gel and the gel was stained using Coomassie Brilliant Blue stain. The prominent bands were cut and analysed using LC-MS/MS.

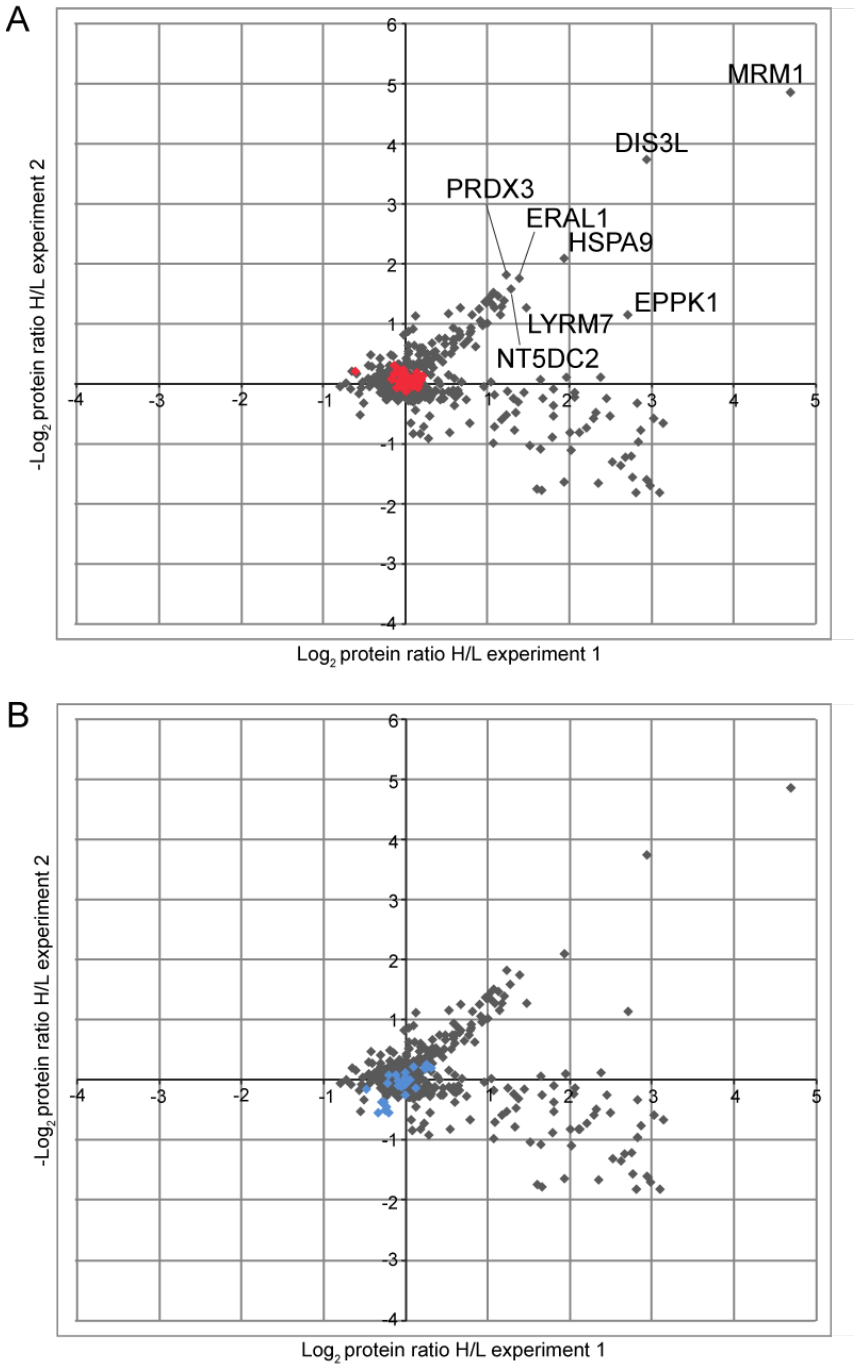

Figure 3.2.2 Proteins associated with MRM1. The doxycycline-inducible cell line was grown in light or heavy SILAC media, one of the two were induced using 100 ng/ml doxycycline, the induced and Uninduced labelled cell lines were mixed in equal proportion and mitochondria were isolated. The lysates were added to flag-affinity beads and eluted using flag peptide. The eluted protein was run on an SDS PAGE gel. Sections of the gel were cut and analysed using LC-MS/MS. The proteins were separated based on stable isotope labelling. The samples were performed in duplicate with reciprocal labelling with each replicate shown on one axis. The graph was plotted using Excel. (A) Components of the mt-LSU are marked with red markers (B) Components of the mt-SSU are marked with red markers

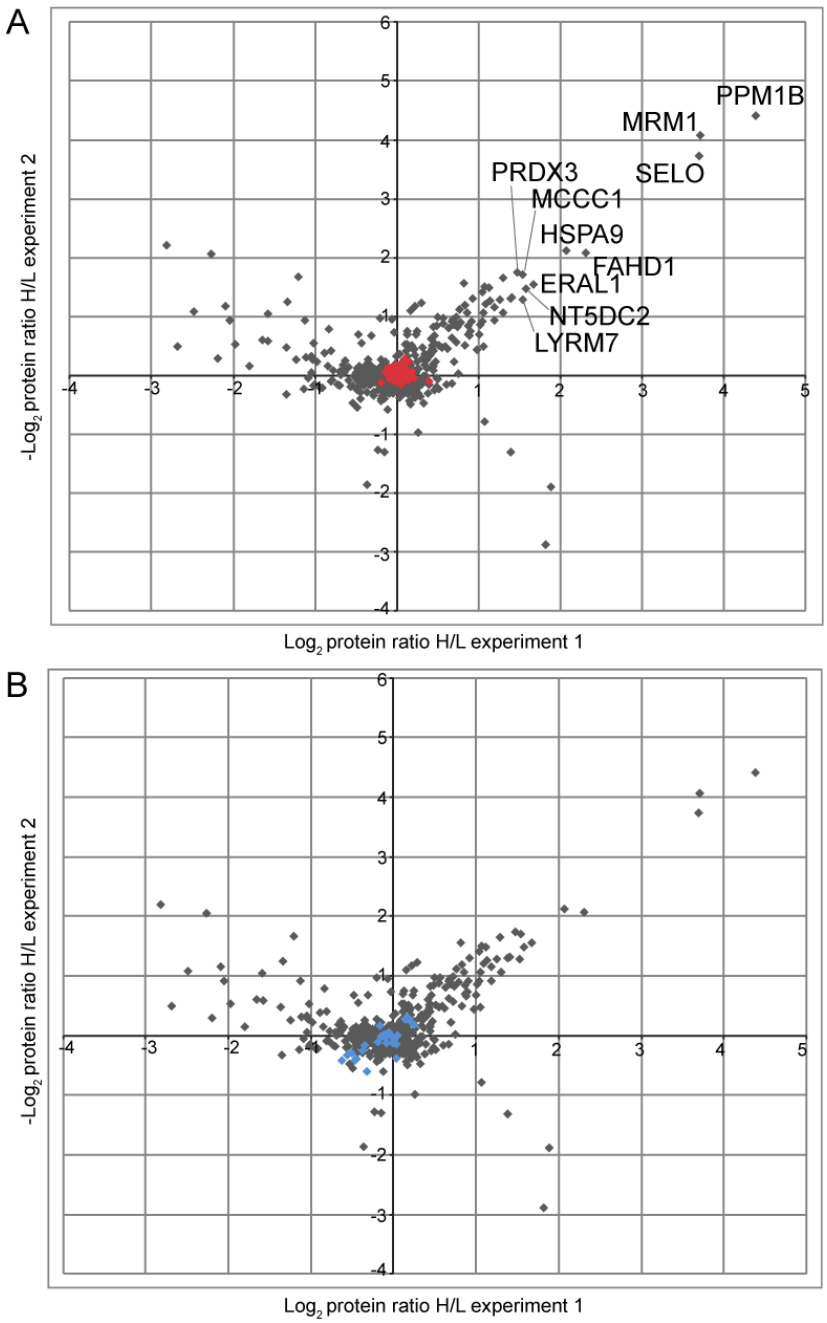

Figure 3.2.3 Proteins associated with MRM1 after benzonase treatment. The doxycycline inducible cell line was grown in light or heavy SILAC media, one of the two were induced using 100 ng/ml doxycycline, the induced and Uninduced labelled cell lines were mixed in equal proportion and mitochondria were isolated. The mitochondrial lysate was split into two, and one sample was treated with 50 U/ml benzonase. The lysates were added to flag-affinity beads and eluted using flag peptide. The eluted protein was run on an SDS PAGE gel. Sections of the gel were cut and analysed using LC-MS/MS. The proteins were separated based on stable isotope labelling. The samples were performed in duplicate with reciprocal labelling with each replicate shown on one axis. The graph was plotted using Excel. (A) Components of the mt-LSU are marked with red markers (B) Components of the mt-SSU are marked with red markers

A recent publication identified that 16S rRNA modifiers interact with the mitoribosome. MRM2 interacts with the mtLSU and the assembled mitoribosome, while MRM3 only interacts with the mtLSU (Rorbach et al., 2014). However, the MRM1 homolog in yeast does not interact with the mitoribosome (Sirum-Connolly and Mason, 1993). It is possible that conditions used in the flag immunoprecipitation may not be idea for preserving MRM1-mitoribosome interactions. Therefore, sucrose gradient fractionation was used to investigate if MRM1 interacts with the mitoribosomes (Figure 3.2.4). This involved resolving the various mitoribosomal assemblies in the cell lysate using a 10-30% (v/v) isokinetic sucrose gradient. Sucrose gradient fractions were then resolved on a 4-12% Tris-glycine SDS-PAGE gel and analysed using western blotting. MRPL12 was used to probe for mt-LSU and MRPLS18b was used to probe for the mt-SSU. This analysis confirmed that MRM1 did not co-localise wth the mt-LSU or the mt-SSU (Figure 3.2.4).

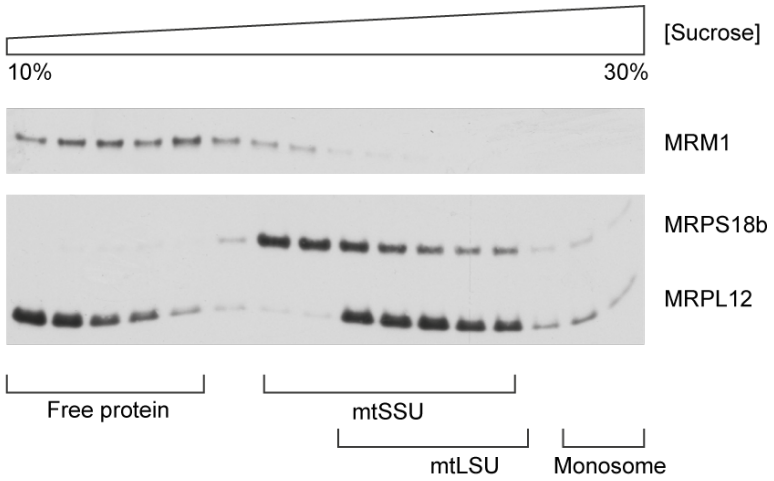

Figure 3.2.4 Analysis of MRM1 interaction with the mitochondrial ribosome. 750 μg of isolated mitochondrial lysate from Hap1 parental cells were separated using 10-30% (v/v) isokinetic sucrose gradient fractionation. 100 μl fractions were then analysed using western blotting. Antibodies against MRPL12 and MRPS18b were used to identify the mt-LSU and mt-SSU, respectively. Antibodies against endogenous MRM1 were used to identify MRM1.

3.2.2 Analysis of the mitoribosomes upon MRM1 overexpression

To analyse the function of MRM1 in the mitochondrial ribosome, overexpression was induced in HEK293T Flp-In cells using 50 ng/ml of doxycycline for 48 hours. Then, the cell lysates were loaded onto an isokinetic sucrose gradient and after ultracentrifugation, 100 µl fractions were resolved in a 4-12% Bis-Tris SDS-PAGE gel. Western blotting using antibodies against components of the mt-LSU (MRPL12) and mt-SSU (MRS18b) were used to analyse changes in ribosomal complexes. This showed no major change in large and small subunits upon MRM1 overexpression. However, a large amount of MRPL12 protein was found in the 'free protein' fractions (fractions 1-4, Figure 3.2.5) in MRM1 overexpression induced cells compared to other sucrose gradients performed before in HEK293T parental or MRM1 deficient cell lines (Section 3.2.5, Figure 3.2.16). Potentially, this could be caused by high levels of MRM1 and suggests that leaky expression of MRM1 in the uninduced cell line may be sufficient to disrupt assembly of the ribosome (Figure 3.2.4).

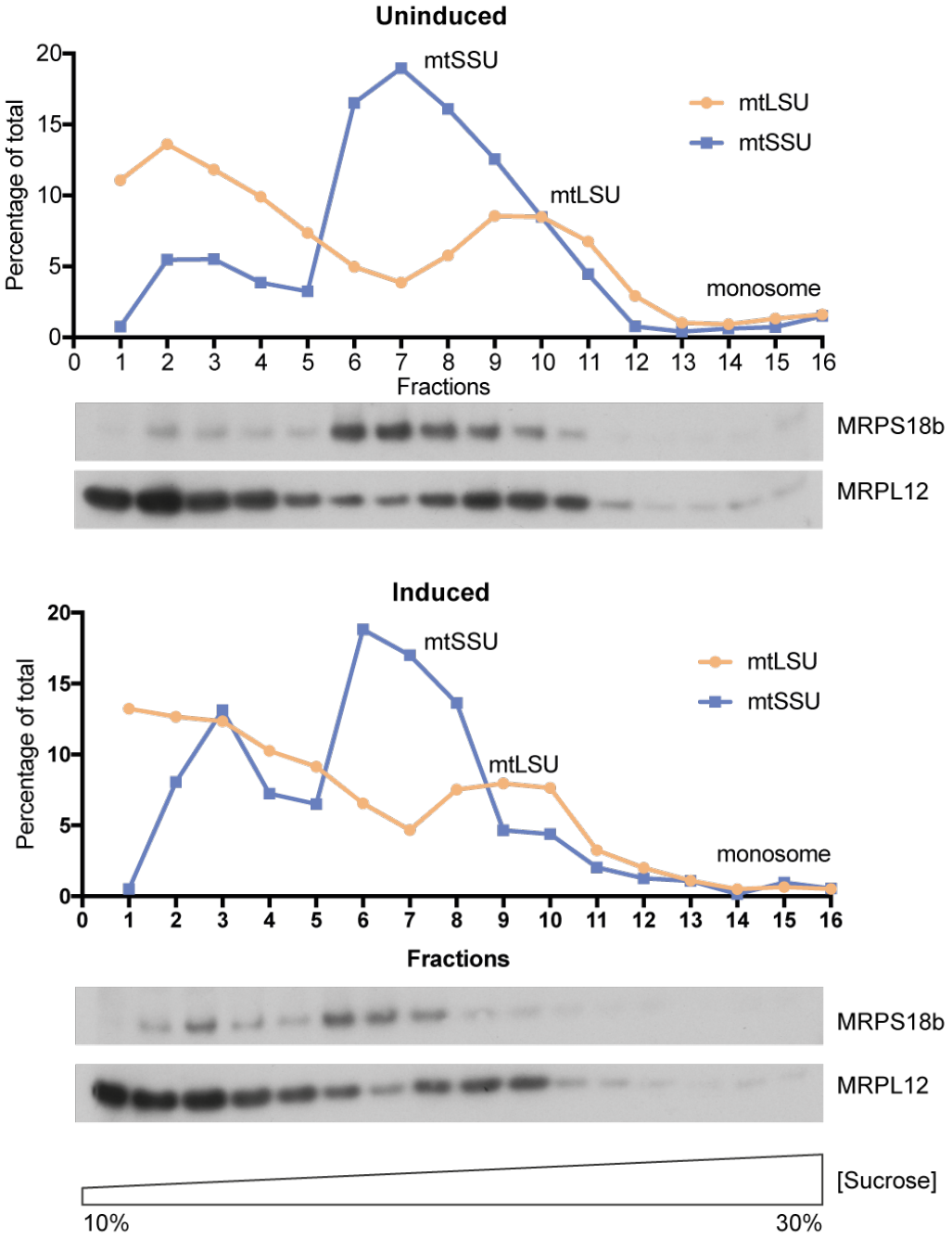

Figure 3.2.5. Assembly of the mitoribosomes in MRM1-overexpressing cells. Total cell lysate from MRM1 overexpressing cells (uninduced and induced for 3 days at 50 ng/ml) were separated in a 0-30% (v/v) isokinetic sucrose gradient and fractionated. The fractions obtained were analysed using western blotting using antibodies specific to mt-LSU (MRPL12) and mt-SSU (MRPS18b). The band intensities were calculated using Image J and the relative band intensity to the total was plotted using Prism 7.

The disadvantage of using isokinetic sucrose gradients followed by western blot detection to investigate mitoribosomal integrity is that only a limited number of mitoribosomal components can be investigated and the comparison of various western blots is mostly qualitative. There, we used complexomic profiling to measure the presence of all the protein components of the mitoribosomes in their various stages of assembly. In this method, mitochondrial membranes from HEK293T control and MRM1 (-/-) cells were isolated, solubilised with detergent and the proteins were resolved on a native PAGE gel. Each lane was cut into 64 X 1 mm slices. The protein composition of each slice was analysed by LC-MS/MS. The intensity of peptide detection was used to generate a heatmap.

As this method had not been previously used to investigate mitoribosomal integrity, various optimisation steps were required namely identifying the correct detergent concentration to solubilise the membrane and freezing the complexes for resolution on a PAGE gel, limiting degradation of the mitoribosomes. The membrane fraction was used because the mitoribosomes is tethered to the inner membrane through the large subunit (Brown et al., 2017; Liu and Spremulli, 2000). The resolved protein complexes were studied by staining the gels with Coomassie Brilliant Blue and western blotting. Inappropriate detergent concentrations caused smearing of the proteins and insufficient membrane solubilisation (as seen in 0.2% DDM, Figure 3.2.6). Above 0.45%, the maximum solubilisation had already occurred, as the western blot bands did not increase in intensity when DDM concentration was increased. Western blot analysis was performed using antibodies against MRPS18b for the small subunit and MRPL3 and MRPL12 for the large subunit. This showed that the gel does not adequately resolve the free mtLSU and mtSSU from the assembled monosome. In the western blot, this appeared as a thick band roughly 2 to 3 MDa in size. In the western blot probing for MRPL12, a smaller band was also observed at about 400 kDa, which corresponds to the ribosomal subcomplex suggested by Wessel *et al.* (2013). Smaller complexes were observed in the soluble fractions (relative to the membrane fractions) indicating possible partially assembled or partially degraded ribosomal complexes (Figure 3.2.6).

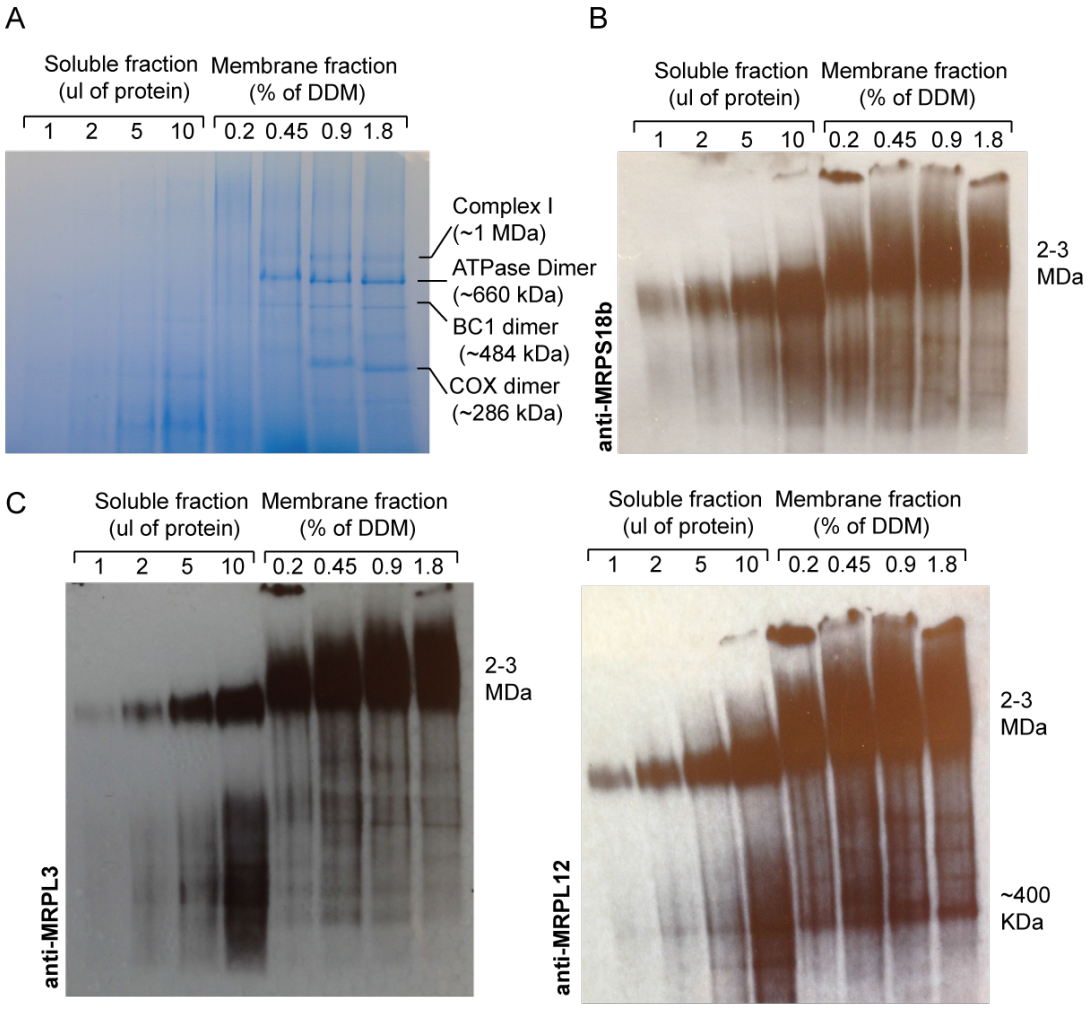

Figure 3.2.6. Optimisation of membrane solubilisation. Isolated mitochondria from HEK293T cells were fractionated into soluble and membrane fractions. Increasing mass of soluble fraction and 2 X 25 μg of membrane fraction solubilised with increasing DDM detergent were resolved on two 3-12% Novex Native PAGE gels. (A) One gel was stained with Coomassie Brilliant Blue to visualise bands corresponding to mitochondrial complexes. (B) Another gel was analysed using western blot using antibodies against mt-SSU component, MRPS18b, and (C) mt-LSU components, MRPL3 and MRPL12.

To verify the results of the sucrose gradients, complexomic profiling was used to analyse cells expressing MRM1. To avoid issues with the side effects of MRM1 leaky expression, HEK293T parental cells were used as the control. Indeed, this showed a marked decrease in ribosomal integrity. Both the mtLSU (Figure 3.2.7) and the mtSSU (Figure 3.2.8) showed a shift in the highest intensity peak to a lower molecular weight (M.W.). This suggested that the highly abundant MRM1 protein in the

overexpression cell line might be interfering with mitoribosomal assembly. This may suggest a role of MRM1 dissociation from the mtLSU as a checkpoint in biogenesis since high abundance of the protein could hinder dissociation of the protein from the rRNA. Moreover, the mtLSU in the overexpression sample shows fewer complexes than the parental control, which shows two major peaks of roughly equal abundance. The mtSSU shows a matching profile to their respective mtLSU profiles, for both the control and the MRM1 overexpression cell line (Figure 3.2.8). Unfortunately, the method does not have sufficient resolution capacity to separate the large and the small subunit.

The multiple peaks in the control sample could have been caused by slightly different treatment of the samples. Therefore, the integrity of Complex I was investigated in both samples (Figure 3.2.9). Complex I in the control sample did not show any notable difference in composition or degradation products. However, compared to the mitoribosomes, Complex I is a smaller complex. It may not be as sensitive to slight differences in treatment. This also showed that an error of approximately 1-2 slices should be considered when approximating the location of the peak. Taking all this into account, the intense peak produced in the overexpression cell line (slice 16) corresponds to the lighter peak of the control sample (slice 15). In particular, the mt-LSU components, MRPL12, MRPL14, MRPL16 and MRPL30 are more abundant in the heavier fraction 13 peak in the control sample than in the lower peak (fraction 15). In the control samples, a majority of the mt-SSU components co-localise with the heavier peak (fraction 13) and the even heavier but less abundant peak in fraction 11. In the overexpression sample, the higher peaks are absent and the mt-SSU co-localised with the lighter fraction 15 mt-LSU peak (Figure 3.2.7 and 3.2.8).

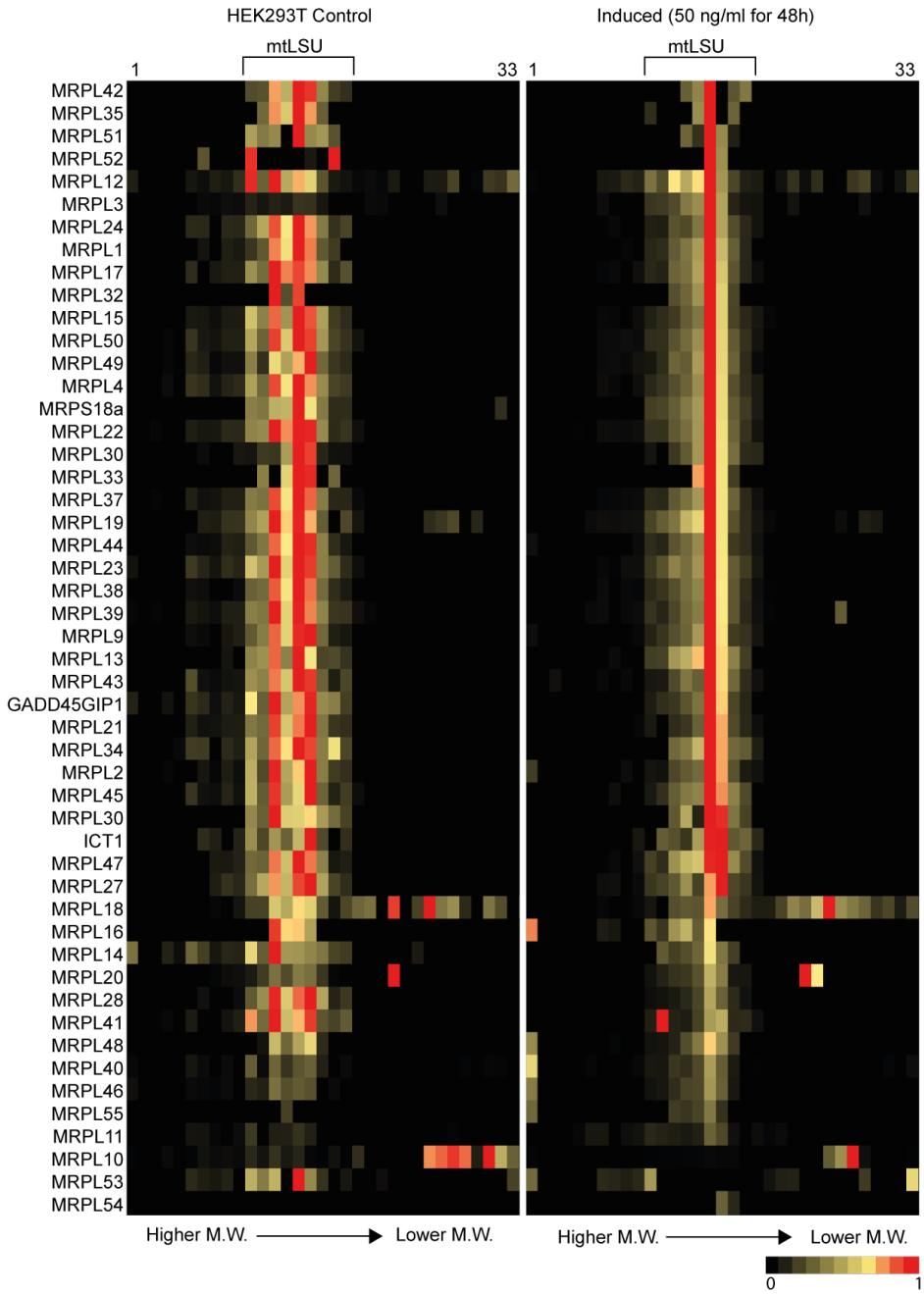

Figure 3.2.7 Analysis of changes to assembly of the mitoribosomal large subunit upon MRM1 overexpression. Mitochondria from parental HEK293T and MRM1-overexpressing cells (induced with 50 ng/ml doxycycline for 48 hours) were extracted. The membrane and soluble fractions were separated. The membrane proteins were solubilized in 0.45% DDM. The protein complexes were resolved on a blue native PAGE gel. The gel was cut into 64 slices and each slice was analysed using mass spectrometry. For each protein and for each slice, peptides common to both samples were found and using the highest abundance as '1', a relative abundance of the peptide was calculated and a heatmap was visualised using Excel. Each column indicates a slice with the top of the gel being at the left of the heatmap. The first 33 slices are shown. The first and the thirty third slice are marked above the heat maps.

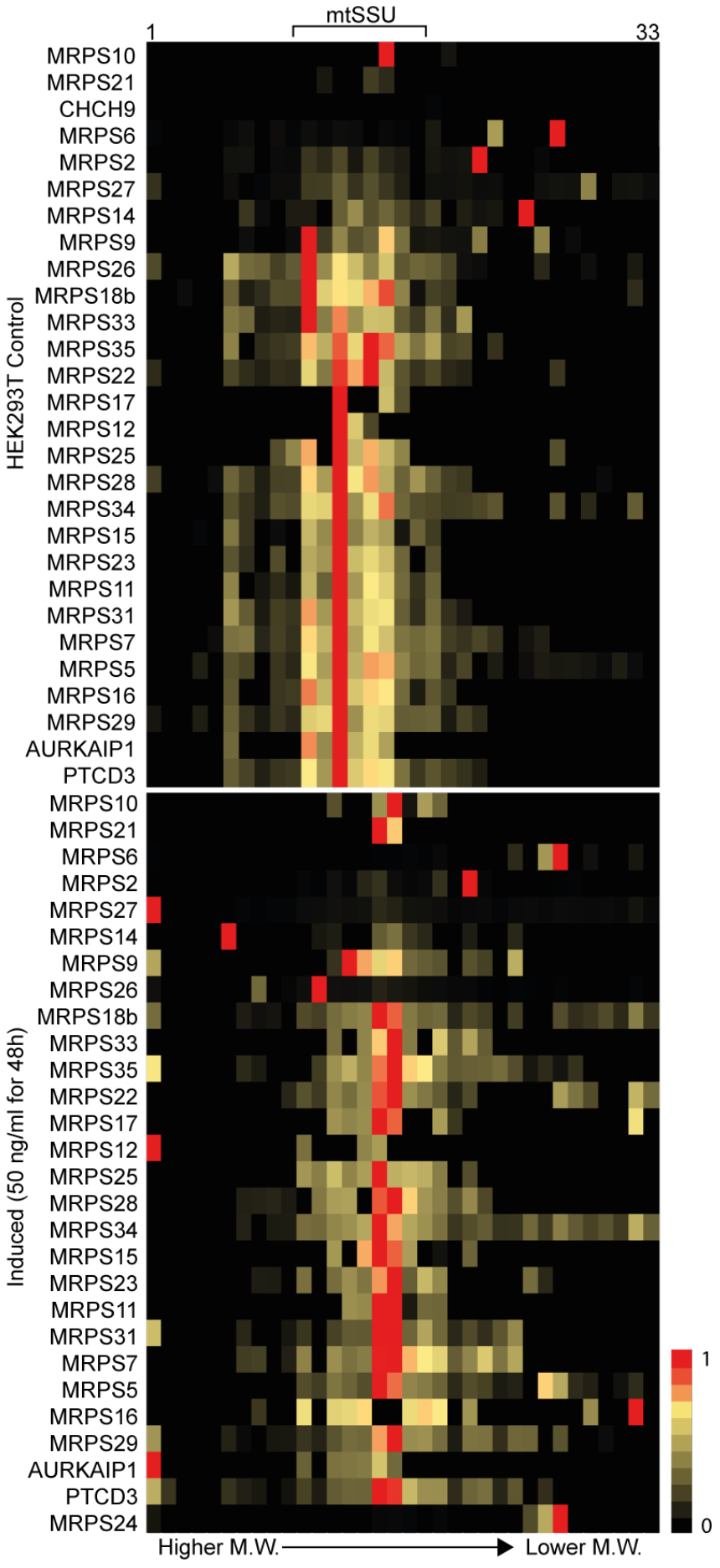
mtSSU
1
33
HEK293T Control
MRPS10
MRPS21
CHCH9
MRPS6
MRPS2
MRPS27
MRPS14
MRPS9
MRPS26
MRPS18b
MRPS33
MRPS35
MRPS22
MRPS17
MRPS12
MRPS25
MRPS28
MRPS34
MRPS15
MRPS23
MRPS11
MRPS31
MRPS7
MRPS5
MRPS16
MRPS29
AURKAIP1
PTCD3
Induced (50 ng/ml for 48h)
MRPS10
MRPS21
MRPS6
MRPS2
MRPS27
MRPS14
MRPS9
MRPS26
MRPS18b
MRPS33
MRPS35
MRPS22
MRPS17
MRPS12
MRPS25
MRPS28
MRPS34
MRPS15
MRPS23
MRPS11
MRPS31
MRPS7
MRPS5
MRPS16
MRPS29
AURKAIP1
PTCD3
MRPS24
1
0
Higher M.W.
Lower M.W.

Figure 3.2.8 Analysis of changes to assembly of the mitoribosomal small subunit upon MRM1 overexpression. Mitochondria from parental HEK293T and MRM1-overexpressing cells (induced with 50 ng/ml doxycycline for 48 hours) were extracted. The membrane and soluble fractions were separated. The membrane proteins were solubilized in 0.45% DDM. The protein complexes were resolved on a blue native PAGE gel. The gel was cut into 64 slices and each slice was analysed using mass spectrometry. For each protein and for each slice, peptides common to both samples were found and using the highest abundance as '1', a relative abundance of the peptide was calculated and a heatmap was visualised using Excel. Each column indicates a slice with the top of the gel being at the left of the heatmap. Note that the order of the proteins is not the same as a different subset of total small subunit components was detected in each sample. The first 33 slices are shown. The first and the thirty third slice are marked above the heat maps.

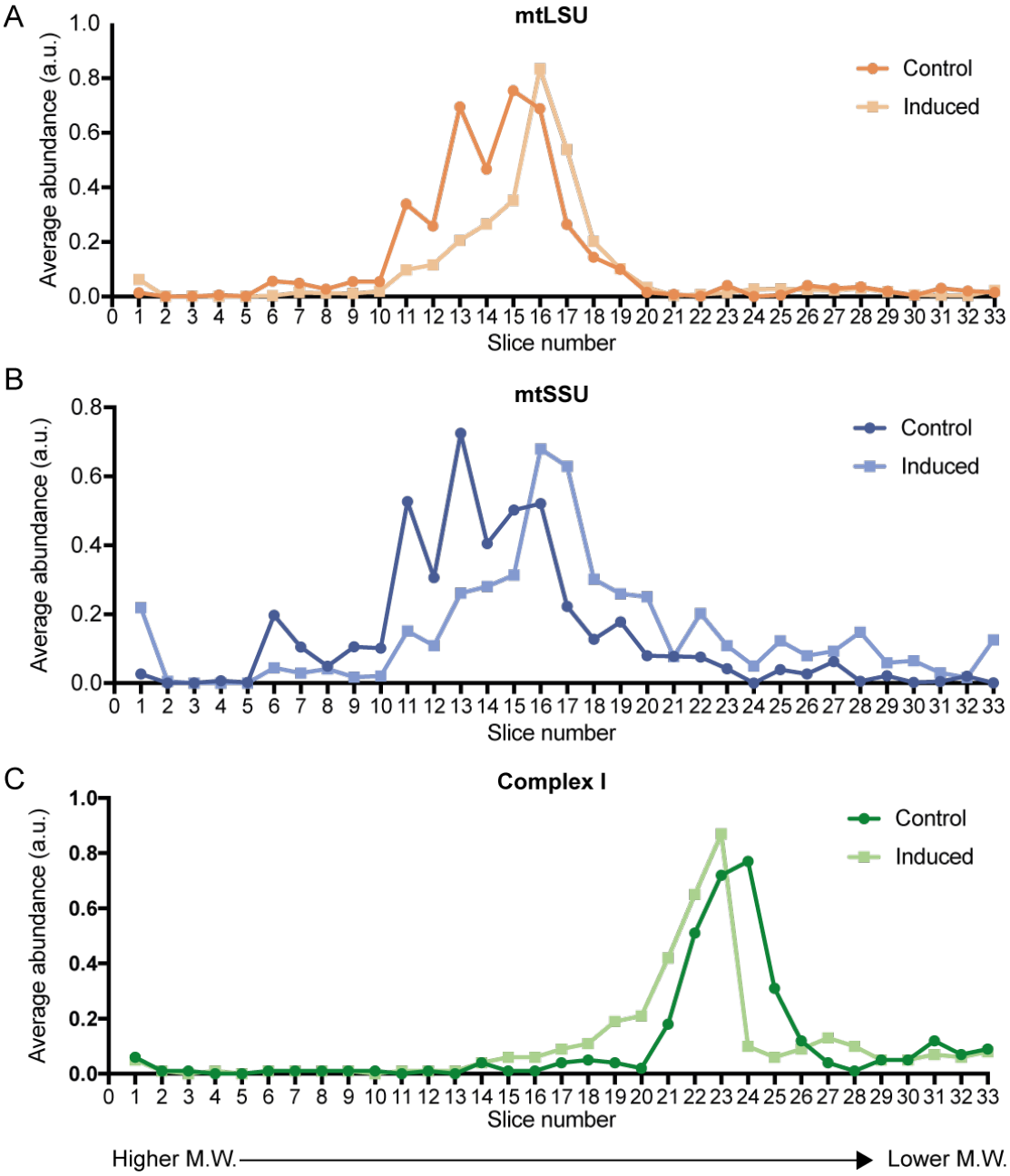

Figure 3.2.9 Analysis of changes to mitoribosomal assembly upon MRM1 overexpression. The average protein abundance of each of the complexes was calculated and plotted using Prism 7. (A) mtLSU (B) mtSSU (C) Complex I control was also used as its abundance should not be affected. As SILAC was not used, this controls for differences in gel running and differences in gel slicing.

3.2.3 MRM1 knockout generation in HEK293T Flp-In cells

Human MRM1 was previously shown to be a 2'-*O*-ribose methyltransferase that methylates G1145 in the mt-LSU 16S rRNA (Lee and Bogenhagen, 2014). However, the function and the reason for the strong conservation of this modification were not clear. Therefore, to decipher the function of the modification in the translation apparatus, a knockout cell line approach was pursued. At the time of creating this knockout, the CRISPR-Cas9 system was still in its infancy and had various issues with off-target cleavage and efficiency that had to be addressed. Various attempts using self-designed guide RNA sequences were made to generate knockout HEK293T Flp-In T-Rex cell lines (not shown). However, this was not successful. Therefore, the well-established method of zinc-finger nuclease (ZFN)-based gene targeting was used. This could be purchased as vectors encoding the two ZFNs that bind to the sense and anti-sense DNA strand and could be easily transfected into the required cell line using lipofection. In addition, the Sigma CompoZr custom ZFN service provided a validated pair of ZFNs that guaranteed high efficiency of gene targeting. The HEK293T Flp-In cell line was used because it contains the Flp-In system, which can be used for a straightforward complementation of the knockout to show rescue of phenotype upon reintroduction of the protein-coding cDNA.

The double strand break produced in the target gene by the ZFN can be repaired by the cell using non-homologous end joining (NHEJ) or homology directed repair (HDR). As a donor-targeting construct for HDR was not supplied to the cell in our experimental system, we relied upon NHEJ to introduce insertions or deletions. The ZFN was targeted to the first exon of the gene and any out-of-frame mutation introduced by NHEJ would produce a premature stop codon.

Prior the ZFN targeting, the HEK293T cells were karyotyped to study the extent of genetic rearrangements in this model cell line. Out of seven clonal cells analysed, chromosomal analysis showed severe aneuploidy and multiple rearrangements between the seven clones. The cells showed between 46 and 58 chromosomes and structural rearrangements were observed in chromosomes 1, 3, 5, 11, 13, 14 and 16, with at least two unidentified marker chromosomes (Figure 3.2.10). The MRM1 gene locus is found on Chromosome 17, which showed three copies of the gene that needed to be targeted by ZFN. Nevertheless, HEK293T Flp-In cells were used to make use of the Flp-In system at a later date.

Figure 3.2.10 Karyotype for HEK293T cells. The cell lines are arrested in metaphase, stained and imaged. The chromosomes are identified based on banding pattern. Karyotyping performed by Cell Guidance Systems Karyotyping service.

Vectors encoding the two ZFNs were transfected into the parental HEK293T Flp-In cell line using nucleofection, and the cells were allowed to recover for 48 hours and diluted to obtain single-cell derived clones in eight 96-well plates at a concentration of 0.2 cells per well. Cells were allowed to recover and single colonies were split in triplicate into three plates. The cells were allowed to reach 60-80% confluency (for two weeks) before being frozen or harvested for screening. To identify potential MRM1 knockout candidates, the cells were lysed using TG lysis buffer and subjected to western blotting using antibodies against endogenous MRM1. Loading was quantified by probing the blot against β-actin (Figure 3.2.11A). Clones identified via western blotting were analysed using PCR across the ZFN target site, TOPO cloning to separate the different alleles and Sanger sequencing (Figure 3.2.11B, C).

Of the 192 clones screened, two clones were identified for further study. Clone 7 showed a complete lack of protein in the western blot analysis. Sequencing the three alleles showed 4 bp, and 7bp (2 alleles) deletions, producing premature stop codons leading to a 167 aa protein and a 120 aa protein, respectively. However, a western blotting analysis showed no detectable MRM1 in the clone 7 sample, suggesting a loss of stability of the produced proteins, efficient nonsense-mediated decay or that the epitope is not on the lost N-terminus (Figure 3.2.11A). Clone 7 will be henceforth referred to as MRM1 (-/-). Similarly, clone 71 was identified on initial western blot screening, which showed strongly depleted MRM1 levels. However, repeated western blotting with protein quantification showed low but detectable amounts of endogenous MRM1. Furthermore, sequencing across the ZFN target site showed that only two of of three alleles had been successfully targeted producing a 14 bp deletion (167 aa protein) and a 2 bp deletion (171 aa protein) (Figure 3.2.11C). Clone 71 will henceforth be referred to as MRM1 (+/-).

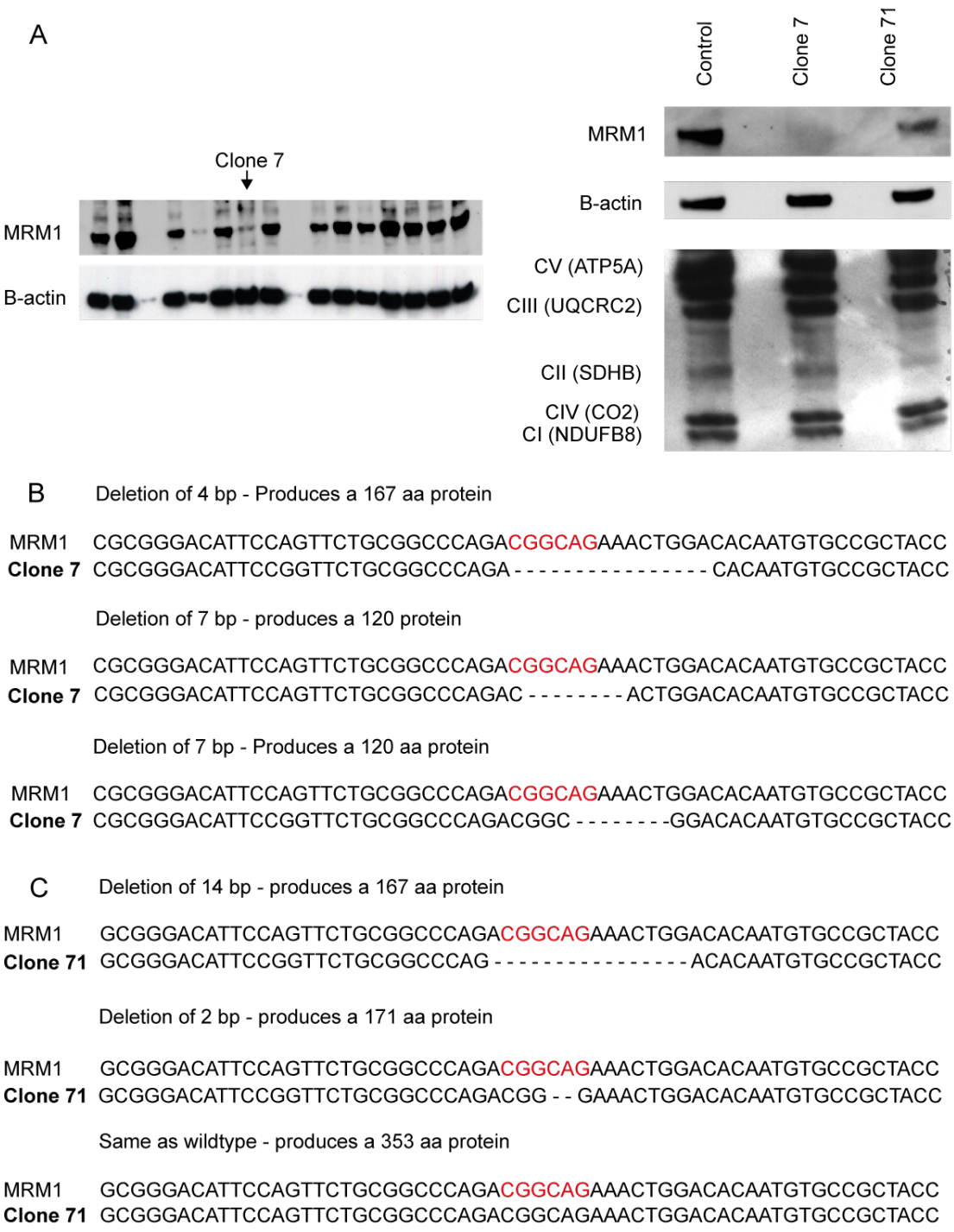

Figure 3.2.11 Screening for MRM1 knockout HEK293T cells. (A) Initial western blot analysis of cell lysate from single cell - derived clones using antibodies against endogenous MRM1, OxPhos complexes and β-actin. Initial screening is shown on the left showed a severe decrease in endogenous MRM1 and a weak non-specific band in its place. Further analysis using quantified protein is shown on the right. (B) PCR products containing the ZFN target site (marked in red) were TOPO cloned, transformed into E. coli, and bacterial colonies were submitted for Sanger sequencing. The sequences were aligned against the wild-type sequence.

MRM1 is responsible for 2'-*O*-ribose methylation of G1145 on the 16S rRNA of the mt-LSU. Therefore, the mitochondrial rRNA for the HEK293T cell lines was analysed for G1145 ribose methylation. This was analysed by reverse transcription primer extension, a method that utilises the inefficiency of reverse transcriptase in reverse transcribing across a modified nucleotide. The knockout cells were also complemented with doxycycline-inducible Flag-tagged MRM1 using the Flp-In recombination system. Confirmation of successful reintroduction of MRM1 was shown using western blotting (Figure 3.2.12). The reintroduction of the modification in these cells would confirm that MRM1 is indeed required for the modification, and that the loss of the modification is caused by the loss of the protein.

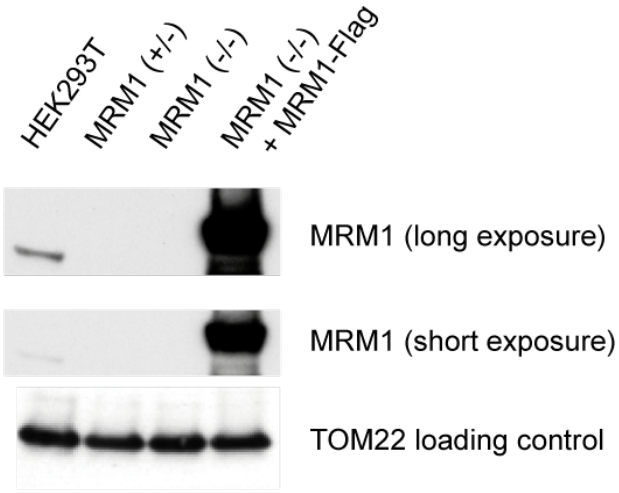

Figure 3.2.12 Complementation of MRM1 (-/-) with MRM1-Flag. Mitochondria were isolated from the HEK293T parental cells, the MRM1-deficient MRM1 (+/-) and MRM1 (-/-) cells and the MRM1-complemented knockout cells (induced for 24 hours with 50 ng/ml doxycycline). Western blotting was performed. Antibodies against endogenous MRM1 were used to show complementation. Antibodies against TOM22 were used as a loading control.

Reverse transcription primer extension involved extracting mitochondrial RNA from the parental HEK293T cells, the MRM1 deficient MRM1 (+/-) and MRM1 (-/-) cells, and the rescued MRM1 (-/-) cells. Two primers were chosen which anneal downstream of the site of the modification. To control for loading internally, dATP was not added to the reverse transcription reaction, therefore, in addition to the pausing at the modified nucleotide, the lack of dATP would cause all reverse

transcription to stall when it encountered a 'U' (a schematic representation is provided for both primers in Figure 3.2.13 and 3.2.14). Therefore, a ratio of primers paused at the modification and those that are stalled due to a lack of dATP could be calculated (Figure 3.2.13A and 3.2.14A). This removed the errors caused by differences in RNA loading. As a further negative control, an *in vitro* transcribed 1059 nucleotide RNA substrate, containing the 16S rRNA position G1145, was used as a negative control to indicate the levels of false positive pausing signals that may be observed. The primers were end-labelled with [^{32}P]-ATP and polynucleotide kinase (PNK) so that reverse transcription products could be visualised using autoradiography (Figure 3.2.13B and 3.2.14B).

For both primers, a substantial decrease is observed in the pausing caused by the Gm1145 modification in MRM1 depleted cells. Moreover, in the knockout cells where MRM1 was reintroduced, a substantial amount of modification-mediated pausing was observed, higher than in control cells. This could be attributed to methylation of immature 16S molecules that would not normally be modified by endogenous MRM1 (Figure 3.2.13C and 3.2.14C).

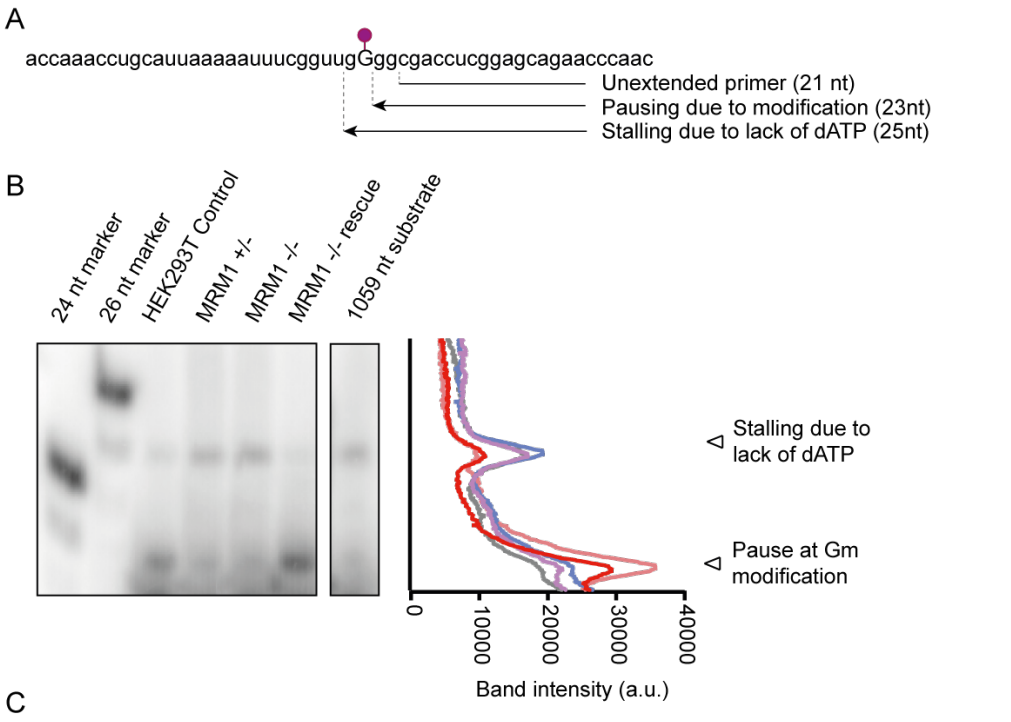

Band intensity	Pausing at Gm	Stalling at U	Pausing / (Pausing + Stalling) Normalised (%)
Control	3806.72	1300.96	100
MRM1(+/-)	924.96	2468.40	30.42
MRM1(-/-)	1910.00	4546.15	15.53
MRM1(-/-) rescue	4000.77	618.33	139.41
1059 nt IVT substrate	468.92	2730.23	11.70

Figure 3.2.13 Identifying G1145 methylation status following MRM1 knockout. [^{32}P]-end-labelled primer complimentary to a sequence downstream to the site of the modification is annealed to the mt-RNA from HEK293T parental, MRM1 (-/-), MRM1 (+/-) and MRM1 (-/-) rescue cells, and 1059 nt RNA substrate, and reverse transcription is carried out. (A) Schematic representation. In the presence of the modification, primer extension by the reverse transcriptase is paused by the modification. Lack of dATP causes complete stalling of the primer extension reaction. (B) The primer (21 nt) produces a 23 nt product when reverse transcription paused by Gm1145 and a 25 nt product when stalled due to lack of dATP. (C) Ratio of band intensities of primer stalling to Gm1145 pausing are calculated using Image J.

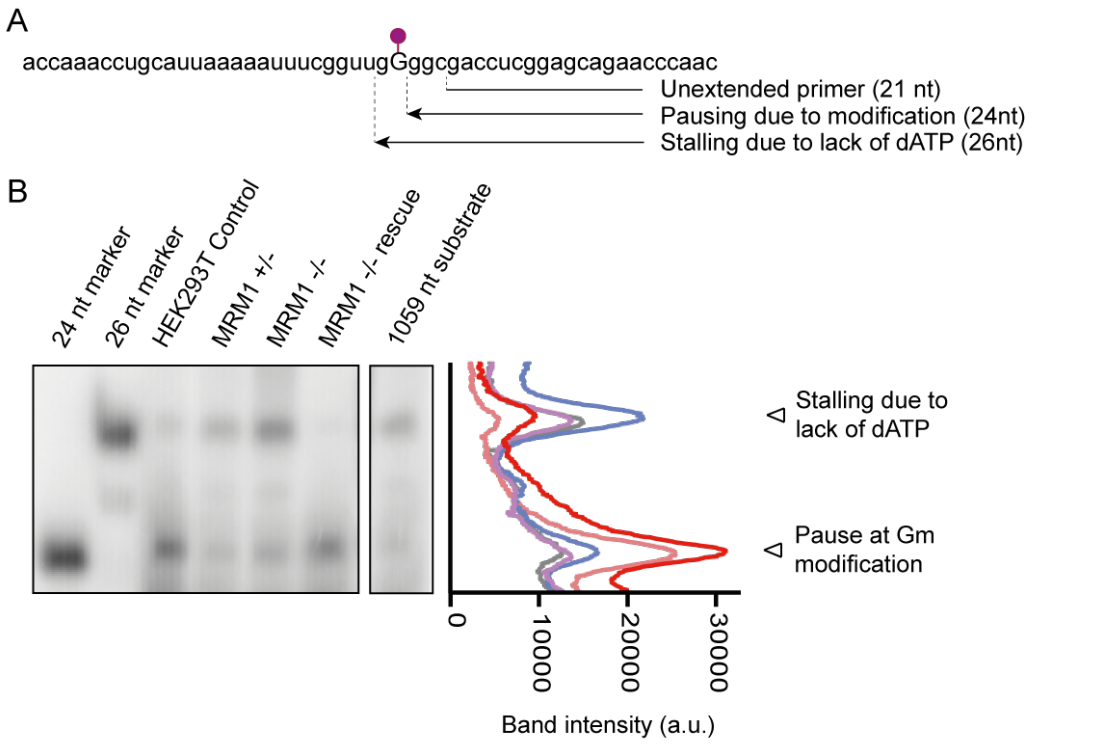

C

Band intensity	Pausing at Gm	Stalling at U	Pausing / (Pausing + Stalling) Normalised (%)
Control	1692.68	990.65	100
MRM1(+/-)	528.86	2226.93	36.57
MRM1(-/-)	300.74	2768.60	39.69
MRM1(-/-) rescue	3727.22	510.99	116.21
1059 nt IVT substrate	186.13	2336.40	19.67

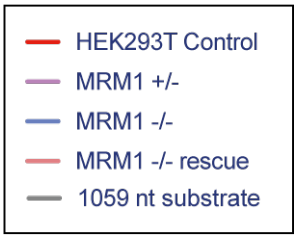

Figure 3.2.14 Identifying G1145 methylation status following MRM1 knockout. [^{32}P]-end-labelled primer complimentary to a sequence downstream to the site of the modification is annealed to the mt-RNA from HEK293T parental, MRM1 (-/-), MRM1 (+/-) and MRM1 (-/-) rescue cells, and 1059 nt RNA substrate, and reverse transcription is carried out. (A) Schematic representation. In the presence of the modification, primer extension by the reverse transcriptase is paused by the modification. Lack of dATP causes complete stalling of the primer extension reaction. (B) The primer (21 nt) produces a 24 nt product when reverse transcription paused by Gm1145 and a 26 nt product when stalled due to lack of dATP. (C) Ratio of band intensities of primer stalling to Gm1145 pausing are calculated using Image J.

3.2.4 Characterisation of growth rate, OxPhos function and mitochondrial translation MRM1 knockout cell lines

Next, the newly generated MRM1 deficient cell lines were characterised to identify the effect of MRM1 ablation on mitochondrial function. Firstly, growth rate of the HEK293T, MRM1 (+/-) and MRM1 (-/-) cell lines was measured in glucose and galactose media. The galactose media forces the cell to rely on mitochondrial respiration for ATP production. This is because galactose metabolism is linked to pyrimidine biosynthesis. The breakdown of galactose requires mitochondrially-produced UTP, which in turn requires dihydroorotate dehydrogenase (DHODH). However, DHODH also functions as an accessory enzyme of OxPhos. Therefore, disruption of OxPhos causes disruption of pyrimidine synthesis and thus, galactose cannot be metabolised by the cell (Gattermann et al., 2004). This stress causes cells with defective mitochondria to suffer and thus reduces cell viability. No significant difference in cell viability was observed in the MRM1 depleted cells (Figure 3.2.15A).
Subsequently, OxPhos function was assessed using microscale oxygraphy using an Extracellular Flux Analyzer to measure oxygen consumption rate of plated cells upon sequential injection of ATP synthase inhibitor, Oligomycin, mitochondrial uncoupler, Bam15, and Complex I and III inhibitors, Rotenone and Antimycin A. No significant difference in oxygen consumption rate was observed between the HEK293T parental, MRM1 (+/-) and MRM1 (-/-) cell lines (Figure 3.2.15B).
Since, the modification is strongly conserved in 16S ribosomal RNA, the effect of the lack of MRM1 on mitochondrial translation was assessed using the incorporation of [^{35}S]-methionine into newly synthesised mitochondrially encoded proteins. To do this, the cells were incubated with cytoplasmic translation inhibitor, emetine. Then, [^{35}S]-methionine was introduced to the cells and incubated for 30 minutes. The cell lysate was run on a SDS-PAGE gel, dried and visualised using autoradiography. This showed no significant difference between the control HEK293T cells and the MRM1 deficient cell lines (Figure 3.2.15C).

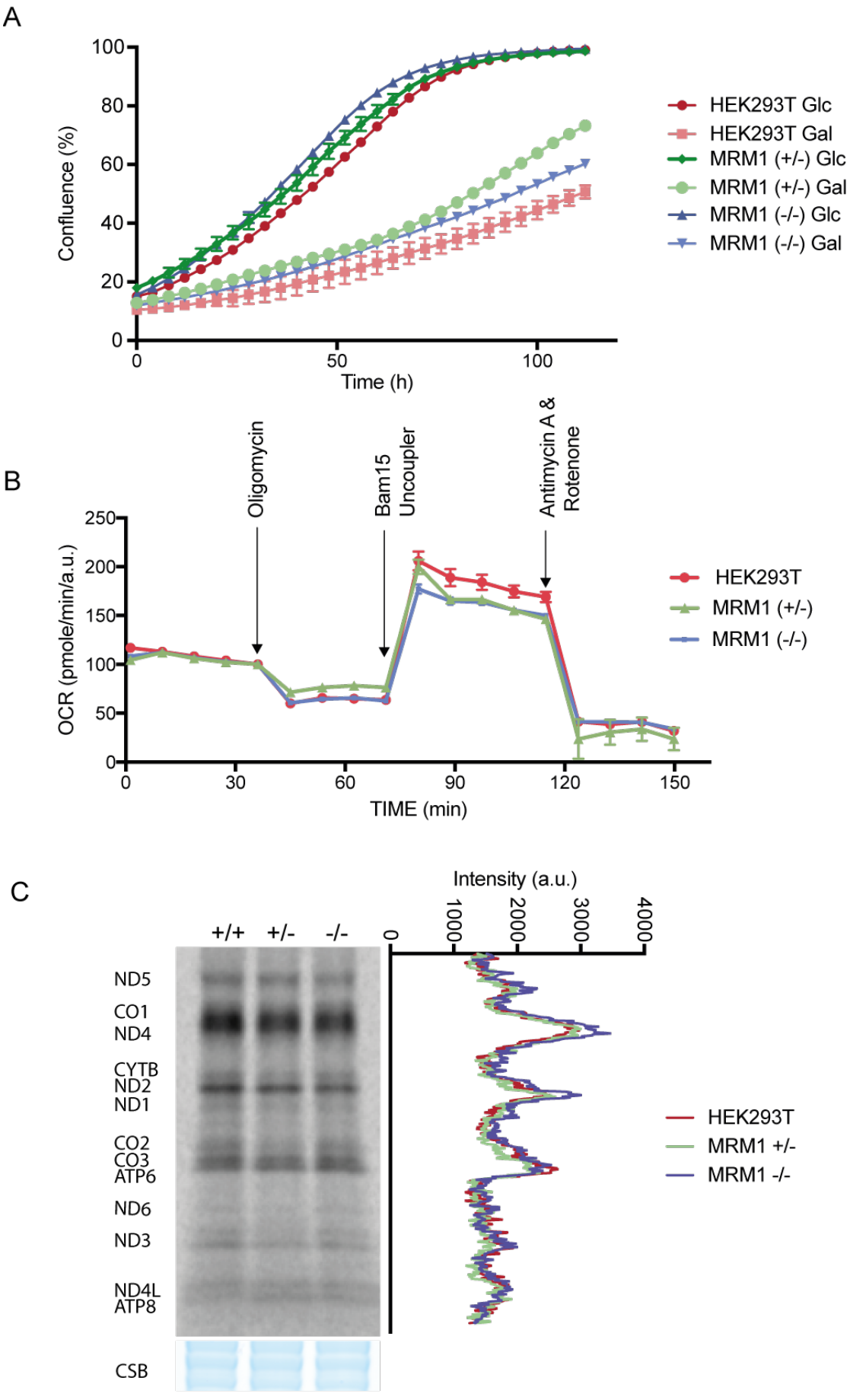
A
Confluence (%)
Time (h)
HEK293T Glc
HEK293T Gal
MRM1 (+/-) Glc
MRM1 (+/-) Gal
MRM1 (-/-) Glc
MRM1 (-/-) Gal
B
OCR (pmole/min/a.u.)
TIME (min)
Oligomycin
Bam15 Uncoupler
Antimycin A & Rotenone
HEK293T
MRM1 (+/-)
MRM1 (-/-)
C
Intensity (a.u.)
+/+
+/-
-/-
ND5
CO1
ND4
CYTB
ND2
ND1
CO2
CO3
ATP6
ND6
ND3
ND4L
ATP8
CSB
HEK293T
MRM1 +/-
MRM1 -/-

Figure 3.2.15 Characterisation of MRM1 knockout cell lines (A) Growth curve. 10,000 cells of the HEK293T parental, MRM1 (+/-) and MRM1 (-/-) cell lines were plated in triplicates in 4.5 g/L glucose or 4.5 g/L galactose and confluence was measured using Incucyte HD. Error bars =1 SEM; n=3. (B) Microscale oxygraphy. 15,000 cells of the three cell lines were plated in a XF96 cell culture microplate 24 hours before the media was replaced with low-buffered DMEM. Using the XF96 Extracellular Flux Analyzer, wells were sequentially injected with Oligomycin (2 μM), Bam15 (2μM) and Antimycin A and Rotenone (1 μM). Oxygen consumption rate was measured before and after the introduction of the inhibitors. Error bars indicate standard error. The experimental protocol was provided by and optimisation of the protocol for HEK293T cells was performed in collaboration with Dr Hannah Bridges. (C) [^{35}S]-methionine labelling of newly synthesised mitochondrial translation products. The three cell lines were incubated in cytoplasmic inhibitor, emetine, for 30 minutes before the addition of the [^{35}S]-methionine. After 30 minutes, the cells were lysed with 0.1 % DDM and 0.1 % SDS and 30 μg of protein were resolved on a 10-20% Tris-glycine SDS-PAGE gel. Coomassie Brilliant Blue staining was used as a loading control. The gel was dried, exposed to a storage phosphor screen and scanned using a Typhoon imager. Band intensity was quantified using Image J and plotted using Prism 7.

3.2.5 The effect of MRM1 depletion on mitoribosomal integrity

To assess if MRM1 depletion has any detrimental effects on the biogenesis of the mitoribosome, we next performed sucrose gradient fractionation and western blotting. This involved resolving the various mitoribosomal assemblies in the cell lysate using a 10-30% (v/v) isokinetic sucrose gradient. Sucrose gradient fractions were then resolved on a 4-12% Tris-glycine SDS-PAGE gel and analysed using western blotting. MRPL3 was used to probe for mt-LSU and MRPLS18b was used to probe for the mt-SSU. No MRM1-specific deficiency in mitoribosomal integrity was observed in MRM1-deficient cells (Figure 3.2.16).

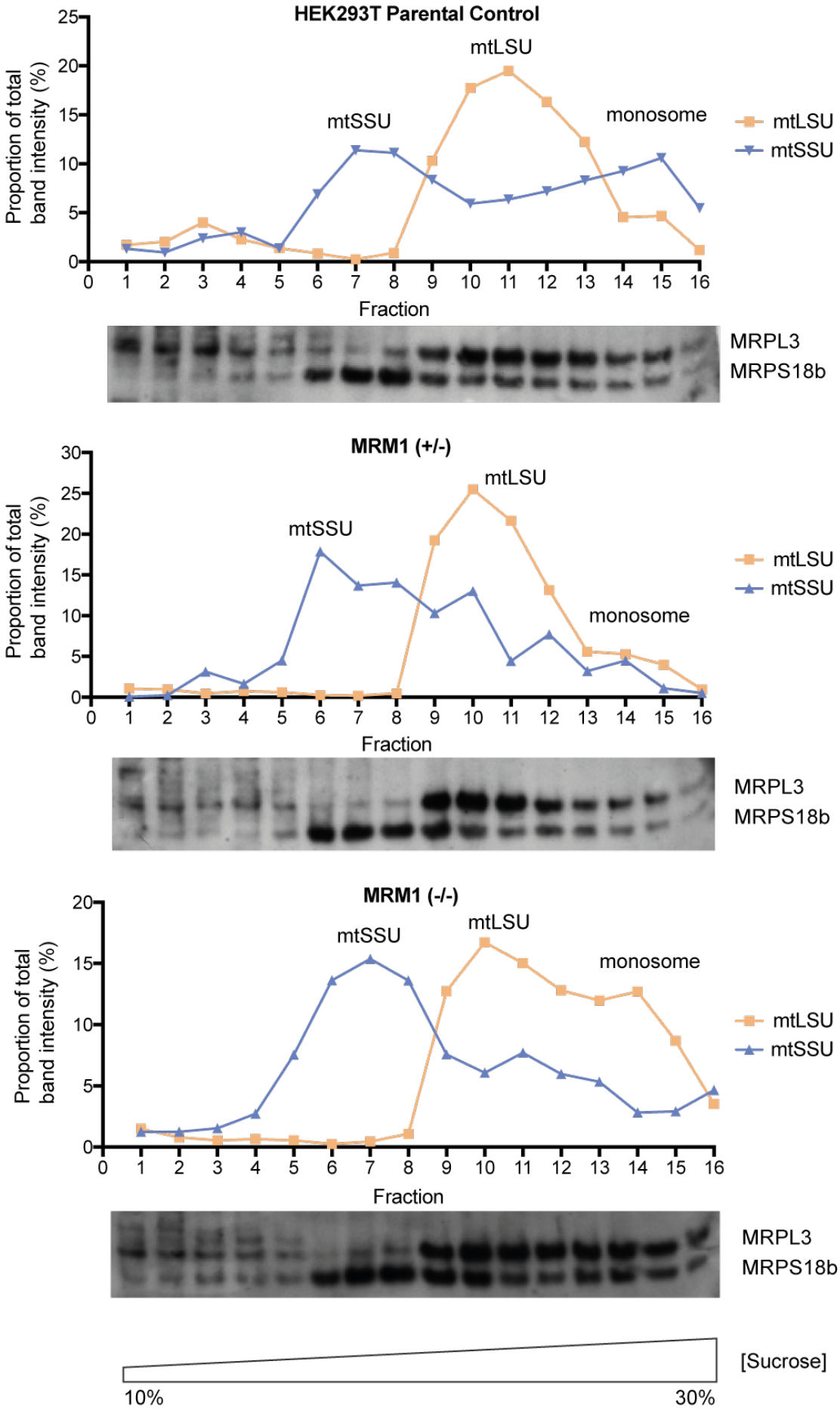
HEK293T Parental Control
mtLSU
mtSSU
monosome
Proportion of total band intensity (%)
Fraction
mtLSU
mtSSU
MRPL3
MRPS18b
MRM1 (+/-)
mtLSU
mtSSU
monosome
Proportion of total band intensity (%)
Fraction
mtLSU
mtSSU
MRPL3
MRPS18b
MRM1 (-/-)
mtSSU
mtLSU
monosome
Proportion of total band intensity (%)
Fraction
mtLSU
mtSSU
MRPL3
MRPS18b
[Sucrose]
10%
30%

Figure 3.2.16 Analysis of mitochondrial ribosome upon MRM1 knockout. 750 μg of cell lysate were separated using 10-30% (v/v) isokinetic sucrose gradient fractionation. 100 μl fractions were then analysed using western blotting. Antibodies against MRPL3 were used to identify the mt-LSU. Antibodies against MRPS18b were used to identify the mt-SSU. Bands were quantified using Image J and plotted as a proportion of total protein using Prism 7.

Small difference between the samples may not be detected due to the low sensitivity of the isokinetic sucrose gradient fractionation method. Therefore, we pursued the use of SILAC and complexomic profiling as described by Vidoni *et al.* (2017) to analyse the mitochondrial ribosomes. Stable isotope labelling by amino acids in cell culture (SILAC) was used to quantitatively compare the composition of the mitoribosomes and any subassemblies identified in the analysis. There are advantages and disadvantages to using SILAC in complexomic profiling. When using SILAC, peptides detected in only one of the two samples are omitted from the data analysis. A comparison of the presence of the protein cannot be made as a lack of detection of the protein does not indicate an absence of the protein. However, the disadvantage of a SILAC-free method is the human error introduced in unequal slicing of the gel between the two samples. The use of SILAC also allows internal normalisation between samples and a direct relative quantification to be made between the samples. Moreover, since the samples from the control and MRM1 knockout cells are mixed before being resolved on a gel, difference in gel slicing and the resulting errors in interpretation of the data are minimised.

For SILAC-complexomics, the HEK293T parental cells and the MRM1 knockout cells were grown in heavy and light SILAC media. They were mixed in equal proportion and the mitochondria were isolated. The rest of the complexomic analysis was carried out as described earlier. The SILAC labelling was used to identify and separate proteins from both samples. For each protein, only peptides common to both samples are used to quantify abundance. An abundance profile is created for each protein using the maximum value from both sets being assigned the value of 1 and the remaining intensities are proportionally scaled. The black to red colour scheme in the heatmap implies an abundance of 0 to 1. Comparison of the complexomic profiles of mt-LSU suggests no major differences in intensity profiles. The smaller subassembly observed in optimisation western blot for MRPL12 was not detected in the mass spectrometry data. Due to the large size of the mt-LSU and mt-SSU, it is not

sufficiently resolved from the monosome (Figure 3.2.17 and 3.2.18). Comparison of the heatmap and profiles of the mtSSU showed that the assembled small subunit does not show accumulation of an assembly intermediate. In addition, a smaller subassembly of the mtSSU is also observed. However, this is also not different between the MRM1 knockout cells and the control cells (Figure 3.2.18). Any differences in presence of a protein could be attributed to variation in peptide detection. This is most noticeable in the profile of the average abundance of all the protein components in the mtLSU and mtSSU (Figure 3.2.19). Taken together, this suggests that neither MRM1 nor the G1145 modification is crucial for mitochondrial assembly and integrity.

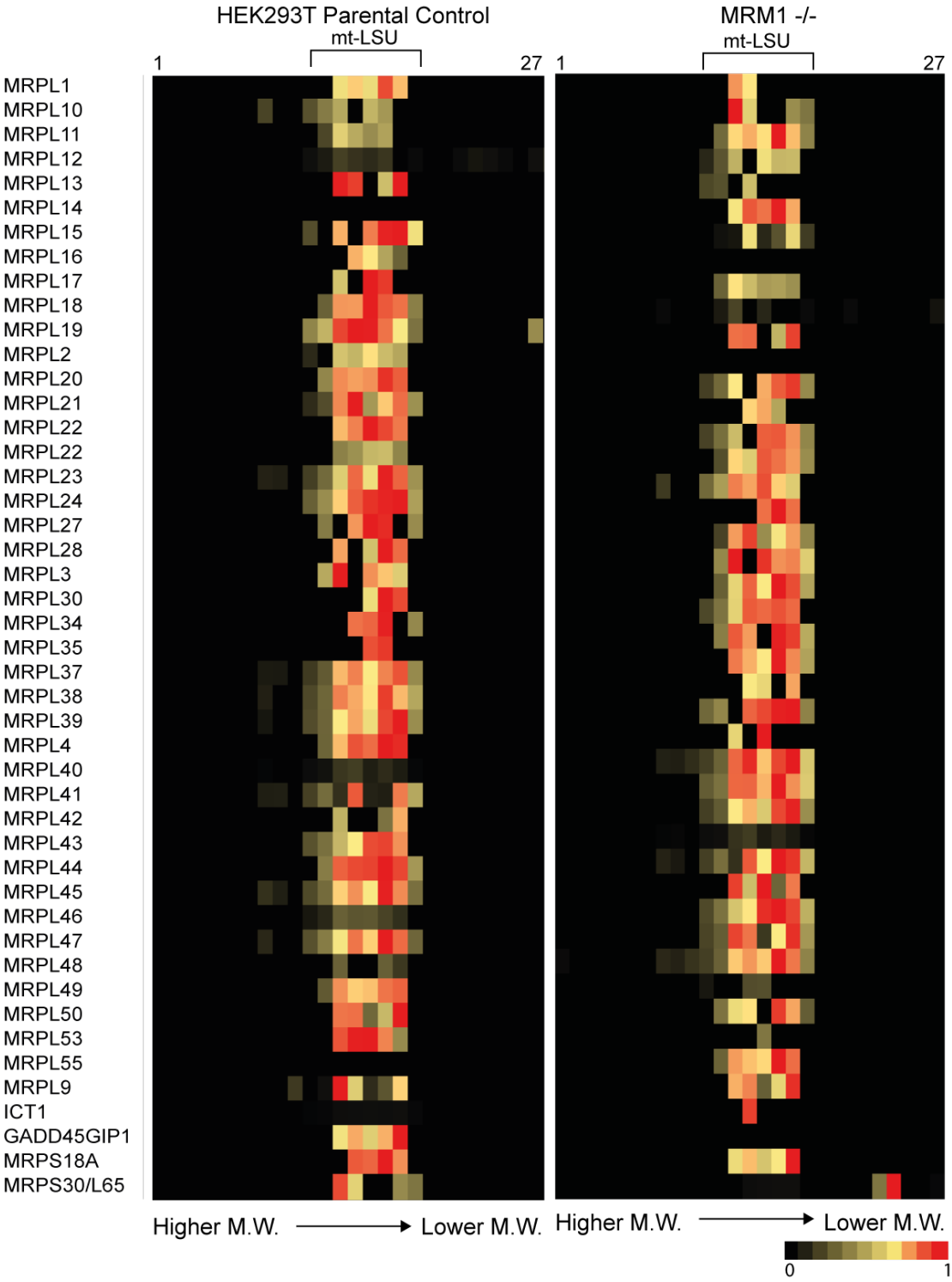

Figure 3.2.17 Analysis of composition of the mitoribosomal large subunit using SILAC-complexomic profiling. (A) Mitochondrial membranes of HEK293T parental cells grown in heavy or light SILAC media and MRM1 (-/-) cells were grown in the other medium (This experiment was repeated with reciprocal labelling) and mixed in equal proportion, were isolated using homogenisation, sonication and ultracentrifugation. 25 μg of membrane proteins were solubilised using 0.45% DDM and run on 3-12% Novex Native PAGE gel for 1 hour at 80 V and for 1 hour at 200 V. Each lane was cut into

64 equal slices and analysed using LC-MS/MS. Heatmap was generated using Excel, using peptides common to both samples such that the maximum abundance of a peptide in both samples was given an abundance of 1 and the remaining slices from both samples were scaled proportionally. Each slice is a column in the heatmap with the highest molecular weight slice from the top of the gel positioned at the left of the heatmap. The rows indicate the protein components of the mitochondrial large subunit detected in both samples. The first 27 slices are shown. Sliec numbers are indicated above the heatmaps. This experiment was performed in collaboration with Dr Michael Harbour.

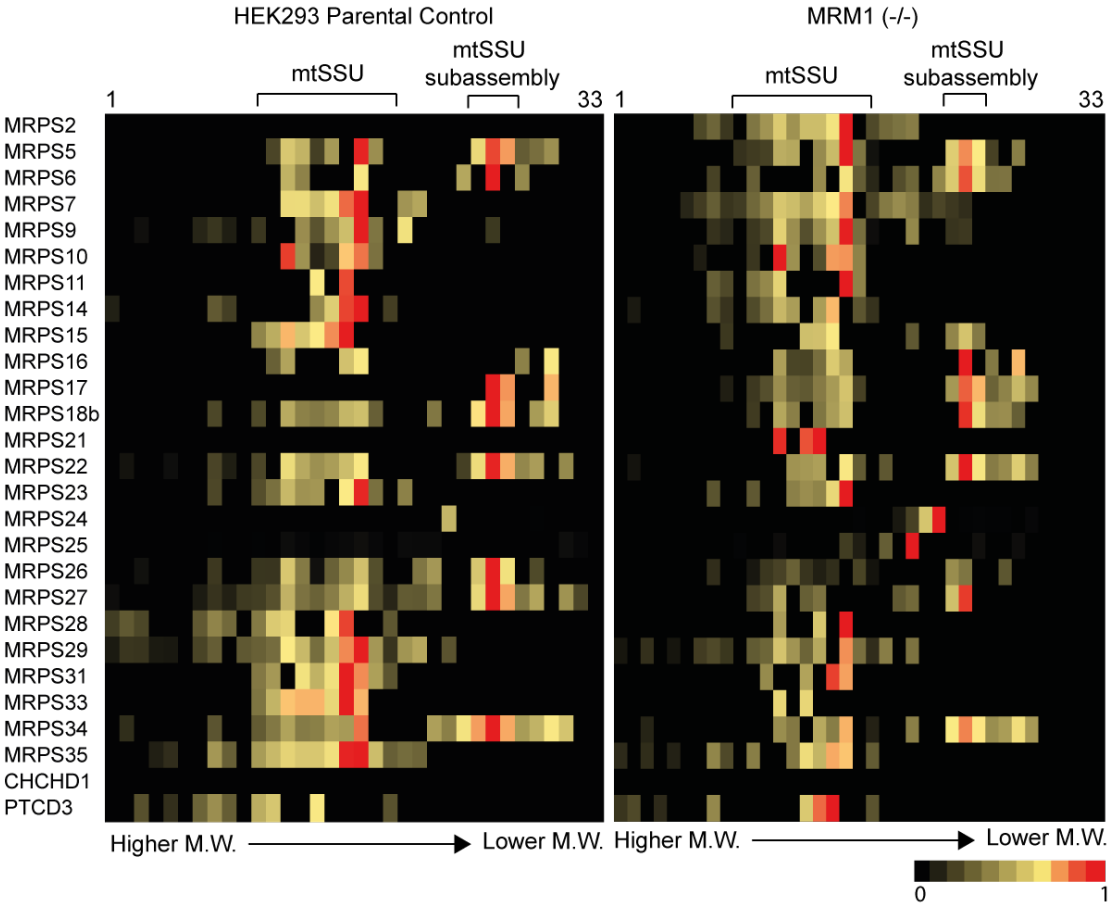

Figure 3.2.18 Analysis of composition of the mitoribosomal small subunit using SILAC-complexomic profiling. (A) Mitochondrial membranes of HEK293T parental cells grown in heavy or light SILAC media and MRM1 (-/-) cells were grown in the other medium (This experiment was repeated with reciprocal labelling) and mixed in equal proportion, were isolated using homogenisation, sonication and ultracentrifugation. 25 μg of membrane proteins was solubilised using 0.45% DDM and run on 3-12% Novex Native PAGE gel for 1 hour at 80 V and for 1 hour at 200 V. Each lane was cut into 64 equal slices and analysed using LC-MS/MS. Heatmap was generated using Excel, using peptides common to both samples such that the maximum abundance of a peptide in both samples was given an abundance of 1 and the remaining slices from both samples were scaled proportionally. Each slice is a

column in the heatmap with the highest molecular weight slice from the top of the gel positioned at the left of the heatmap. The rows indicate the protein components of the mitochondrial small subunit detected in both samples. The first 33 slices are shown. Sliec numbers are indicated above the heatmaps. This experiment was performed in collaboration with Dr Michael Harbour.

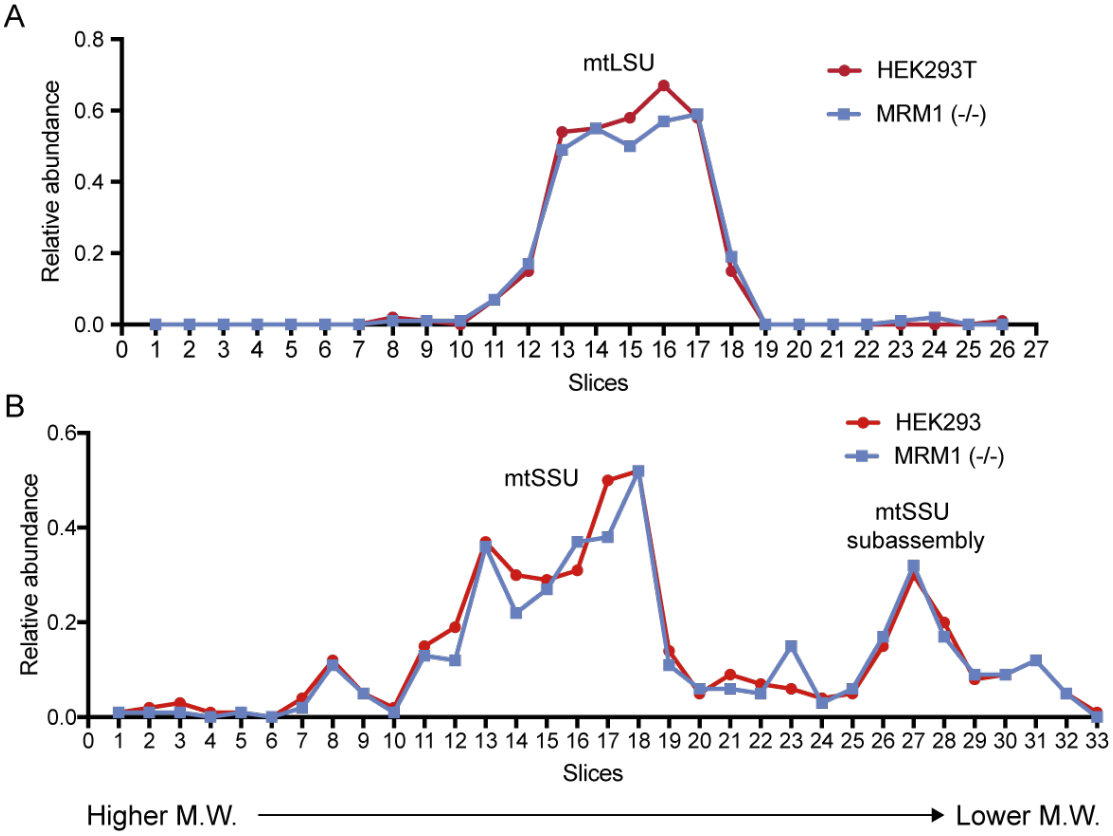

Figure 3.2.19 Analysis of composition of the mitoribosomal subunits using SILAC-complexomic profiling. The average abundance of all the components of the (A) large subunit and (B) small subunit was calculated and plotted using Excel. Only 26 slices are shown for the mt-LSU and 33 slices are shown for the mt-SSU.

3.3 MRM1 - Discussion

In mammalian mitochondria, the ribosomal RNA undergoes ten highly conserved modifications found in close proximity to the catalytic centre of the mitoribosome, including base methylations, 2'-*O*-ribose methylations and pseudouridylation. This works aims to characterise in particular the highly conserved G1145 2'-*O*-ribose methylation and its role in mitoribosomal biogenesis. While this work was in progress, Lee and Bogenhagen (2014) demonstrated that MRM1 catalyses the formation of Gm1145 on the P-loop of the 16S rRNA of the mitochondrial large ribosomal subunit. The importance of this modification varies depending on species. In bacteria, lack of this modification does not seem to affect ribosomal assembly and function (Lovgren and Wikstrom, 2001). However, it is indispensable in yeast (Connolly et al., 1995). Therefore, knockout cells were generated to identify the function of MRM1 and purpose of this modification. We showed that despite being highly conserved, knockout of the methyltransferase does not affect OxPhos function, mitochondrial translation and mitoribosomal biogenesis.

3.3.1 MRM1 is required for G1145 methylation

In the MRM1 knockout cells, a small amount of pausing of reverse transcription at the site of modification is still observed in the knockout cells. However, this pausing is also seen in *in vitro* transcribed substrates suggesting that this observed pausing is not specific to the modification and may be due to the specific sequence. A substantial increase in pausing of reverse transcriptase at the site of modification upon expression of MRM1 in knockout cells suggests that there is a pool of 16S rRNA that is unmodified and that MRM1 concentration is the rate-limiting step. Alternatively, it is more likely that these unmodified RNA molecules are earlier in the stages of maturation and the excess of MRM1 causes a deregulation in the hierarchy of 16S rRNA maturation. This would suggest that MRM1 modification does not happen co-transcriptionally.

Other methods have also been used previously to identify the presence of a modification such as mass spectrometric analysis of 16S rRNA extracted from sucrose gradient fractionated samples (Su et al., 2014), or a direct comparison of parental and knockout cell 16S rRNA using Nanopore techniques (Marchand et al., 2016).

3.3.2 MRM1 depletion does not affect cell viability and mitochondrial gene expression

The modification of the guanine in the peptidyl transferase loop of domain V of 16S rRNA is highly conserved (Baer & Dubin, 1981). However, the effect of loss of the MRM1-induced modification is variable across various species. In *E. coli*, loss of RlmB, homolog of MRM1, does not cause any changes to cell viability (Lovgren and Wikstrom, 2001). In *S. cerevisiae* mitochondria, loss of the homolog, Pet56p, led to a strong respiratory defect and a reduction in growth in media containing non-fermentable carbon source (Connolly et al., 1995). In *S. cerevisiae* cytoplasmic ribosomes, knockout of snoRNA snR67 required for the methylation of the equivalent site (G2619) causes a mild defect in growth in basal medium. However, loss of the modification does not affect sensitivity to ribosomal inhibitors and extraribosomal stresses (Esguerra et al., 2008). In our HEK293T knockout cells, the absence of MRM1 does not lead to a reduction in cell viability in glucose or galactose medium. Further analysis also showed that MRM1 and the G1145 methylation is not required for the synthesis of mitochondrially-encoded components of the respiratory chain. Any inefficiencies introduced by the lack of modification to the effective decoding of the mRNA did not lead to any measurable deficiencies in OxPhos function.

A similar lack of phenotype has been observed in other cells where conserved tRNA modifiers have been lost. However, upon further knockdown of one or more other modifiers, a deficiency in translation was observed. For example, in yeast, independent deletion of TRM140 and TRM1 modifiers of the tRNA anti-codon loop do not have any effect on translation or cell viability. However, deletion strains lacking both proteins show a modest growth phenotype, but only in the presence of a translation inhibitor, cyclohexamide (D'Silva et al., 2011). In the case of MRM1, a similar model with multiple deletions may be required to elicit a translation defect.

3.3.3 The role of MRM1 in mitoribosome biogenesis

The biogenesis of the mitoribosome involves the methylation of multiple sites by different conserved methyltransferases. The loss of Um1369 and Gm1370 by methyltransferases related to MRM1 (MRM2 and MRM3), causes a defect in mt-LSU assembly, which subsequently leads to a respiratory deficiency (Lee and Bogenhagen, 2014; Rorbach et al., 2014). It then stands to reason that MRM1, being a highly conserved protein involved in a highly prevalent modification should be also

important for mitoribosome biogenesis. Analysis of different species lacking this methyltransferase activity seems to give mixed results. In bacteria, loss of the MRM1 homolog does not lead to changes in ribosome assembly (Lovgren & Wikstrom, 2001). However, in yeast mitochondria, depletion of the MRM1 homolog leads to a defect in mt-LSU assembly with an associated accumulation of lower sedimenting particles lacking Mrp7p (homolog of bL27 and MRPL27) (Sirum-Connolly & Mason., 1993; Sirum-Connolly et al., 1995). However, knockout of MRM1 in HEK293T cells did not show any detectable differences in mitoribosome subunit assembly and composition.

This lack of a phenotype in MRM1 knockout cells implies that its function is either very subtle and cannot be identified by the experiments performed, or that the effects of the modification may only come into play under certain contexts, such as under certain environmental stresses, in specific cell types or at certain stages of development. It is also possible that under standard conditions testing in this work, the lack of this modification does not hinder translation. As previously described, a double or triple knockout of multiple modifications or a suitable environmental stress may be required to bring about significant differences in translation (D'Silva et al., 2011).

Recent structural work on a ribosome with a tRNA in the P-site showed that G1145 (target of MRM1) and G1146 base pairs with C75 and C74 of the universally conserved aminoacylated CCA sequence at the 3' of the tRNAs (figure 3.3.1) (Greber et al., 2015). In this context, the 2'-O-ribose methylation of rRNA could have another structural function. The methylation of the hydroxyl group, often prevents it from hydrogen binding and stabilises the structure (Motorin and Helm, 2010). Esguerra *et al.* (2008) also suggest that strategically placed modifications may also serve a function analogous to 'ball bearings' which facilitate the repetitive ratchet-like mechanism of ribosome and tRNA movement during translation. For example, in the bacterial ribosome, when the P-site substrate is bound, U2585 points towards the A-site until the A-site substrate enters. This causes a shift in conformation such that it faces away from the tRNA-amino acid ester group. This change in conformation positions the amino and carbonyl groups such that nucleophilic attach can occur and leading to the formation of the peptide bond (Steitz, 2008). In bacteria, this is the region where RrmJ (MRM2 homolog) methylates U2552 and this modification may function as the 'ball bearing' facilitating conformational change.

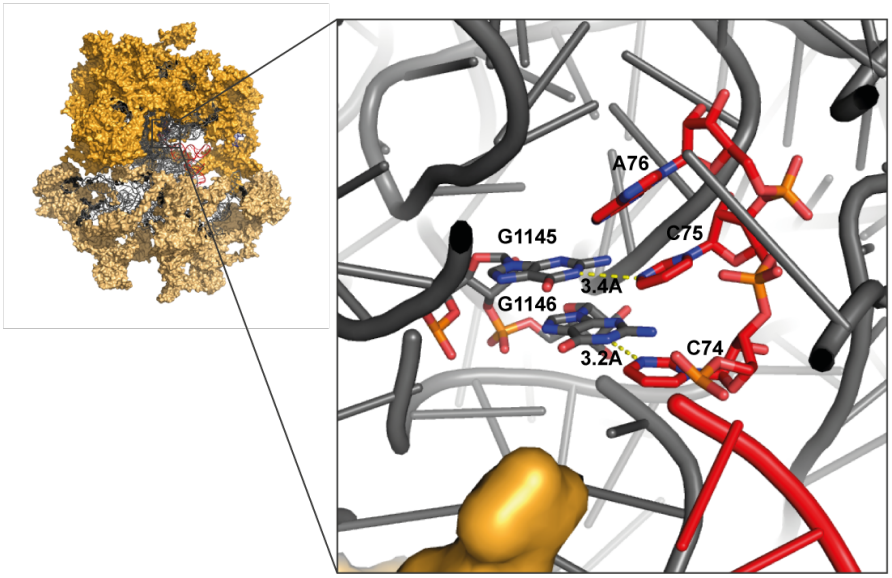

Figure 3.3.1 G1145 in the P-site. Orange, MRPLs; dark grey, rRNA; light orange, MRPSs; red, P-site tRNA. The 3' CCA and G1145-1146 are depicted as cartoons by element showing that they are roughly hydrogen bonding distance away from each other. The structure does not contain information about the tRNA sequence and hence Watson-Crick bonding could not be shown. (Modelled using Pymol molecular visualisation system, PDB 3J9M)

Complexomic profiling using proteins labelled with stable isotopes is a novel method with a potential for the analysis of the large complexes, including mitoribosome. However, there are some issues that still need to be addressed with this method. The enormity of the mitoribosome and its subunits prevent them from being sufficiently resolved by the blue native PAGE gel. There is a strong overlap between the peaks of the large and small subunits. However, to a certain extent, SILAC labelling compensates for this and allows for a direct comparison between the parental and knockout samples.

Our results did not show any substantial differences between the HEK293T parental cells and the MRM1 knockout cells. However, this method also revealed certain previously unidentified characteristics of the mitoribosome. The complexomic profile of the mt-LSU is much less diffused than that of the mt-SSU. In addition, the mt-LSU has fewer major peaks. This may suggest that as in bacterial ribosomal assembly, the large subunit also has fewer assembly intermediates, and thus assembly pathways than the small subunit. Variations in sample handling between experiments can also affect the integrity of the protein complex. For example, the mt-SSU subassembly detected in the different HEK293T cell lines reproducibly contains the subunits MRPS26,

MRPS17, MRPS34, MRPS27, MRPS18b, MRPS5, MRPS6 and MRPS22 and may represent an assembly intermiadiate. When visualised on the 3D structure, these subunits seemed to cluster together. However, the detection and the composition of this subassembly may vary depending on these variations (Figure 3.3.2).

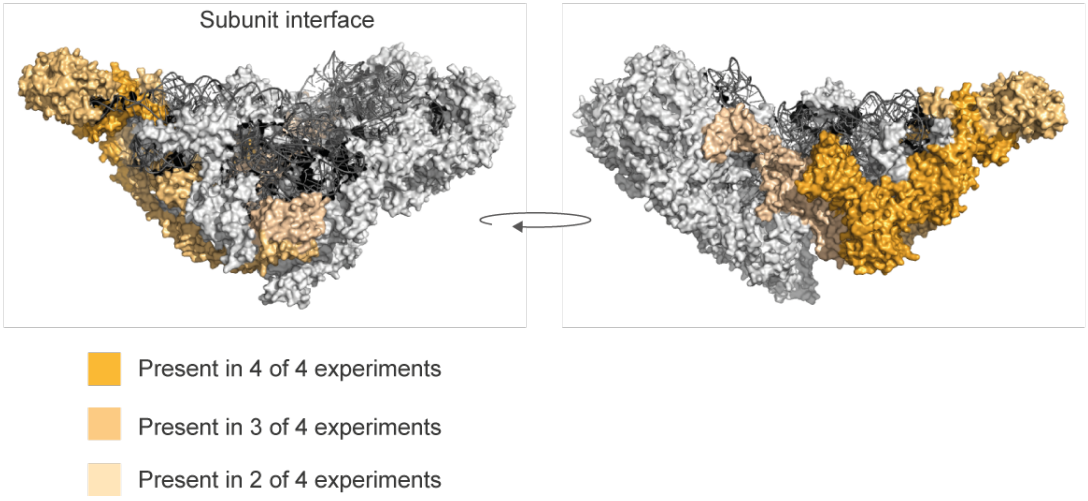

Figure 3.3.2 Subassembly of the small subunit observed in various SILAC-complexomics results. The darkness of the orange signifies how repeatable the presence of the protein is. Light grey, MRPSs, Dark grey, 12S rRNA (PDB:3J9M)

In cells overexpressing MRM1, both sucrose gradient fractionation and complexomic profiling identified a block in the assembly of mt-LSU and the mt-SSU. This is clearly visible in the average protein abundance of each slice of the complexomic profiles (Figure 3.2.8). In particular, the stalled subassembly of the mt-LSU lacked subunits lack subunits MRPL16, MRPL14, MRPL28 and MRPL41 (Figure 3.3.3). However, the composition of the stalled mt-SSU was the same as the control sample. The reason for the lower molecular weight cannot be attributed to the absence of specific protein components. This could be a non-specific side effect of the overexpression of an RNA-binding protein. Alternatively, this could be explained by the abundant MRM1 preventing the dissociation of the protein from 16S rRNA, which in turn prevents the association of MRPs and the progression of assembly. Many of the mitoribosome biogenesis factors, namely GTPases, rely of the hydrolysis of GTP to induce dissociation, which in turn causes assembly to progress (See section 1.7.4.1). In the case of MRM1, one assumes that the affinity of MRM1 to its substrate decreases after 2'-O-ribose methylation, which leads to dissociation. However, the high abundance of the protein in overexpression cell lines may compensate for this lower affinity and may cause the rRNA site to be constantly occupied by MRM1.

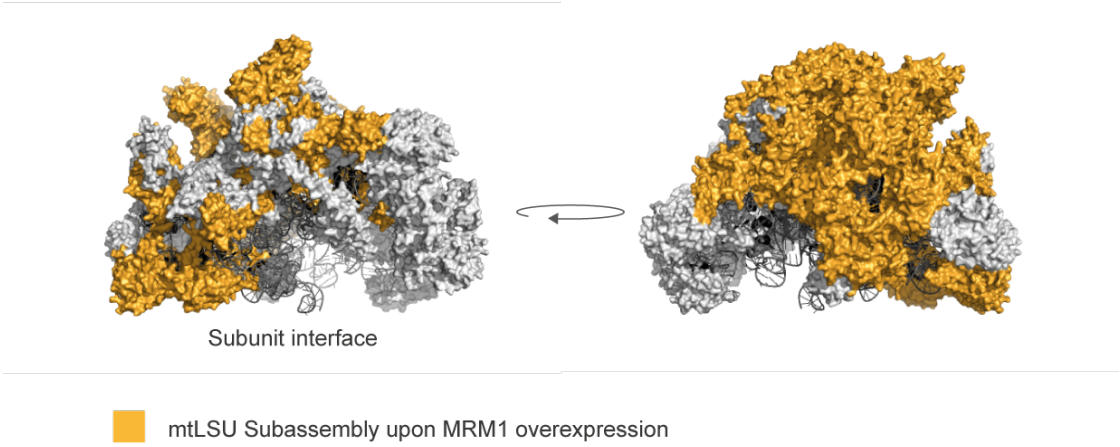

Figure 3.3.3 Subassembly of the large subunit observed in complexomic profiling of MRM1 overexpression cells. The orange signifies proteins found in the subassembly of the mt-LSU found in slice 16 of the complexomic profile shown in Figure 3.2.6 (where abundance of the protein is highest, red) (PDB:3J9M)

3.3.3.1 MRM1 does not interact with mitoribosomal proteins or other known biogenesis factors

Previously identified 16S rRNA methyltransferases strongly interact with the mitoribosome. MRM2 interacts with the mt-LSU and the assembled mitoribosome, while MRM3 only interacts with the mt-LSU (Rorbach et al., 2014). Therefore, it was assumed that MRM1 would also show similar interactions. Western blotting and complexomic profiling did not identify MRM1 co-localising with the mitoribosome. Proteins immunopurified after treatment with benzonase, to identify interactions independent of RNA interaction, identified direct interactions between the proteins independent of RNA intermediaries. However, even though MRM1 binds and modifies 16S rRNA, it failed to pull down known 16S rRNA-associated MRPs or biogenesis factors. Instead, mt-SSU biogenesis factor, ERAL1, was pulled down as a weak interactor. In addition, LYRM7, a late stage assembly factor of Complex III was also immunopurified. However, a role in co-translational assembly of the complex is discounted by the fact that OxPhos function and steady state level of complex III subunit was not changed by the absence of MRM1. Interestingly, NT5DC2, a predicted mitochondrial nucleotidase is also common to both immunopurifications with and without benzonase treatment. As a nucleotidase, it is capable of binding RNA, and thus may play a role in ribosome biogenesis. However, the protein remains uncharacterised and could be an interesting subject for further studies. The failure of

MRM1 to bind to mitoribosome-associated proteins suggests that MRM1 may act on 16S rRNA at an early stage of biogenesis. A summary of the proteins pulled down by MRM1, their cellular localisation and previously characterised roles in the cell are detailed in tables 3.3.1 and 3.3.2.

Interactors	**Localisation**	**Function**	**References**
DIS3L	Found predominantly in the cytoplasm.	3'-5' exoribonuclease activity. Possible RNA-binding contaminant as it is removed by benzonase treatment.	Tomecki et al. (2010)
HSPA9	Mitochondria	Heat shock protein possibly produced as a result of overexpression of the MRM1 bait protein.	Wadhwa et al. (2002)
EPPK1	Cytoplasm	Cytoskeleton maintenance	Jang et al. (2005)
ERAL1	Mitochondria	mt-SSU biogenesis factor (see section 1.7.4)	Dennerlein et al. (2010)
LYRM7	Mitochondrial inner membrane	Complex III assembly factor	Sanchez et al. (2013)
PRDX3	Mitochondria	Antioxidant protein	Watabe et al., 1997
NT5DC2	Predicted mitochondrial	Not characterised. Contains domains for hydrolase and 5'-nucleotidase activity.	-

Table 3.3.1 Function of MRM1 immunoaffinity proteins in the absence of benzonase

Interactors	Localisation	Function	References
PPM1B	Nucleus	Mg2+/Mn2+ dependent protein phosphatase	Tasdelen et al. (2013)
SELO	Mitochondria	Antioxidant protein	Han et al. (2014)
FAHD1	Mitochondria	Fumarylacetoacetate hydrolase activity in tyrosine catabolism pathway	Pircher at al. (2011)
HSPA9		See Table 3.3.1	
ERAL1		See Table 3.3.1	
NT5DC2		See Table 3.3.1	
MCCC1	Mitochondria	3-methylcrotonyl-coA carboxylase activity in leucine catabolism pathway	Obata et al. (2001)
PRDX3		See Table 3.3.1	
LYRM7		See table 3.3.1	

Table 3.3.2 Function of MRM1 immunoaffinity proteins in the presence of benzonase

Only 7 of these proteins were identified in three independent complexomic profiling data sets of HEK293T control cells (Figure 3.3.4). Of these, PRDX3 and HSPA9 were found evenly spread in all the lanes indicating that the proteins indiscriminately bind to proteins in the mitochondria. ERAL1, a known late-stage assembly factor of the mt-SSU seems to co-migrate with the assembled mt-LSU/mt-SSU (complex A) (Figure 3.3.3 assembly labelled 'A'). Since the assembled mt-LSU and mt-SSU are not adequately resolved on the blue native gel, it is difficult to conclude which complex the protein is bound to. However, in the third of the three experiments shown, ERAL1 does not seem to co-migrate with the complex A indicating variability in the results and that a lack of an observed interaction does not indicate an absence of an interaction. Similarly, NT5DC2 is seen co-migrating with both the assembled mitoribosomal complexes and the mt-SSU subassembly described earlier (Figure 3.3.4). FAHD1 co-migrates with complex A in one of the three experiments. LYRM7 and MCCC1 are both detected in the same fraction as the mt-SSU subassembly (complex B). However, if this is a true co-migration, why mt-SSU-interacting proteins would be pulled down with MRM1 is unclear.

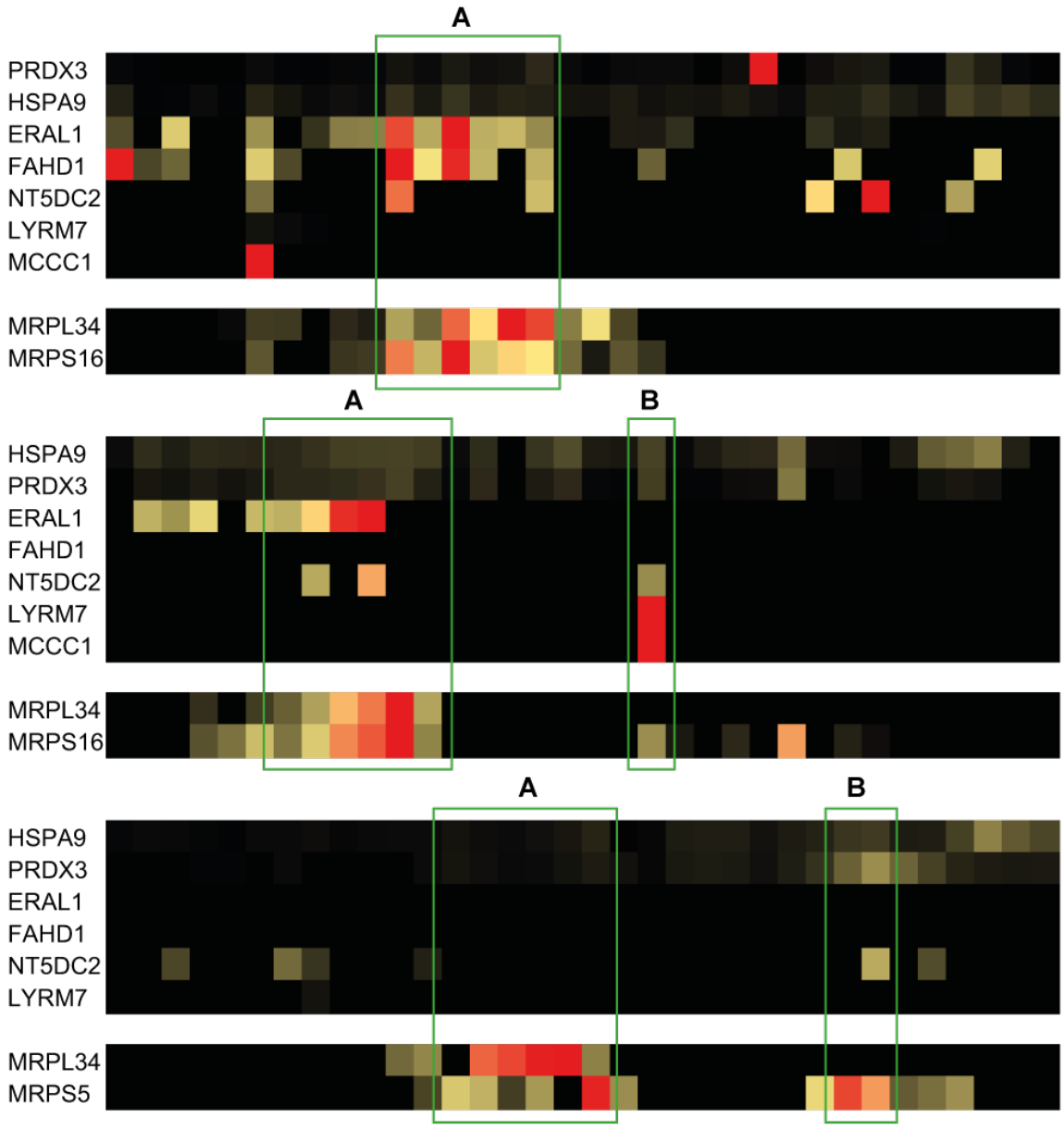

Figure 3.3.4 Immunoaffinity purified MRM1 interactors in complexomic profiles of HEK293T cells. The membrane fraction of mitochondria extracted from parental HEK293T cells was resolved on a blue native PAGE gel. The lane was cut into 64 slices and each slice was analysed via mass spectrometry. The colour of the heatmap indicates the intensity of detection of the protein in that fraction where red indicates the maximum intensity and black indicates the minimum. Green box A – mt-LSU/mt-SSU assembled complexes, Green Box B – mt-SSU subassembly

4 YbeY – A novel mitochondrially-targeted endonuclease required for mitoribosomal biogenesis

4.1 YbeY – A novel mitochondrially-targeted endoribonuclease

Human YbeY protein encoded by the *C21orf57* gene is an uncharacterised protein predicted to be a mitochondrially-localised by mitochondrial localisation database MitoCarta 2.0 and MitoMiner 4.0 (Calvo *et al.*, 2016, Smith and Robinson, 2016).

YbeY is conserved in prokaryotes, some protists, a few plant species and higher metazoans. However, it has been lost in a majority of protists, plants, fungi and lower metazoans (Figure 4.1.1). The *E. coli* homolog, eYbeY (UPF0054 protein family), was identified as one of 206 genes that are vital for viability and comprise the 'minimal bacterial genome' set (Gil *et al.*, 2004). Deletion of the protein in *E.* coli leads to a severe sensitivity to temperature, detergents, oxidative stress, β-lactam antibiotics and aminoglycoside antibiotics (Davies et al, 2010). Furthermore, YbeY is essential for pathogenesis in bacteria. Without the protein, *Vibrio cholerae* are incapable of correctly expressing small RNAs required for virulence, causing an inability to colonise mice or to produce biofilm. Similarly, YbeY is required by *Yersinia enterocolitica* for the expression of virulence factors required for adhesion and infection of eukaryotic cells (Leskinen et al., 2015). This necessity of YbeY also extends to symbiosis. In *Sinorhizobium meliloti,* the lack of YbeY prevents the nitrogen-fixing bacteria from effectively forming a symbiotic relationship with their legume hosts (Davies and Walker, 2008).

This is in contrast with in fungi, which have lost the YbeY-coding gene, and expression of the human YbeY in *Saccharomyces cerevisiae* causes a strong growth phenotype and extreme toxicity (Ghosal *et al.*, 2017).

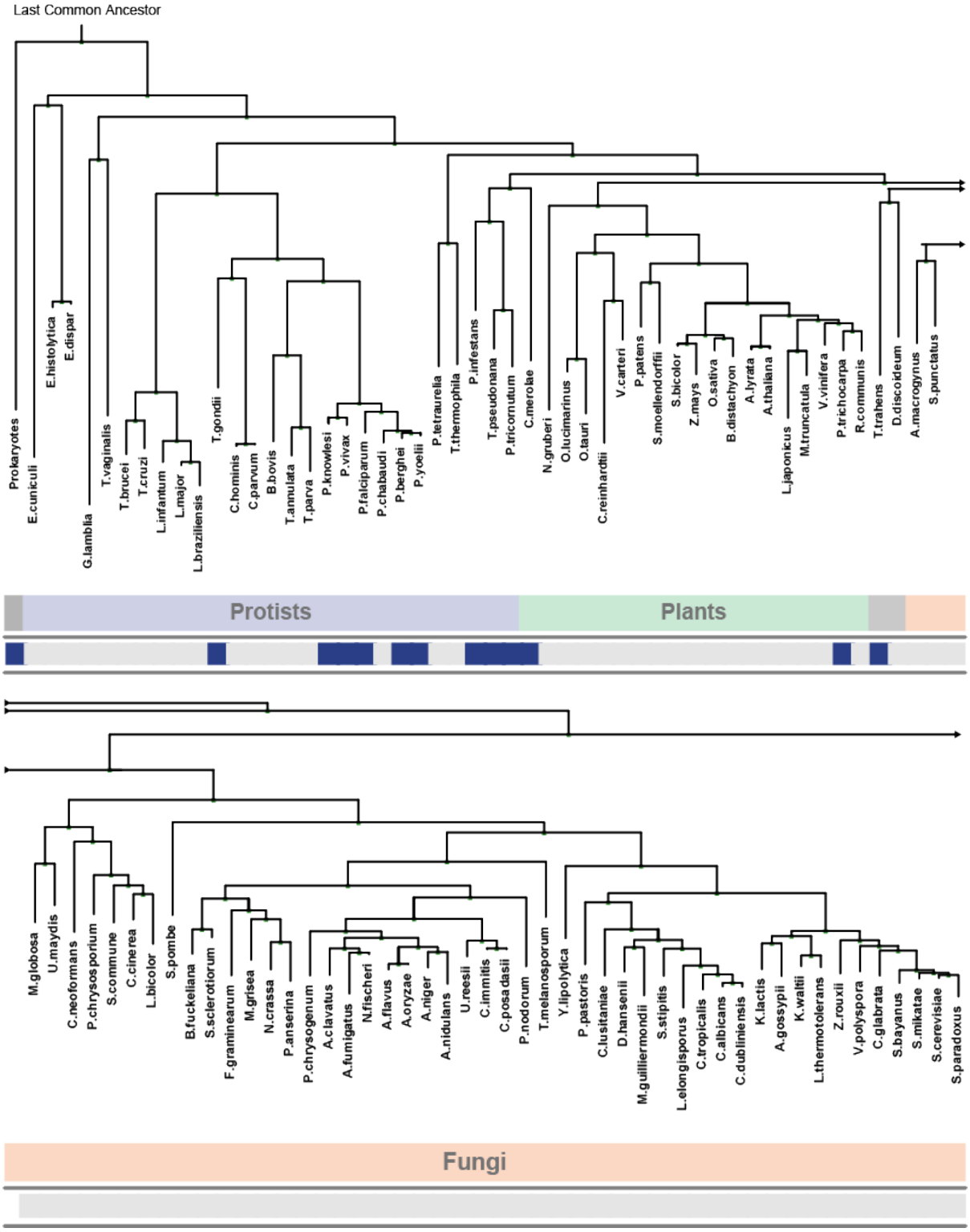
Last Common Ancestor
Prokaryotes
E.cuniculi
E.histolytica
E.dispar
G.lamblia
T.vaginalis
T.brucei
T.cruzi
L.infantum
L.major
L.braziliensis
T.gondii
C.hominis
C.parvum
B.bovis
T.annulata
T.parva
P.knowlesi
P.vivax
P.falciparum
P.chabaudi
P.berghei
P.yoelii
P.tetraurelia
T.thermophila
P.infestans
T.pseudonana
P.tricornutum
C.merolae
N.gruberi
O.lucimarinus
O.tauri
C.reinhardtii
V.carteri
P.patens
S.moellendorffii
S.bicolor
Z.mays
O.sativa
B.distachyon
A.lyrata
A.thaliana
L.japonicus
M.truncatula
V.vinifera
P.trichocarpa
R.communis
T.trahens
D.discoideum
A.macrogynus
S.punctatus
Protists
Plants
M.globosa
U.maydis
C.neoformans
P.chrysosporium
S.commune
C.cinerea
L.bicolor
S.pombe
B.fuckeliana
S.sclerotiorum
F.graminearum
M.grisea
N.crassa
P.anserina
P.chrysogenum
A.clavatus
A.fumigatus
N.fischeri
A.flavus
A.oryzae
A.niger
A.nidulans
U.reesii
C.immitis
C.posadasii
P.nodorum
T.melanosporum
Y.lipolytica
P.pastoris
C.lusitaniae
D.hansenii
M.guilliermondii
S.stipitis
L.elongisporus
C.tropicalis
C.albicans
C.dubliniensis
K.lactis
A.gossypii
K.waltii
L.thermotolerans
Z.rouxii
V.polyspora
C.glabrata
S.bayanus
S.mikatae
S.cerevisiae
S.paradoxus
Fungi

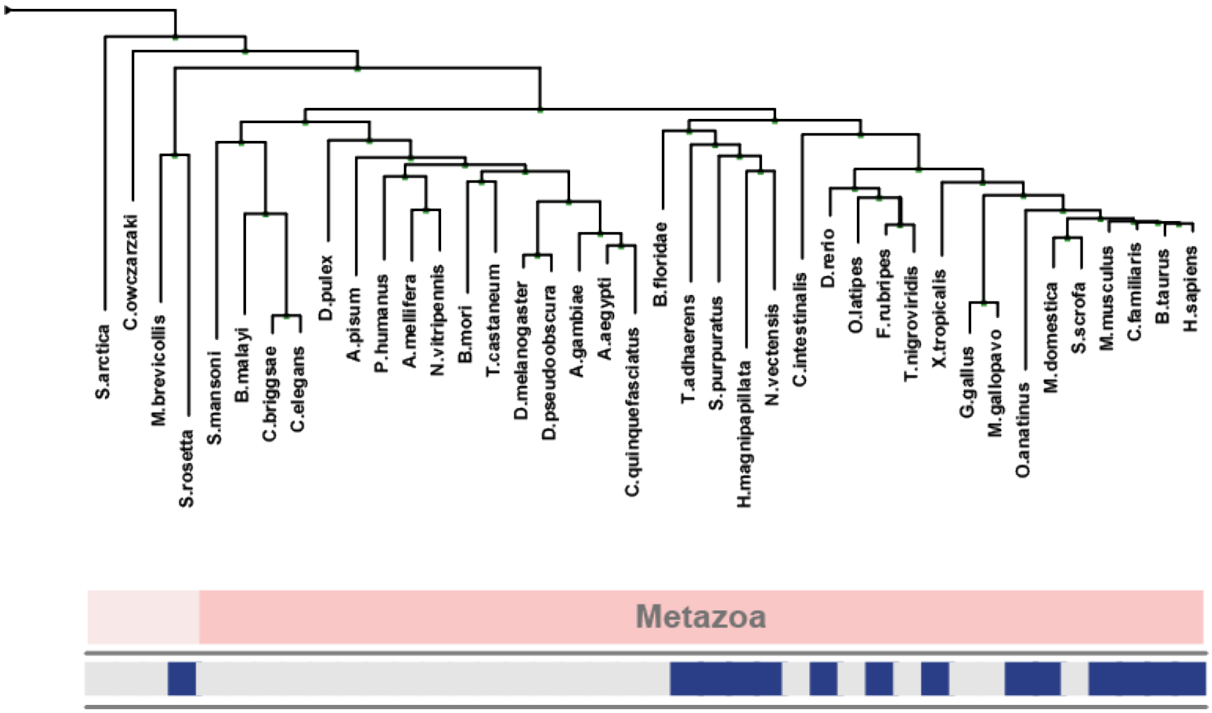

Figure 4.1.1 Conservation and phylogeny of YbeY. Evolutionary conservation of YbeY was calculated using CLIME portal online web service (gene-clime.org). The bottom bar indicates the presence of the protein in the species indicated above on the evolutionary tree. Grey indicates absence of the protein while blue indicates presence of the protein. The length of the branches in the phylogenetic tree indicate divergence of the protein since a common ancestor.

Bacterial YbeY is a single strand-specific endoribonuclease, which contains a highly conserved Arg59 residue for RNA binding and a zinc ion-coordinating histidine triad (H3XH5XH) domain for endonucleolytic cleavage (Davies *et al.*, 2010; Jacob et al., 2013). Human YbeY shares 23% sequence identity with its bacterial homolog. 3D homology modelling of human YbeY using the *E. coli* protein as a template (PDB 1XM5) shows that the catalytically important residues are conserved in humans (see Figure 4.2.1). Therefore, it is predicted that RNA binding and endonuclease function is retained in the human version of the protein.

In *E. coli*, eYbeY has been assigned various rRNA maturation functions. It is responsible for the 3' end processing of the SSU rRNA (16S in *E.* coli) and depletion of eYbeY leads to a loss of translation caused by the depletion of the 30S SSU (Rasouly et al., 2009; Rasouly et al., 2010).

Furthermore, it has been shown to play a role in the maturation of the 23S LSU rRNA and 5S RNA molecule (Jacob *et al.,*2013). Early studies with eYbeY showed

that it interacts with exonuclease, RNase R, rRNA maturation factor, RNase III and exoribonuclease, PNPase. In association with exonuclease RNase R, eYbeY was shown to specifically degrade rRNA from late stage 70S ribosomes with defective 30S SSUs, without degrading rRNA from unassembled LSU and SSU (Jacob et al., 2013) and as such plays a role in ribosomal quality control (Davies et al., 2010).

Recent bacterial 2-hybrid analysis with eYbeY showed that it interacts with ribosomal protein, S11, GTPase Era, a protein that acts as a checkpoint in 30S ribosomal subunit maturation and GTPase Der which is a 50S ribosomal subunit maturation switch (Vercruysse *et al.*, 2016), stress regulator SpoT and YbeZ. The interaction with S11 occurs through a conserved four-stranded β-sheet distinct from the catalytic site. The residues involved in this interaction are conserved in human YbeY (Figure 4.2.29). A disruption of the eYbeY-S11 interaction led to an increase in the 16S rRNA precursor and a subsequent increase in sensitivity to stress (Vercruysse *et al.*, 2016).

YbeY has also been investigated in eukaryotic models. In *Arabadopsis thaliana*, YbeY has been shown to co-localise to the chloroplast where it is involved with maturation of the 23S, 16S and the 4.5S rRNA components. Consequently, mutations in YbeY lead to deficiencies in ribosomal biogenesis and translation in the chloroplast. YbeY null mutants showed seedling lethality and YbeY knockdown showed slow growth and impaired photosynthesis (Liu *et al.* 2015).

Recent work on human YbeY identified non-specific ribonucleolytic activity of the protein, in *in vitro* assays. Notably, the expression of human YbeY in bacterial cell lines lacking the protein, partially rescued the phenotype of the cells investigated by measuring changes in sensitivity of the cells to various stresses. However, a completion of 16S processing was not observed in these cells. This partial rescue was not observed with catalytically inactive human YbeY (Ghosal et al., 2017). This suggests that the divergence of the human YbeY sequence coincides with a divergence of function. In the mitochondria, the function of YbeY is unclear. The mammalian mitochondrial rRNA is assembled into the ribosomes without the need for end-processing as observed in bacteria. Both the 12S mtSSU and 16S mtSSU mt-rRNAs are flanked by tRNAs and excision of these tRNAs by RNase P and ELAC2 is sufficient to liberate mt-rRNA ready for assembly into the mitochondrial ribosome (Dubin et al., 1982; Mercer et al., 2011). Therefore, the human orthologue of YbeY is likely to have a different function in the mitochondria, yet the exact role of YbeY in mammalian mitochondria is still unknown. In this section, we aim to show mitochondrial

localisation of the protein and elucidate the function of the protein through characterisation of YbeY-deficient cell lines and immunoaffinity-based protein-protein interaction assays.

4.2 Identification of the role of YbeY in mitochondria using YbeY-deficient and YbeY-overexpressing cell lines

4.2.1 Structural analysis of YbeY

YbeY is not conserved in many clades of the evolutionary tree. However, it's endonucleolytic function is vital in bacteria. To identify if this function is preserved in human YbeY, the sequence conservation of YbeY was investigated by aligning the amino acid sequence of the protein to that of various species using the Clustal omega online tool (figure 4.2.1). Previously arg59 (bacterial numbering) and a histidine triad (H3XH5XH) have been identified as vital for endonucleolytic activity of the bacterial enzyme. The sequence comparison showed that these catalytically important residues are conserved in humans. Then, homology modelling of human YbeY was performed to predict the 3D structure using the bacterial structure as a template (Figure 4.2.2A). The SwissDock ligand docking software was used to dock ADP into YbeY, to identify whether it is still capable of binding RNA, and whether the predicted site of docking corresponds to the catalytic site. The software output also provides an electrostatic surface, which showed that the catalytic cavity, where the conserved residues reside, has an electropositive surface (Figure 4.2.2B, blue), suitable for binding the negatively charged nucleic acid backbone. The software provides a large number of candidate sites where the ligand may bind the protein surface. The first 50 probable docking configurations were modelled on the protein surface (Figure 4.2.2C). The top 49 docking configurations of ADP were found to be within the catalytic site. This indicated the human YbeY contains a conserved RNA binding pocket similar to the bacterial protein.

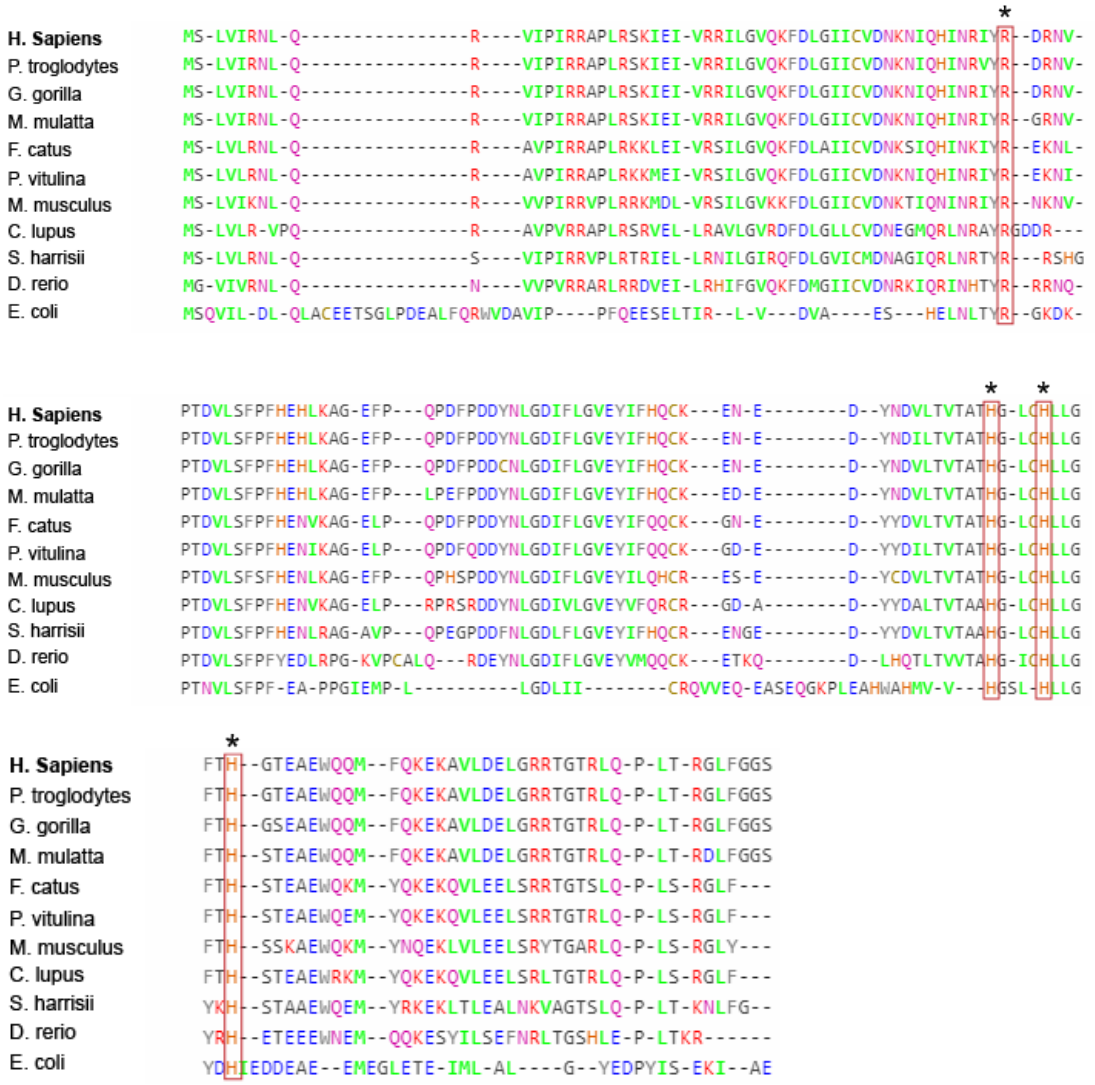

Figure 4.2.1 Sequence alignment of YbeY.

The YbeY amino acid sequences for various species were aligned using the Clustal Omega online tool (www.ebi.ac.uk/Tools/msa/clustalo). The catalytically-important RNA-binding arginine and the zinc ion binding H3XH5XH motif are highly conserved and indicated with a red box and an asterisk.

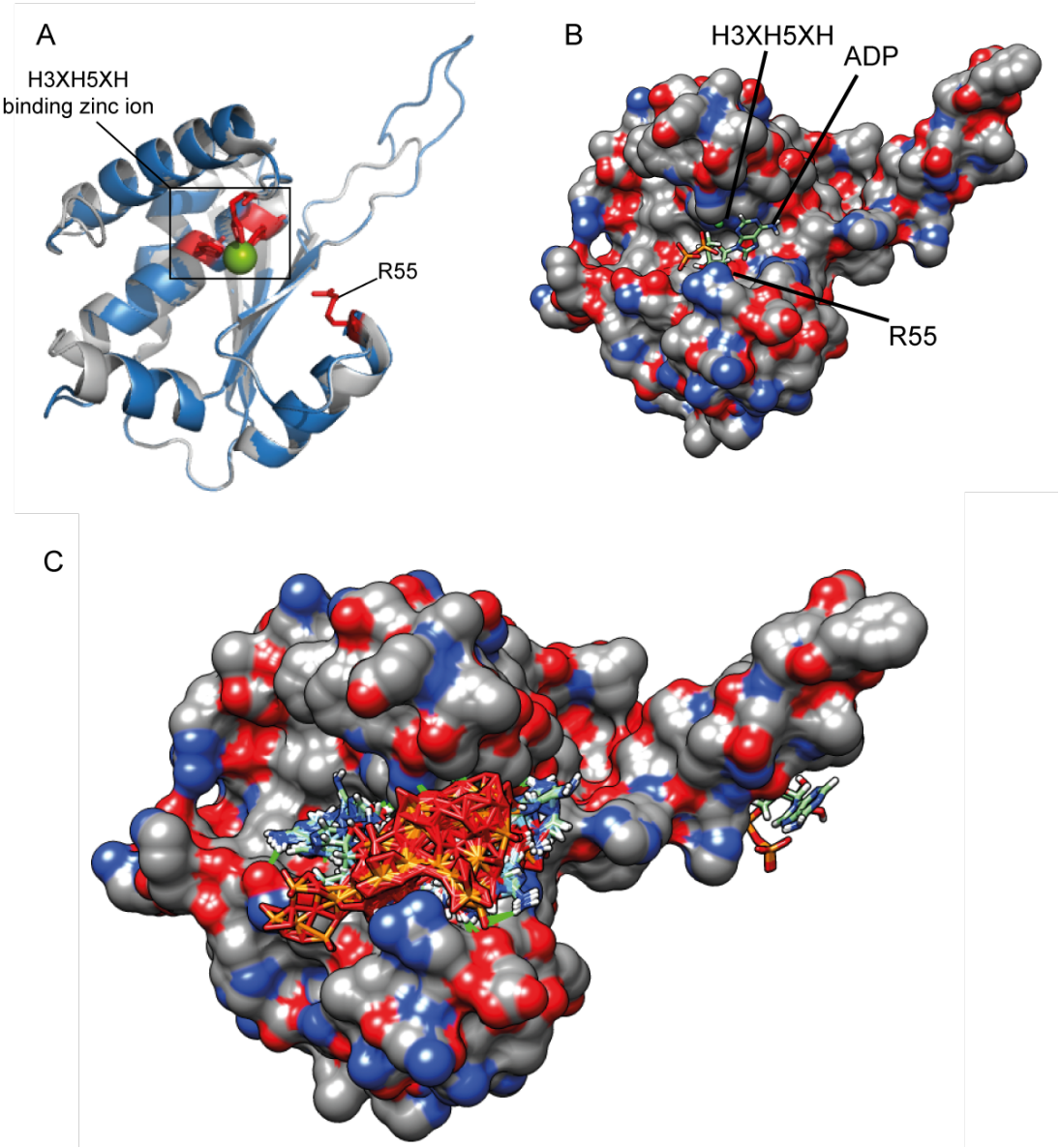

Figure 4.2.2 Structural analysis of Human YbeY (A) Homology modelling of YbeY using E. coli YbeY as a template (PDB: 1XM5). Blue, human YbeY; grey, bacterial YbeY; red, catalytically important residues; green, zinc ion. Homology modelling was performed using Swiss-Model homology modelling server and visualised using PyMol. (B) Most probable ADP docking site in homology modelled human YbeY with catalytically important residues identified. The protein is colour based on electrostatic surface charge. Blue, electropositive; red, electronegative; dark grey, neutral. Docking analysis and electrostatic surface charge analysis was performed using the SwissDock web service (C) 50 most probable ADP docking sites on the YbeY surface as calculated by the SwissDock web service. The docking models were visualised using Chimera.

4.2.2 Localisation of YbeY in the cell

Mitochondrial localisation prediction compendia such as MitoCarta2.0 and MitoMiner 4.0, had already predicted the localisation of YbeY in the mitochondria (Calvo et al., 2016, Smith and Robinson, 2016). Additionally, *in silico* analysis of the N-terminus of the protein was used to assess subcellular localisation of a protein to the mitochondria. This method looks for a consensus sequence, also called the mitochondrial targeting sequence, which composes of amphipathic α-helices and targets the protein for mitochondrial import. There are two variants of YbeY produced by alternative transcription start sites (Genbank Accession number: BC022828). However, only transcript 1 produces a protein with the catalytic site (see Section 4.2.1). Bioinformatic analysis of the N-terminal sequence of the YbeY protein produced from transcript 1 showed a high probability of mitochondrial localisation (Table 4.1).

	Probability of mitochondrial localisation
Predotar	87%
TargetP	86.2%
Mitoprot II	95.8%

Table 4.2.1 In silico analysis of mitochondrial localisation of YbeY. Analysis of the probability of mitochondrial localisation was performed using Predotar (Small et al, 2004), TargetP (Emanuelsson et al., 2000) and Mitoprot (Claros and Vincens, 1996), by analysing the composition of the N-terminus of the protein.

To analyse this prediction experimentally, YbeY cDNA was cloned into a pcDNA5/FRT/TO flag/strep2 plasmid, transiently transfected into HeLa cells. Upon fixing, cells were subjected to ICC, using antibodies against the flag epitope to detect YbeY (anti-mouse secondary, green). Antibodies against mitochondrial outer membrane translocase, TOM20 were used to label mitochondrial membranes (red). Overlap of the red and green signal is visualised as yellow. This shows co-localisation of the YbeY signal in the mitochondria (Figure 4.2.3A).

Then, to assess if the protein co-localises within mitochondrial RNA granules (MRGs) within the mitochondria, immunocytochemistry was performed using antibodies against GRSF1 to label MRGs (Antonicka et al., 2013). MRGs appear as distinct

puncta whereas YbeY seems to be distributed throughout the mitochondria (Figure 4.3B). This showed that YbeY is exclusively localised in the mitochondria and not found in MRGs.

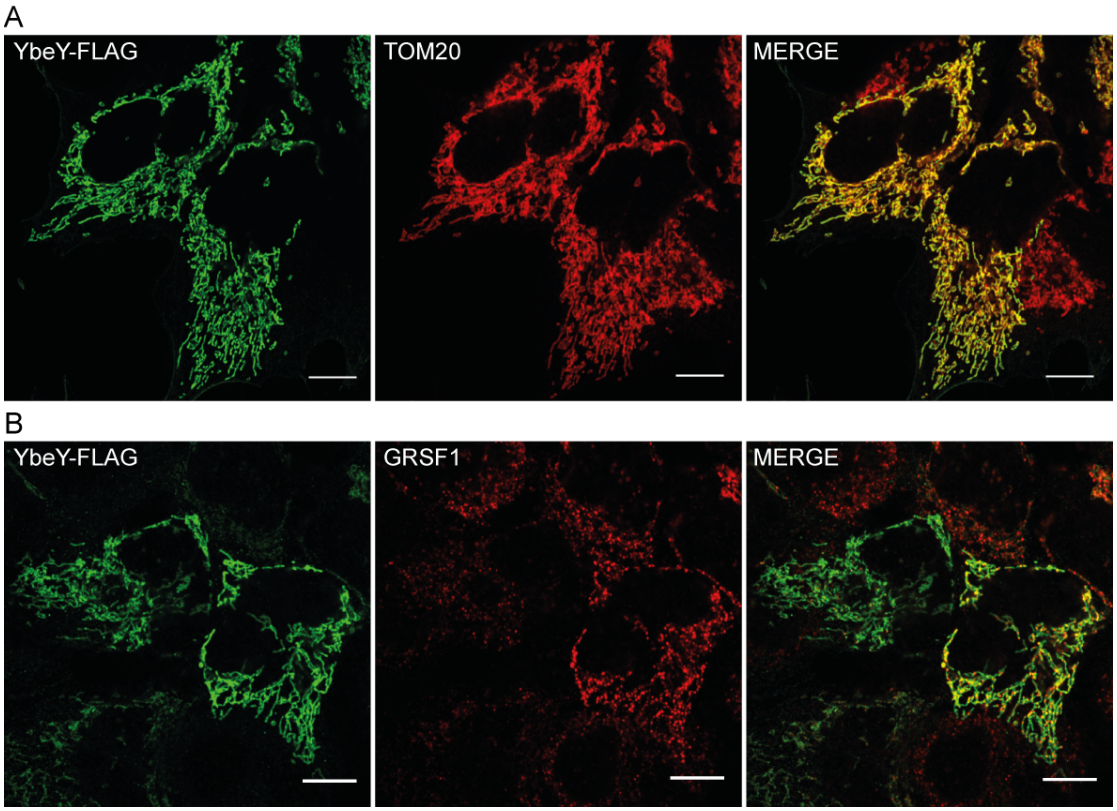

Figure 4.2.3 Immunocytochemistry of YbeY. Flag-tagged YbeY was transiently expressed in Hela cells and visualised using anti-flag antibodies (goat anti-mouse IgG, Alexa fluor 488, green, left). (A) The mitochondrial network was stained using antibodies against mitochondrial outer membrane translocase, TOM20 (goat anti-rabbit, Alexa fluor 594, red, middle). Co-localisation of YbeY and TOM20 is shown in yellow (right). (B) RNA granules were stained using antibodies against GRSF1 (red, middle). The digitally merged image does not show distinct yellow puncta that would indicate co-localisation of GRSF1 and YbeY in RNA granules (yellow, right). White scale bar at the bottom right indicates 10 μm. Immunocytochemistry and microscopy was performed by Pedro Guiomar.

The subcellular localisation of endogenous YbeY antibody was also analysed using western blotting of subcellular fractions of HEK293T cells. Homogenisation and centrifugation was used to isolate nuclear, cell debris, cytosolic and mitochondrial fractions. An additional Proteinase-K treatment was used to degrade proteins bound to the exterior of the mitochondria. Proteins in the mitochondrial fraction, that are resistant to Proteinase-K treatment, can be inferred to be in the mitochondrial matrix. Antibodies were used against cytosolic GAPDH, outer membrane translocase

TOM22, inner mitochondrial complex I component, NDUFS1, and endogenous YbeY. TOM22, NDUFS1 and YbeY, but not GAPDH, were enriched in the mitochondrial fractions. Both NDUFS1 and YbeY show resistance to Proteinase K treatment indicating that the proteins are localised within the mitochondrial matrix (Figure 4.2.4).

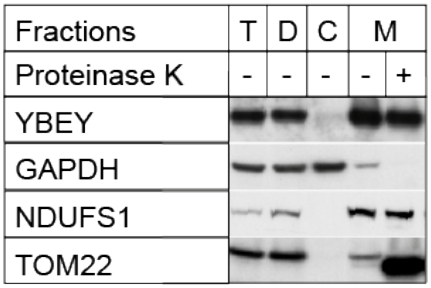

Figure 4.2.4 Localisation of YbeY in Subcellular fractions. Subcellular fractions of HEK293T cells were isolated and assessed using western blot. Antibodies were used to against endogenous YbeY and various protein markers for the subcellular fractions, namely, GAPDH (cytosol), TOM22 (outer membrane), NDUFS1 (mitochondrial matrix). T, total cell lysate; D, cell debris; C, cytoplasm; M, mitochondria

4.2.3 Role of YbeY in Cleavage of the ATP8/6-CO3 junction in mitochondrial RNA precursor

Structural analysis of YbeY showed that the catalytically important residues required for RNA binding (R59 in *E. coli*) and endonucleolytic activity (H3XH5XH motif) are strongly conserved in the human enzyme (Davies et al., 2010) (Figure 4.2.2A). This led us to postulate a role of YbeY in the processing of the non-canonical cleavage sites that are not catered for by the Punctuation model. There are a few of these sites in the polycistronic precursor, namely the ATP8/6-CO3 junction, the ND5-Cytb junction, the 3' end of ND6 and the 5' end of CO1 (Figure 4.2.5).

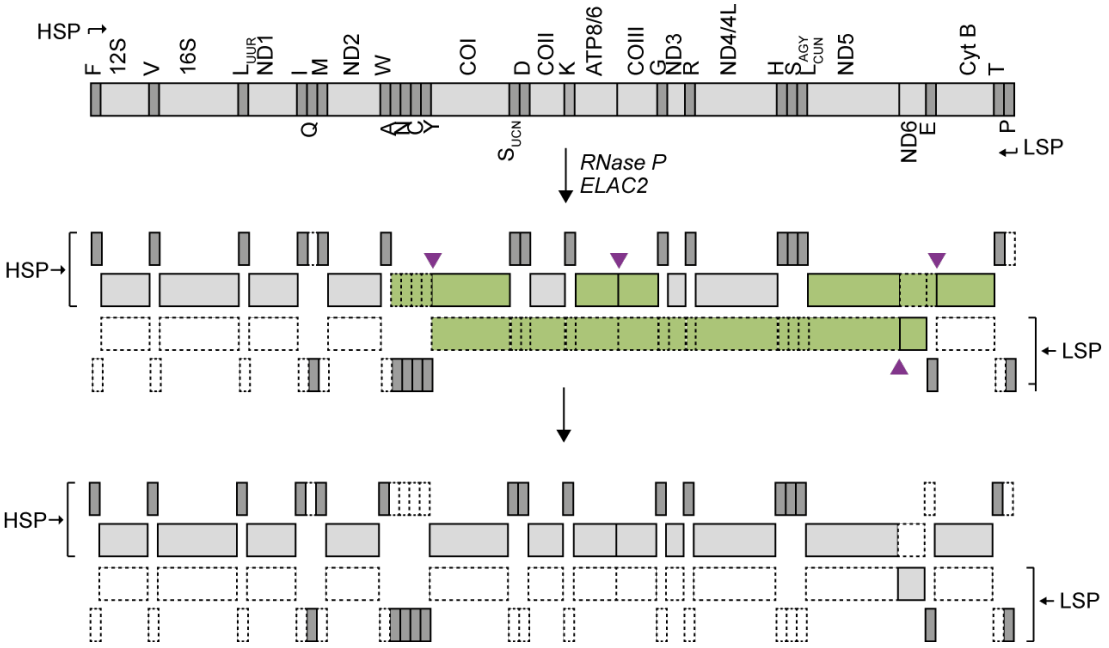

Figure 4.2.5 Non-canonical cleavage sites. RNase P and ELAC2 cleave the 5' and 3' ends of tRNAs in the polycistronic precursor molecules transcribed from the HSP and LSP. Light grey regions depict mRNAs and rRNAs. Dark grey regions depict tRNAs. Green regions depict immature molecules produced by RNase P and ELAC2 that require further maturation through non-canonical cleavage. Non-canonical cleavage sites are indicated with purple triangles. Regions contained within a dotted line are non-coding regions.

To investigate if YbeY is involved in the cleavage of non-canonical mtRNA sites, YbeY was knocked down using siRNA and transcripts were analysed using northern blotting and qPCR. In preliminary experiments, an accumulation of the ATP8/6-CO3 precursor was observed in cells transfected with siRNA and stressed with galactose media as the only carbon source where the cells were forced to be dependent on mitochondrial ATP production (Figure 4.2.6C and 4.2.6E). We hypothesised that growing cells in galactose media would lead to up-regulation of mitochondrial transcription, which would lead to an accumulation of unprocessed precursor transcripts due to a reduction in YbeY. No change was observed in control mtRNAs (16S rRNA, 12S rRNA, ND5 rRNA) (Figure 4.2.6B). However, this observation did not lead to defects in translation of the ATP8/6 or CO3 mRNA nor to changes in steady state levels of OxPhos complexes IV and V when analysed using western blot analysis (Figure 4.2.6D). This lack of a translational defect was attributed to there being sufficient YbeY in the knockdown cells to produce the required transcripts for mitochondrial translation. However, our preliminary hypothesis was

that, in mammalian mitochondria, YbeY had evolved to process the non-canonical cleavage sites, namely the ATP8/6-CO3 precursor transcript (Figure 4.2.8).

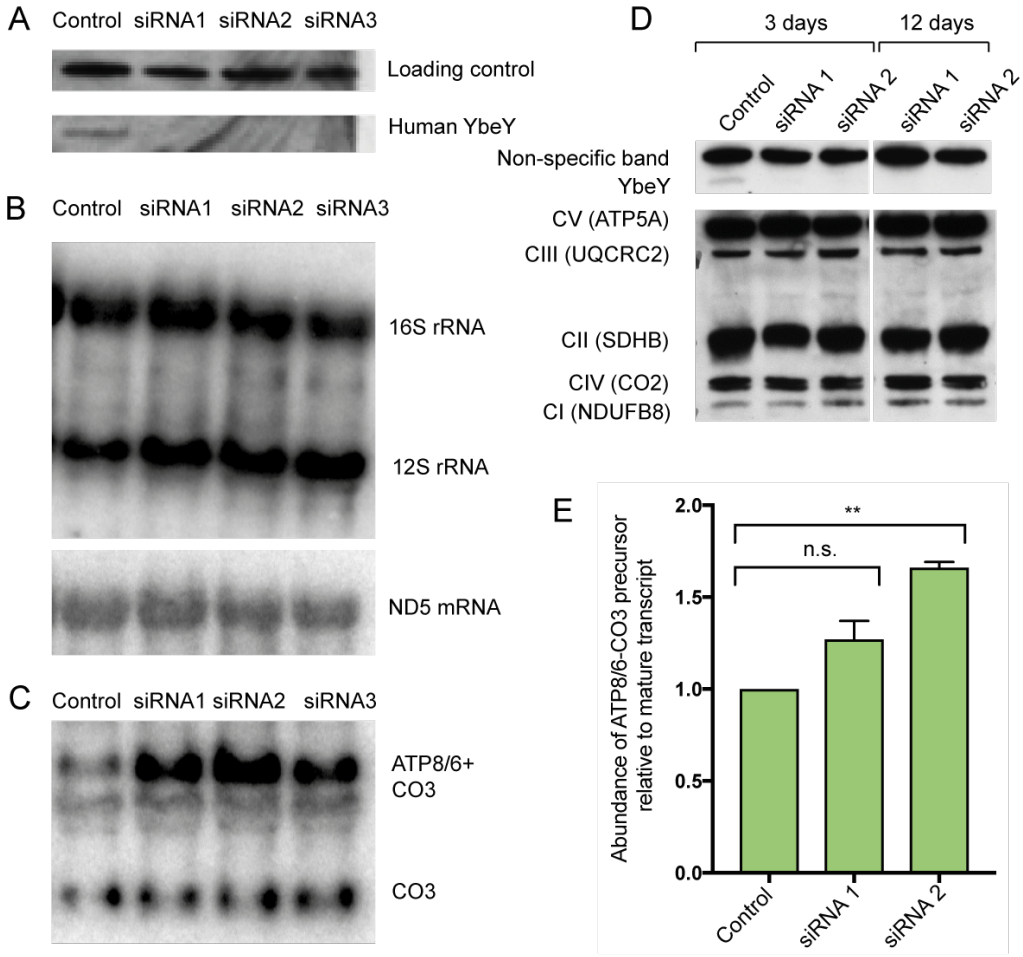

*Figure 4.2.6 Western blot and northern blot analysis of HeLa cells transfect with siRNA and grown in galactose media. (A) Western blot analyses of HeLa cells transfected with control siRNA (against GFP) and three different siRNAs against YbeY, probed with anti-YbeY antibody. (B) Northern blot probing for 16S rRNA, 12S rRNA and ND5 mRNA. (C) Northern blot analysis probing for CO3 which also binds to the ATP8/6-CO3 precursor transcript (Northern blot analysis performed by Dr Joanna Rorbach). (D) Western blot analysis of the siRNA knockdown cells after 1 transfection (3 days) and 4 transfections (12 days) with antibodies against the mitochondrial complexes. (E) qPCR analysis was performed on the RNA extracted from HeLa cells treated with YbeY siRNAs. Student's t-test was used to determine statistical significance (n.s., not significant; ** $p<0.01$). qPCR reaction was performed by Dr Christopher Jackson*

YbeY endonucleolytic cleavage of RNA in bacteria leads to the formation of a 5' hydroxyl and 3' phosphate group. We speculated that this biochemical feature is

conserved in the human enzyme. To analyse the nature of cleavage of the ATP8/6-CO3 precursor, we used the Terminator exonuclease that allows the phosphorylation state of the 5' end of the CO3 mature transcript to be assessed. Terminator exonuclease degrades RNA that has a 5'-monophosphate. It is incapable of degrading RNA with a 5' di/triphosphate, cap or hydroxyl group. In addition, the terminator assay was repeated after phosphatase treatment which would remove the 5'-phosphates in a di/triphosphate, leaving behind a monophosphate which is susceptible to Terminator-mediated degradation. Dephosphorylation of the di/triphosphate 5' end would then make the RNA susceptible to Terminator exonuclease. The RNA products were then analysed using northern blotting. A probe against CO1 was used as a control as it is known that it contains the 5'-monophosphate and would be susceptible to degradation (Mercer *et al.*, 2011).

The CO1 mRNA and the ATP8/6-CO3 precursor transcript was degraded by the Terminator exonuclease confirming the presence of a 5'-monophosphate. On the other hand, the CO3 mRNA was not degraded by the exonuclease. In addition, phosphatase treatment caused some of the CO3 to be degraded by the exonuclease. This analysis showed that CO3 does not have a 5'-monophosphate, suggesting the presence of a 5' di/triphosphate, cap and/or hydroxyl group. It seems that at least a small population of molecules are phosphorylated after cleavage. The 5' end of ATP8/6 contains a 5' monophosphate which is produced by ELAC2 upon excision of tRNA-lysine (Figure 4.2.7). Differences observed in the degradation of CO1 and CO3 could also be attributed in part to secondary structure of the RNA and availability of the RNA to the Terminator nuclease.

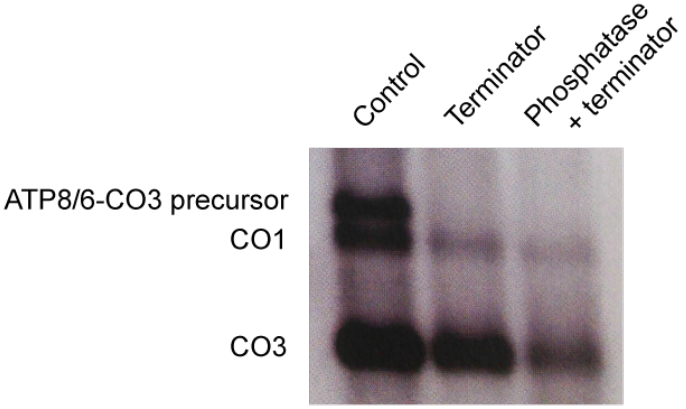

Band intensity relative to control (%)	Control	Terminator	Phosphatase + Terminator
CO1	100	32	24.4
ATP8/6-CO3	100	12.2	6
CO3	100	85.5	38.2

Figure 4.2.7 Terminator assay. RNA extracted from HEK293T cells was treated with Terminator nuclease or with Phosphatase and Terminator nuclease. The control sample was untreated. The RNA was then analysed using northern blotting, probing for CO1, and CO3. Bands were quantified using Image J and plotted using Prism 7. Experiments performed in collaboration with Dr Christopher Powell.

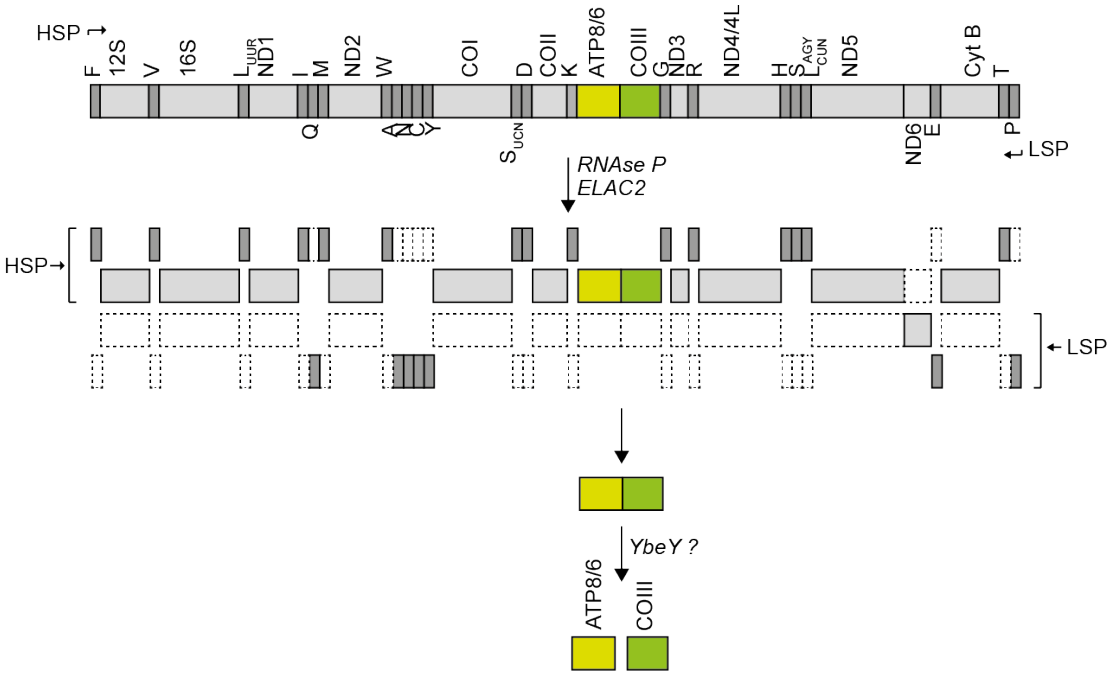

Figure 4.2.8 Primary hypothesis of the function of YbeY. The model shows canonical cleavage at the 5' and 3' ends of tRNAs by RNaseP and ELAC2 to produce the majority of mRNAs, tRNAs and rRNAs in the mitochondria. YbeY may be responsible for the cleavage of the ATP8/6-CO3 precursor transcript, which is not punctuated by tRNAs.

In order to directly investigate the cleavage activity of YbeY, HEK293/FRT/TO Flp-In cell lines were generated in which the expression of wild-type and catalytically inactive (R55A) YbeY could be induced using doxycycline. Arg55 (equivalent to *E.coli* Arg59) is important for RNA binding and indispensable for endonucleolytic cleavage in bacteria. The recombinant YbeY contained a C-terminal flag/strep2-tag that could then be purified from isolated mitochondria using streptavidin beads. Elution was confirmed using antibodies against the flag epitope and CBB staining (Figure 4.2.9A). Using this purified wild-type and mutant protein, *in vitro* cleavage assays were performed using *in vitro* transcribed α[^{32}P]-UTP-labelled RNA substrates. A 60 nucleotide control sequence encoding a sequence downstream in the ATP8/6-CO3 junction and a 70 nucleotide sequence spanning the ATP8/6-CO3 junction were used as substrates. This would indicate if YbeY has site-specific endonucleolytic activity. Furthermore, the concentration of the protein in the assay was varied from 0 to 20 pmol to show a concentration-dependant increase in cleavage. Cleavage activity would have been indicated with concentration-dependant increase in smaller cleavage products. No junction-specific cleavage or non-specific cleavage activity of the endonuclease was observed (Figure 4.2.9B). YbeY is a zinc-ion dependant endonuclease with a conserved zinc-ion binding H3XH5XH motif required for catalysis. Work in *Sinorhizobium meliloti* showed that the catalytic activity of the bacterial protein was also supported by other divalent metal ions such as Mg2+, Mn^{2+}, and Ca^{2+} (Samarago et al., 2016). Therefore, the metal ion composition of the reactions was changed to elucidate if this would have an effect on cleavage activity. However, no metal ion-specific effect on cleavage of the RNA substrates was observed (Figure 4.9C).

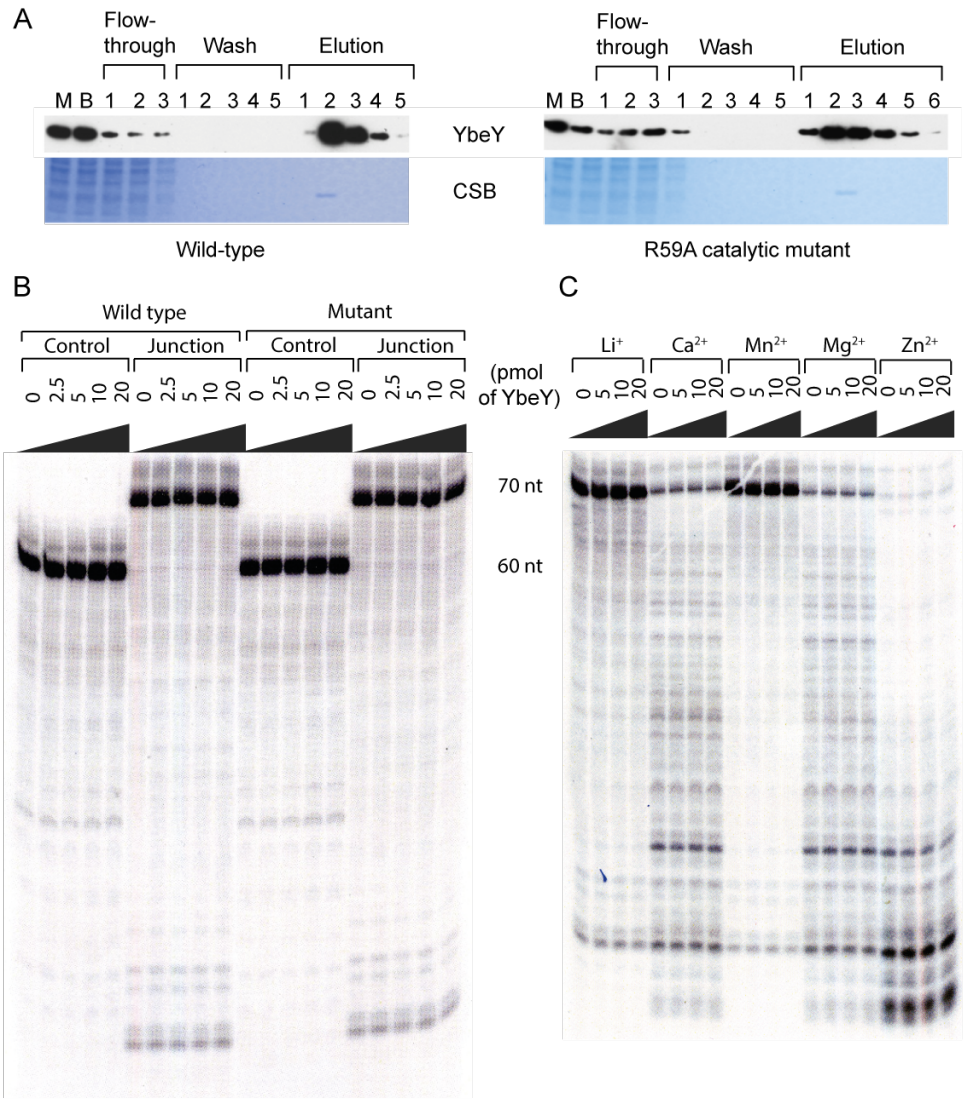

Figure 4.2.9 Affinity-purification of YbeY and In vitro cleavage assay. (A) HEK293T Flp-In cells containing wild-type (left) and catalytic mutant (R55A, right) were induced using 50 ng/ml doxycycline. Mitochondria were isolated and recombinant flag/strep2 – tagged protein was affinity purified using a streptactin column. Antibody against the flag epitope was used to detect YbeY. The SDS-PAGE gels were stained using coomassie Brilliant Blue stain. The prominent band in the elution fraction corresponds to purified YbeY-flag/strep2 protein. M - Mitochondrial fraction, B – Beads (B) Different concentrations (0-20 pmols) of purified recombinant protein were incubated with ~400 ng of radiolabelled in vitro transcribed RNA of length 60 (control, mtDNA positions 9371-9421) and 70 (ATP8/6-CO3 junction, mtDNA positions 9183-9251) nucleotides. (C) The cleavage assays were repeated with the 70 nt RNA substrate (~400ng) and wild-type YbeY (20 pmol) with different metal ions (10 mM) in the reaction. These experiments were performed in collaboration with Dr Thomas Nicholls.

4.2.4 YbeY Knockout and Complementation cell lines

4.2.4.1 Knockout generation in HEK293T cells

The results obtained from the siRNA experiments and the lack of confirmation of the preliminary hypothesis from *in vitro* experiments led us to pursue the creation of a knockout cell line. This would enable direct study of effects of lack of YbeY on the mitochondrial transcriptome, especially the non-canonical cleavage sites. Initially, when this was being attempted, the CRISPR-Cas9 technology was still in its infancy and the efficiency and specificity of the targeted DNA cleavage was still low. Karyotyping of the HEK293T cell line showed major rearrangements of the genome (see section 3.2.1). However, YbeY is positioned on chromosome 21, which showed no rearrangements and two or three copies of the chromosomes that needed to be targeted.

Zinc-finger nucleases (ZFN) were used to target the YbeY gene. The Sigma CompoZr custom ZFN service provides custom designed and validated ZFN pairs for the required gene target. Through this, we purchased two constructs targeting the first exon of YbeY. The double strand breaks created by the ZFNs would induce DNA repair through non-homologous end joining (NHEJ) or homology directed repair (HDR). HDR could be used to specifically direct gene editing using a donor targeting construct. However, in our system, NHEJ was harnessed to introduce insertions or deletions (indels), which would lead to a frameshift mutation and the generation of a premature stop codon.

HEK293T Flp-In cells were transfected with the ZFN vectors using lipofectamine and single colonies were split for freezing and screening. The protocol was the same as that used to produce MRM1 knockout clones in section 3.2.1. Initially candidates were identified using western blotting against endogenous YbeY and β-actin for loading. According to our preliminary hypothesis, we believe YbeY is required for effective production of mature transcripts. Therefore, antibodies against OxPhos complexes were also used to identify any other characteristics that might identify a potential YbeY knockout (Figure 4.2.10A).

Of the 192 clones screened, nine clones showing a lower level or complete lack of YbeY were selected from this initial screen. These candidates were analysed with PCR which would give a product spanning the ZFN target site, and thus, the site most likely to contain the NHEJ-mediated mutation. The PCR reaction mix was sent for

Sanger sequencing. Aligning the sequence against the wild-type sequence showed lower consensus after the ZFN cut site in cases where indels had caused a frameshift. The PCR products from candidates identified in this step were cloned into a pCR4 vector using the Zero Blunt TOPO cloning kit and multiple bacterial colonies for each clone were sent for Sanger sequencing. This is required because the indels produced by NHEJ could be different in each copy of the gene. In the case of YbeY, we expected to find 2-3 copies of YbeY per cell and therefore, we expected to see up to three different indels per clone. However, of the many clones screened, no complete knockout was identified with all alleles containing out-of-frame indels. Figure 4.2.10 shows two clones that were used for subsequent experiments.

In clone 4, four alleles of YbeY were identified with a 4 bp insertion (allele 1), a deletion of 13 bp and an insertion of 1 bp (allele 2), a deletion of 8 bp (allele 3) and a deletion of 67 bp (allele 4). In the first two alleles, a frameshift mutation led to a premature stop codon. In the third allele, the indel led to an inframe frameshift leading to a change in 12 amino acids in the protein. In the fourth allele, a large deletion led to the removal of the start codon. This hemizygous clone will subsequently be referred to as YbeY (-/m) (Figure 4.2.10B). In this clone, preliminary western blotting against the respiratory complexes showed a depletion in Complexes I and IV.

In clone 7, five copies of YbeY were identified. Three of these alleles (alleles 1, 2 and 4) contained indels which led to premature stop codons which would lead to early termination of translation. Allele 3 contained an in frame frameshift leading to the loss of two amino acids from the protein. The fifth allele was not affected (Figure 4.2.10C). The heterozygous clone will subsequently be referred to as YbeY (+/-). The two cell lines were thawed and screened further using western blotting and sequencing.

A

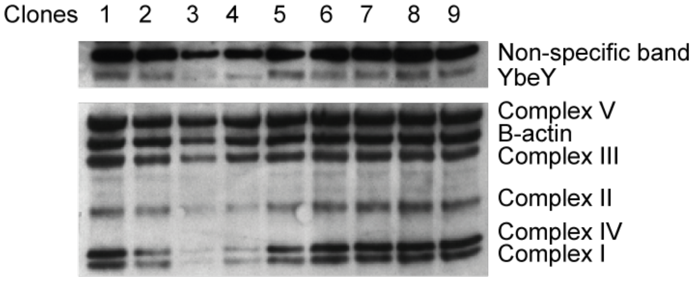

B

1. Insertion of 4 bp - Produces a 24 aa protein

YbeY AATGAGTTTGGTGATTAGAAATCTGCAGCGAGTCATCCCCATCAG - - - - GAGAG CGCCACTTCGCAGTA
Clone 4 ANGTGTTTTGTGAC-TAGAAATCTGCAGCGAGTCATCCCCATCAGGAGGGAGAG CGCCACTTCGCAGTA

2. Deletion of 13 bp and insertion of 1 bp - produces a 163 protein

YbeY AATGAGTTTGGTGATTAGAAATCTGCAGCGAGTCATCCCCATCAGGAGAGCGCCACTTCGCAGTAAGATC
Clone 4 AATGAGTTTGGTGATTAGAAATCTGCAGCGAGTCATCCCCATCAGGAG - - - - - - - - - - - - - TAGTAAGATC

3. Deletion of 8 bp - Produces a 18 aa protein

YbeY GATTAGAAATCTGCAGCGAGTCATCCCCATCAGGAGAG CGCCACTTCGCAGTAAGATCGAGATTGTAAG
Clone 4 GATTAGAAATCTGCAGCGAGTCAT - - - - - - - - GGAGAG CGCCACTTCGCAGTAAGATCGAGATTGTAAG

4. Deletion of 67 bp - No start codon

YbeY TAAAGGGC TGGTTATTCTTCCTGAAATGAGTTTGGTGATTAGAAATCTGCAGCGAGTCATCCCCATCAGGAGA
Clone 4 T - GGAGA

C

1. Deletion of 14 bp - produces a 16 aa protein

YbeY AATGAGTTTGGTGATGCAGCGAGTCATCCC CATCAGGAGAGCGCCACTTCGCAGTAAGATCGAGATTG
Clone 7 AATGAGTTTGGTGATGCAGCGAGTC - - - - - - - - - - - - - - AGCGCCACTTCGCAGTAAGATCGAGATTG

2. Deletion of 4 bp - produces a 24 aa protein

YbeY AATGAGTTTGGTGATGCAGCGAGTCATCCC CATCAGGAGAGCGCCACTTCGCAGTAAGATCGAGATTG
Clone 7 AATGAGTTTGGTGATGCAGCGAGTCATCCC CATCA - - - - -AGCGCCACTTCGCAGTAAGATCGAGATTG

3. Deletion of 3 bp and insertion of 6 bp - produces a 166 aa protein

YbeY TTTGGTGATGCAGCGAGTCATCCCCATC - - - - - - - - -AGGAGAGCGCCACTTCGCAGTAAGATCGAGATT
Clone 7 NTTGNNGATGCAGNGAGTCATCCCCNTCNGTCAGAGGA - - - -GGCCACTTCGCAGTAAGATCGAGATT

4. Insertion of 4 bp - produces a 22 aa protein

YbeY AATGAGTTTGGTGATGCAGCGAGTCATCCCCATCA - - - - -GGAGAGCGCCACTTCGCAGTAAGATCGAG
Clone 7 AATGAGTTTGGTGATGCAGCGAGTCATCCCCATCAGGAGGGAGAGCGCCACTTCGCAGTAAGATCGAG

5. No indel - produces wild-type 168 aa protein

YbeY AATGAGTTTGGTGATGCAGCGAGTCATCCCCATCAGGAGAGCGCCACTTCGCAGTAAGATCGAGATTGT
Clone 7 AATGAGTTTGGTGATGCAGCGAGTCATCCCCATCAGGAGAGCGCCACTTCGCAGTAAGATCGAGATTGT

Figure 4.2.10 Screening for YbeY knockout HEK293T cells. (A) Western blot analysis of cell lysate from single cell-derived clones using antibodies against endogenous YbeY, OxPhos complexes and β-

actin. (B) PCR products containing the ZFN target site (marked in red) were TOPO cloned and bacterial colonies were submitted for Sanger sequencing. The sequences were aligned against the wild-type sequence.

4.2.4.2 Hap1 knockout cells

At the same time, a YbeY knockout Hap1 cell line (Product ID: HZGHC002765c022) became available with a 13 bp insertion which produced a premature stop codon leading to an 80 amino acid truncated protein instead of the wild-type 168 amino acid wild-type protein. The resultant protein, if stable, would contain the catalytically important R55 (equivalent to R59 in the bacterial homolog), but would lack the H3XH5XH motif that chelates the zinc ion necessary for endonucleolytic activity.

4.3.4.3 Characterisation of growth rate, OxPhos function and mitochondrial translation in YbeY-deficient cell lines

Initial culturing of cells showed slower growth of the YbeY deficient HEK293T cells. Furthermore, the YbeY knockout Hap1 cells (YbeY (-/-)) showed rapid acidification of the media and higher sensitivity to media acidification than Hap1 parental cells, identified by the change in colour of phenol red pH indicator in the DMEM culture media. This indicates a strong reliance on glycolysis for ATP production and a resultant production of acidic lactate. The YbeY (-/-) had an extreme growth defect and required supplementation with 20% foetal calf serum and regular media changes. To determine that these defects are caused by a deficiency of YbeY, the knockout cell line was complemented with wild-type and H117A mutant (equivalent to H114 in the bacterial homolog) cDNA using lentiviral infection. The cDNA of wild-type YbeY and predicted catalytic H117A mutant were cloned into the pBMN vector which were packaged into lentivirus by Phoenix-AMPHO cells. Media from these cells were then filtered to remove any packaging cells and the viruses were added to the YbeY (-/-) cells. Hygromycin section was used to select for select for cells that successfully incorporated the cDNA. Interestingly, the mitochondrial translation phenotype was rescued by both wild-type YbeY and YbeY lacking the His117 residue predicted to be required for zinc sequestration and endonucleolytic activity.

To investigate the deficiency in oxidative phosphorylation in these cell lines, growth rate was measured and western blot analysis were carried out, probing for components of the five respiratory complexes.

The western blot analysis of the HEK293T cell lines showed that, in the YbeY (-/m) cells, there was a strong reduction in steady-state levels of Complex I and IV compared to wild-type parental cells. This was not seen in heterozygous YbeY (+/-) HEK293T cells which had comparable protein levels to wild-type. On the other hand, Complex V and Complex II levels were not affected by reduction of YbeY (Figure 4.2.11A). Complex II was entirely encoded in the nucleus and its components were imported into the mitochondria, and can be used as a loading control. Therefore, this indicates that the depletion is a product of a mitochondrial translation defect. To investigate how reduced translation affects growth rate in these cells, rate of proliferation was calculated by growing 10,000 cells in a 6-well plate in high glucose medium (4.5 g/L DMEM) which allows ATP production using glycolysis, or galactose-containing medium (4.5 g/L DMEM) which forces the cell to rely on OxPhos for their ATP production. The parental HEK293T, YbeY (+/-) and YbeY (-/m) cell lines showed a marked decrease in growth rate in galactose media and furthermore, the change in growth rates depending on presence of YbeY was similar in both media types. Growth rate in the YbeY (+/-) cells was partially reduced with reduction of YbeY, while growth in the YbeY (-/m) cells was the most inhibited (Figure 4.2.11B).

Similarly, western blot analysis of components of the mitochondrial respiratory complexes was performed on the Hap1 cell lines. This showed a corresponding loss of mitochondrially-encoded OxPhos complexes I, III and IV, and a mild decrease in the band size for complex V. No significant change was observed in nuclear encoded Complex II. An antibody against mitochondrial translocase, TOM22 was used as a loading control. However, upon complementation of the knockout cell line with constitutively expressed wild-type and H117A mutant transgene, the phenotype is rescued. Surprisingly, the introduction of YbeY with a mutation that is predicted to inhibit catalytic activity does not prevent rescue of translation in the mitochondria. This indicates that its endonucleolytic cleavage is not its primary function and is not necessary to rescue mitochondrial translation. Anti-YbeY antibody was used to probe for YbeY. Furthermore, despite having been completely rescued, the YbeY antibody could not bind as effectively to the mutant YbeY as the wild-type, suggesting a

possible change to protein structure and the antibody's epitope, or a difference in expression levels upon transfection (Figure 4.2.11C).

In addition to this, proliferation in the knockout cells was assessed using the Incucyte system that measures changes in cell confluence. The cells were plated at 10% confluence in wells of a 6-well plate, in high glucose and glutamine IMDM media with 20% fetal calf serum. In this medium, the knockout cells displayed extremely limited growth (Figure 4.2.11D). To further investigate the reliance of the knockout cells on glycolysis, the cells were also grown in varying concentration of glucose and galactose containing DMEM media with 20% fetal calf serum. However, the parental Hap1 cells showed a strong reduction in growth rate in the DMEM media independent of the glucose concentration, and the YbeY (-/-) cells showed a loss of viability in this growth media (Figure 4.2.11E). It seems that DMEM media is not conducive to the growth of Hap1 cells. A repetition of the experiment with galactose-containing IMDM media was not financially justifiable as the effect in high glucose media was very strong.

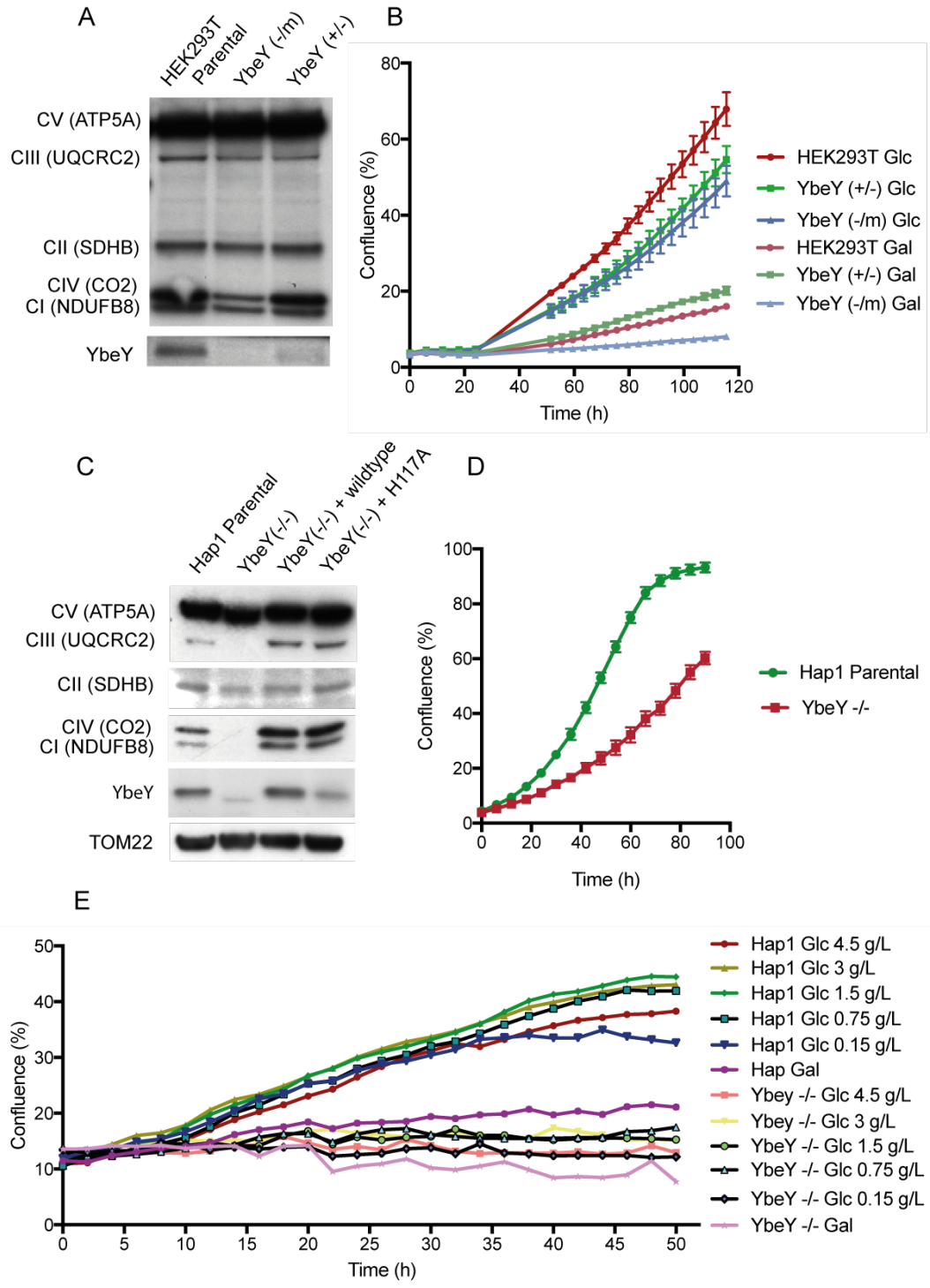

Figure 4.2.11 Characterisation of the HEK293T and Hap1 cells with depleted YbeY. (A) Total cell lysate of the HEK293T parental cells, heterozygous (+/-) and hemizygous (-/m) cell lines were analysed with western blotting. The membrane was probed with anti-OxPhos and anti-YbeY antibody. Complex II antibody functions as a loading control in this blot. (B) 10,000 cells of the various HEK293T cell lines were plates in wells of a 6 well plate in high glucose (Glc) and galactose (Gal) medium. Growth rate, indicated by change in confluence, was measured using the Incucyte HD

and graphs were plotted using Prism 7. (C) Total cell lysate of the Hap1 parental, knockout (-/-), wild-type-complemented knockout and mutant-complement knockout cell line were analysed via western blotting. The membrane was probed with anti-OxPhos and anti-YbeY antibody. Anti-TOM22 was used as a loading control. A faint band is also observed in the YbeY(-/-) cell line which we believe to be a non-specific band. (D) 10,000 cells of the Hap1 parental and knockout cell lines were plated in wells of a 6 well plate in high glucose and glutamine IMDM media containing 20% FBS. As above, confluence was measured using Incucyte HD and plotted using Prism 7. (E) Hap1 cells were plated and measured as in (D). However, the cells were plated in DMEM media with 20% FBS with galactose media or increasing concentrations of glucose (0.15, 0.75, 1.5, 3 and 4 g/L)

4.2.4.4 Measuring cellular respiration of cells with perturbed YbeY expression

Due to the strong effect of YbeY depletion on translation and growth of Hap1 cells, OxPhos function was directly assessed using microscale oxygraphy. Oxygen consumption rate (OCR) was measured using an Extracellular Flux Analyzer upon sequential injection of ATP synthase inhibitor, Oligomycin, mitochondrial uncoupler, Bam15, and Complex I and III inhibitors, Rotenone and Antimycin A. In YbeY (-/-) cells, baseline oxygen consumption was incredibly low, suggesting a near complete lack of mitochondrial oxidative phosphorylation to generate ATP (Figure 4.2.12B).

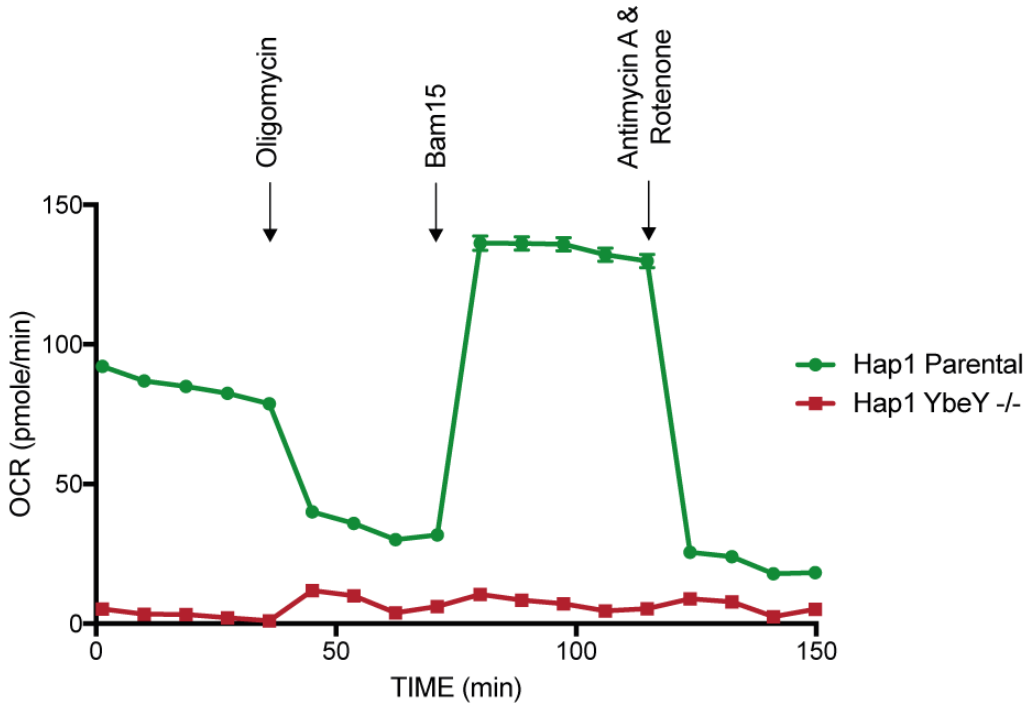

Figure 4.2.12 Oxygen consumption rate in Hap1 YbeY (-/-) cells. 60,000 cells of control and knockout cells were plated onto XF96 cell culture microplates in 20% FCS containing IMDM media, 4 hours before the media was replaced with low buffered DMEM so that the cells could adhere to the plate. Using the XF96 Extracellular Flux Analyzer, wells were sequentially injected with Oligomycin (2 μM), Bam15 (2μM) and Antimycin A and Rotenone (1 μM). Oxygen consumption rate was measured before and after the introduction of the inhibitors. Error bars = SEM, n=46. Experiments were performed in collaboration with Dr Hannah Bridges.

4.2.4.5 Assessing effects of YbeY depletion on mitochondrial translation using ^{35}S labelling

The effect of YbeY knockout on mitochondrial translation was further assessed using *in vivo* incorporation of [^{35}S]-methionine into newly synthesised mitochondrially encoded proteins. After incubating the cells in media lacking methionine and containing non-competitive cytoplasmic translation inhibitor, emetine, for 30 minutes, radiolabelled methionine was added to the media. In this manner, any nascent peptide would contain would be radiolabelled. The cells were then lysed, the membrane solubilized with detergent and the protein was run on a SDS-PAGE gel. Coomassie Brilliant Blue staining was used as a loading control. The gel was dried and the proteins were then visualised using autoradiography. The assay demonstrated

a global mitochondrial translation defect with no visible translation product after 30 minutes of incubation with radiolabelled methionine (Figure 4.2.13A). When the experiment was performed with the HEK293T parental, YbeY (+/-) and YbeY (-/m) cell lines, an intermediate translation defect was observed in the hemizygous clone, suggesting a dose-dependent effect of YbeY depletion (Figure 4.2.13B).

To confirm that the loss of translation is mitochondria-specific, the experiment was repeated without any inhibitor or with chloramphenicol (CAP), a competitive inhibitor of mitochondrial translation. The latter required that the cells be incubated in CAP for 22 hours before [^{35}S]-methionine could be introduced, with the rest of the protocol being the same as above. This experiment showed that without any inhibitors, the profile of labelled proteins is the same in the control and the knockout cells. This indicated that ^{35}S-methioinine import into the cell and incorporation into cytoplasmic translation products is not impaired. However, in the cells in which only mitochondrial translation was inhibited with CAP, the control cells showed a much higher incorporation rate. This can be attributed to the detrimental effects of inhibiting mitochondrial translation over a long period of time in already defective YbeY (-/-) cells. Predictably, inhibiting both cytoplasmic and mitochondrial translation led to a complete lack of newly synthesised proteins being produced, confirming efficiency of inhibition (Figure 4.2.13C).

Western blot analysis suggested that mitochondrial translation is not completely ablated in YbeY knockout cells (Figure 4.2.11B). Therefore, to assess the rate of translation in the knockout cells further, a time course experiment was carried out where the cells were incubated in [^{35}S]-methionine for longer periods of time. This was carried out to a maximum of two hours. In this time, the intensity of the protein profile did not reach the levels in the control Hap1 cells suggesting that either the turnover of the proteins is higher in the knockout cells or that production of the proteins is strongly reduced (Figure 4.2.13D). Overall, this global effect on mitochondrial translation also contradicts the initial hypothesis of ATP8/6-CO3 RNA cleavage by YbeY.

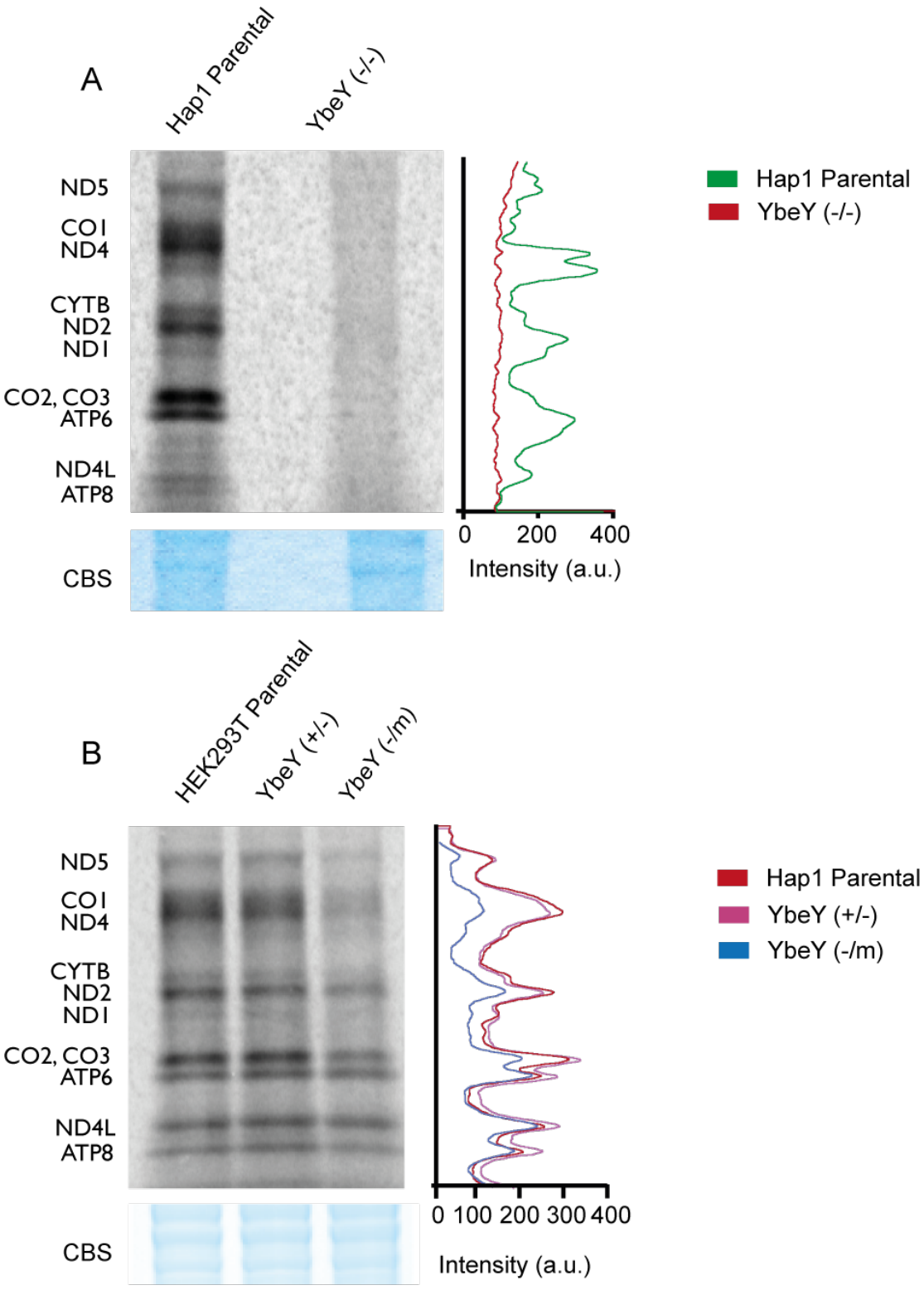
A
Hap1 Parental
YbeY (-/-)
ND5
CO1
ND4
CYTB
ND2
ND1
CO2, CO3
ATP6
ND4L
ATP8
CBS
0
200
400
Intensity (a.u.)
Hap1 Parental
YbeY (-/-)
B
HEK293T Parental
YbeY (+/-)
YbeY (-/m)
ND5
CO1
ND4
CYTB
ND2
ND1
CO2, CO3
ATP6
ND4L
ATP8
CBS
0 100 200 300 400
Intensity (a.u.)
Hap1 Parental
YbeY (+/-)
YbeY (-/m)

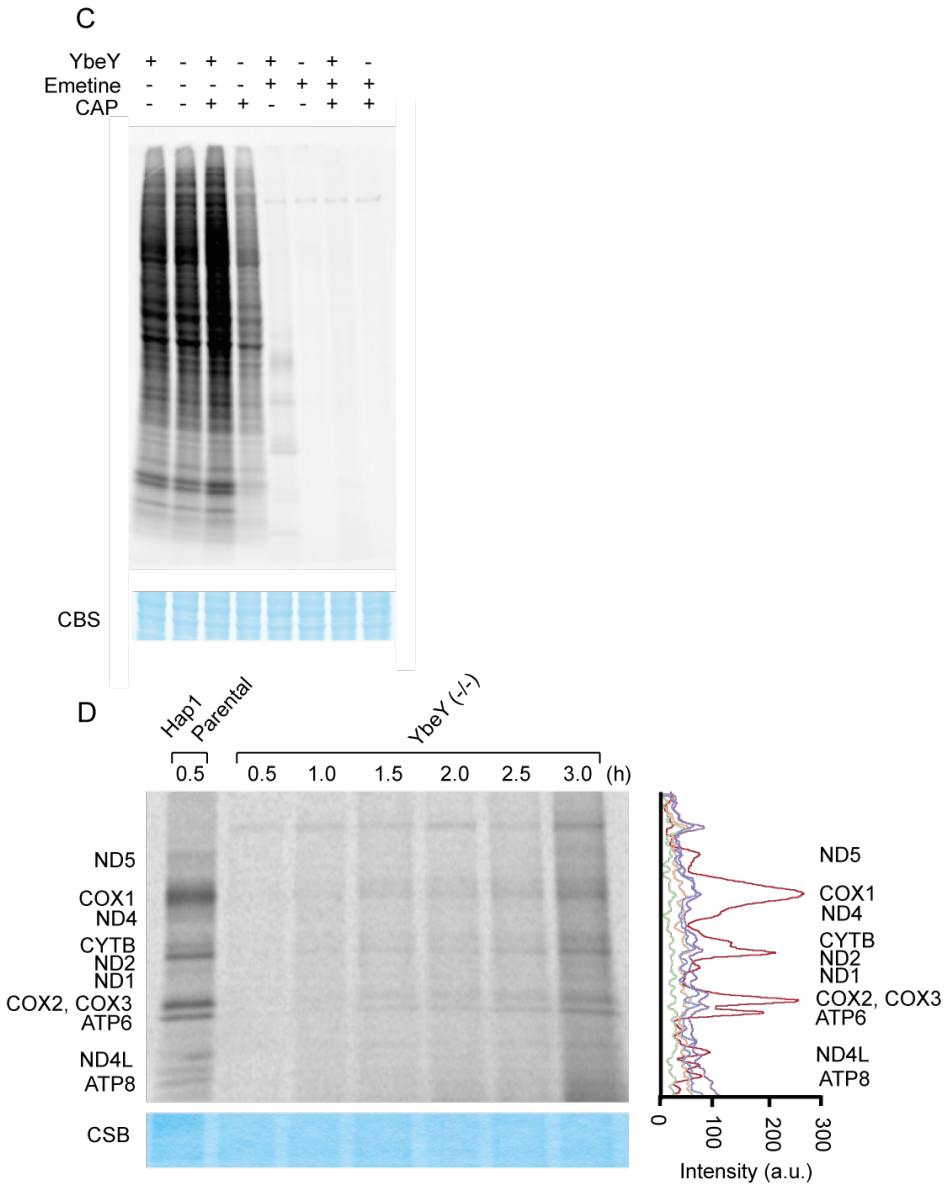

Figure 4.2.13 [^{35}S]-methionine labelling of newly synthesised mitochondrial translation products in YbeY deficient cells. (A, B) The Hap1, YbeY (-/-), HEK293, YbeY (+/-) and YbeY (-/m) cells were incubated in cytoplasmic inhibitor, emetine, for 30 minutes before the addition of the radiolabelled methionine. After 30 minutes, the cells were lysed with 0.1 % DDM and 0.1 % SDS and 30 μg of protein were resolved on a 10-20% Tris-glycine SDS-PAGE gel. Coomassie Brilliant Blue staining was used as a loading control. The gel was dried, exposed to a storage phosphor screen and scanned using a Typhoon imager. (C) The experimental methodology was the same as in (A, B) but in the case of the chloramphenicol (CAP) treatment, the cells were incubated with CAP for 22 hours prior to the introduction of [^{35}S]-methionine. (D) The experimental methodology is the same as in (A, B) but the time of incubation with the radiolabelled methionine is increased in the difference samples in 30 min intervals for up to 3 h. Coomassie Brilliant Blue staining was used as a loading control.

4.2.5 Effect of YbeY knockout of the mitochondrial transcriptome

4.2.5.1 Assessing cleavage products of ATP8/6-CO3 non-canonical cleavage in YbeY-deficient cells

Cells lacking YbeY showed a strong translation phenotype. Therefore, to identify the cause of the severe defect, we analysed the mitochondrial transcriptome to see if the translational defect is caused by a deficiency in the maturation of the transcriptome. Initially, we looked to investigate the preliminary hypothesis of YbeY's role in the endonucleolytic cleavage of the ATP8/6-CO3 non-canonical junction. In both the HEK293T cell lines (Figure 4.2.14A) and the Hap1 cell lines (Figure 4.2.14B), northern blot analysis showed no increase in the ratio of the precursor to the mature transcript. Indeed, in the Hap1 YbeY (-/-) cell lines a decrease in precursor molecule was observed. This was analysed using probes for both CO3 and ATP8/6.

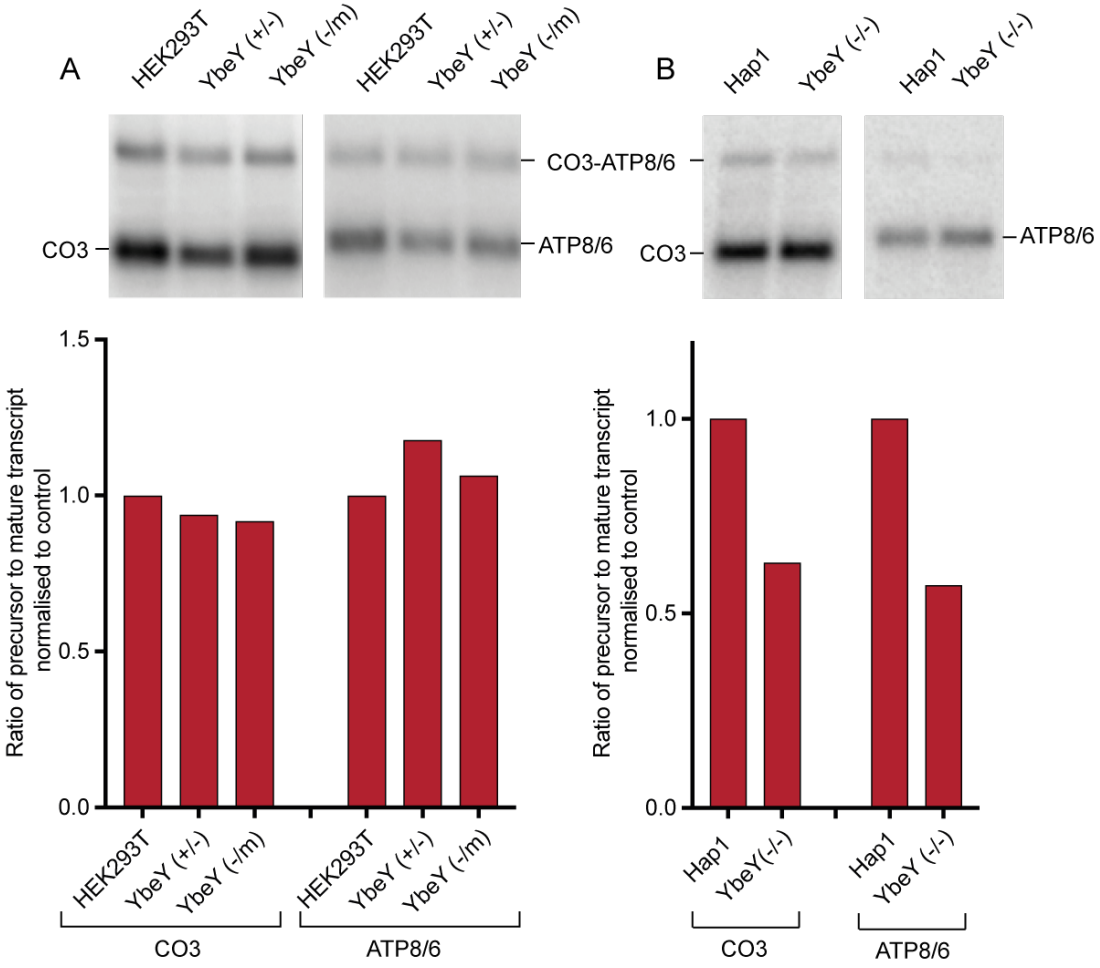

Figure 4.2.14 Northern blot analysis (top) and quantification (bottom) of the ATP8/6-CO3 precursor transcript in YbeY deficient cells. 4 μg of RNA extracted from control, YbeY (+/-) and YbeY (-/m) HEK293T cells (A), and control and YbeY (-/-) Hap1 cells (B) were run on a 1.2% agarose gel containing 1x MOPS and 3% formaldehyde. a[^{32}P]-labelled probes complementary to the ATP8/6 or CO3 mRNAs were used for northern blotting. Quantification was performed using image J and graph were plotted using Prism 7.

Next, we analysed mitochondrial rRNAs and mRNAs using northern blotting to identify potential changes in steady-state levels on the mature transcripts. A mild decrease in 12S SSU rRNA and no substantial change in 16S LSU rRNA was observed. In the coding regions, mRNAs for ATP8/6, CO2 and CO3 showed no substantial change. The ND3 mRNA, ND5 mRNA, the ATP8/6-CO3 precursor (RNA14) and the 16S+Leu(UUR)+ND1 precursor (RNA19) showed a decrease in abundance. An increase was only observed in ND1, ND2 and CytB mRNAs. This has been previously observed in cells with deficient RNA metabolism (Metodiev et al., 2009; Pearce *et al.*, 2017) and is thought to be a mitochondrial compensatory mechanism. 5S RNA was used a loading control (Figure 4.2.15). Despite these observed changes in mitochondrial RNA levels, the changes are not large enough to justify the severe and global reduction in mitochondrial translation.

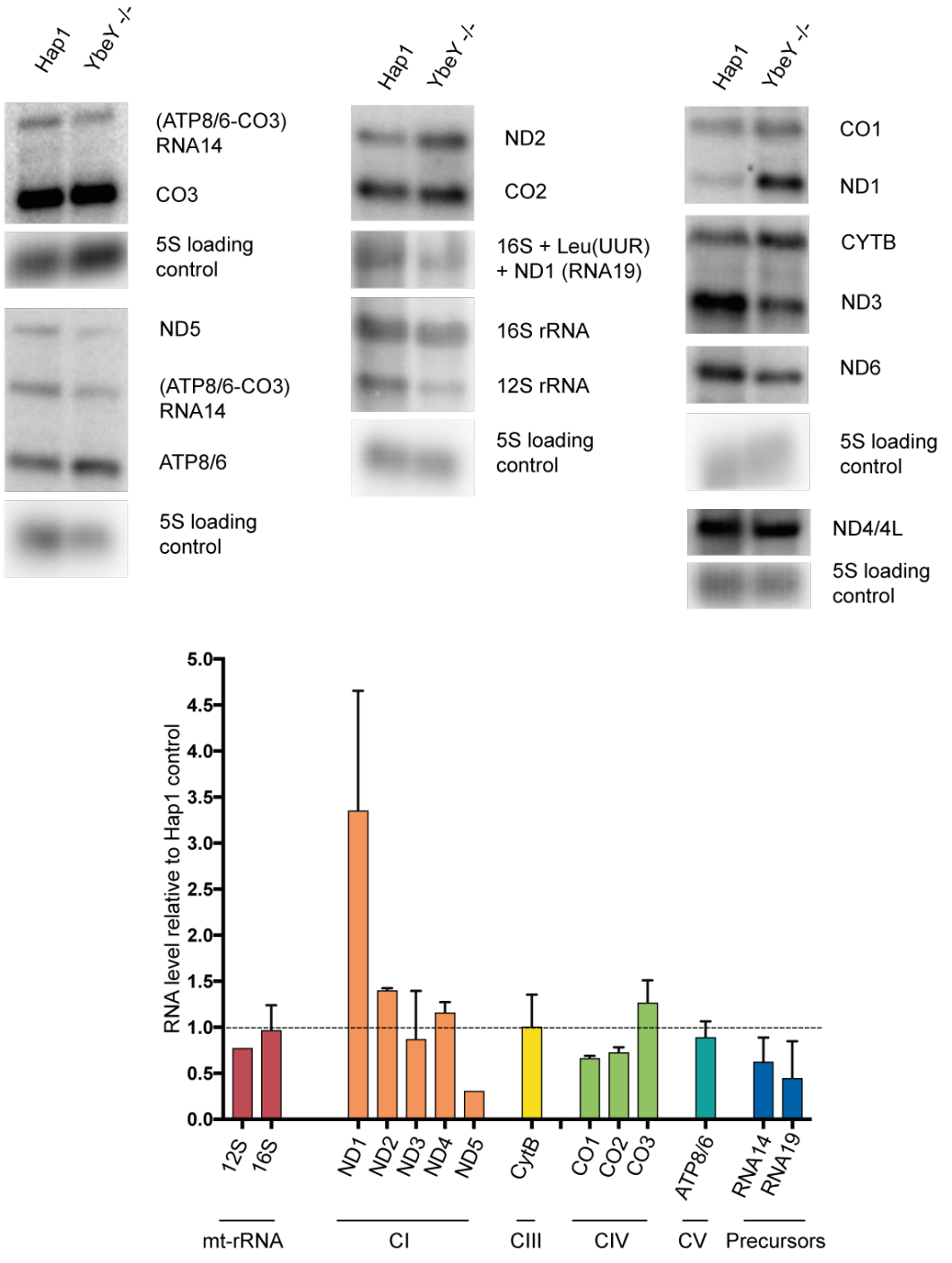

Figure 4.2.15 Northern blot analysis of mitochondrial mRNAs in the absence of YbeY. 4 μg of RNA extracted from parental and YbeY (-/-) Hap1 cells were run on a 1.2% agarose gel containing 1 x MOPS and 3% formaldehyde. a[^{32}P]-labelled probes complementary to mitochondrial rRNAs and mRNAs were used for northern blotting. Probes against 5S cytoplasmic rRNA were used as a loading control. Quantification was performed using image J and graph were plotted using Prism 7. Error bars (SEM) are plotted for experiments where n>=2.

4.2.5.2 Northern blot analysis of mitochondrial tRNAs in YbeY (-/-) cells

Next, potential changes in abundance of mitochondrial tRNAs were analysed using northern blotting. All the tRNAs tested, except for mt-tRNA$^{Ser(AGY)}$ showed no change in steady state levels. In the northern blot, mt-tRNA$^{Ser(AGY)}$ is observed as two peaks. The lower band showed no change in intensity. However, the higher band is substantially reduced in the YbeY (-/-) cells (Figure 4.2.16).

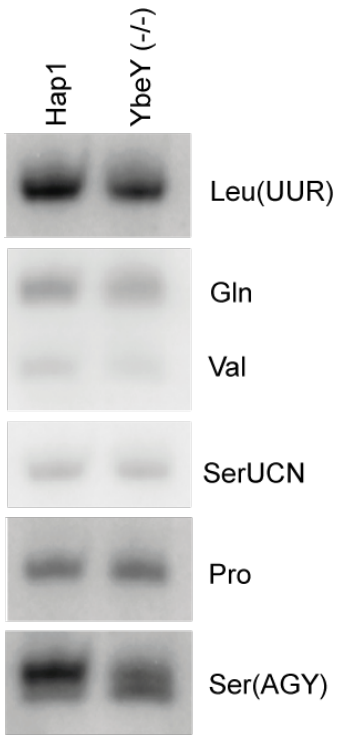

Figure 4.2.16 Northern blot analysis of mitochondrial tRNAs. 1 μg of RNA extracted from isolated mitochondria from parental Hap1 and YbeY (-/-) Hap1 cells were run on a high-resolution polyacrylamide gel. a[^{32}P]-labelled probes complementary to the tRNAs were used for northern blotting.

4.2.5.3 Determining the status of RNA processing in YbeY knockout cells

The bacterial homolog of YbeY is responsible for the processing of the 5' and 3' termini of the SSU rRNA (16S in bacteria) and the maturation of the 5' end of bacterial 23S LSU rRNA and 5S rRNA molecules (Davies et al., 2010). However, these functions are not required in mammalian mitochondria as transcribed spacers do not need to be processed from mitochondrial rRNA. Moreover, due to the strong conservation of the RNA binding and endonucleolytic activity amino acids, we employed circularisation RT-PCR to determine if YbeY is associated with correct

processing or maturation of mtRNAs. Northern blotting showed minor effects of the absence of YbeY on the steady state levels of the two mitochondrial rRNAs (Figure 4.2.15). In circularisation RT-PCR, RNA from isolated mitochondria were purified, circularized and reverse transcribed across the junction formed by the ligated 3' and 5' ends. PCR was used to amplify the junction, which was then cloned into a pCR 4Blunt TOPO vector and analysed by Sanger sequencing. It must be noted that the data is limited by the size of the primer and any misprocessed tRNA that was smaller that the size of the two primers would not be detected. Moreover, since the ligation step is performed at 37°C, ligation would be biased towards incorrectly processed RNAs with weaker secondary structure that are more susceptible to melting than the correctly processed tRNAs and rRNAs with stronger secondary structures (Zhuang et al., 2012). The size and composition of the mt-tRNAs also skews the efficiency of the PCR reactions. Hence, the number of clones analysed for each mt-tRNA varied substantially. In this experiment, no significant difference between parental Hap1 and YbeY (-/-) cells was observed in the lengths of the tRNAs Ile, Gln and Leu(UUR) (Figure 4.2.17A). However, only 0.71% (2 out of 192) of the Ser(AGY) tRNAs were correctly cleaved from the primary transcript along with the correct addition of the 3' CCA in YbeY (-/-) cells, compared to 85% in the control (Figure 4.2.18B). Alignment of the 5' ends showed a preference for cleavage at the 12^{th} and 14^{th} nucleotide from the 5' end with only 20.4% correctly processed, and alignment of the 3' end showed a lower number of the $tRNA^{Ser(AGY)}$ molecules (63.7%) with correctly processed ends compared to the parental Hap1 control cells (Figure 4.2.18A).

No significant changes in the lengths of the 12S (expected size of 955 nucleotides) and 16S (expected size of 1559 nucleotides) mitochondrial rRNA was observed (Figure 4.2.17 A, B). Interestingly, a large number of 16S rRNA molecules were 4 nucleotides larger than expected with the 3' end, 4 nucleotides into the Leu(UUR) tRNA sequence, as previously described in Pearce *et al.* (2017). As rRNA lengths are not affected by the absence of YbeY, this suggests that even though the residues required for endonucleolytic activity are conserved, the bacterial function of YbeY in cleavage-based processing of ribosomal RNA are not conserved.

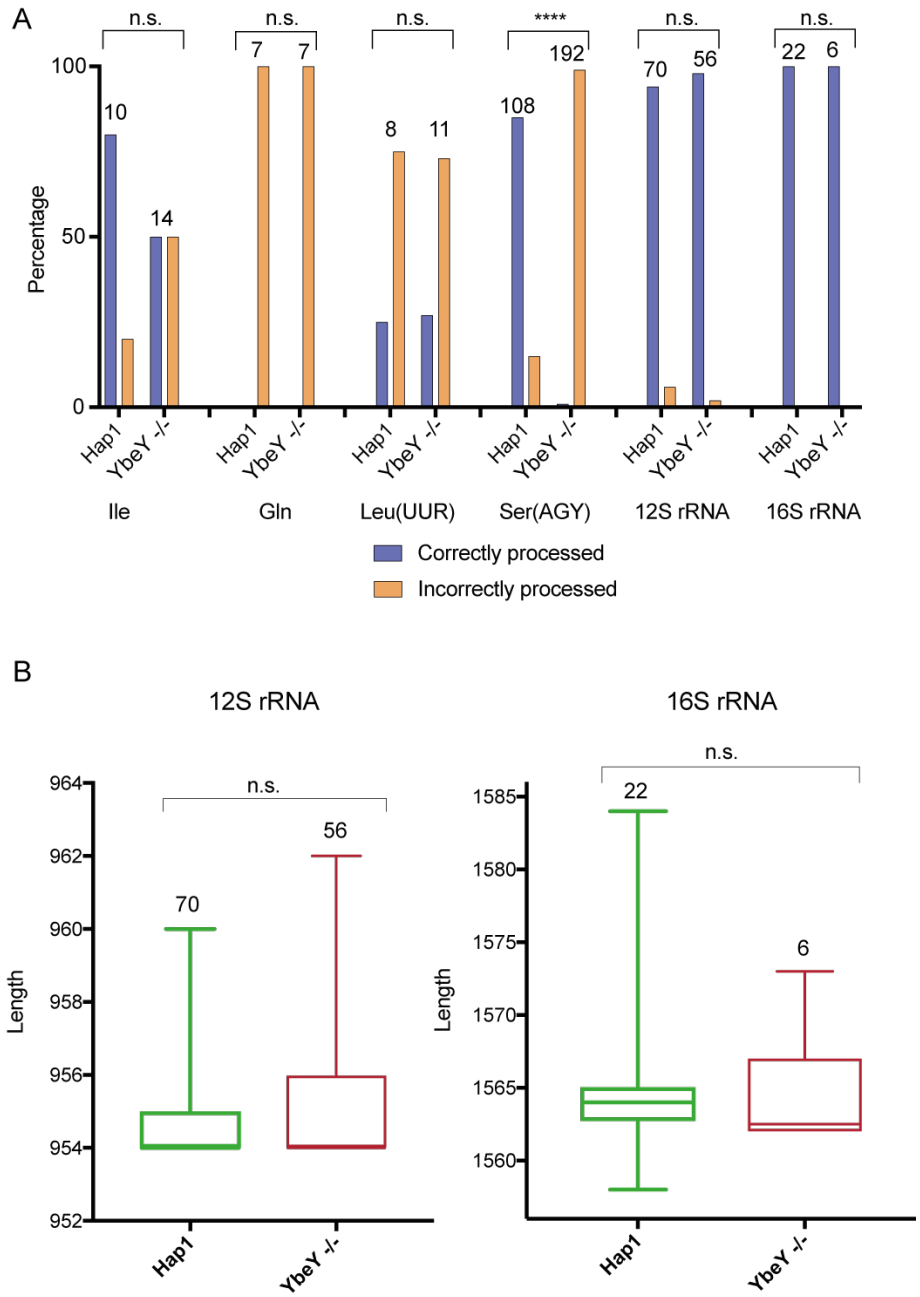

*Figure 4.2.17 Circularisation RT-PCR to assess changes in RNA processing upon YbeY knockout. RNA from isolated mitochondria from Hap1 parental and YbeY knockout cells were circularised and the 5' and 3' ends were analysed using RT-PCR and Sanger sequencing. (A) The analysis was performed for mt-tRNAs$^{Leu(UUR)}$, mt-tRNA^{Ile}, mt-tRNA^{Gln}, mt-tRNA$^{Ser(AGY)}$, and the 12S and 16S mt-rRNAs. Analysis of significance was calculated using Fisher's exact test. N=above bar graphs, ****p<0.0001 (B) The lengths of the 16S and 12S were measured and plotted in a box and whisker plot using Prism 7. The lines indicate the minimum and maximum values. The edges of the box indicate the upper and lower quartile. The middle line indicates the median. Number of data points are written above the box and whiskers plot. Significance was calculated using an unpaired Student's T-test (n.s., not significant).*

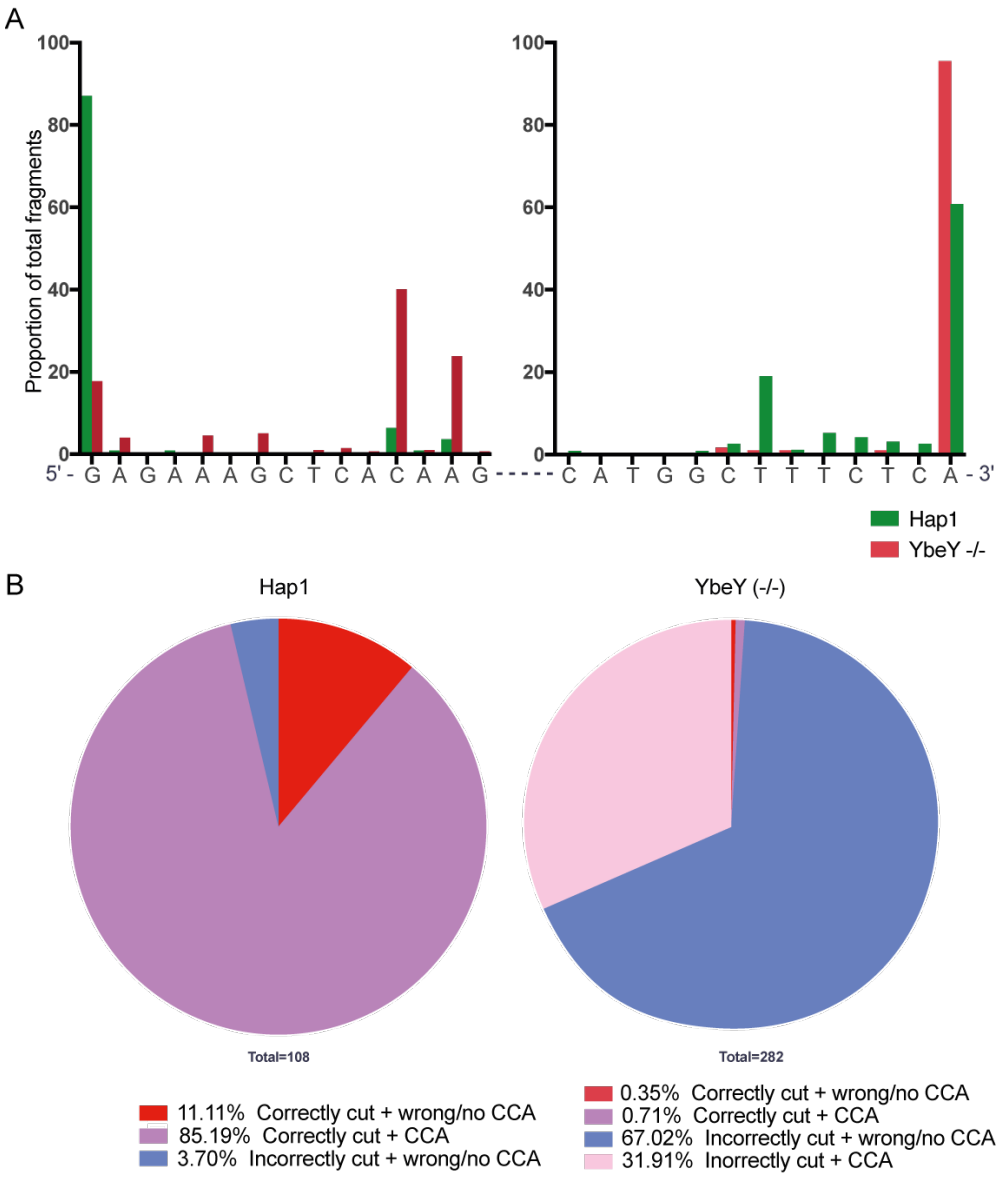

Figure 4.2.18 Analysis of the processing of 5' and 3' ends of tRNA$^{Ser(AGY)}$ (A) Mapping the 5' and 3' ends to the wild-type sequence of tRNA$^{Ser(AGY)}$ in Hap1 parental and YbeY (-/-) cells. The sequencing results obtained from the circularisation RT-PCR were analysed manually. The 5' and 3' ends were deduced from the sequenced PCR products and mapped against the wild-type sequence. The 5' and 3' ends were plotted independently as a percentage of the total 5' reads and 3' reads respectively. (B) Proportion of tRNA$^{Ser(AGY)}$ that are correctly cut at the primary transcript and with the correct addition of CCA at the 3' end. The graphs were plotted using Prism 7.

4.2.5.4 Analysis of the mitochondrial transcriptome using RNA-Seq in YbeY deficient HEK293T cells

Since, in mitochondrial YbeY, the residues required for endonucleolytic activity are conserved, the effect of YbeY knockout on the transcriptome was investigated. Compared to northern blot analysis done previously, deep sequencing provided a high-throughput comprehensive analysis of the mitochondrial transcriptome, including non-coding regions. To do this, mitochondria were isolated from parental HEK293T, YbeY (+/-) and YbeY (-/m) cells and RNA was extracted. The mt-RNA was treated with RiboZero Gold to remove the highly abundant mitoribosomal rRNA which drowns out the signal from other less abundant RNAs. Illumina TruSeq Stranded RNA libraries were prepared and deep sequencing was performed. Since YbeY may be associated with RNA endonucleolytic processing, conventional alignment would discard any reads that do not align at the 5' and 3' ends. Therefore, the mapped reads were aligned against the mitochondrial genome giving higher priorities to alignment of the sequence to the interior of the genes. This was to avoid discarding reads produced from misprocessed ends. Finally, the sequencing reads corresponding to RNA molecules produced from the heavy and light strand were separated.

Firstly, we compared the four non-canonical junctions (marked with a dotted red line) at the 5' end of CO1 (Figure 4.2.19A), between ND5 and CytB (Figure 4.2.19B), between ATP8/6 and CO3 (Figure 4.2.19C), and the 3' end of ND6 (within ND5 antisense) as presented schematically in Figure 4.2.5. The dips in the graphs marking the sites of cleavage (marked with a dotted line). Due to mitochondrial isolation before RNA extraction and ribozero Gold treatment to remove rRNA, comparison of reads can only be made between the mt-mRNAs and mt-tRNAs. This only gives a comparison of abundance of one RNA relative to the another. No significant differences were observed in the cleavage of these molecules at the non-canonical cleavage sites (Figure 4.2.19).

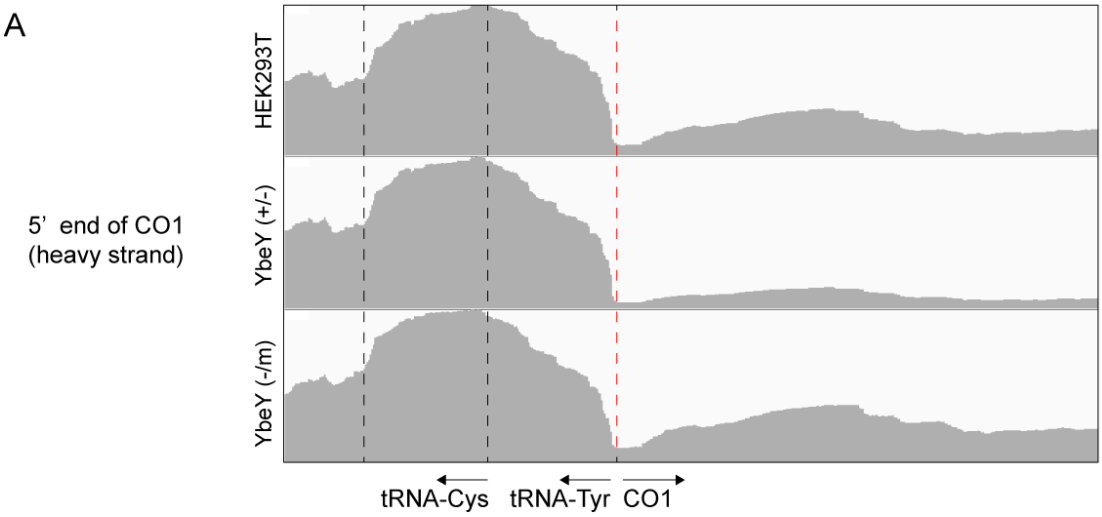
A
5’ end of CO1
(heavy strand)
HEK293T
YbeY (+/-)
YbeY (-/m)
tRNA-Cys
tRNA-Tyr
CO1

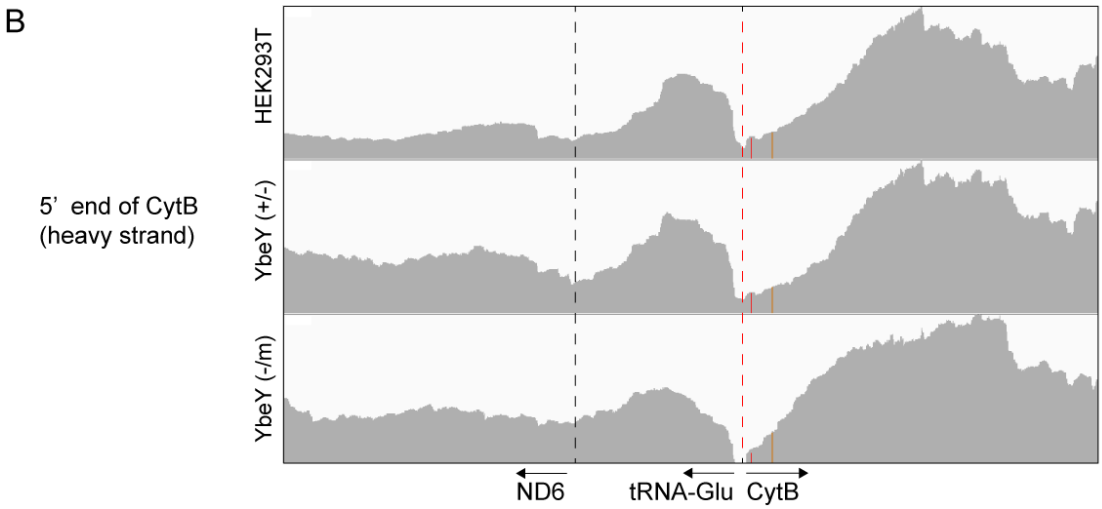
B
5’ end of CytB
(heavy strand)
HEK293T
YbeY (+/-)
YbeY (-/m)
ND6
tRNA-Glu
CytB

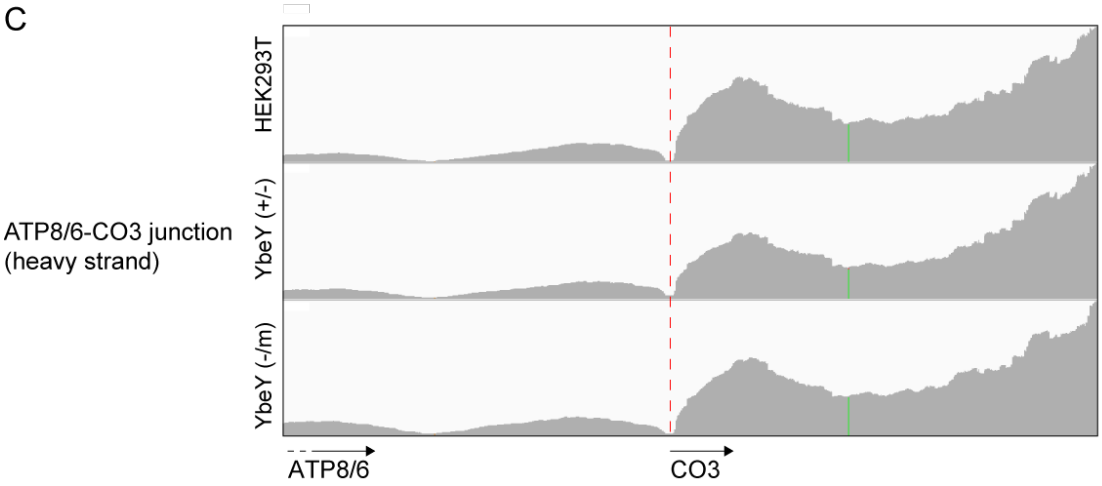
C
ATP8/6-CO3 junction
(heavy strand)
HEK293T
YbeY (+/-)
YbeY (-/m)
ATP8/6
CO3

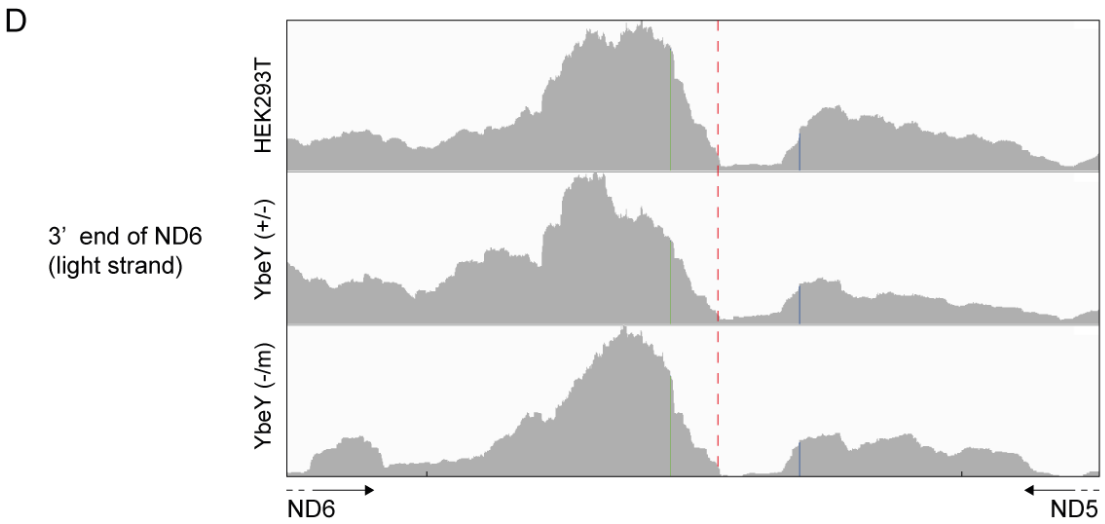

Figure 4.2.19 RNA-Seq of RNA spanning the non-canonical cleavage junction encoded in the heavy and the light strand. Mitochondrial RNA from extracted from parental HEK293, YbeY (+/-) and YbeY (-/m) cells, rRNA was depleted using RiboZero Gold, a library was prepared and deep sequenced using the Illumina MiSeq platform. The sequencing reads were aligned against the mitochondrial genome. The cleavage sites are delineated with dotted lines. Non-canonical cleavage sites are marked with a red dotted line.Three biological repeats were performed for each cell line. Bioinformatic analysis was performed by Dr Lindsey Van Haute. (A) 5' end of CO1, (B) 5' of CytB (C) ATP8/6-CO3 junction (D) 3' end of ND6

Comparison of relative abundance of the various mature transcripts showed that the lack of YbeY had the strongest effect on certain mt-tRNAs. All the effects described below were most noticeable in the YbeY (-/m) cells but not in the YbeY (+/-) cells. This was similar to the phenotype observed in YbeY (-/m) cells in the [^{35}S]-methionine incorporation assay and western blotting. Hence, the YbeY (+/-) cells could be assessed as another control for comparison as the amount of wildtype YbeY protein present in this cell line in sufficient to maintain a healthy cell. Since the strongest effect was observed with tRNA$^{Ser(AGY)}$, which is found between two tRNAs tRNA^{His} and tRNA$^{Leu(UUR)}$, tRNAs not immediately flanked by two mRNAs were studied to see if YbeY is required for their maturation. Assessment of RNAs produced from the heavy strand showed a strong reduction in RNA-Seq read coverage for mt-tRNA^{Ile} and tRNA^{Met} (Figure 4.2.20A), and mt-tRNA^{Phe} (Figure 4.2.20D) and a smaller decrease in mt-tRNA^{His}, mt-tRNA$^{Ser(AGY)}$ and mt-tRNA$^{Leu(CUN)}$ (Figure 4.2.20C). The number of reads spanning the region covering tRNA^{Trp} was very low.

Therefore, any conclusion made about $tRNA^{Trp}$ cannot be made with a much certainty (Figure 4.2.20B).

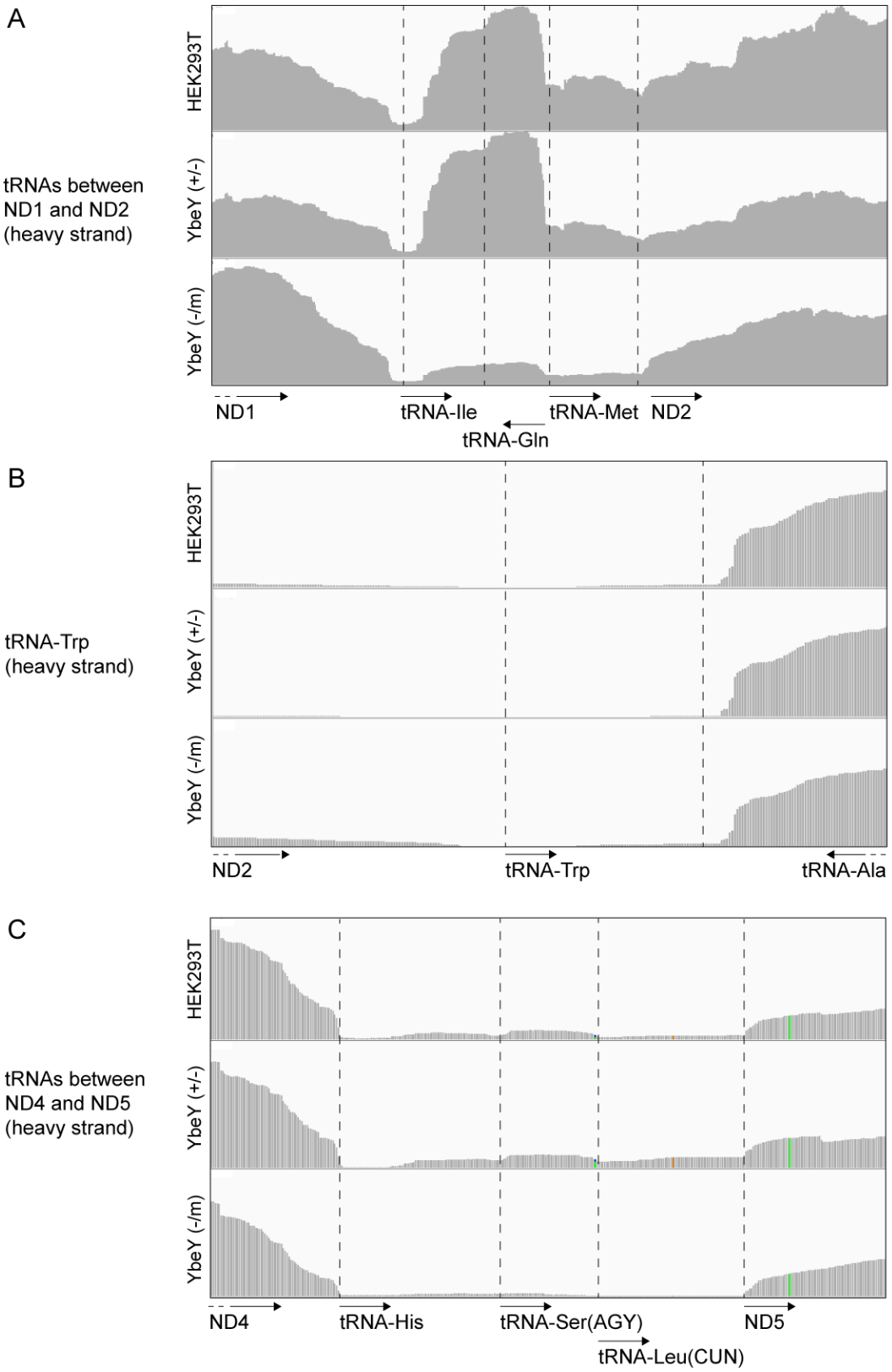

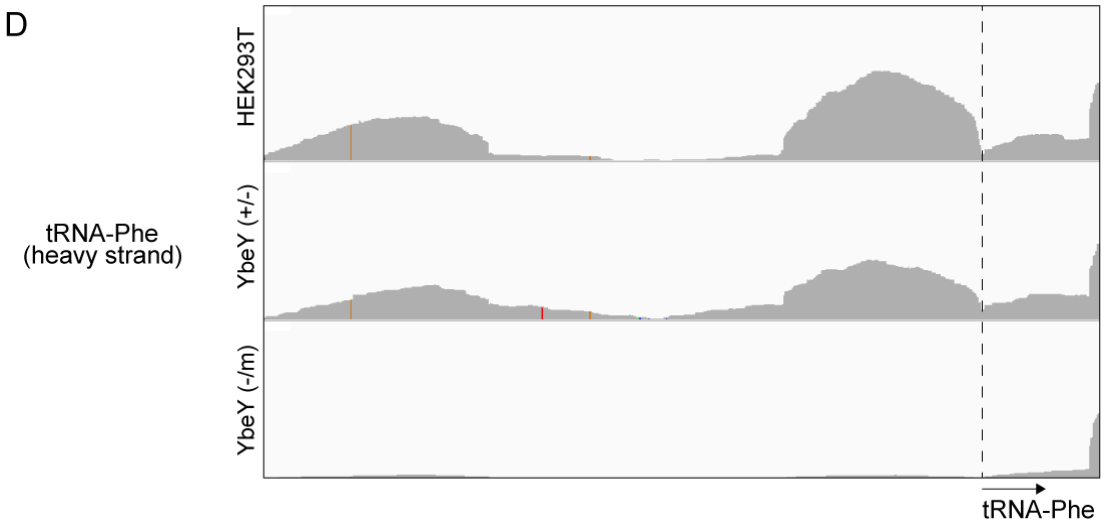

Figure 4.2.20 RNA-Seq of mtRNAs encoded in the heavy strand. Mitochondrial RNA was extracted from parental HEK293T, YbeY (+/-) and YbeY (-/m) cells, rRNA was depleted using RiboZero Gold, a library was prepared and deep sequenced using the Illumina MiSeq platform. The sequencing reads were aligned against the mitochondrial genome. Three biological repeats were performed for each cell line. Bioinformatic analysis was performed by Dr Lindsey Van Haute. The separate genes are delineated with dotted lines. (A) mt-tRNAs between ND1 and ND2 (B) tRNA^{Trp} (C) mt-tRNAs between ND4 and ND5 (D) tRNA^{Phe}

Mitochondrial tRNAs encoded by the light strand were also assessed. This showed lower read coverage for mature tRNA^{Glu} and CytB mRNA relative to ND6 (Figure 4.2.21A). However, since this method of evaluating abundance is qualitative and requires comparison with adjacent regions, this could also be caused by a relative increase in ND6 levels. Moreover, tRNA^{Asn} and tRNA^{Ala} also show a relative decrease (Figure 4.2.21B). The tRNAs for Tyr, Cys (Figure 4.20B) and Gln (Figure 4.2.21C) showed no marked difference between the control HEK293T cells and the cells with depleted YbeY levels.

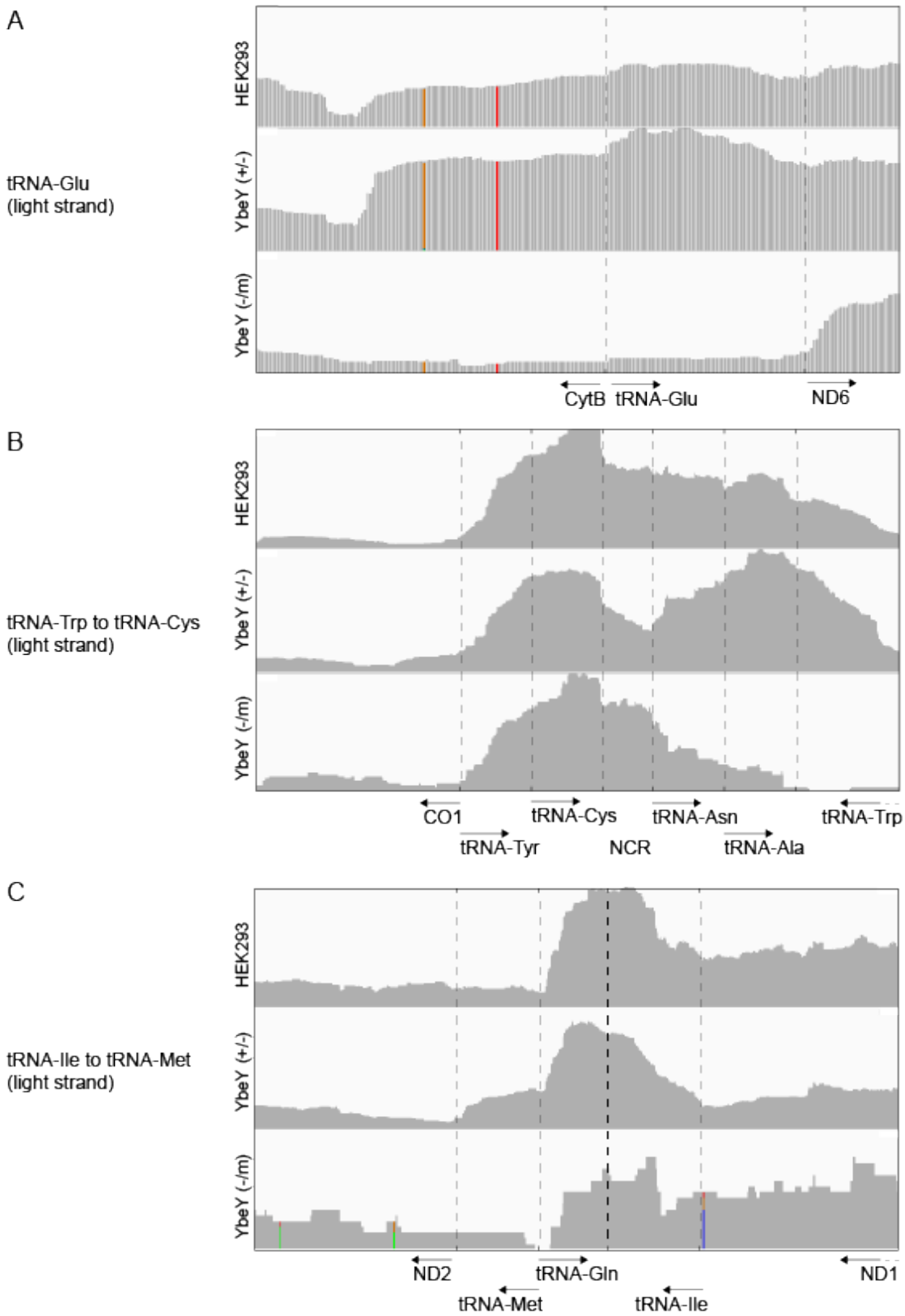

Figure 4.2.21 RNA-Seq of mtRNAs encoded in the light strand. Mitochondrial RNA from extracted from parental HEK293T, YbeY (+/-) and YbeY (-/m) cells, rRNA was depleted using RiboZero

Gold, a library was prepared and deep sequenced using the Illumina MiSeq platform. The sequencing reads were aligned against the mitochondrial genome. Three biological repeats were performed for each cell line. The separate genes are delineated with dotted lines. Bioinformatic analysis was performed by Dr Lindsey Van Haute. (A) tRNA^{Glu} (B) tRNA^{Trp} to tRNA^{Cys} (C) tRNAs^{Ile} to tRNA^{Met}

Finally, analysis of other non-coding regions in the mitochondrial transcriptome showed a large decrease in the abundance of ncRNA located in the D-loop (pre-tRNA^{Phe}) in the YbeY-depleted cells. These reads map to the region corresponding to the 7S RNA species transcribed from the L-strand, required for mitochondrial DNA replication (Crews et al., 1979). (Figure 4.2.22). This implies that YbeY may play a role in stability of the 7S RNA and thus may have knock-on effects on DNA replication.

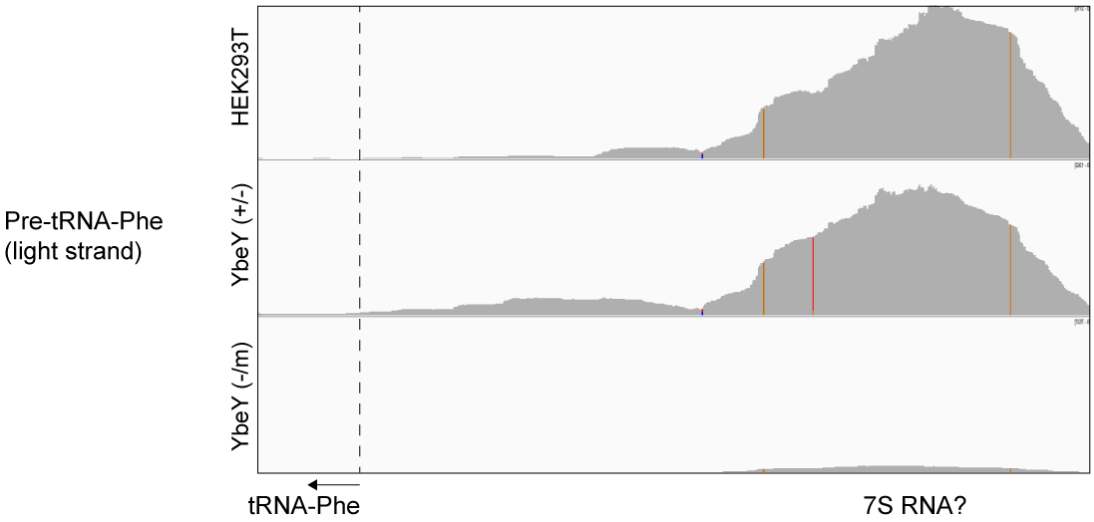

Figure 4.2.22 RNA-Seq of the D-loop region or RNA transcribed from the L-strand. Mitochondrial RNA from extracted from parental HEK293, YbeY (+/-) and YbeY (-/m) cells, rRNA was depleted using RiboZero Gold, a library was prepared and deep sequenced using the Illumina MiSeq platform. The sequencing reads were aligned against the mitochondrial genome. The 5' end of antisense tRNA^{Phe} is marked with a dotted line. Three biological repeats were performed for each cell line. Bioinformatic analysis was performed by Dr Lindsey Van Haute.

Transcriptomic analysis of HEK293T cells with depleted YbeY showed a depletion of specific RNA molecules, especially tRNA$^{Ser(AGY)}$. The decrease in steady state levels of tRNA$^{Ser(AGY)}$ was also observed in northern blotting. This loss of tRNA$^{Ser(AGY)}$ may be

the cause of the effect on global mitochondrial translation. The small amounts of the tRNA observed in northern blots and the RNA-seq data would lead stalling of translation. However, previous work has shown that stalling of translation affects larger translation products more than the smaller translation products (Pearce et al., 2017). This is observed in the [35S] *in vivo* translation assay performed on the YbeY deficient HEK293T cell lines, however, other causes of translational failure were investigated in YbeY-deficient cells.

4.2.5.5 Analysis of mtDNA copy in YbeY (-/-) cells

As there is a strong depletion of RNA transcribed from the light strand corresponding to the 7S RNA in YbeY (-/m) HEK293T cells, the mtDNA copy number in the knockout Hap1 cells was compared to the control cells. We assumed that the effect on 7S RNA abundance is a result of YbeY depletion. This could identify any repercussions of 7S RNA depletion on mitochondrial DNA replication (figure 4.2.23). We showed that in YbeY (-/-) Hap1 cells, there is no difference in mtDNA copy number as compared to Hap1 parental control cells.

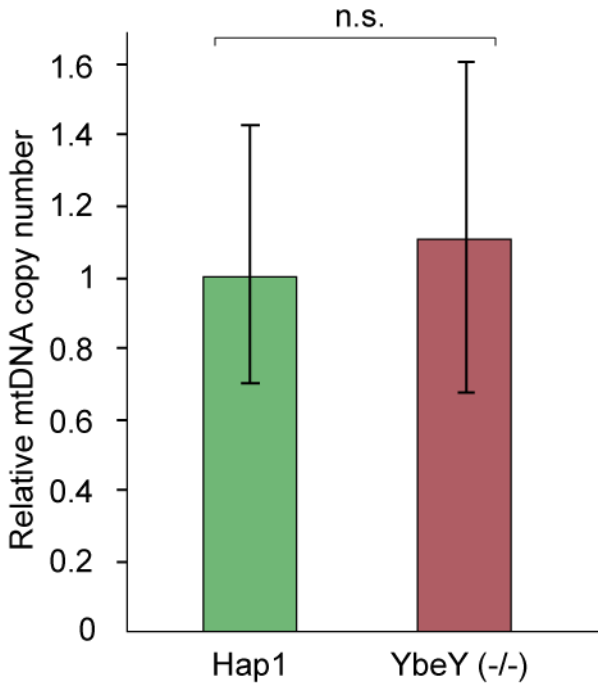

Figure 4.2.23 Quantitative real-time PCR of control Hap1 parental and YbeY (-/-) Hap1 cells was performed to determine mtDNA copy number. N =3. The qPCR experiment was performed by Dr Lindsey Van Haute.

4.2.5.6 Analysis of the mitochondrial ribosome in the absence of YbeY

As described earlier, the translation defect that affects all mtDNA-encoded OxPhos subunits could not be completely attributed to a deficiency in RNA processing and a decrease in tRNA steady state levels. Therefore, in order to identify if the loss of translation is caused by the deterioration of the translation apparatus, the integrity of the mitochondrial ribosome was investigated using a 10-30% isokinetic sucrose gradient. This involved resolving a cell lysate using the sucrose gradient, and separating the protein components in 100 µl fractions in a SDS-PAGE gel and analysing the profile of mt-LSU (MRPL3) and mt-SSU (MRPS17) proteins using western blotting. An increase in levels of assembled mt-LSU was observed for the mt-LSU subunit (fractions 7- 11) and potentially a small decrease was observed in the mt-LSU present in the monosome (fractions 11-13) in YbeY (-/-) cells. This accumulation of assembled mt-LSU was potentially caused by a stalling of monosome assembly in YbeY-deficient cells. However, a much stronger effect was seen in the small subunit in the knockout cells. In the absence of YbeY, the amount of free mt-SSU protein is increased, and a sharp reduction in assembled small subunit and mt-SSU in the monosome was observed (Figure 4.2.24).

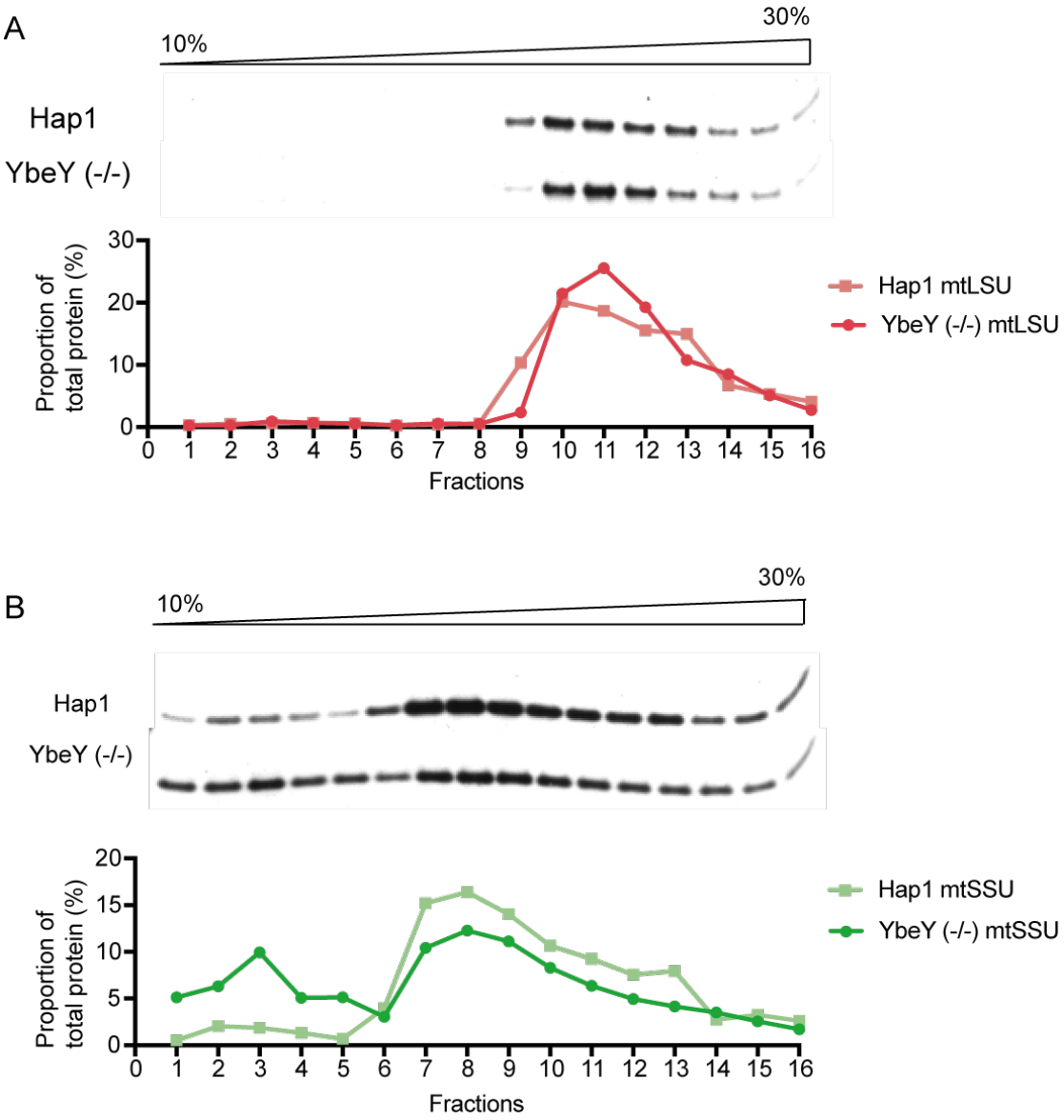

Figure 4.2.24 Analysis of mitochondrial ribosome upon YbeY knockout. Mitoribosomal subassemblies in 750 µg of cell lysate were resolved using 10-30% (v/v) isokinetic sucrose gradient fractionation. Fractions were then analysed using western blotting. (A) Antibodies against MRPL3 were used to identify the mt-LSU. (B) Antibodies against MRPS17 were used to identify the mt-SSU. Bands were quantified using Image J and plotted as a proportion of total protein using Prism 7.

The decrease in mt-SSU integrity indicated that YbeY is involved in mitoribosomal biogenesis. Various mitoribosomal biogenesis factors show interaction with rRNA, assembled subunits or monosomes depending on stage at which they assist mitoribosomal biogenesis. Therefore, sucrose gradient-fractionated mitoribosomes were probed for endogenous YbeY using western blotting (figure 4.2.25). This showed

that YbeY does not interact with the large or small subunit. This may be because YbeY only interacts transiently, weakly or indirectly with the assembling ribosome.

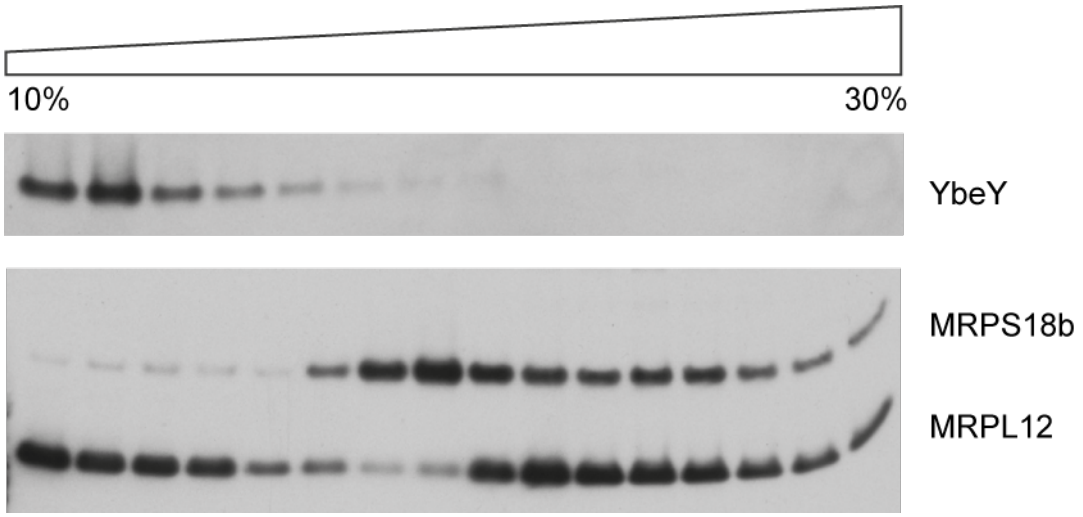

Figure 4.2.25 Analysis of YbeY interaction with the mitochondrial ribosome. 750 ug of isolated mitochondria from Hap1 cells were separated using 10-30% (v/v) isokinetic sucrose gradient fractionation. 100 µl fractions were then analysed using western blotting. Antibodies against MRPL12 were used to identify the mt-LSU. Antibodies against MRPS18b were used to identify the mt-SSU. Antibodies against endogenous YbeY were used to identify YbeY.

To quantitively assess changes in composition and the stability of the mitoribosome in YbeY (-/-) cells, we used quantitative - gradient fractionation – mass spectrometry (qGFMS). This involves growing the control and knockout cells in SILAC media, mixing them in equal proportion and isolating mitochondria. The mitochondria are then lysed and the ribosomal subassemblies are resolved using 10-30 % isokinetic sucrose gradient density fractionation. 100 µl fractions are extracted and run into a 4-12 % bis-tris gel. These are stained with Coomassie Brilliant Blue and the stained protein bands are extracted and analysed using mass spectrometry. The proteins from the two cell lines are resolved by identifying heavy or light stable isotope labelling. Peptides common to both samples are identified and intensity of detection is measured for each fraction. The maximum intensity for each protein in the two samples is marked as the maximum value and the remaining intensity profile is scaled proportional to this value. The profile is then coloured from black to red corresponding to the increasing intensity. Each row signifies a different mitoribosomal

component. However, the intensity profiles can only be qualitatively compared between different proteins. This is because different proteins have different ionisation properties and thus their detection is not a function of their abundance. Therefore, the intensity profiles cannot be used to infer stoichiometry.

Analysis of mitoribosomal integrity using qGFMS showed that, similar to the western blots and northern blot analysis of 12S rRNA, the large subunit was more abundant and the small subunit was less abundant in the YbeY knockout cells (Figure 4.2.26 and Figure 4.2.27). However, the monosomal peak was lower for both the mt-LSU and mt-SSU in the YbeY (-/-) sample. A comparison of the ratio of free assembled subunit to the monosome showed that for both mt-LSU and mt-SSU, there is a larger proportion of subunit that is not assembled into the monosome (Figure 4.2.27).

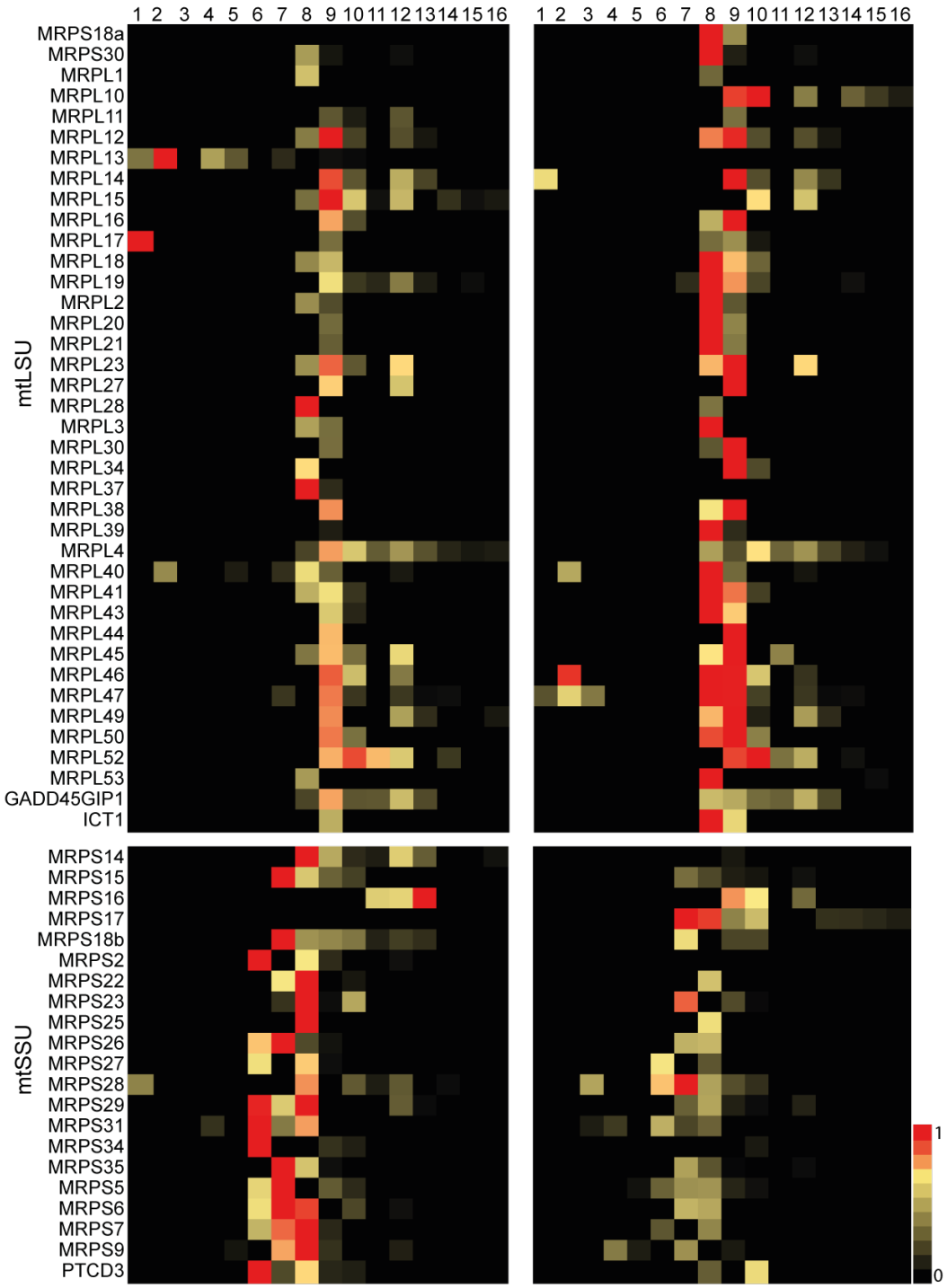

Figure 4.2.26 Mitochondria from parental Hap1 and YbeY (-/-) cells, grown in heavy and light SILAC media respectively, were isolated and the lysates were separated using a 10-30% isokinetic sucrose gradient. Fractions were analysed using mass spectrometry. A heatmap was generated from the intensity of detection of peptides common to both samples with the red value containing maximum proportion of the peptide between the two samples. Each row depicts the abundance profile of a different mitoribosomal protein. This experiment was performed in collaboration with Pedro Giuomar and Mike Harbour.

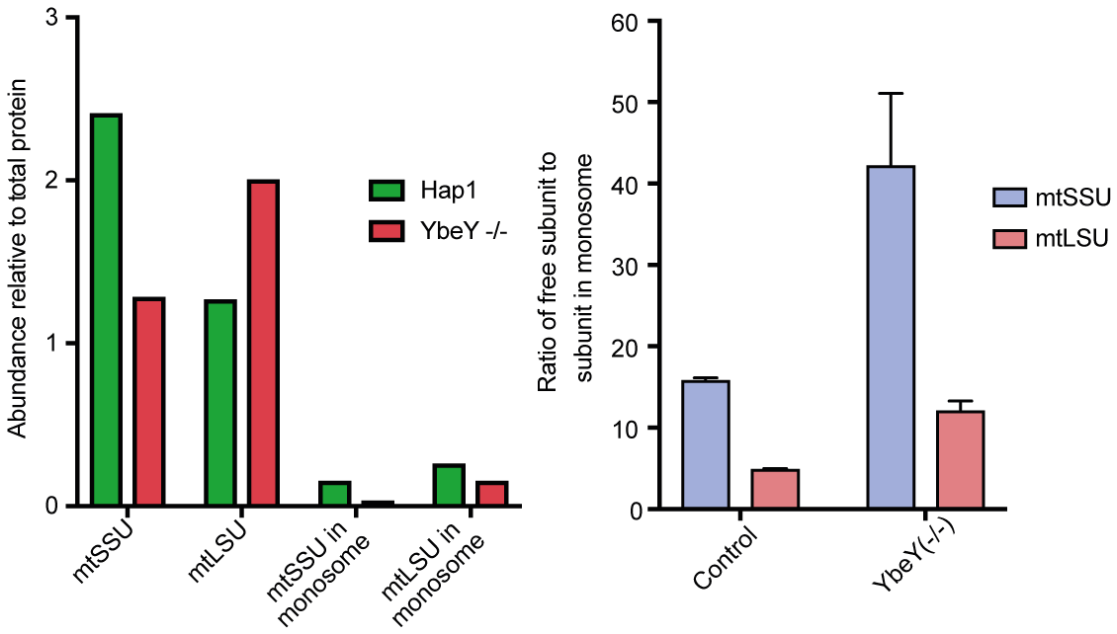

Figure 4.27 Proportion of protein components in subunits relative those found assembled in monosomes. (A) The total abundance of the MRPs was calculated from the quantitative sucrose gradient fractionation-mass spectrometry results shown in Figure 4.26, for the unbound mt-LSU (fractions 8-10), unbound mt-SSU (fractions 6-8) and monosome (fraction 12). (B) The proportion of free subunit to assembled monosome was calculated for the Hap1 parental and YbeY (-/-) cells, and plotted using Prism 7. N=2

The decrease in mitoribosomal SSU integrity might explain the strong reduction in mitochondrial translation that affects all mtDNA-encoded OxPhos subunits. However, how YbeY affects ribosomal biogenesis was unclear. Since, translation in YbeY (-/-) cells are completely restored upon complementation with the mutant protein predicted to lack endonucleolytic activity, it stands to reason that endonucleolytic activity may not be required for its ribosome-associated function. In addition, the loss of tRNASer(AGY) steady state levels may be a contributing factor to the loss of mitochondrial translation. Therefore, to elucidate the mode of action of YbeY, immunoprecipitation was used to identify interactors of YbeY. This could potentially indicate the interacting protein partners and, possibly shed some light on the mechanism by which YbeY influences ribosomal biogenesis and translation.

4.2.6 Immunoaffinity purification of YbeY to identify potential interactors

Even though the effect of YbeY depletion had been extensively characterised, and various effects on RNA metabolism and mitoribosomal biogenesis were identified, the exact mechanism, site of action and substrate of YbeY was still unclear. Therefore, immunoaffinity purification was used to identify potential interactors of YbeY.

To perform this, overexpression of flag/strep-2 tagged YbeY was induced in HEK293T Flp-In cells, the cell lysate was incubated with beads coated with anti-Flag antibody and the interacting proteins were eluted using flag peptide. The proteins were resolved on a 4-12% bis-tris polyacrylamide gel, prominent bands were cut and identified using mass spectrometry. Flag-tagged Luceriferase pulldown was used as a control to identify interactors non-specific to YbeY. A strong candidate was identified by mass spectrometric analysis as P32 (C1qBP) (Figure 4.2.28A). The other weaker band could not be identified. P32 is a multifunction mitochondrial chaperone protein that has been shown to bind to C1q complement component, Hyaluronic acid, and a large number of intracellular and extracellular proteins (Storz et al., 2000; Fogal et al., 2010). To identify if this observed interaction with P32 was YbeY-specific and not a side-effect of YbeY overexpression, reciprocal immunopurification of Flag-tagged P32 was used. However, this did not pull down YbeY. Only a smaller band was identified as the post pre-sequence cleavage product of P32 (Figure 4.2.28B). This suggested that P32 might be upregulated in the cell as a response to overexpression of YbeY and therefore, is not a specific interactor of YbeY.

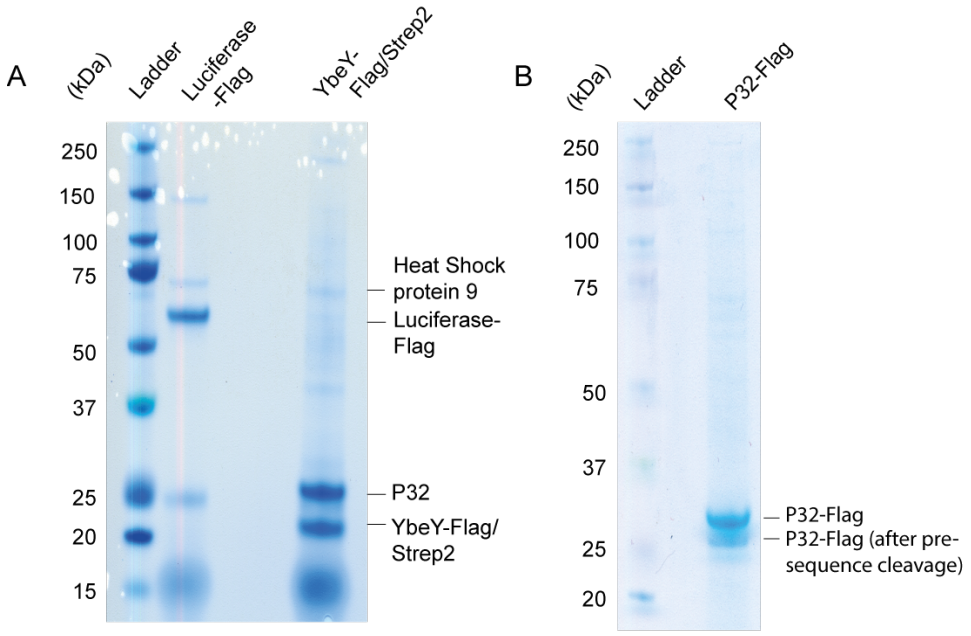

Figure 4.2.28 Immunopurification of YbeY and P32. Proteins containing a C-terminal flag tag were overexpressed in HEK293T Flp-In cell lines using 100 ng/ml doxycycline, mitochondria were isolated from the cells, the mitochondrial lysate was incubated with the beads coated with antibodies against the Flag epitope and the bound proteins were eluted using flag peptide. The eluent was resolved on a 4-12% Bis-Tris SDS-PAGE gel and prominent bands were cut for analysis using LC-MS/MS (A) Flag/Strep2-tagged YbeY (n=2). Flag-tagged Luciferase was used as a control. (B) Flag-tagged P32

Next, we performed a more sensitive and quantitative SILAC-based immunoaffinity purification using anti-flag antibodies. Instead of using the Flag/Strep2-tagged protein, a flag-tagged YbeY was used. Flag-tagged YbeY HEK293T Flp-In cells were grown in heavy and light stable isotope labelled amino acids. One of the two were induced with doxycycline to overexpress YbeY-flag. The cells were mixed in equal proportion, the mitochondria were extracted and the mitochondrial lysates were incubated with anti-flag antibody-covered beads. After multiple washes, the proteins were eluted using flag peptide. These proteins were then analysed using mass spectrometry. The proteins from the uninduced and induced cell lines were separated based on their stable isotope labelling. Peptides common to both samples were used to calculate the ratio of the amount pulled down with the overexpressed YbeY to the proteins pulled down due to non-specific interaction. The SILAC labelling allows for

the level of interaction to be quantified and allows weak and specific interactions to be identified. The experiment was performed with reciprocal labelling which also acts as an independent repeat. The log_2(ratio of induced/uninduced) was plotted for both experiments.

The top right quadrant of the graph signifies proteins that have been enriched in the overexpression cell line in reciprocal experiments. The proteins depicted in the lower left quandrant indicate those proteins that are more abundant in the control cell line. Proteins in the top left and bottom right quandrant are considered noise in the data that showed an increase in one sample but a decrease in the other (Figure 4.2.29A).

A limitation of the SILAC method could be that when the mitochondria are lysed, the overexpressed YbeY may interact with proteins from the control cell line. This would dilute the signal of the interaction. This would lead to a lack of strong interactors of YbeY (Figure 4.2.29A). P32 was not identified as one of the major interactors of YbeY, possibly due to the different C-terminal tag used for pulldown. YbeY was highly abundant in the 'induced sample' (Figure 4.2.29A). YbeY was removed from the graph and the scales were adjusted to identify the strongest interactors of YbeY. This identified various mt-LSU (red diamonds in Figure 4.2.29B) and mt-SSU (blue diamonds in Figure 4.2.29B) component proteins, and other proteins related to mitoribosome biogenesis. The strongest interactor of YbeY was identified to be MRPS11. The next highest interactors were mt-LSU components MRPL2, MRPL4, MRPL20, MRPL21, MRPL42, MRPL43, MRPL50 and GADD5GIP1 (GADD45), and mt-SSU component MRPS26. The other strongest interactors included, heat shock protein, HSPA9, Aminoadipate-Semialdehyde Synthase, AASS1 (Sacksteder K.A. et al., 2010), ERAL1, a 12S ribosomal rRNA chaperone (Dennerlein S. et al., 2010) and Large 60S Subunit Nuclear Export GTPase 1 and LSG1 (Kallstrom,G et al., 2003) (Figure 4.2.29B). This strongly suggests a role of YbeY in mitoribosomal biogenesis.

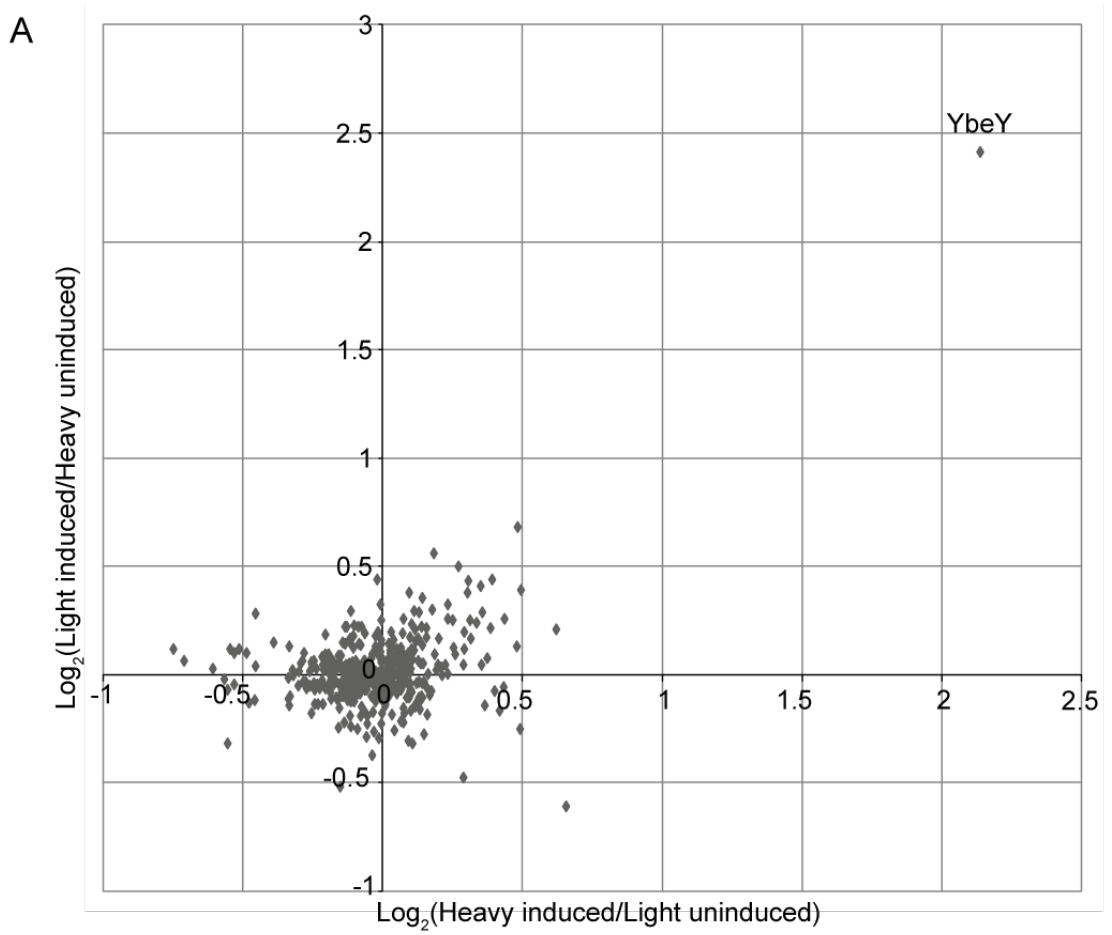
A
YbeY
Log2(Light induced/Heavy uninduced)
Log2(Heavy induced/Light uninduced)
3
2.5
2
1.5
1
0.5
0
-0.5
-1
-1
-0.5
0
0.5
1
1.5
2
2.5

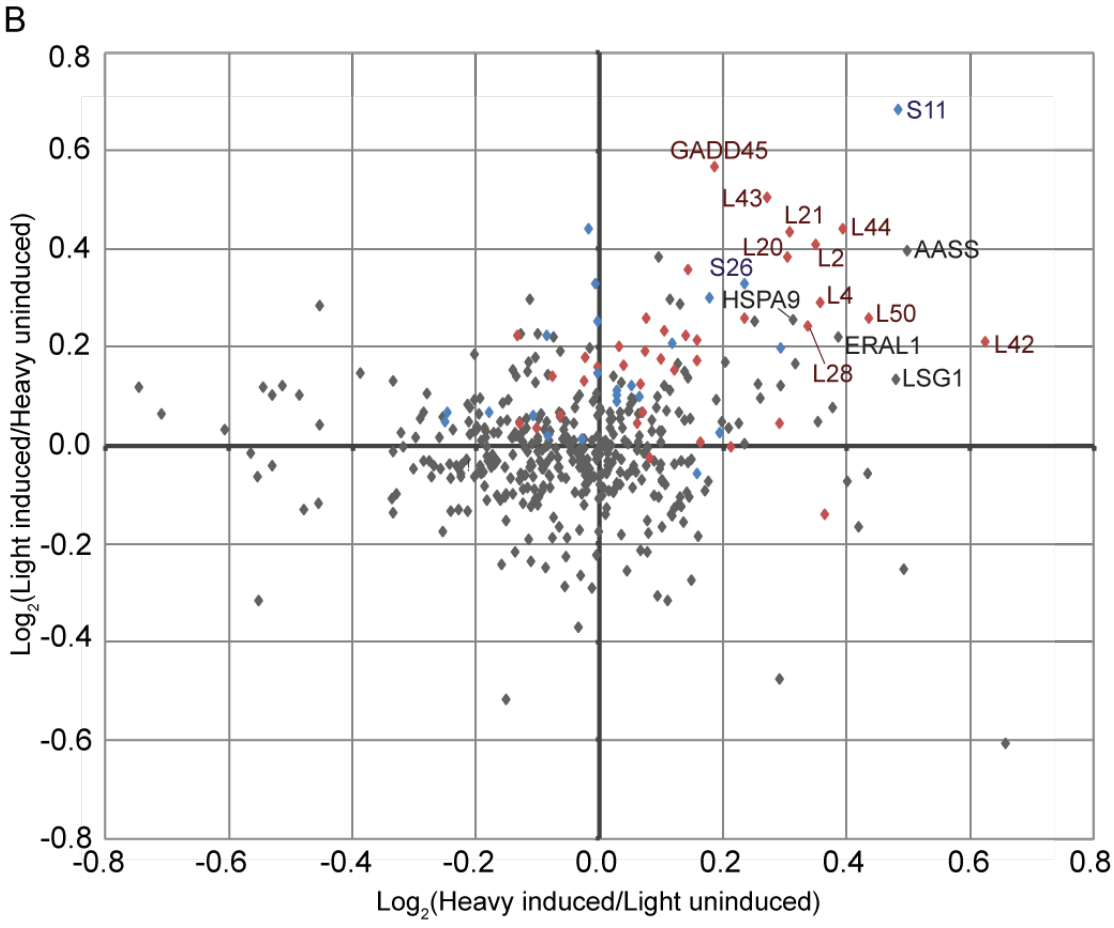
B
S11
GADD45
L43
L21
L44
L20
L2
AASS
S26
HSPA9
L4
L50
ERAL1
L42
L28
LSG1
Log2(Light induced/Heavy uninduced)
Log2(Heavy induced/Light uninduced)
0.8
0.6
0.4
0.2
0.0
-0.2
-0.4
-0.6
-0.8
-0.8
-0.6
-0.4
-0.2
0.0
0.2
0.4
0.6
0.8

Figure 4.2.29 Immunoaffinity purification of flag-tagged YbeY. Overexpression of flag-tagged YbeY was induced in HEK293T flp-In cells grown in SILAC media (heavy or light) while cells grown in the opposite SILAC media were not induced. Cells were mixed in equal proportion and mitochondria were isolated. YbeY was pulled down from the mitochondrial lysate using beads coated with antibodies against the flag epitope and eluted using flag peptide. The immunopurified proteins were identified using mass spectrometry. The log_2(ratio of peptide abundance in induced cells to peptide abundance in uninduced cells) were plotted on the X and Y axes from reciprocally- labelled experiments. Proteins in top right quadrant are those that were more abundant in the sample with YbeY overexpression and immunopurification while proteins in the lower left quandrant are more abundant in the control uninduced sample. (A) The graph was plotted with YbeY to show overexpression (B) and without YbeY for better resolution of pulldown products. Blue diamond, mt-SSU components, Red diamonds, mt-LSU components, grey diamonds, other.

4.3 YbeY – Discussion

The maturation of the mitoribosome involves RNA folding and the assembly of the nuclearly-encoded protein components. The biogenesis factors that direct this process remain largely unidentified. Here, we identify a novel mitochondrially-targeted putative RNA endonuclease called YbeY. In bacteria, this protein is vital for the removal of internal transcribed spacers from precursors of the ribosomal RNA and the degradation of improperly assembled ribosomes. However, in human mitochondria, this processing function is not required as the 16S and 12S rRNA do not have internal transcribed spacers that need to be removed. To identify the role of Ybey in the human mitochondria, we generate YbeY-deficient cell lines using zinc finger nuclease technology and show that the absence of YbeY leads to a loss of cell viability and OxPhos function, resulting from severely compromised translation. An initial hypothesis of the role of YbeY in processing of precursor mtRNA at non-canonical cleavage sites between ATP6/8 and CO3 mRNAs was refuted via northern blotting and RNA-Seq analysis. However, we identified $tRNA^{Ser(AGY)}$ as a potential target of the endonucleolytic function of YbeY. Moreover, quantitative sucrose gradient fractionation and mass spectrometry of mitoribosomal assembly stages showed that in particular, biogenesis of the mt-SSU is impaired in YbeY knockout cells. Immunoaffinity purification of YbeY also identified mt-SSU component, MRPS11 as a key interactor. We propose that YbeY is a mitoribosomal biogenesis

factor that coordinates the assembly if the small subunit through hits interaction with MRPS11.

4.3.1 YbeY is a vital for mitochondrial function

YbeY is not a highly conserved protein. YbeY is absent in large sections of the evolutionary tree and the lack of a bacteria-like rRNA operon in mammalian mitochondria suggests a reassignment of YbeY's function. *In silico* analysis of the amino acid sequence and the predicted structure showed that the residues involved in catalysis are conserved. The 3D structure modelling of the human YbeY using the *E. coli* homolog as a template showed that the structure of the catalytic site is conserved along with the Arg55 residue (equivalent to bacterial Arg59, PDB 1XM5) and the H3XH5XH zinc ion-binding motif, which are required for RNA binding and nuclease activity, respectively (Davies *et al.*, 2010; Zhan et al., 2005). They also lie within an electropositive pocket which is the site predicted for nucleic acid docking. The zinc ion coordinated by the histidine triad is vital for catalysis as addition of a chelating agent, EDTA, inhibits RNase activity of the enzyme (Jacob et al., 2013). Previous analysis of the human YbeY also showed that certain residues required for protein-protein interactions in bacterial YbeY, namely Asp85 are conserved. There is an addition of nine amino acids (Gly75-Pro83) between two conserved beta sheets, which may confer additional protein interaction capabilities compared to its bacterial homolog (Ghosal et al., 2017). Taken together, this suggests that the endonucleolytic function of YbeY is conserved in humans.

Using immunofluorescence analysis of YbeY localisation we show that YbeY is solely localised in the mitochondria implying that it does not play a role in nuclear gene expression. Western blot analysis of the fractionated human cells showed that YbeY is found in the mitochondrial matrix. This confirmed prediction made by mitochondrial localisation databases, Mitocarta 2.0 and Mitominer 4.0, based on information gathered from analysis of the mitochondrial proteome and bioinformatic analysis of the mitochondrial targeting sequence and comparison to the homolog in *Rickettsia* (Calvo et al., 2016; Hung et al., 2014, Smith and Robinson, 2016). Furthermore, the absence of YbeY in mitochondrial RNA granules does not necessarily suggest that it does not play a role in processing the nascent transcript because some RNA-processing enzymes such as PUS1 are not found in RNA granules (Antonicka et al., 2015).

In further work on YbeY, we confirmed that the protein is vital for mitochondrial function and cell viability. This result is consistent with studies in bacteria which show that YbeY is crucial for cell viability (Davies et al., 2010). Recently, Arroyo et al. (2016) created a 'death screen', which used CRISPR technology to delete genes in immortalised human cell lines. Then, the cells were replica plated in glucose medium or galactose medium, which forced the cells to rely on their mitochondria for ATP production. This identified YbeY as a protein vital for mitochondrial function and cell viability.

4.3.2 Absence of YbeY leads to aberrant mt-RNA processing

In *E. coli*, YbeY facilitates the processing of the 3' end of 16S rRNA (SSU), the maturation of the 23S (LSU) and 5S rRNA molecules, and the degradation of defective late stage 70S ribosomes (Jacob *et al.*, 2013). However, these cleavage steps are not required in mammalian mitochondria as there are no transcribed spacers encoded in the mitochondrial genome that need to be removed. The 12S and 16S mammalian mitochondrial rRNA-coding sequences are immediately preceded and succeeded by tRNA molecules (Figure 4.4). Furthermore, the 5S rRNA molecule in not encoded in mammalian mtDNA and in human mt-LSU has been replaced by a mt-tRNA^{Val} (Amunts et al., 2015). All the mt-rRNA coding regions do not need to be processed similar to their bacterial equivalents. Instead, they are excised by RNase P and RNase Z as described by the Punctuation Model (see Introduction section 1.4). Therefore, the mammalian orthologue of YbeY is likely to have an alternate function in the mitochondria. YbeY may still be involved in the quality control and degradation of defective small subunit.

This led us to propose that YbeY is involved in the processing of the non-canonical cleavage sites. Four major non-canonical cleavage sites have been identified that are not catered for by the Punctuation Model. These include the ATP8/6-CO3 junction, the ND5-Cytb junction, the 3' end of ND6 and the 5' end of CO1. The deletion of PTCD2 (Penticopeptide repeat domain protein 2) in mice led to a reduction in the processing of the ND5-CytB cleavage site. Similarly, FASTKD2 (FAST domain-containing protein 2) is a kinase that binds to multiple sites along the ND6 mRNA and cooperates with the degradosome to facilitate the maturation of the ND6 precursor transcript (Jourdain et al., 2015; Popow et al., 2015; Xu et al., 2008). No

proteins have been identified that enable the maturation of the ATP8/6-CO3 and CO1 precursor transcripts.

The mitochondrially-targeted endoribonuclease we had identified appeared as a candidate for this purpose. However, our results show conclusively that YbeY is not responsible for these two cleavage events. Northern blotting of mtRNA form YbeY knockdown and YbeY knockout cells showed that ATP8/6-CO3 precursor levels were not affected by depletion of YbeY. In addition, transcriptomic analysis of YbeY YbeY-deficient HEK293T cells shows that the levels of all four non-canonical cleavage sites remain unperturbed. We also identified that the CO3 cleavage product of ATP8/6-CO3 processing contains an unusual di- or tri-phosphorylated or a hydroxyl group at its 5' terminus. This is confirmed by a recent mitotranscriptomic analysis which showed a distinct lack of a 5' monophosphate on CO3 (Rackham et al., 2016). Recent characterisation of bacterial YbeY showed that YbeY cleavage activity produces a 5' hydroxyl and 3' phosphate terminus (Jacob et al., 2013). Since the residues involved in endonucleolytic cleavage activity in bacteria are conserved in humans, it stands to reason that the mechanism of cleavage is also conserved. Therefore, any cleavage product of human YbeY must also have a 5' hydroxyl group. Our results show that CO3 does not have a 5' monophosphate, and thus may have a 5' hydroxyl group. This indicates that YbeY may indeed be responsible for the processing of the ATP8/6-CO3 precursor. However, northern blot analysis and RNA-Seq showed that the ATP8/6-CO3 precursor is not affected by the depletion of YbeY.

Interesting, we observed a plethora of other changes to steady state levels potentially caused by aberrant processing events in YbeY-deficient cells. Northern blotting identified an increase in Complex I transcripts and decrease in Complex IV transcripts. However, this has been observed previously in mitochondria with deficient RNA metabolism. In PDE12 knockout cells where the lack of the poly-(A) exoribonuclease leads to spurious polyadenylation of mt-rRNAs and mt-tRNAs, and conditional TFB1M knockout mice lacking the methylation of two adenines on 12S rRNA, leads to a similar signature of increased complex I transcript and decreased complex IV transcripts (Metodiev et al., 2009; Pearce et al., 2017; Sharoyko et al., 2014). This implies that these observed effects on mRNA stability are not specific to YbeY deficiency and are likely compensatory effects of mitochondrial translation deficiency. A noticeable reduction was observed in the RNA-seq analysis of the steady

state level of various tRNAs in YbeY (-/m) cells, namely tRNAs for Ser(AGY), Ile, Ala, Trp, Met, Leu(CUN) and Glu. A closer inspection of mt-tRNA$^{Ser(AGY)}$ showed that its steady-state level was reduced in northern blots in YbeY (-/-) cells. Circularisation RT-PCR showed that in YbeY (-/-) cells there was a severe reduction in mt-tRNA$^{Ser(AGY)}$ with correctly processed 5' and 3' ends, with the strongest change observed at the 5' end.

Human mt-tRNA$^{Ser(AGY)}$ is found between two other mt-tRNAs, tRNA^{His} and tRNA$^{Leu(UUR)}$. Previous work had demonstrated that the 5' end processing of mt-tRNA$^{Ser(AGY)}$ is not performed by RNase P. Instead, using mitochondrial extracts on *in vitro* transcribed radiolabelled RNA substrates, Rossmanith (1997) showed that the 5' of mt-tRNA$^{Ser(AGY)}$ is probably released through the action of 3' endonucleolytic processing of mt-tRNA^{His}. This cleavage event does not take place in the absence of mt-tRNA^{His}. On the other hand, the presence of mt-tRNA$^{Leu(UUR)}$ is dispensable for mt-tRNA$^{Ser(AGY)}$ 3' end processing. The 5' end mt-tRNA^{His}- mt-tRNA$^{Ser(AGY)}$ end-to-end junction is conserved in all vertebrates, while the 3' end of mt-tRNA$^{Ser(AGY)}$ is variable. For example, in the platypus, there is a 4 nucleotide overlap between the 3' end of Ser(AGY) and the 5' end of Leu(UUR). This implies that the sequence or structure of mt-tRNA^{His} is necessary of the recognition of the cleavage site at the 5' end of mt-tRNA$^{Ser(AGY)}$ (Rosmanith, 1997).

Normally, 5' processed products of RNase P are preferred substrates of 3' end processing of tRNA by RNase Z activity (Brzezniak et al.,2011, Rossmanith, 1997, Rackham et al., 2016). However, this is not the case for mt-tRNA$^{Ser(AGY)}$ which shows cleavage activity in a non-hierarchical cleavage of the 5' and 3' end independent of 3' and 5' cleavage respectively (Rossmanith. 1997). A recent mitotranscriptomic analysis of MRPP3-deficient mice showed that indeed, the steady state levels of mt-tRNA$^{Ser(AGY)}$ are not affected by lack of RNase P activity. However, the effect on the other tRNAs mentioned above is not as pronounced, suggesting a possible redundancy in the system for these tRNAs (Rackham et al., 2016). Therefore, this analysis shows that YbeY is required for the accurate processing of tRNA$^{Ser(AGY)}$ from the primary transcript. In the absence of YbeY, the 5' and 3' ends of the tRNA are erroneously identified. It is unclear if YbeY directly cleaves the transcript itself or if it is responsible for the recognition of the tRNA termini and targeting of the nuclease to these sites for accurate cleavage.

The depletion of YbeY also led to a distinct decrease in 7S RNA produced from the L-strand. This RNA species is required for the synthesis of 7S DNA and the initiation of DNA replication. However, no change was observed in mt-DNA copy number, suggesting that 7S levels are not the rate-limiting step in DNA replication. A similar effect on 7S RNA is seen in MRPP3-deficient cells and may be a consequence of a disruption of RNaseP activity (Rackham et al., 2016). This suggests that disruption of primary transcript processing (due to a lack of MRPP3 or YbeY) may lead to a compensatory switch from DNA replication to transcription, preventing the termination of LSP transcription elongation at CSB2. This would lead to the observed 7S RNA depletion in the YbeY (-/-) cells.

4.3.3 YbeY is necessary for mitoribosome biogenesis

YbeY in bacteria plays a key role in the biogenesis and quality control of the ribosome. It is responsible for the maturation of SSU rRNA, LSU rRNA and 5S rRNA. In addition, YbeY identifies and degrades 70S ribosomes containing defective SSUs, thus facilitating ribosomal quality control. We sought to elaborate on the source of the mitochondrial dysfunction further. Cells lacking YbeY showed a high reliance on glycolysis. They were incapable of growing in galactose medium and OxPhos function was severely affected by the lack of YbeY. Western blot analysis of components of the respiratory complexes showed a reduction in complexes which have mitochondrially-encoded components suggesting a deterioration of mitochondrial translation in YbeY deficient cells. Furthermore, labelling of newly synthesised translation products with [^{35}S]-methionine showed that mitochondrial translation was reduced in a YbeY dose dependent manner. A reduced amount of YbeY in the hemizygous HEK293T cells led to a reduced effect on translation. However, a lack of YbeY led to a lack of measurable translation products after 30 minutes of labelling. Moreover, translation was uniformly decreased irrespective of the size of the translation product. In a recent paper by Pearce et al. (2017), larger translation products were affected more than the smaller translation products caused by translational stalling due to lack of a specific tRNAs. This suggests that the translation problem we observe is due to defective ribosomes rather than translational stalling. Moreover, surprisingly, reintroduction of YbeY lacking the H117 residue, required for zinc sequestration and catalysis, led to a rescue of mitochondrial

translation. This indicates that the function of YbeY in mitochondrial translation is independent of its endonucleolytic activity.

To identify the effect of YbeY on mitoribosomal integrity, we used *in vivo* SILAC labelling of parental and knockout cells, sucrose gradient fractionation of the cell lysate and mass spectrometric analysis (qGFMS). This allowed us to successfully resolve the assembled ribosome, the individual subunits and their subunits, and quantify changes in their composition. This method has been successfully used in the past to identify subassemblies in bacterial small subunit assembly (Sashital et al., 2014). Using this method, we identified a decrease in mt-SSU levels and higher levels of mt-LSU. Moreover, a decrease was observed in the levels of mt-LSU assembled into monosomes. However, this effect on the mt-LSU was not as severe as in the mt-SSU. This increase in mt-LSU may be a compensatory effect as a response to a lack of mt-SSU assembled into monosomes. Alternatively, these differences in levels may be caused by a decrease in stability of improperly assembled ribosomes.

The compensatory increase in mt-LSU has been previously observed in mice containing a mutation in MRPS34, which show a loss of mt-SSU assembly. In these mice, there is an increase in mt-LSU protein levels and a decrease in monosome assembly (Richman et al., 2015). Northern blotting also showed that 12S rRNA steady state levels are reduced in the absence of YbeY. Overall, this indicates that YbeY plays a role in mt-SSU assembly and a loss of YbeY leads to a defect in mitoribosomal biogenesis. However, the interaction between YbeY is transient or weak as YbeY did not co-migrate with the mitochondrial small or large subunit in sucrose gradients.

4.3.3.1 YbeY assists mt-SSU assembly via interactions with MRPS11

In bacteria, YbeY is responsible for 3' end processing of the SSU rRNA, the maturation of the 23S LSU rRNA and 5S RNA molecule, and the degradation of assembled ribosomes containing defective SSUs (Jacob *et al.,* 2013). In our experiment, YbeY showed a clear role in mt-SSU biogenesis. A rescue of knockout translation by a catalytic mutant suggests that this role in mitoribosomal biogenesis may not be related to its endonucleolytic activity. However, bacteria lacking YbeY complimented with human YbeY do not show a rescue of SSU rRNA processing. These cells did show a partial rescue of stress sensitivity when human YbeY was introduced. This partial rescue was not observed with catalytically inactive human YbeY (Ghosal et al., 2017). This suggests a divergence of human YbeY function from

its bacterial homolog and that the endonucleolytic function may be independent of its function in assisting mitochondrial translation.

We next looked into identifying the mechanism by which YbeY influences mitoribosome biogenesis. To do this, we performed SILAC-based immunoaffinity purification of flag-tagged YbeY. Interestingly, we identified various mt-LSU components, including, MRPL2, MRPL4, MRPL20, MRPL21, MRPL28, MRPL42, MRPL43, MRPL44, MRPL50 and GADD45GIP1 (Figure 4.3.1). Investigation of these proteins in the qGFMS data showed that these proteins were not depleted in response to the loss of YbeY, which suggests that the interaction may be indirect through RNA. Three non-mitoribosomal proteins were also identified - HSPA9, LSG1 and AASS (Table 4.3.1).

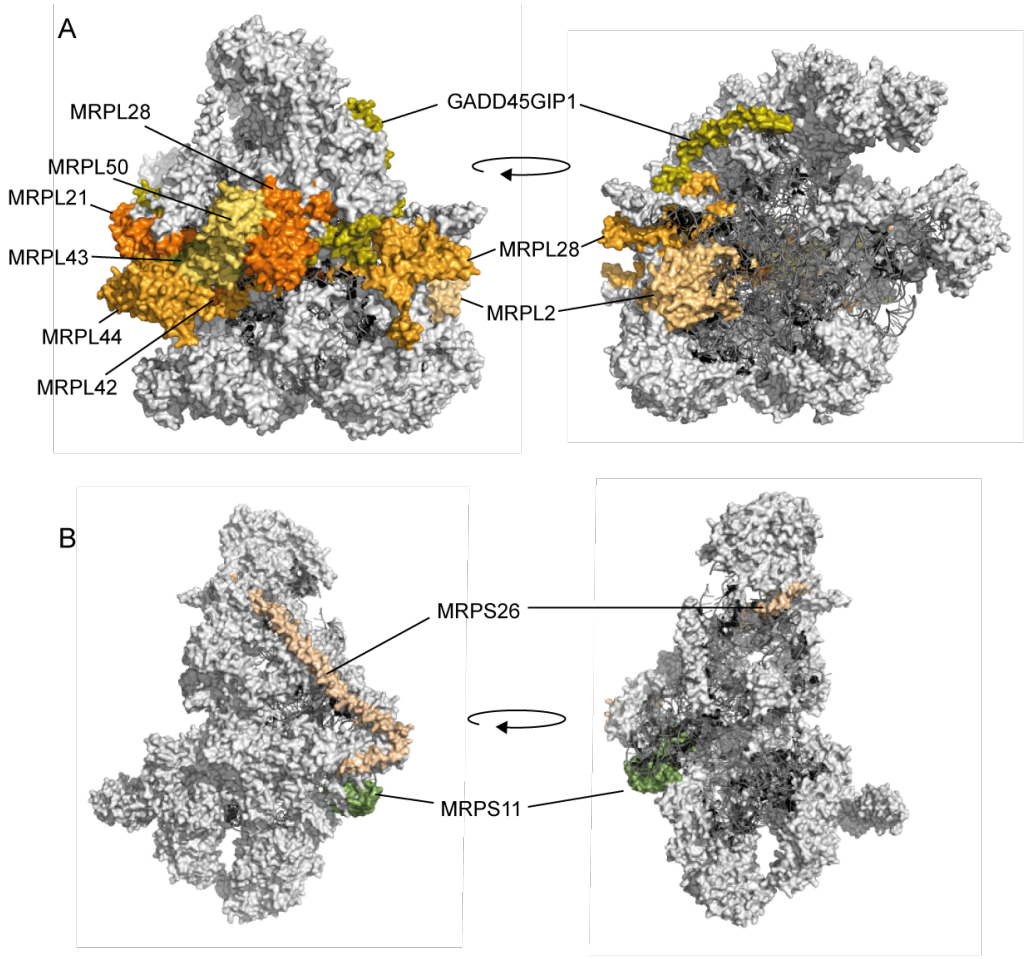

Figure 4.3.1 YbeY interactors on the mitoribosomes. Light grey, mitoribosomal proteins; Dark grey, rRNA (A) mt-LSU. Interactors form a belt around the middle of the protein. (B) mt-SSU. Interactors are also found around the exterior of the protein. The structure was visualised using PyMol molecular graphics system (PDB: 3J9M)

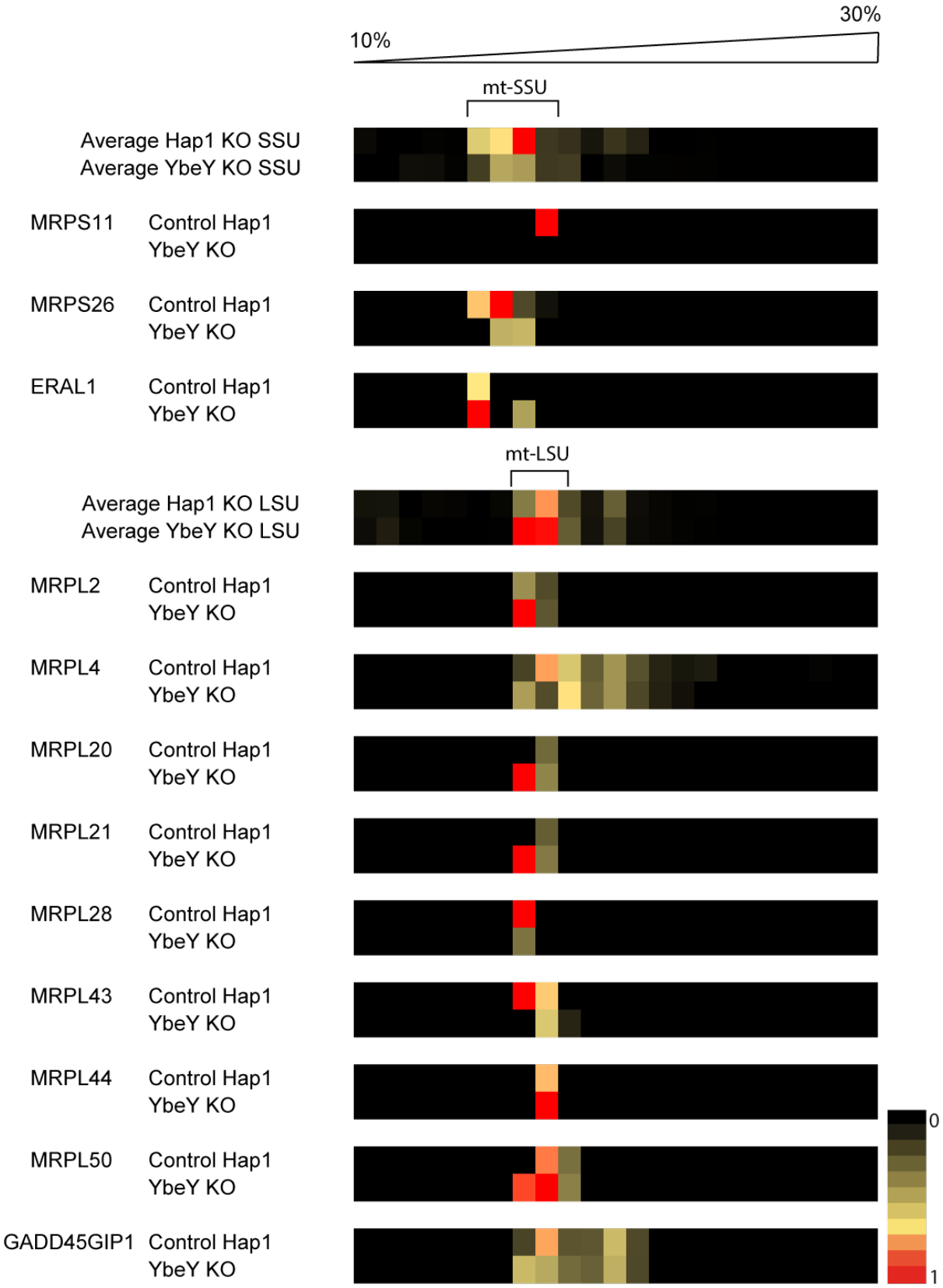

Figure 4.3.2 Effect of YbeY knockout on sucrose gradient fractionation of interactors of YbeY. Heatmap from figure 4.23 filtered for interactors of YbeY. Red indicates maximum intensity of detection while black indicated lack of detection of the protein in that fraction. In the case of

MRPS11, the heatmap was generated from the unmixed SILAC sampels as MRPS11 was not detected in the knockout cells and thus a comparison could not be generated. It must be noted that the lack of detection of MRPS11 does not necessarily indicate absence of protein.

Protein	Localisation	Function	Reference
HSPA9		See Table 3.3.1	
LSG1	Nucleus, Endoplasmic reticulum, cytoplasm	GTPase involved with cytoplasmic ribosomal biogenesis	Reynaud et al. (2005)
AASS	Mitochondria	Lysine degradation pathway	Markovitz et al. (1984)

Table 4.3.1 Non-mitoribosomal protein interactors of YbeY

However, the strongest interactor of human YbeY was identified to be MRPS11. In bacteria, YbeY interacts with the small subunit component, S11 and small subunit biogenesis factor, Era. A recent pulse quantitative proteomic analysis of bacterial SSU assembly identified that S11 is one of the last proteins to assemble, as there are essentially no precursor pools with S11 in them (Chen et al., 2012). Era is a GTPase that binds to the precursor of 30S bacterial ribosomal small subunit close to the 3' terminus of the 16S rRNA, while interacting with S2, S7, S11 and S18. In bacteria, it facilitates maturation of the RNA by acting as a chaperone. Era is displaced by ribosomal protein S1 on the final assembly step, completing the maturation of the bacterial small subunit. *In vitro* and *in silico* analysis showed that bacterial YbeY interacts with Era and S11 suggesting that YbeY may interact with the assembling small subunit at the 3' terminus of the rRNA. Furthermore, investigation of bacterial YbeY interaction through targeted mutations indicated that the interaction between YbeY and Era is indirect, through its interaction with S11. The efficacy of YbeY in the maturation of 16S rRNA in bacteria is highly dependent on its interaction with S11. Given that no RNA-targeting domain has been identified in YbeY that could confer sequence specificity, this interaction may target the nuclease to its substrate (Vercruysse et al., 2016).

Human YbeY not only showed an interaction with MRPS11, it also showed a weaker (and possibly indirect) interaction with ERAL1 (homolog of bacterial Era). In the

qGFMS data, MRPS11 was not detectable in the YbeY KO samples while ERAL1 levels increased in response to the absence of YbeY. This suggests that like in the bacteria, the interaction with ERAL1 is indirect mediated through its interaction with MRPS11. This also implies that the site of interaction of YbeY is conserved and lies at the 3' end of the SSU rRNA. In the mammalian mitoribosome, the region adjacent to S11 are protruding out of the structure and could be the potential site for YbeY binding (see figure 4.3.3) (Greber and Ban, 2015). Here, similar to its bacterial ortholog, YbeY may degrade improperly assembled SSU rRNA. The bacterial YbeY only cleaves single stranded RNA. It is incapable of cleaving dsRNA, RNA that contain 2'-O-ribose methylations, hairpin loops, and 3' ssRNA extensions after hairpin loops that are 10 nucleotides or fewer (Jacob et al., 2013). MRPS11 binds to two distal regions of the 12S rRNA (see figure 4.3.3). The secondary structure of these regions is predominantly base paired. Moreover, the hairpin loop at the 3' end of the rRNA is not only bound by ERAL1 (Uchiumi et al., 2010), but is also dimethylated by TFB1M. YbeY may act as a part of quality control mechanism as it would only be able to degrades rRNA that is not base paired or methylated. In the mitochondrial SSU, YbeY may facilitate late stage assembly and quality control of final maturation of the small subunit.

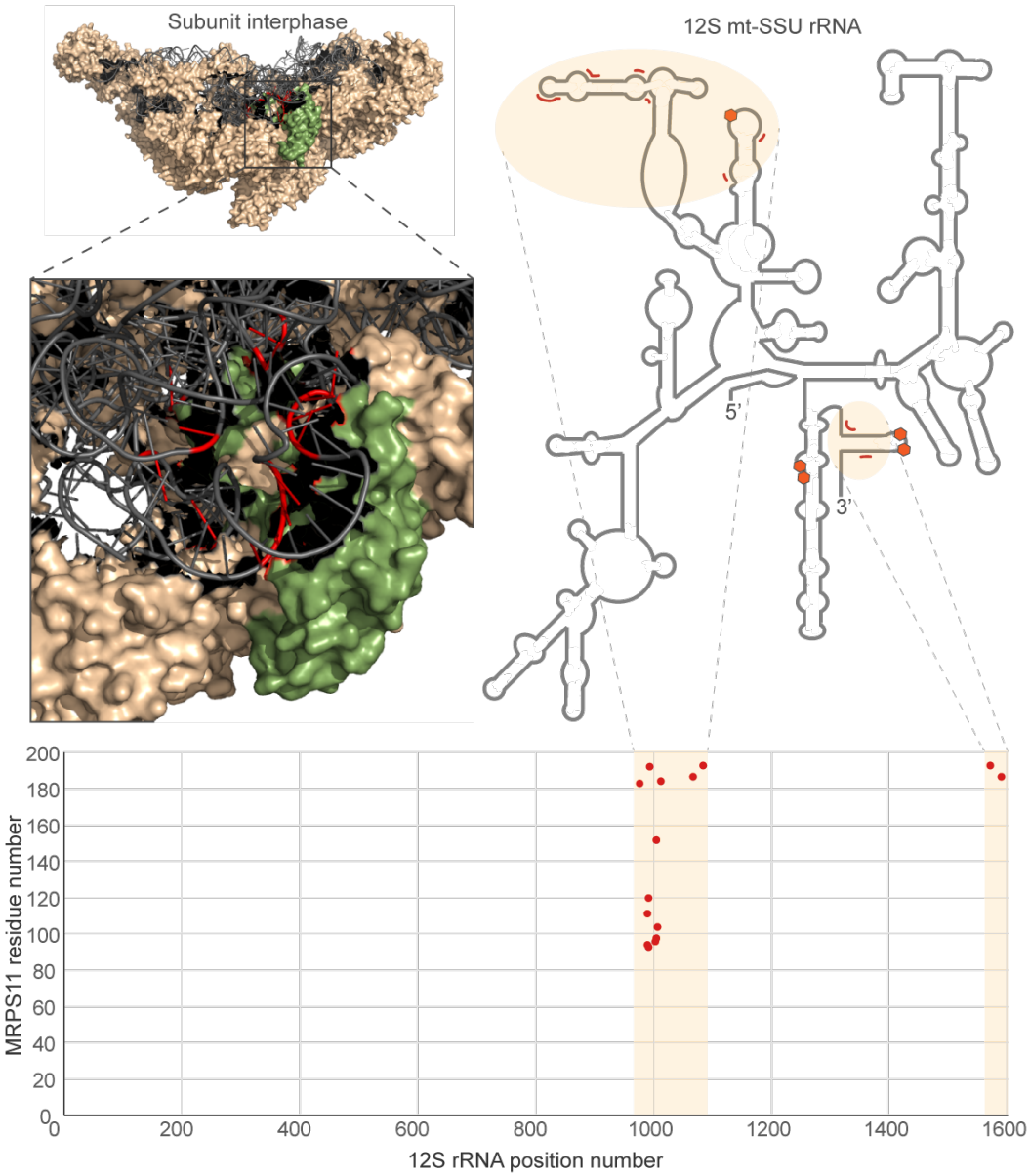

Figure 4.3.3 In silico footprinting of MRPS11. (Right and below) The distance of each amino acid of MRPS11 to each nucleotide of 12S rRNA was calculated. From this, all the nucleotides within hydrogen bonding distance were filtered out and mapped onto the schematic diagram of 12S rRNA. Red lines around the 12S rRNA indicate sites at which MRPS11 comes within 3Å of the rRNA. Orange hexagons indicate sites of modification on the rRNA. (Left) The 3D structure of the small subunit where the rRNA is in gray and the MRPSs are in wheat. MRPS11 is depicted in green. The sites of MRPS11 interaction on the rRNA are shown in red. This structure also illustrates the exposed rRNA to which both ERAL1 and YbeY can bind (Uchiumi et al., 2010). The structure was visualised using PyMol molecular graphics system (PDB: 3J9M)

Interactomic analysis of bacterial YbeY showed that it does not associate with various translation apparatus-associated factors such as translation initiation factors (IF2 and IF3) and ribosome biogenesis factors (KsgA, GsgA, RbfA and RimM). YbeY also does not interact with exoribonuclease, RNase R with which it degrades improperly assembly 70S ribosomes. One interesting protein bound to bacterial YbeY was YbeZ, which is a protein of unknown function with a NTP hydrolase domain (Kazakov et al., 2003). It's function in YbeY's role in ribosome biogenesis and quality control is unknown. However, as a NTPase, it may be required for dissociation of YbeY from the ribosome fuelled by the hydrolysis of ATP or GTP. In human, no homolog of YbeZ has been identified. Our results also fail to identify a mitochondrially-targeted NTPase interactor. Hence, this role may not be conserved in humans.

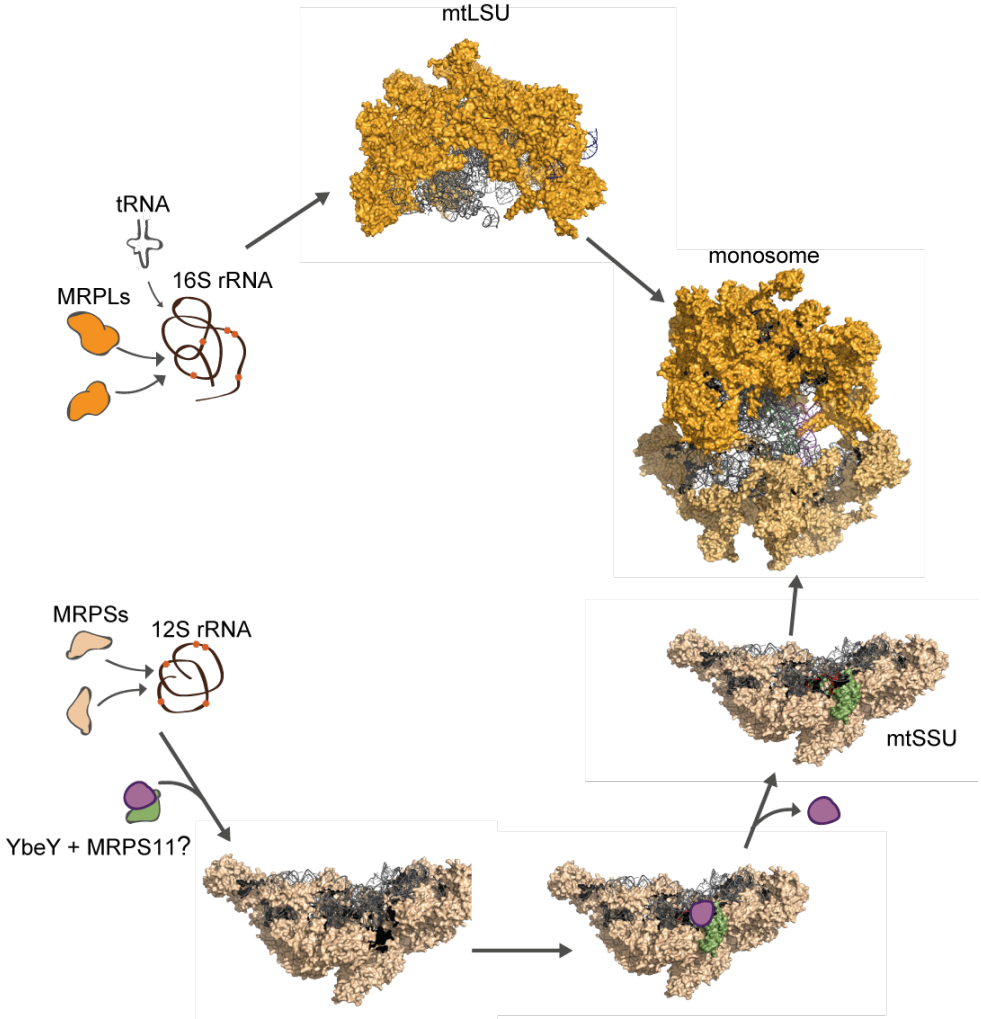

Figure 4.3.4 Schematic model of YbeY in mitoribosomal biogenesis. YbeY (purple) assists mt-SSU assembly through its interaction with MRPS11 (green). After its transient interaction with the mt-SSU, it dissociates and allows monosome formation.

5 Concluding remarks and future directions

The work presented here describes two distinct responses to knockouts of factors involved in mitoribosomal biogenesis. Studies performed on knockout and overexpression cell lines, provide evidence for the dispensability of MRM1 and the G1145 rRNA methylation on various aspects of mitoribosomes maturation, mitochondrial translation and function. We have also not identified any mitoribosomal component interactors of MRM1. For further research, we aim to directly confirm complete loss of methylation using mass spectrometry in order to exclude the possibility that the lack of observed phenotype is caused by the presence of a few molecules with the Gm1145 modification. It is also possible that redundancies in the system may cause a few RNA molecules to be modified by alternative proteins that are not detectable by the primer extension assay. Further research needs to focus on finding conditions where mitoribosomes will show a measurable impact of loss of the modification. This may be in the form of intraribosomal stresses, such as antibiotics and inhibitors, or through the generation of double mutants or cell lines expressing dominant negative protein.

In this work, we have also identified YbeY as a novel factor, vital for mitoribosomal assembly and integrity. We have shown that YbeY is mitochondrially-localised and depletion of YbeY leads to a loss of mitochondrial translation resulting in a reduction of OxPhos function and consequently, a loss of cell viability. Northern blotting and RNA-Seq analysis identified mitochondrial $tRNA^{Ser(AGY)}$ as a potential target for YbeY endoribonucleolytic activity. Loss of YbeY had a detrimental effect on the levels of assembled mt-SSU. Immunoaffinity purification identified MRPS11 as a key interactor of YbeY and a potential mechanism through which mt-SSU biogenesis could be affected by YbeY. Further evidence needs to be gathered to confirm the interaction of YbeY and the mt-SSU through the MRPS11 and the role this interaction plays in mt-SSU assembly. We aim to perform further crosslinking studies to confirm the YbeY-MRPS11 interaction and CLIP assays to identify RNA targets of YbeY.

YbeY also seems to have independent endonucleolytic functions in the mitochondria as loss of mitochondrial translation can be rescued through the reintroduction of predicted catalytically inactive protein. However, the loss of endonucleolytic activity

needs to be confirmed through RNA-Seq and northern blotting against $tRNA^{Ser(AGY)}$. If the tRNAs are still improperly processed in these cells rescued with predicted catalytically inactive protein, this would imply that YbeY performs endonucleotytic functions independent of its role in assisting mitoribosomal biogenesis. Northern blot analysis needs to be extended to all the tRNAs shown to be affected in the RNA-Seq data. Furthermore, RNA-Seq analysis of Hap1 knockout cells needs to be performed to confirm the observed effects on RNA steady state levels observed in YbeY-deficient HEK293T cells.

This work has contributed to the building body of knowledge on the role of chemical modifications of rRNA on mitoribosomal biogenesis, and has identified a novel mitoribosomal biogenesis factor that may also have a role in RNA processing in the mitochondria. The latter discovery points towards a possible mechanism that connects mitochondrial RNA processing to mitoribosomal biogenesis and translation.

6 References

Achila, D., Gulati, M., Jain, N., and Britton, R.A. (2012). Biochemical characterization of ribosome assembly GTPase RbgA in Bacillus subtilis. J Biol Chem *287*, 8417-8423.

Adilakshmi, T., Ramaswamy, P., and Woodson, S.A. (2005). Protein-independent folding pathway of the 16S rRNA 5' domain. J Mol Biol *351*, 508-519.

Agaronyan, K., Morozov, Y.I., Anikin, M., and Temiakov, D. (2015). Mitochondrial biology. Replication-transcription switch in human mitochondria. Science *347*, 548-551.

Al-Furoukh, N., Goffart, S., Szibor, M., Wanrooij, S., and Braun, T. (2013). Binding to G-quadruplex RNA activates the mitochondrial GTPase NOA1. Biochim Biophys Acta *1833*, 2933-2942.

Alexandrov, A., Chernyakov, I., Gu, W., Hiley, S.L., Hughes, T.R., Grayhack, E.J., and Phizicky, E.M. (2006). Rapid tRNA decay can result from lack of nonessential modifications. Mol Cell *21*, 87-96.

Amunts, A., Brown, A., Bai, X.C., Llacer, J.L., Hussain, T., Emsley, P., Long, F., Murshudov, G., Scheres, S.H.W., and Ramakrishnan, V. (2014). Structure of the yeast mitochondrial large ribosomal subunit. Science *343*, 1485-1489.

Amunts, A., Brown, A., Toots, J., Scheres, S.H., and Ramakrishnan, V. (2015). Ribosome. The structure of the human mitochondrial ribosome. Science *348*, 95-98.

Anand, B., Surana, P., and Prakash, B. (2010). Deciphering the catalytic machinery in 30S ribosome assembly GTPase YqeH. PloS one *5*, e9944.

Andersen, N.M., and Douthwaite, S. (2006). YebU is a m5C methyltransferase specific for 16 S rRNA nucleotide 1407. J Mol Biol *359*, 777-786.

Anderson, P., and Kedersha, N. (2009). Stress granules. Curr Biol *19*, R397-398.

Anderson, S., Bankier, A.T., Barrell, B.G., de Bruijn, M.H., Coulson, A.R., Drouin, J., Eperon, I.C., Nierlich, D.P., Roe, B.A., Sanger, F., et al. (1981). Sequence and organization of the human mitochondrial genome. Nature *290*, 457-465.

Andersson, S.G., Zomorodipour, A., Andersson, J.O., Sicheritz-Ponten, T., Alsmark, U.C., Podowski, R.M., Naslund, A.K., Eriksson, A.S., Winkler, H.H., and Kurland, C.G. (1998). The genome sequence of Rickettsia prowazekii and the origin of mitochondria. Nature *396*, 133-140.

Ansmant, I., Massenet, S., Grosjean, H., Motorin, Y., and Branlant, C. (2000). Identification of the Saccharomyces cerevisiae RNA:pseudouridine synthase responsible for formation of psi(2819) in 21S mitochondrial ribosomal RNA. Nucleic Acids Res *28*, 1941-1946.

Antonicka, H., Choquet, K., Lin, Z.Y., Gingras, A.C., Kleinman, C.L., and Shoubridge, E.A. (2017). A pseudouridine synthase module is essential for mitochondrial protein synthesis and cell viability. EMBO Rep *18*, 28-38.

Antonicka, H., Sasarman, F., Nishimura, T., Paupe, V., and Shoubridge, E.A. (2013). The mitochondrial RNA-binding protein GRSF1 localizes to RNA granules and is

required for posttranscriptional mitochondrial gene expression. Cell metabolism *17*, 386-398.

Antonicka, H., and Shoubridge, E.A. (2015). Mitochondrial RNA Granules Are Centers for Posttranscriptional RNA Processing and Ribosome Biogenesis. Cell reports.

Arroyo, J.D., Jourdain, A.A., Calvo, S.E., Ballarano, C.A., Doench, J.G., Root, D.E., and Mootha, V.K. (2016). A Genome-wide CRISPR Death Screen Identifies Genes Essential for Oxidative Phosphorylation. Cell metabolism.

Baer, R.J., and Dubin, D.T. (1981). Methylated regions of hamster mitochondrial ribosomal RNA: structural and functional correlates. Nucleic Acids Res *9*, 323-337.

Bai, Y., Srivastava, S.K., Chang, J.H., Manley, J.L., and Tong, L. (2011). Structural basis for dimerization and activity of human PAPD1, a noncanonical poly(A) polymerase. Molecular cell *41*, 311-320.

Bar-Yaacov, D., Frumkin, I., Yashiro, Y., Chujo, T., Ishigami, Y., Chemla, Y., Blumberg, A., Schlesinger, O., Bieri, P., Greber, B., et al. (2016). Mitochondrial 16S rRNA Is Methylated by tRNA Methyltransferase TRMT61B in All Vertebrates. PLoS Biol *14*, e1002557.

Barrientos, A., Korr, D., Barwell, K.J., Sjulsen, C., Gajewski, C.D., Manfredi, G., Ackerman, S., and Tzagoloff, A. (2003). MTG1 codes for a conserved protein required for mitochondrial translation. Mol Biol Cell *14*, 2292-2302.

Bauerschmitt, H., Mick, D.U., Deckers, M., Vollmer, C., Funes, S., Kehrein, K., Ott, M., Rehling, P., and Herrmann, J.M. (2010). Ribosome-binding proteins Mdm38 and Mba1 display overlapping functions for regulation of mitochondrial translation. Mol Biol Cell *21*, 1937-1944.

Baughman, J.M., Nilsson, R., Gohil, V.M., Arlow, D.H., Gauhar, Z., and Mootha, V.K. (2009). A computational screen for regulators of oxidative phosphorylation implicates SLIRP in mitochondrial RNA homeostasis. PLoS Genet *5*, e1000590.

Becker, L., Kling, E., Schiller, E., Zeh, R., Schrewe, A., Holter, S.M., Mossbrugger, I., Calzada-Wack, J., Strecker, V., Wittig, I., et al. (2014). MTO1-Deficient Mouse Model Mirrors the Human Phenotype Showing Complex I Defect and Cardiomyopathy. PloS one *9*, e114918.

Bertram, G., Innes, S., Minella, O., Richardson, J., and Stansfield, I. (2001). Endless possibilities: translation termination and stop codon recognition. Microbiology *147*, 255-269.

Bestwick, M.L., and Shadel, G.S. (2013). Accessorizing the human mitochondrial transcription machinery. Trends Biochem Sci *38*, 283-291.

Bhargava, K., and Spremulli, L.L. (2005). Role of the N- and C-terminal extensions on the activity of mammalian mitochondrial translational initiation factor 3. Nucleic Acids Res *33*, 7011-7018.

Bhargava, K., Templeton, P., and Spremulli, L.L. (2004). Expression and characterization of isoform 1 of human mitochondrial elongation factor G. Protein Expr Purif *37*, 368-376.

Boehm, E., Zornoza, M., Jourdain, A.A., Delmiro Magdalena, A., Garcia-Consuegra, I., Torres Merino, R., Orduna, A., Martin, M.A., Martinou, J.C., De la Fuente, M.A., et al. (2016). Role of FAST Kinase Domains 3 (FASTKD3) in Post-transcriptional Regulation of Mitochondrial Gene Expression. J Biol Chem *291*, 25877-25887.

Bogenhagen, D.F., Martin, D.W., and Koller, A. (2014). Initial steps in RNA processing and ribosome assembly occur at mitochondrial DNA nucleoids. Cell metabolism *19*, 618-629.

Bogenhagen, D.F., Rousseau, D., and Burke, S. (2008). The layered structure of human mitochondrial DNA nucleoids. J Biol Chem *283*, 3665-3675.

Bohnsack, M.T., and Sloan, K.E. (2017). The mitochondrial epitranscriptome: the roles of RNA modifications in mitochondrial translation and human disease. Cell Mol Life Sci.

Borowski, L.S., Dziembowski, A., Hejnowicz, M.S., Stepien, P.P., and Szczesny, R.J. (2013). Human mitochondrial RNA decay mediated by PNPase-hSuv3 complex takes place in distinct foci. Nucleic Acids Research *41*, 1223-1240.

Bratic, A., Clemente, P., Calvo-Garrido, J., Maffezzini, C., Felser, A., Wibom, R., Wedell, A., Freyer, C., and Wredenberg, A. (2016). Mitochondrial Polyadenylation Is a One-Step Process Required for mRNA Integrity and tRNA Maturation. PLoS Genet *12*, e1006028.

Bratic, A., Wredenberg, A., Gronke, S., Stewart, J.B., Mourier, A., Ruzzenente, B., Kukat, C., Wibom, R., Habermann, B., Partridge, L., et al. (2011). The bicoid stability factor controls polyadenylation and expression of specific mitochondrial mRNAs in Drosophila melanogaster. PLoS Genet *7*, e1002324.

Bricker, D.K., Taylor, E.B., Schell, J.C., Orsak, T., Boutron, A., Chen, Y.C., Cox, J.E., Cardon, C.M., Van Vranken, J.G., Dephoure, N., et al. (2012). A mitochondrial pyruvate carrier required for pyruvate uptake in yeast, Drosophila, and humans. Science *337*, 96-100.

Brown, A., Amunts, A., Bai, X.C., Sugimoto, Y., Edwards, P.C., Murshudov, G., Scheres, S.H., and Ramakrishnan, V. (2014). Structure of the large ribosomal subunit from human mitochondria. Science *346*, 718-722.

Brown, A., Rathore, S., Kimanius, D., Aibara, S., Bai, X.C., Rorbach, J., Amunts, A., and Ramakrishnan, V. (2017). Structures of the human mitochondrial ribosome in native states of assembly. Nat Struct Mol Biol *24*, 866-869.

Brule, H., Holmes, W.M., Keith, G., Giege, R., and Florentz, C. (1998). Effect of a mutation in the anticodon of human mitochondrial tRNAPro on its post-transcriptional modification pattern. Nucleic Acids Research *26*, 537-543.

Bruni, F., Gramegna, P., Oliveira, J.M.a., Lightowlers, R.N., and Chrzanowska-Lightowlers, Z.M.a. (2013). REXO2 is an oligoribonuclease active in human mitochondria. PloS one *8*, e64670.

Brzezniak, L.K., Bijata, M., Szczesny, R.J., and Stepien, P.P. (2011). Involvement of human ELAC2 gene product in 3' end processing of mitochondrial tRNAs. RNA Biol *8*, 616-626.

Bubunenko, M., Korepanov, A., Court, D.L., Jagannathan, I., Dickinson, D., Chaudhuri, B.R., Garber, M.B., and Culver, G.M. (2006). 30S ribosomal subunits can be assembled in vivo without primary binding ribosomal protein S15. RNA *12*, 1229-1239.

Caldas, T., Binet, E., Bouloc, P., Costa, A., Desgres, J., and Richarme, G. (2000a). The FtsJ/RrmJ heat shock protein of Escherichia coli is a 23 S ribosomal RNA methyltransferase. J Biol Chem *275*, 16414-16419.

Caldas, T., Binet, E., Bouloc, P., and Richarme, G. (2000b). Translational defects of Escherichia coli mutants deficient in the Um(2552) 23S ribosomal RNA methyltransferase RrmJ/FTSJ. Biochemical and biophysical research communications *271*, 714-718.

Calvo, S.E., Clauser, K.R., and Mootha, V.K. (2016). MitoCarta2.0: an updated inventory of mammalian mitochondrial proteins. Nucleic Acids Res *44*, D1251-1257.

Camara, Y., Asin-Cayuela, J., Park, C.B., Metodiev, M.D., Shi, Y., Ruzzenente, B., Kukat, C., Habermann, B., Wibom, R., Hultenby, K., et al. (2011). MTERF4 regulates translation by targeting the methyltransferase NSUN4 to the mammalian mitochondrial ribosome. Cell metabolism *13*, 527-539.

Camasamudram, V., Fang, J.K., and Avadhani, N.G. (2003). Transcription termination at the mouse mitochondrial H-strand promoter distal site requires an A/T rich sequence motif and sequence specific DNA binding proteins. European journal of biochemistry / FEBS *270*, 1128-1140.

Cerritelli, S.M., Frolova, E.G., Feng, C., Grinberg, A., Love, P.E., and Crouch, R.J. (2003). Failure to produce mitochondrial DNA results in embryonic lethality in Rnaseh1 null mice. Mol Cell *11*, 807-815.

Chaban, Y., Boekema, E.J., and Dudkina, N.V. (2014). Structures of mitochondrial oxidative phosphorylation supercomplexes and mechanisms for their stabilisation. Biochim Biophys Acta *1837*, 418-426.

Chacinska, A., and Boguta, M. (2000). Coupling of mitochondrial translation with the formation of respiratory complexes in yeast mitochondria. Acta Biochim Pol *47*, 973-991.

Chang, D.D., and Clayton, D.A. (1984). Precise identification of individual promoters for transcription of each strand of human mitochondrial DNA. Cell *36*, 635-643.

Chang, D.D., and Clayton, D.A. (1985). Priming of human mitochondrial DNA replication occurs at the light-strand promoter. Proc Natl Acad Sci U S A *82*, 351-355.

Charollais, J., Pflieger, D., Vinh, J., Dreyfus, M., and Iost, I. (2003). The DEAD-box RNA helicase SrmB is involved in the assembly of 50S ribosomal subunits in Escherichia coli. Mol Microbiol *48*, 1253-1265.

Chatzispyrou, I.A., Alders, M., Guerrero-Castillo, S., Zapata Perez, R., Haagmans, M.A., Mouchiroud, L., Koster, J., Ofman, R., Baas, F., Waterham, H.R., et al. (2017). A homozygous missense mutation in ERAL1, encoding a mitochondrial rRNA chaperone, causes Perrault syndrome. Hum Mol Genet *26*, 2541-2550.

Chen, J.Y., and Martin, N.C. (1988). Biosynthesis of tRNA in yeast mitochondria. An endonuclease is responsible for the 3'-processing of tRNA precursors. J Biol Chem *263*, 13677-13682.

Chen, S.S., Sperling, E., Silverman, J.M., Davis, J.H., and Williamson, J.R. (2012). Measuring the dynamics of E. coli ribosome biogenesis using pulse-labeling and quantitative mass spectrometry. Mol Biosyst *8*, 3325-3334.

Choi, S.K., Lee, J.H., Zoll, W.L., Merrick, W.C., and Dever, T.E. (1998). Promotion of met-tRNAiMet binding to ribosomes by yIF2, a bacterial IF2 homolog in yeast. Science *280*, 1757-1760.

Choi, S.K., Olsen, D.S., Roll-Mecak, A., Martung, A., Remo, K.L., Burley, S.K., Hinnebusch, A.G., and Dever, T.E. (2000). Physical and functional interaction between the eukaryotic orthologs of prokaryotic translation initiation factors IF1 and IF2. Molecular and cellular biology *20*, 7183-7191.

Chow, C.S., Lamichhane, T.N., and Mahto, S.K. (2007). Expanding the nucleotide repertoire of the ribosome with post-transcriptional modifications. ACS Chem Biol *2*, 610-619.

Chrzanowska-Lightowlers, Z.M., and Lightowlers, R.N. (2015). Response to "Ribosome Rescue and Translation Termination at Non-standard Stop Codons by ICT1 in Mammalian Mitochondria". PLoS Genet *11*, e1005227.

Chujo, T., Ohira, T., Sakaguchi, Y., Goshima, N., Nomura, N., Nagao, A., and Suzuki, T. (2012). LRPPRC/SLIRP suppresses PNPase-mediated mRNA decay and promotes polyadenylation in human mitochondria. Nucleic Acids Res *40*, 8033-8047.

Chujo, T., and Suzuki, T. (2012). Trmt61B is a methyltransferase responsible for 1-methyladenosine at position 58 of human mitochondrial tRNAs. RNA (New York, N.Y.) *18*, 2269-2276.

Clayton, D.A. (1982). Replication of animal mitochondrial DNA. Cell *28*, 693-705.

Clemente, P., Pajak, A., Laine, I., Wibom, R., Wedell, A., Freyer, C., and Wredenberg, A. (2015). SUV3 helicase is required for correct processing of mitochondrial transcripts. Nucleic Acids Res *43*, 7398-7413.

Cordin, O., Banroques, J., Tanner, N.K., and Linder, P. (2006). The DEAD-box protein family of RNA helicases. Gene *367*, 17-37.

Cotney, J., and Shadel, G.S. (2006). Evidence for an early gene duplication event in the evolution of the mitochondrial transcription factor B family and maintenance of rRNA methyltransferase activity in human mtTFB1 and mtTFB2. J Mol Evol *63*, 707-717.

Crews, S., Ojala, D., Posakony, J., Nishiguchi, J., and Attardi, G. (1979). Nucleotide sequence of a region of human mitochondrial DNA containing the precisely identified origin of replication. Nature *277*, 192-198.

Crosby, A.H., Patel, H., Chioza, B.A., Proukakis, C., Gurtz, K., Patton, M.A., Sharifi, R., Harlalka, G., Simpson, M.A., Dick, K., et al. (2010). Defective mitochondrial mRNA maturation is associated with spastic ataxia. Am J Hum Genet *87*, 655-660.

Culver, G.M., and Noller, H.F. (1999). Efficient reconstitution of functional Escherichia coli 30S ribosomal subunits from a complete set of recombinant small subunit ribosomal proteins. RNA *5*, 832-843.

Culver, G.M., and Noller, H.F. (2000). In vitro reconstitution of 30S ribosomal subunits using complete set of recombinant proteins. Methods Enzymol *318*, 446-460.

D'Silva, S., Haider, S.J., and Phizicky, E.M. (2011). A domain of the actin binding protein Abp140 is the yeast methyltransferase responsible for 3-methylcytidine modification in the tRNA anti-codon loop. RNA *17*, 1100-1110.

Dalla Rosa, I., Durigon, R., Pearce, S.F., Rorbach, J., Hirst, E.M., Vidoni, S., Reyes, A., Brea-Calvo, G., Minczuk, M., Woellhaf, M.W., et al. (2014). MPV17L2 is required for ribosome assembly in mitochondria. Nucleic Acids Research *42*, 8500-8515.

Davies, B.W., Kohrer, C., Jacob, A.I., Simmons, L.A., Zhu, J., Aleman, L.M., Rajbhandary, U.L., and Walker, G.C. (2010). Role of Escherichia coli YbeY, a highly conserved protein, in rRNA processing. Mol Microbiol *78*, 506-518.

Davies, B.W., and Walker, G.C. (2008). A highly conserved protein of unknown function is required by Sinorhizobium meliloti for symbiosis and environmental stress protection. J Bacteriol *190*, 1118-1123.

Davies, S.M., Rackham, O., Shearwood, A.M., Hamilton, K.L., Narsai, R., Whelan, J., and Filipovska, A. (2009). Pentatricopeptide repeat domain protein 3 associates with the mitochondrial small ribosomal subunit and regulates translation. FEBS Lett *583*, 1853-1858.

Davis, D.R. (1995). Stabilization of RNA stacking by pseudouridine. Nucleic acids research *23*, 5020-5026.

De Silva, D., Fontanesi, F., and Barrientos, A. (2013). The DEAD box protein Mrh4 functions in the assembly of the mitochondrial large ribosomal subunit. Cell metabolism *18*, 712-725.

Decatur, W.A., and Fournier, M.J. (2002). rRNA modifications and ribosome function. Trends Biochem Sci *27*, 344-351.

Dennerlein, S., Rozanska, A., Wydro, M., Chrzanowska-Lightowlers, Z.M., and Lightowlers, R.N. (2010). Human ERAL1 is a mitochondrial RNA chaperone involved in the assembly of the 28S small mitochondrial ribosomal subunit. Biochem J *430*, 551-558.

Diges, C.M., and Uhlenbeck, O.C. (2001). Escherichia coli DbpA is an RNA helicase that requires hairpin 92 of 23S rRNA. EMBO J *20*, 5503-5512.

Dubin, D.T., Montoya, J., Timko, K.D., and Attardi, G. (1982). Sequence analysis and precise mapping of the 3' ends of HeLa cell mitochondrial ribosomal RNAs. J Mol Biol *157*, 1-19.

Dudek, J., Rehling, P., and van der Laan, M. (2013). Mitochondrial protein import: common principles and physiological networks. Biochim Biophys Acta *1833*, 274-285.

Dunn, J.J., and Studier, F.W. (1973). T7 early RNAs are generated by site-specific cleavages. Proc Natl Acad Sci U S A *70*, 1559-1563.

Dziembowski, A., Piwowarski, J., Hoser, R., Minczuk, M., Dmochowska, A., Siep, M., van der Spek, H., Grivell, L., and Stepien, P.P. (2003). The yeast mitochondrial degradosome. Its composition, interplay between RNA helicase and RNase activities and the role in mitochondrial RNA metabolism. J Biol Chem *278*, 1603-1611.

Esguerra, J., Warringer, J., and Blomberg, A. (2008). Functional importance of individual rRNA 2'-O-ribose methylations revealed by high-resolution phenotyping. RNA *14*, 649-656.

Fairman-Williams, M.E., Guenther, U.P., and Jankowsky, E. (2010). SF1 and SF2 helicases: family matters. Curr Opin Struct Biol *20*, 313-324.

Falkenberg, M., Gaspari, M., Rantanen, A., Trifunovic, A., Larsson, N.G., and Gustafsson, C.M. (2002). Mitochondrial transcription factors B1 and B2 activate transcription of human mtDNA. Nat Genet *31*, 289-294.

Feaga, H.A., Quickel, M.D., Hankey-Giblin, P.A., and Keiler, K.C. (2016). Human Cells Require Non-stop Ribosome Rescue Activity in Mitochondria. PLoS Genet *12*, e1005964.

Fearnley, I.M., and Walker, J.E. (1987). Initiation codons in mammalian mitochondria: differences in genetic code in the organelle. Biochemistry *26*, 8247-8251.

Fernandez-Vizarra, E., Berardinelli, A., Valente, L., Tiranti, V., and Zeviani, M. (2007). Nonsense mutation in pseudouridylate synthase 1 (PUS1) in two brothers affected by myopathy, lactic acidosis and sideroblastic anaemia (MLASA). Journal of medical genetics *44*, 173-180.

Fisher, R.P., and Clayton, D.A. (1985). A transcription factor required for promoter recognition by human mitochondrial RNA polymerase. Accurate initiation at the heavy- and light-strand promoters dissected and reconstituted in vitro. J Biol Chem *260*, 11330-11338.

Fogal, V., Richardson, A.D., Karmali, P.P., Scheffler, I.E., Smith, J.W., and Ruoslahti, E. (2010). Mitochondrial p32 protein is a critical regulator of tumor metabolism via maintenance of oxidative phosphorylation. Molecular and cellular biology *30*, 1303-1318.

Frazer-Abel, A.A., and Hagerman, P.J. (2008). Core flexibility of a truncated metazoan mitochondrial tRNA. Nucleic Acids Res *36*, 5472-5481.

Fuller-Pace, F.V., Nicol, S.M., Reid, A.D., and Lane, D.P. (1993). DbpA: a DEAD box protein specifically activated by 23s rRNA. EMBO J *12*, 3619-3626.

Fung, S., Nishimura, T., Sasarman, F., and Shoubridge, E.A. (2013). The conserved interaction of C7orf30 with MRPL14 promotes biogenesis of the mitochondrial large ribosomal subunit and mitochondrial translation. Mol Biol Cell *24*, 184-193.

Fuste, J.M., Wanrooij, S., Jemt, E., Granycome, C.E., Cluett, T.J., Shi, Y., Atanassova, N., Holt, I.J., Gustafsson, C.M., and Falkenberg, M. (2010). Mitochondrial RNA polymerase is needed for activation of the origin of light-strand DNA replication. Mol Cell *37*, 67-78.

Gaignard, P., Gonzales, E., Ackermann, O., Labrune, P., Correia, I., Therond, P., Jacquemin, E., and Slama, A. (2013). Mitochondrial Infantile Liver Disease due to TRMU Gene Mutations: Three New Cases. JIMD Rep *11*, 117-123.

Gao, Y., Katyal, S., Lee, Y., Zhao, J., Rehg, J.E., Russell, H.R., and McKinnon, P.J. (2011). DNA ligase III is critical for mtDNA integrity but not Xrcc1-mediated nuclear DNA repair. Nature *471*, 240-244.

Garcia-Gomez, S., Reyes, A., Martinez-Jimenez, M.I., Chocron, E.S., Mouron, S., Terrados, G., Powell, C., Salido, E., Mendez, J., Holt, I.J., et al. (2013). PrimPol, an archaic primase/polymerase operating in human cells. Mol Cell *52*, 541-553.

Garrido, N., Griparic, L., Jokitalo, E., Wartiovaara, J., van der Bliek, A.M., and Spelbrink, J.N. (2003). Composition and dynamics of human mitochondrial nucleoids. Mol Biol Cell *14*, 1583-1596.

Gattermann, N., Dadak, M., Hofhaus, G., Wulfert, M., Berneburg, M., Loeffler, M.L., and Simmonds, H.A. (2004). Severe impairment of nucleotide synthesis through inhibition of mitochondrial respiration. Nucleosides Nucleotides Nucleic Acids *23*, 1275-1279.

Gaur, R., Grasso, D., Datta, P.P., Krishna, P.D., Das, G., Spencer, A., Agrawal, R.K., Spremulli, L., and Varshney, U. (2008). A single mammalian mitochondrial translation initiation factor functionally replaces two bacterial factors. Mol Cell *29*, 180-190.

Ghezzi, D., Baruffini, E., Haack, T.B., Invernizzi, F., Melchionda, L., Dallabona, C., Strom, T.M., Parini, R., Burlina, A.B., Meitinger, T., et al. (2012). Mutations of the mitochondrial-tRNA modifier MTO1 cause hypertrophic cardiomyopathy and lactic acidosis. Am J Hum Genet *90*, 1079-1087.

Ghosal, A., Kohrer, C., Babu, V.M.P., Yamanaka, K., Davies, B.W., Jacob, A.I., Ferullo, D.J., Gruber, C.C., Vercruysse, M., and Walker, G.C. (2017). C21orf57 is a human homologue of bacterial YbeY proteins. Biochemical and biophysical research communications *484*, 612-617.

Gil, R., Silva, F.J., Pereto, J., and Moya, A. (2004). Determination of the core of a minimal bacterial gene set. Microbiol Mol Biol Rev *68*, 518-537, table of contents.

Ginsburg, D., and Steitz, J.A. (1975). The 30 S ribosomal precursor RNA from Escherichia coli. A primary transcript containing 23 S, 16 S, and 5 S sequences. J Biol Chem *250*, 5647-5654.

Gohil, V.M., Nilsson, R., Belcher-Timme, C.a., Luo, B., Root, D.E., and Mootha, V.K. (2010). Mitochondrial and nuclear genomic responses to loss of LRPPRC expression. Journal of Biological Chemistry *285*, 13742-13747.

Greber, B.J., and Ban, N. (2016). Structure and Function of the Mitochondrial Ribosome. Annu Rev Biochem *85*, 103-132.

Greber, B.J., Bieri, P., Leibundgut, M., Leitner, A., Aebersold, R., Boehringer, D., and Ban, N. (2015). Ribosome. The complete structure of the 55S mammalian mitochondrial ribosome. Science *348*, 303-308.

Greber, B.J., Boehringer, D., Leibundgut, M., Bieri, P., Leitner, A., Schmitz, N., Aebersold, R., and Ban, N. (2014). The complete structure of the large subunit of the mammalian mitochondrial ribosome. Nature *515*, 283-286.

Green, R., and Noller, H.F. (1999). Reconstitution of functional 50S ribosomes from in vitro transcripts of Bacillus stearothermophilus 23S rRNA. Biochemistry *38*, 1772-1779.

Green, R., Samaha, R.R., and Noller, H.F. (1997). Mutations at nucleotides G2251 and U2585 of 23 S rRNA perturb the peptidyl transferase center of the ribosome. J Mol Biol *266*, 40-50.

Gupta, N., and Culver, G.M. (2014). Multiple in vivo pathways for Escherichia coli small ribosomal subunit assembly occur on one pre-rRNA. Nat Struct Mol Biol *21*, 937-943.

Haack, T.B., Kopajtich, R., Freisinger, P., Wieland, T., Rorbach, J., Nicholls, T.J., Baruffini, E., Walther, A., Danhauser, K., Zimmermann, F.A., et al. (2013). ELAC2 mutations cause a mitochondrial RNA processing defect associated with hypertrophic cardiomyopathy. Am J Hum Genet *93*, 211-223.

Haag, S., Sloan, K.E., Ranjan, N., Warda, A.S., Kretschmer, J., Blessing, C., Hubner, B., Seikowski, J., Dennerlein, S., Rehling, P., et al. (2016). NSUN3 and ABH1 modify the wobble position of mt-tRNAMet to expand codon recognition in mitochondrial translation. EMBO J *35*, 2104-2119.

Hammarsund, M., Wilson, W., Corcoran, M., Merup, M., Einhorn, S., Grander, D., and Sangfelt, O. (2001). Identification and characterization of two novel human mitochondrial elongation factor genes, hEFG2 and hEFG1, phylogenetically conserved through evolution. Hum Genet *109*, 542-550.

Han, S.J., Lee, B.C., Yim, S.H., Gladyshev, V.N., and Lee, S.R. (2014). Characterization of mammalian selenoprotein o: a redox-active mitochondrial protein. PloS one *9*, e95518.

Haque, M.E., Elmore, K.B., Tripathy, A., Koc, H., Koc, E.C., and Spremulli, L.L. (2010). Properties of the C-terminal tail of human mitochondrial inner membrane protein Oxa1L and its interactions with mammalian mitochondrial ribosomes. J Biol Chem *285*, 28353-28362.

Haque, M.E., and Spremulli, L.L. (2008). Roles of the N- and C-terminal domains of mammalian mitochondrial initiation factor 3 in protein biosynthesis. J Mol Biol *384*, 929-940.

Harmel, J., Ruzzenente, B., Terzioglu, M., Spåhr, H., Falkenberg, M., and Larsson, N.G. (2013). The leucine-rich pentatricopeptide repeat-containing protein (LRPPRC) does not activate transcription in mammalian mitochondria. Journal of Biological Chemistry *288*, 15510-15519.

Harrington, K.M., Nazarenko, I.A., Dix, D.B., Thompson, R.C., and Uhlenbeck, O.C. (1993). In vitro analysis of translational rate and accuracy with an unmodified tRNA. Biochemistry *32*, 7617-7622.

He, J., Cooper, H.M., Reyes, A., Di Re, M., Kazak, L., Wood, S.R., Mao, C.C., Fearnley, I.M., Walker, J.E., and Holt, I.J. (2012). Human C4orf14 interacts with the mitochondrial nucleoid and is involved in the biogenesis of the small mitochondrial ribosomal subunit. Nucleic Acids Res *40*, 6097-6108.

Heidler, J., Al-Furoukh, N., Kukat, C., Salwig, I., Ingelmann, M.E., Seibel, P., Kruger, M., Holtz, J., Wittig, I., Braun, T., et al. (2011). Nitric oxide-associated

protein 1 (NOA1) is necessary for oxygen-dependent regulation of mitochondrial respiratory complexes. J Biol Chem *286*, 32086-32093.

Held, W.A., Mizushima, S., and Nomura, M. (1973). Reconstitution of Escherichia coli 30 S ribosomal subunits from purified molecular components. J Biol Chem *248*, 5720-5730.

Held, W.A., and Nomura, M. (1975). Escherichia coli 30 S ribosomal proteins uniquely required for assembly. J Biol Chem *250*, 3179-3184.

Helm, M., Brule, H., Degoul, F., Cepanec, C., Leroux, J.P., Giege, R., and Florentz, C. (1998). The presence of modified nucleotides is required for cloverleaf folding of a human mitochondrial tRNA. Nucleic Acids Res *26*, 1636-1643.

Helm, M., Giegé, R., and Florentz, C. (1999). A Watson−Crick Base-Pair-Disrupting Methyl Group (m 1 A9) Is Sufficient for Cloverleaf Folding of Human Mitochondrial tRNA Lys. Biochemistry *38*, 13338-13346.

Hennon, S.W., Soman, R., Zhu, L., and Dalbey, R.E. (2015). YidC/Alb3/Oxa1 Family of Insertases. J Biol Chem *290*, 14866-14874.

Herrmann, J.M., Woellhaf, M.W., and Bonnefoy, N. (2013). Control of protein synthesis in yeast mitochondria: the concept of translational activators. Biochim Biophys Acta *1833*, 286-294.

Herzig, S., Raemy, E., Montessuit, S., Veuthey, J.L., Zamboni, N., Westermann, B., Kunji, E.R., and Martinou, J.C. (2012). Identification and functional expression of the mitochondrial pyruvate carrier. Science *337*, 93-96.

Holmes, J.B., Akman, G., Wood, S.R., Sakhuja, K., Cerritelli, S.M., Moss, C., Bowmaker, M.R., Jacobs, H.T., Crouch, R.J., and Holt, I.J. (2015). Primer retention owing to the absence of RNase H1 is catastrophic for mitochondrial DNA replication. Proc Natl Acad Sci U S A *112*, 9334-9339.

Holzmann, J., Frank, P., Loffler, E., Bennett, K.L., Gerner, C., and Rossmanith, W. (2008). RNase P without RNA: identification and functional reconstitution of the human mitochondrial tRNA processing enzyme. Cell *135*, 462-474.

Hung, V., Zou, P., Rhee, H.W., Udeshi, N.D., Cracan, V., Svinkina, T., Carr, S.A., Mootha, V.K., and Ting, A.Y. (2014). Proteomic mapping of the human mitochondrial intermembrane space in live cells via ratiometric APEX tagging. Mol Cell *55*, 332-341.

Hyvarinen, A.K., Kumanto, M.K., Marjavaara, S.K., and Jacobs, H.T. (2010). Effects on mitochondrial transcription of manipulating mTERF protein levels in cultured human HEK293 cells. BMC Mol Biol *11*, 72.

Jacob, A.I., Kohrer, C., Davies, B.W., RajBhandary, U.L., and Walker, G.C. (2013). Conserved bacterial RNase YbeY plays key roles in 70S ribosome quality control and 16S rRNA maturation. Mol Cell *49*, 427-438.

Jang, S.I., Kalinin, A., Takahashi, K., Marekov, L.N., and Steinert, P.M. (2005). Characterization of human epiplakin: RNAi-mediated epiplakin depletion leads to the disruption of keratin and vimentin IF networks. J Cell Sci *118*, 781-793.

Jimenez-Menendez, N., Fernandez-Millan, P., Rubio-Cosials, A., Arnan, C., Montoya, J., Jacobs, H.T., Bernado, P., Coll, M., Uson, I., and Sola, M. (2010).

Human mitochondrial mTERF wraps around DNA through a left-handed superhelical tandem repeat. Nat Struct Mol Biol *17*, 891-893.

Jomaa, A., Jain, N., Davis, J.H., Williamson, J.R., Britton, R.A., and Ortega, J. (2014). Functional domains of the 50S subunit mature late in the assembly process. Nucleic Acids Res *42*, 3419-3435.

Jourdain, A.A., Boehm, E., Maundrell, K., and Martinou, J.C. (2016). Mitochondrial RNA granules: Compartmentalizing mitochondrial gene expression. J Cell Biol *212*, 611-614.

Jourdain, A.A., Koppen, M., Rodley, C.D., Maundrell, K., Gueguen, N., Reynier, P., Guaras, A.M., Enriquez, J.A., Anderson, P., Simarro, M., et al. (2015). A mitochondria-specific isoform of FASTK is present in mitochondrial RNA granules and regulates gene expression and function. Cell reports *10*, 1110-1121.

Jourdain, A.A., Koppen, M., Wydro, M., Rodley, C.D., Lightowlers, R.N., Chrzanowska-Lightowlers, Z.M., and Martinou, J.C. (2013). GRSF1 regulates RNA processing in mitochondrial RNA granules. Cell metabolism *17*, 399-410.

Kaberdin, V.R., and Blasi, U. (2013). Bacterial helicases in post-transcriptional control. Biochim Biophys Acta *1829*, 878-883.

Kaczanowska, M., and Ryden-Aulin, M. (2007). Ribosome biogenesis and the translation process in Escherichia coli. Microbiol Mol Biol Rev *71*, 477-494.

Kaur, J., and Stuart, R.A. (2011). Truncation of the Mrp20 protein reveals new ribosome-assembly subcomplex in mitochondria. EMBO Rep *12*, 950-955.

Kaushal, P.S., Sharma, M.R., Booth, T.M., Haque, E.M., Tung, C.S., Sanbonmatsu, K.Y., Spremulli, L.L., and Agrawal, R.K. (2014). Cryo-EM structure of the small subunit of the mammalian mitochondrial ribosome. Proc Natl Acad Sci U S A *111*, 7284-7289.

Kazakov, A.E., Vassieva, O., Gelfand, M.S., Osterman, A., and Overbeek, R. (2003). Bioinformatics classification and functional analysis of PhoH homologs. In Silico Biol *3*, 3-15.

Klootwijk, J., Klein, I., and Grivell, L.A. (1975). Minimal post-transcriptional modification of yeast mitochondrial ribosomal RNA. J Mol Biol *97*, 337-350.

Kolanczyk, M., Pech, M., Zemojtel, T., Yamamoto, H., Mikula, I., Calvaruso, M.A., van den Brand, M., Richter, R., Fischer, B., Ritz, A., et al. (2011). NOA1 is an essential GTPase required for mitochondrial protein synthesis. Mol Biol Cell *22*, 1-11.

Kopajtich, R., Nicholls, T.J., Rorbach, J., Metodiev, M.D., Freisinger, P., Mandel, H., Vanlander, A., Ghezzi, D., Carrozzo, R., Taylor, R.W., et al. (2014). Mutations in GTPBP3 Cause a Mitochondrial Translation Defect Associated with Hypertrophic Cardiomyopathy, Lactic Acidosis, and Encephalopathy. Am J Hum Genet *95*, 708-720.

Korhonen, J.A., Gaspari, M., and Falkenberg, M. (2003). TWINKLE Has 5' -> 3' DNA helicase activity and is specifically stimulated by mitochondrial single-stranded DNA-binding protein. J Biol Chem *278*, 48627-48632.

Korhonen, J.A., Pham, X.H., Pellegrini, M., and Falkenberg, M. (2004). Reconstitution of a minimal mtDNA replisome in vitro. EMBO J *23*, 2423-2429.

Kornblum, C., Nicholls, T.J., Haack, T.B., Scholer, S., Peeva, V., Danhauser, K., Hallmann, K., Zsurka, G., Rorbach, J., Iuso, A., et al. (2013). Loss-of-function mutations in MGME1 impair mtDNA replication and cause multisystemic mitochondrial disease. Nat Genet *45*, 214-219.

Kotani, T., Akabane, S., Takeyasu, K., Ueda, T., and Takeuchi, N. (2013). Human G-proteins, ObgH1 and Mtg1, associate with the large mitochondrial ribosome subunit and are involved in translation and assembly of respiratory complexes. Nucleic Acids Res *41*, 3713-3722.

Krzyzosiak, W., Denman, R., Nurse, K., Hellmann, W., Boublik, M., Gehrke, C.W., Agris, P.F., and Ofengand, J. (1987). In vitro synthesis of 16S ribosomal RNA containing single base changes and assembly into a functional 30S ribosome. Biochemistry *26*, 2353-2364.

Kukat, C., Davies, K.M., Wurm, C.A., Spahr, H., Bonekamp, N.A., Kuhl, I., Joos, F., Polosa, P.L., Park, C.B., Posse, V., et al. (2015). Cross-strand binding of TFAM to a single mtDNA molecule forms the mitochondrial nucleoid. Proc Natl Acad Sci U S A *112*, 11288-11293.

Lafontaine, D.L., Preiss, T., and Tollervey, D. (1998). Yeast 18S rRNA dimethylase Dim1p: a quality control mechanism in ribosome synthesis? Molecular and cellular biology *18*, 2360-2370.

Lagouge, M., Mourier, A., Lee, H.J., Spahr, H., Wai, T., Kukat, C., Silva Ramos, E., Motori, E., Busch, J.D., Siira, S., et al. (2015). SLIRP Regulates the Rate of Mitochondrial Protein Synthesis and Protects LRPPRC from Degradation. PLoS Genet *11*, e1005423.

Lakshmipathy, U., and Campbell, C. (1999). The human DNA ligase III gene encodes nuclear and mitochondrial proteins. Molecular and cellular biology *19*, 3869-3876.

Lamichhane, T.N., Blewett, N.H., Crawford, A.K., Cherkasova, V.A., Iben, J.R., Begley, T.J., Farabaugh, P.J., and Maraia, R.J. (2013). Lack of tRNA modification isopentenyl-A37 alters mRNA decoding and causes metabolic deficiencies in fission yeast. Molecular and cellular biology *33*, 2918-2929.

Lane, N., and Martin, W. (2010). The energetics of genome complexity. Nature *467*, 929-934.

Lapkouski, M., and Hallberg, B.M. (2015). Structure of mitochondrial poly(A) RNA polymerase reveals the structural basis for dimerization, ATP selectivity and the SPAX4 disease phenotype. Nucleic Acids Res *43*, 9065-9075.

Larsson, N.G., Wang, J., Wilhelmsson, H., Oldfors, A., Rustin, P., Lewandoski, M., Barsh, G.S., and Clayton, D.A. (1998). Mitochondrial transcription factor A is necessary for mtDNA maintenance and embryogenesis in mice. Nat Genet *18*, 231-236.

Lee, J.H., Choi, S.K., Roll-Mecak, A., Burley, S.K., and Dever, T.E. (1999). Universal conservation in translation initiation revealed by human and archaeal homologs of bacterial translation initiation factor IF2. Proc Natl Acad Sci U S A *96*, 4342-4347.

Lee, K.W., and Bogenhagen, D.F. (2014). Assignment of 2'-O-methyltransferases to modification sites on the mammalian mitochondrial large subunit 16 S ribosomal RNA (rRNA). J Biol Chem *289*, 24936-24942.

Lee, K.W., Okot-Kotber, C., LaComb, J.F., and Bogenhagen, D.F. (2013). Mitochondrial ribosomal RNA (rRNA) methyltransferase family members are positioned to modify nascent rRNA in foci near the mitochondrial DNA nucleoid. J Biol Chem *288*, 31386-31399.

Leskinen, K., Varjosalo, M., and Skurnik, M. (2015). Absence of YbeY RNase compromises the growth and enhances the virulence plasmid gene expression of Yersinia enterocolitica O:3. Microbiology *161*, 285-299.

Levy, S., Allerston, C.K., Liveanu, V., Habib, M.R., Gileadi, O., and Schuster, G. (2016). Identification of LACTB2, a metallo-beta-lactamase protein, as a human mitochondrial endoribonuclease. Nucleic Acids Res *44*, 1813-1832.

Li, H., Handsaker, B., Wysoker, A., Fennell, T., Ruan, J., Homer, N., Marth, G., Abecasis, G., Durbin, R., and Genome Project Data Processing, S. (2009). The Sequence Alignment/Map format and SAMtools. Bioinformatics *25*, 2078-2079.

Li, N., Chen, Y., Guo, Q., Zhang, Y., Yuan, Y., Ma, C., Deng, H., Lei, J., and Gao, N. (2013). Cryo-EM structures of the late-stage assembly intermediates of the bacterial 50S ribosomal subunit. Nucleic Acids Res *41*, 7073-7083.

Li, X., Li, R., Lin, X., and Guan, M.-X. (2002). Isolation and characterization of the putative nuclear modifier gene MTO1 involved in the pathogenesis of deafness-associated mitochondrial 12 S rRNA A1555G mutation. The Journal of biological chemistry *277*, 27256-27264.

Li, Z., Pandit, S., and Deutscher, M.P. (1999a). Maturation of 23S ribosomal RNA requires the exoribonuclease RNase T. RNA *5*, 139-146.

Li, Z., Pandit, S., and Deutscher, M.P. (1999b). RNase G (CafA protein) and RNase E are both required for the 5' maturation of 16S ribosomal RNA. EMBO J *18*, 2878-2885.

Liao, H.X., and Spremulli, L.L. (1990). Identification and initial characterization of translational initiation factor 2 from bovine mitochondria. J Biol Chem *265*, 13618-13622.

Liao, Y., Smyth, G.K., and Shi, W. (2013). The Subread aligner: fast, accurate and scalable read mapping by seed-and-vote. Nucleic Acids Res *41*, e108.

Linder, P., and Jankowsky, E. (2011). From unwinding to clamping - the DEAD box RNA helicase family. Nat Rev Mol Cell Biol *12*, 505-516.

Ling, M., Merante, F., Chen, H.S., Duff, C., Duncan, A.M., and Robinson, B.H. (1997). The human mitochondrial elongation factor tu (EF-Tu) gene: cDNA sequence, genomic localization, genomic structure, and identification of a pseudogene. Gene *197*, 325-336.

Litonin, D., Sologub, M., Shi, Y., Savkina, M., Anikin, M., Falkenberg, M., Gustafsson, C.M., and Temiakov, D. (2010). Human mitochondrial transcription revisited: only TFAM and TFB2M are required for transcription of the mitochondrial genes in vitro. J Biol Chem *285*, 18129-18133.

Liu, J., Zhou, W., Liu, G., Yang, C., Sun, Y., Wu, W., Cao, S., Wang, C., Hai, G., Wang, Z., et al. (2015). The conserved endoribonuclease YbeY is required for chloroplast ribosomal RNA processing in Arabidopsis. Plant Physiol *168*, 205-221.

Liu, M., and Spremulli, L. (2000). Interaction of mammalian mitochondrial ribosomes with the inner membrane. J Biol Chem *275*, 29400-29406.

Lodeiro, M.F., Uchida, A., Bestwick, M., Moustafa, I.M., Arnold, J.J., Shadel, G.S., and Cameron, C.E. (2012). Transcription from the second heavy-strand promoter of human mtDNA is repressed by transcription factor A in vitro. Proc Natl Acad Sci U S A *109*, 6513-6518.

Lopez, M.F., Kristal, B.S., Chernokalskaya, E., Lazarev, A., Shestopalov, A.I., Bogdanova, A., and Robinson, M. (2000). High-throughput profiling of the mitochondrial proteome using affinity fractionation and automation. Electrophoresis *21*, 3427-3440.

Love, M.I., Huber, W., and Anders, S. (2014). Moderated estimation of fold change and dispersion for RNA-seq data with DESeq2. Genome biology *15*, 550.

Lovgren, J.M., and Wikstrom, P.M. (2001). The rlmB gene is essential for formation of Gm2251 in 23S rRNA but not for ribosome maturation in Escherichia coli. J Bacteriol *183*, 6957-6960.

Lu, B., Lee, J., Nie, X., Li, M., Morozov, Y.I., Venkatesh, S., Bogenhagen, D.F., Temiakov, D., and Suzuki, C.K. (2013). Phosphorylation of human TFAM in mitochondria impairs DNA binding and promotes degradation by the AAA+ Lon protease. Mol Cell *49*, 121-132.

Maden, B.E., Corbett, M.E., Heeney, P.A., Pugh, K., and Ajuh, P.M. (1995). Classical and novel approaches to the detection and localization of the numerous modified nucleotides in eukaryotic ribosomal RNA. Biochimie *77*, 22-29.

Martin, M., Cho, J., Cesare, A.J., Griffith, J.D., and Attardi, G. (2005). Termination factor-mediated DNA loop between termination and initiation sites drives mitochondrial rRNA synthesis. Cell *123*, 1227-1240.

Martin, W., and Muller, M. (1998). The hydrogen hypothesis for the first eukaryote. Nature *392*, 37-41.

Mercer, T.R., Neph, S., Dinger, M.E., Crawford, J., Smith, M.A., Shearwood, A.M., Haugen, E., Bracken, C.P., Rackham, O., Stamatoyannopoulos, J.A., et al. (2011). The human mitochondrial transcriptome. Cell *146*, 645-658.

Metodiev, M.D., Lesko, N., Park, C.B., Camara, Y., Shi, Y., Wibom, R., Hultenby, K., Gustafsson, C.M., and Larsson, N.G. (2009). Methylation of 12S rRNA is necessary for in vivo stability of the small subunit of the mammalian mitochondrial ribosome. Cell metabolism *9*, 386-397.

Metodiev, M.D., Spahr, H., Loguercio Polosa, P., Meharg, C., Becker, C., Altmueller, J., Habermann, B., Larsson, N.G., and Ruzzenente, B. (2014). NSUN4 is a dual function mitochondrial protein required for both methylation of 12S rRNA and coordination of mitoribosomal assembly. PLoS Genet *10*, e1004110.

Minczuk, M., Dmochowska, A., Palczewska, M., and Stepien, P.P. (2002). Overexpressed yeast mitochondrial putative RNA helicase Mss116 partially

restores proper mtRNA metabolism in strains lacking the Suv3 mtRNA helicase. Yeast *19*, 1285-1293.

Minczuk, M., He, J., Duch, A.M., Ettema, T.J., Chlebowski, A., Dzionek, K., Nijtmans, L.G., Huynen, M.A., and Holt, I.J. (2011). TEFM (c17orf42) is necessary for transcription of human mtDNA. Nucleic Acids Res *39*, 4284-4299.

Montoya, J., Christianson, T., Levens, D., Rabinowitz, M., and Attardi, G. (1982). Identification of initiation sites for heavy-strand and light-strand transcription in human mitochondrial DNA. Proc Natl Acad Sci U S A *79*, 7195-7199.

Montoya, J., Gaines, G.L., and Attardi, G. (1983). The pattern of transcription of the human mitochondrial rRNA genes reveals two overlapping transcription units. Cell *34*, 151-159.

Motorin, Y., and Helm, M. (2010). tRNA stabilization by modified nucleotides. Biochemistry *49*, 4934-4944.

Mourier, A., Ruzzenente, B., Brandt, T., Kühlbrandt, W., and Larsson, N.-G. (2014). Loss of LRPPRC causes ATP synthase deficiency. Human molecular genetics *23*, 2580-2592.

Nagaike, T., Suzuki, T., Katoh, T., and Ueda, T. (2005). Human mitochondrial mRNAs are stabilized with polyadenylation regulated by mitochondria-specific poly(A) polymerase and polynucleotide phosphorylase. The Journal of biological chemistry *280*, 19721-19727.

Nagaike, T., Suzuki, T., Tomari, Y., Takemoto-Hori, C., Negayama, F., Watanabe, K., and Ueda, T. (2001). Identification and characterization of mammalian mitochondrial tRNA nucleotidyltransferases. J Biol Chem *276*, 40041-40049.

Nakano, S., Suzuki, T., Kawarada, L., Iwata, H., Asano, K., and Suzuki, T. (2016). NSUN3 methylase initiates 5-formylcytidine biogenesis in human mitochondrial tRNA(Met). Nat Chem Biol *12*, 546-551.

Nicholls, T.J., Zsurka, G., Peeva, V., Scholer, S., Szczesny, R.J., Cysewski, D., Reyes, A., Kornblum, C., Sciacco, M., Moggio, M., et al. (2014). Linear mtDNA fragments and unusual mtDNA rearrangements associated with pathological deficiency of MGME1 exonuclease. Hum Mol Genet *23*, 6147-6162.

Ojala, D., Montoya, J., and Attardi, G. (1981). tRNA punctuation model of RNA processing in human mitochondria. Nature *290*, 470-474.

Patton, J.R., Bykhovskaya, Y., Mengesha, E., Bertolotto, C., and Fischel-Ghodsian, N. (2005). Mitochondrial myopathy and sideroblastic anemia (MLASA): missense mutation in the pseudouridine synthase 1 (PUS1) gene is associated with the loss of tRNA pseudouridylation. J Biol Chem *280*, 19823-19828.

Pearce, S.F., Rorbach, J., Van Haute, L., D'Souza, A.R., Rebelo-Guiomar, P., Powell, C.A., Brierley, I., Firth, A.E., and Minczuk, M. (2017). Maturation of selected human mitochondrial tRNAs requires deadenylation. Elife *6*.

Piwowarski, J., Grzechnik, P., Dziembowski, A., Dmochowska, A., Minczuk, M., and Stepien, P.P. (2003). Human polynucleotide phosphorylase, hPNPase, is localized in mitochondria. J Mol Biol *329*, 853-857.

Poulsen, J.B., Andersen, K.R., Kjaer, K.H., Durand, F., Faou, P., Vestergaard, A.L., Talbo, G.H., Hoogenraad, N., Brodersen, D.E., Justesen, J., et al. (2011). Human

2'-phosphodiesterase localizes to the mitochondrial matrix with a putative function in mitochondrial RNA turnover. Nucleic Acids Res *39*, 3754-3770.

Powell, C.A., Kopajtich, R., D'Souza, A.R., Rorbach, J., Kremer, L.S., Husain, R.A., Dallabona, C., Donnini, C., Alston, C.L., Griffin, H., et al. (2015). TRMT5 Mutations Cause a Defect in Post-transcriptional Modification of Mitochondrial tRNA Associated with Multiple Respiratory-Chain Deficiencies. Am J Hum Genet *97*, 319-328.

Rackham, O., Davies, S.M., Shearwood, A.M., Hamilton, K.L., Whelan, J., and Filipovska, A. (2009). Pentatricopeptide repeat domain protein 1 lowers the levels of mitochondrial leucine tRNAs in cells. Nucleic Acids Res *37*, 5859-5867.

Reiter, V., Matschkal, D.M.S., Wagner, M., Globisch, D., Kneuttinger, A.C., Müller, M., and Carell, T. (2012). The CDK5 repressor CDK5RAP1 is a methylthiotransferase acting on nuclear and mitochondrial RNA. Nucleic acids research *40*, 6235-6240.

Rorbach, J., Gammage, P.A., and Minczuk, M. (2012). C7orf30 is necessary for biogenesis of the large subunit of the mitochondrial ribosome. Nucleic Acids Res *40*, 4097-4109.

Rorbach, J., Gao, F., Powell, C.A., D'Souza, A., Lightowlers, R.N., Minczuk, M., and Chrzanowska-Lightowlers, Z.M. (2016). Human mitochondrial ribosomes can switch their structural RNA composition. Proc Natl Acad Sci U S A.

Rorbach, J., and Minczuk, M. (2012). The post-transcriptional life of mammalian mitochondrial RNA. Biochem J *444*, 357-373.

Rorbach, J., Nicholls, T.J., and Minczuk, M. (2011). PDE12 removes mitochondrial RNA poly(A) tails and controls translation in human mitochondria. Nucleic Acids Res *39*, 7750-7763.

Rossmanith, W. (2011). Localization of human RNase Z isoforms: dual nuclear/mitochondrial targeting of the ELAC2 gene product by alternative translation initiation. PloS one *6*, e19152.

Rossmanith, W., and Holzmann, J. (2009). Processing mitochondrial (t) RNAs. Cell Cycle *8*.

Ruzzenente, B., Metodiev, M.D., Wredenberg, A., Bratic, A., Park, C.B., Cámara, Y., Milenkovic, D., Zickermann, V., Wibom, R., Hultenby, K., et al. (2012). LRPPRC is necessary for polyadenylation and coordination of translation of mitochondrial mRNAs. The EMBO journal *31*, 443-456.

Sagan, L. (1967). On the origin of mitosing cells. J Theor Biol *14*, 255-274.

Sanchez, M.I., Mercer, T.R., Davies, S.M., Shearwood, A.M., Nygard, K.K., Richman, T.R., Mattick, J.S., Rackham, O., and Filipovska, A. (2011). RNA processing in human mitochondria. Cell Cycle *10*, 2904-2916.

Sasarman, F., Nishimura, T., Antonicka, H., Weraarpachai, W., Shoubridge, E.A., and Consortium, L. (2015a). Tissue-specific responses to the LRPPRC founder mutation in French Canadian Leigh Syndrome. Hum Mol Genet *24*, 480-491.

Sasarman, F., Thiffault, I., Weraarpachai, W., Salomon, S., Maftei, C., Gauthier, J., Ellazam, B., Webb, N., Antonicka, H., Janer, A., et al. (2015b). The 3' addition of

CCA to mitochondrial tRNASer(AGY) is specifically impaired in patients with mutations in the tRNA nucleotidyl transferase TRNT1. Hum Mol Genet.

Seidel-Rogol, B.L., McCulloch, V., and Shadel, G.S. (2003). Human mitochondrial transcription factor B1 methylates ribosomal RNA at a conserved stem-loop. Nat Genet *33*, 23-24.

Shi, Y., Dierckx, A., Wanrooij, P.H., Wanrooij, S., Larsson, N.G., Wilhelmsson, L.M., Falkenberg, M., and Gustafsson, C.M. (2012). Mammalian transcription factor A is a core component of the mitochondrial transcription machinery. Proc Natl Acad Sci U S A *109*, 16510-16515.

Sirum-Connolly, K., and Mason, T.L. (1993). Functional requirement of a site-specific ribose methylation in ribosomal RNA. Science *262*, 1886-1889.

Slomovic, S., Laufer, D., Geiger, D., and Schuster, G. (2005). Polyadenylation and Degradation of Human Mitochondrial RNA : the Prokaryotic Past Leaves Its Mark. Molecular and cellular biology *25*, 6427-6435.

Slomovic, S., and Schuster, G. (2008). Stable PNPase RNAi silencing : Its effect on the processing and adenylation of human mitochondrial RNA. RNA *14*, 310-323.

Small, I.D., and Peeters, N. (2000). The PPR motif - a TPR-related motif prevalent in plant organellar proteins. Trends Biochem Sci *25*, 46-47.

Sondheimer, N., Fang, J.K., Polyak, E., Falk, M.J., and Avadhani, N.G. (2010). Leucine-rich pentatricopeptide-repeat containing protein regulates mitochondrial transcription. Biochemistry *49*, 7467-7473.

Spahr, H., Habermann, B., Gustafsson, C.M., Larsson, N.G., and Hallberg, B.M. (2012). Structure of the human MTERF4-NSUN4 protein complex that regulates mitochondrial ribosome biogenesis. Proc Natl Acad Sci U S A *109*, 15253-15258.

Sterky, F.H., Ruzzenente, B., Gustafsson, C.M., Samuelsson, T., and Larsson, N.-G. (2010). LRPPRC is a mitochondrial matrix protein that is conserved in metazoans. Biochemical and biophysical research communications *398*, 759-764.

Suzuki, T., Wada, T., Saigo, K., and Watanabe, K. (2002). Taurine as a constituent of mitochondrial tRNAs: new insights into the functions of taurine and human mitochondrial diseases. The EMBO journal *21*, 6581-6589.

Szczesny, R.J., Borowski, L.S., Brzezniak, L.K., Dmochowska, A., Gewartowski, K., Bartnik, E., and Stepien, P.P. (2010). Human mitochondrial RNA turnover caught in flagranti: involvement of hSuv3p helicase in RNA surveillance. Nucleic Acids Res *38*, 279-298.

Temperley, R., Richter, R., Dennerlein, S., Lightowlers, R.N., and Chrzanowska-Lightowlers, Z.M. (2010a). Hungry codons promote frameshifting in human mitochondrial ribosomes. Science *327*, 301.

Temperley, R.J., Seneca, S.H., Tonska, K., Bartnik, E., Bindoff, L.A., Lightowlers, R.N., and Chrzanowska-Lightowlers, Z.M. (2003). Investigation of a pathogenic mtDNA microdeletion reveals a translation-dependent deadenylation decay pathway in human mitochondria. Hum Mol Genet *12*, 2341-2348.

Temperley, R.J., Wydro, M., Lightowlers, R.N., and Chrzanowska-Lightowlers, Z.M. (2010b). Human mitochondrial mRNAs--like members of all families, similar but different. Biochimica et biophysica acta *1797*, 1081-1085.

Terzioglu, M., Ruzzenente, B., Harmel, J., Mourier, A., Jemt, E., Lopez, M.D., Kukat, C., Stewart, J.B., Wibom, R., Meharg, C., et al. (2013). MTERF1 binds mtDNA to prevent transcriptional interference at the light-strand promoter but is dispensable for rRNA gene transcription regulation. Cell metabolism *17*, 618-626.

Tiranti, V., Savoia, A., Forti, F., D'Apolito, M.F., Centra, M., Rocchi, M., and Zeviani, M. (1997). Identification of the gene encoding the human mitochondrial RNA polymerase (h-mtRPOL) by cyberscreening of the Expressed Sequence Tags database. Hum Mol Genet *6*, 615-625.

Tomecki, R., Dmochowska, A., Gewartowski, K., Dziembowski, A., and Stepien, P.P. (2004). Identification of a novel human nuclear-encoded mitochondrial poly(A) polymerase. Nucleic acids research *32*, 6001-6014.

Tu, Y.T., and Barrientos, A. (2015). The Human Mitochondrial DEAD-Box Protein DDX28 Resides in RNA Granules and Functions in Mitoribosome Assembly. Cell reports.

Urbonavicius, J., Qian, Q., Durand, J.M., Hagervall, T.G., and Bjork, G.R. (2001). Improvement of reading frame maintenance is a common function for several tRNA modifications. EMBO J *20*, 4863-4873.

Van Haute, L., Dietmann, S., Kremer, L., Hussain, S., Pearce, S.F., Powell, C.A., Rorbach, J., Lantaff, R., Blanco, S., Sauer, S., et al. (2016). Deficient methylation and formylation of mt-tRNA(Met) wobble cytosine in a patient carrying mutations in NSUN3. Nature communications *7*, 12039.

Van Haute, L., Powell, C.A., and Minczuk, M. (2017). Dealing with an Unconventional Genetic Code in Mitochondria: The Biogenesis and Pathogenic Defects of the 5-Formylcytosine Modification in Mitochondrial tRNAMet. Biomolecules *7*.

Vilardo, E., Nachbagauer, C., Buzet, A., Taschner, A., Holzmann, J., and Rossmanith, W. (2012). A subcomplex of human mitochondrial RNase P is a bifunctional methyltransferase--extensive moonlighting in mitochondrial tRNA biogenesis. Nucleic Acids Res *40*, 11583-11593.

Villarroya, M., Prado, S., Esteve, J.M., Soriano, M.A., Aguado, C., Perez-Martinez, D., Martinez-Ferrandis, J.I., Yim, L., Victor, V.M., Cebolla, E., et al. (2008). Characterization of human GTPBP3, a GTP-binding protein involved in mitochondrial tRNA modification. Molecular and cellular biology *28*, 7514-7531.

Wang, D.D.-H., Guo, X.E., Modrek, A.S., Chen, C.-F., Chen, P.-L., and Lee, W.-H. (2014). Helicase SUV3, polynucleotide phosphorylase, and mitochondrial polyadenylation polymerase form a transient complex to modulate mitochondrial mRNA polyadenylated tail lengths in response to energetic changes. The Journal of biological chemistry *289*, 16727-16735.

Wang, G., Chen, H.-W., Oktay, Y., Zhang, J., Allen, E.L., Smith, G.M., Fan, K.C., Hong, J.S., French, S.W., McCaffery, J.M., et al. (2010). PNPASE regulates RNA import into mitochondria. Cell *142*, 456-467.

Wang, Z., Cotney, J., and Shadel, G.S. (2007). Human mitochondrial ribosomal protein MRPL12 interacts directly with mitochondrial RNA polymerase to modulate mitochondrial gene expression. J Biol Chem *282*, 12610-12618.

Wanrooij, P.H., Uhler, J.P., Simonsson, T., Falkenberg, M., and Gustafsson, C.M. (2010). G-quadruplex structures in RNA stimulate mitochondrial transcription termination and primer formation. Proc Natl Acad Sci U S A *107*, 16072-16077.

Wanschers, B.F., Szklarczyk, R., Pajak, A., van den Brand, M.A., Gloerich, J., Rodenburg, R.J., Lightowlers, R.N., Nijtmans, L.G., and Huynen, M.A. (2012). C7orf30 specifically associates with the large subunit of the mitochondrial ribosome and is involved in translation. Nucleic Acids Res *40*, 4040-4051.

Wilson, W.C., Hornig-Do, H.T., Bruni, F., Chang, J.H., Jourdain, A.A., Martinou, J.C., Falkenberg, M., Spahr, H., Larsson, N.G., Lewis, R.J., et al. (2014). A human mitochondrial poly(A) polymerase mutation reveals the complexities of post-transcriptional mitochondrial gene expression. Hum Mol Genet *23*, 6345-6355.

Wredenberg, A., Lagouge, M., Bratic, A., Metodiev, M.D., Spahr, H., Mourier, A., Freyer, C., Ruzzenente, B., Tain, L., Gronke, S., et al. (2013). MTERF3 regulates mitochondrial ribosome biogenesis in invertebrates and mammals. PLoS Genet *9*, e1003178.

Wydro, M., Bobrowicz, A., Temperley, R.J., Lightowlers, R.N., and Chrzanowska-Lightowlers, Z.M. (2010). Targeting of the cytosolic poly(A) binding protein PABPC1 to mitochondria causes mitochondrial translation inhibition. Nucleic Acids Res *38*, 3732-3742.

Xu, F., Ackerley, C., Maj, M.C., Addis, J.B.L., Levandovskiy, V., Lee, J., Mackay, N., Cameron, J.M., and Robinson, B.H. (2008a). Disruption of a mitochondrial RNA-binding protein gene results in decreased cytochrome b expression and a marked reduction in ubiquinol-cytochrome c reductase activity in mouse heart mitochondria. The Biochemical journal *416*, 15-26.

Xu, Z., O'Farrell, H.C., Rife, J.P., and Culver, G.M. (2008b). A conserved rRNA methyltransferase regulates ribosome biogenesis. Nat Struct Mol Biol *15*, 534-536.

Yakubovskaya, E., Mejia, E., Byrnes, J., Hambardjieva, E., and Garcia-Diaz, M. (2010). Helix unwinding and base flipping enable human MTERF1 to terminate mitochondrial transcription. Cell *141*, 982-993.

Yarham, J.W., Lamichhane, T.N., Pyle, A., Mattijssen, S., Baruffini, E., Bruni, F., Donnini, C., Vassilev, A., He, L., Blakely, E.L., et al. (2014). Defective i6A37 modification of mitochondrial and cytosolic tRNAs results from pathogenic mutations in TRIT1 and its substrate tRNA. PLoS Genet *10*, e1004424.

Zaganelli, S., Rebelo-Guiomar, P., Maundrell, K., Rozanska, A., Pierredon, S., Powell, C.A., Jourdain, A.A., Hulo, N., Lightowlers, R.N., Chrzanowska-Lightowlers, Z.M., et al. (2017). The Pseudouridine Synthase RPUSD4 Is an Essential Component of Mitochondrial RNA Granules. J Biol Chem *292*, 4519-4532.

Zeharia, A., Shaag, A., Pappo, O., Mager-Heckel, A.M., Saada, A., Beinat, M., Karicheva, O., Mandel, H., Ofek, N., Segel, R., et al. (2009). Acute infantile liver failure due to mutations in the TRMU gene. Am J Hum Genet *85*, 401-407.